A BOUNDARY ELEMENT SCHEME FOR THREE-DIMENSIONAL ACOUSTIC RADIATION WITH FLOW

A THESIS

SUBMITTED IN PARTIAL FULFILMENT

OF THE REQUIREMENTS FOR THE DEGREE OF

MASTER OF ENGINEERING

IN

MECHANICAL ENGINEERING

AT

THE UNIVERSITY OF CANTERBURY

BY

JAMES GREGORY BAIN, B.SC.(HONS)

1985

ABSTRACT

A boundary element approach is proposed for acoustical radiation in non-uniform, low Mach number flows. The formulation utilizes a transformation, valid at low Mach number for short wavelength disturbances, which converts this problem into an analogous no-flow problem for the same geometry. Two distinct boundary integral schemes are considered. An overdetermined combined surface-interior formulation and a combined surface-surface derivative formulation are both used to calculate the velocity potential due to the vibration of an arbitrary body in a uniform mean flow. Results are presented for the test cases of pulsating and juddering spheres in low Mach number flows. Good agreement is established between the results produced by the present boundary element formulations and those obtained from an analytic solution and an alternative numerical (finite element) scheme.

ACKNOWLEDGEMENT

The support and guidance provided by my supervisor, Dr R.J. Astley, is gratefully acknowledged. His suggestions, patience and time spent in discussion have been much appreciated.

I am sincerely grateful to Mrs Christine McEntee for typing this thesis.

Finally I wish to acknowledge the enduring qualities displayed by my flatmates; Iain McInnes, Wendy Mein, Helen Redshaw and Susan Strowger while I was writing this thesis.

TABLE OF CONTENTS

LIST OF FIGURES

LIST OF SYMBOLS

a	Radius of a mean sphere
$\underline{b}$	External body force
$\overset{*}{c}$	Total speed of sound
D_-	Interior domain (bounded externally by the body surface S)
D_+	Exterior domain (i.e. the complement of D_- S)
$\frac{D(\ )}{Dt}$	Material derivative
$h_n^{(2)}$	Spherical Hankel function of the second kind and n-th order
k	Wavenumber
L_A	Characteristic lengthscale of an acoustic disturbance
L_M	Characteristic lengthscale of the mean flow
$\underline{M}$	Mach number vector
$\underline{\hat{n}}$	Unit normal vector
N	Total number of elements or nodes
p	Fluid pressure
P_n^m	Legendre function of the first kind, m-th order and n-th degree
P	A singularity point
Q	A point on the surface S. An integration point (see section 2 of chapter 4).
R	Radius of a large spherical surface
$\hat{R}_1$, $\hat{R}_2$	Non-dimensional nodal radii
$r(P,Q)$	Distance between points P and Q
S	The surface of the radiating body
S_R	The surface of a large sphere
S_d	Surface area of discretized model
t	Time variable
T	Characteristic time scale or transformed time variable (2.6.7)
$\underline{U}$	Mean flow velocity
$\underline{V}$	Total velocity in the flow field (2.3.1)
W_k	The k-th weight of a numerical integration (see 4.2.1)
$\underline{x} = (x,y,z)$	Rectangular Cartesian coordinate system
$\underline{X} = (X,Y,Z)$	Rectangular Cartesian coordinate system in the transformed space
α	Curvilinear coordinate normal to the surface S or a complex coupling constant (3.4.3) or a residual weighting factor (4.3.13)
β_1, β_2	Curvilinear coordinates on the surface S
c	The local speed of sound

γ Ratio of specific heats (2.3.3)

γ_i Distance from element centroid to the interior singularity point

δ The perturbed density (2.3.21) or Dirac delta function (3.1.8)

ϵ Small perturbation parameter

η Surface displacement (2.4.1) or a surface point or base triangle coordinate

θ Spherical coordinate (5.4.2) or viscous term (2.3.6)

λ Acoustic wavelength

μ Coefficient of shear viscosity

ν Integration coordinate (4.2.1)

ξ Coefficient of bulk viscosity or a surface point or base triangle coordinate

ρ Total fluid density

$\overline{\rho}$ Density of steady mean flow

$\overset{*}{\phi}$ Total velocity potential

ϕ Acoustic velocity potential

$\overline{\phi}$ Velocity potential of the steady mean flow

$\hat{\phi} = \frac{\overline{\phi}}{U_\infty}$ A flow related velocity potential

Φ Amplitude of acoustic velocity potential (3.1.1) or a reference value of ϕ (section 5 of chapter 2)

Ψ Amplitude of transformed acoustic velocity potential (3.1.3)

ψ Spherical coordinate (5.4.2)

χ Residual function (4.3.13)

ω Harmonic frequency

$\cup$ Union operator

$\cap$ Intersection operator

$\underline{\nabla}$ Del operator

SUBSCRIPTS

o Stagnation conditions or solution of homogeneous integral equation

r A reference state

∞ Steady far field conditions (at infinity)

x Transformed quantity

SUPERSCRIPTS

* Complex conjugate

I Interior quantity

I. INTRODUCTION

The general acoustic field problem is concerned with the description of the acoustical field that is produced or perturbed by real sources within an acoustic medium.

The calculation of acoustical fields propagating in subsonic mean flows and the interaction of such fields both with the mean flow itself and with reflecting boundaries is the general problem represented in this study.

The solution of this problem is important in the analysis of the sound fields generated by aircraft. Typical aeroacoustic problems are concerned with the prediction of propellor generated noise, the noise resulting from flow-fuselage interaction and the fan noise from the nacelle inlet of a turbofan aircraft engine. As in most aeroacoustic problems the dimensions of the radiating body will be many times larger than the acoustical wavelengths corresponding to the major energy carrying frequencies.

In modelling this sort of problem for realistic sound levels the acoustical field can be regarded as linear. This particular problem is similar in general character to many other problems involving linear radiation in a mean flow.

A review of available methods which have been used to model the general radiation problem is presented below.

In the no-flow problem, closed form analytic solutions exist for a limited number of simple geometries. Such solutions range from the variables separable and source distribution methods of Rayleigh and others,[1],[2] to studies in which the Weiner-Hopf technique [3],[4],[5] has been used. For the more general mean flow problem two restrictive analytic solutions are available. Dowling,[6], has solved for the acoustic field generated by flow over compact vibrating bodies. Taylor,[7], has given solutions for the simple case of a vibrating sphere in a low Mach number flow for a frequency parameter (ka) of order 1.

None of these analytic solutions can be extended to the problem of an arbitrary body within a mean flow. Consequently, use is often made of numerical techniques such as finite differences (FD) and finite element (FE) methods.

The direct application of a FD method or a conventional FE method over a large portion of an unbounded domain would be computationally impractical. The wavelike nature of the solution typically demands the use of a fine mesh in order to resolve the problem accurately. This requirement is compounded in the relative high frequency/short wavelength limit characteristic of many aeroacoustic problems.

The usual approach at this stage is to divide the exterior domain into two subregions, that is;

(i) a relatively small inner region surrounding the body or inlet;

(ii) and an outer region which meets the inner region at some arbitrary interface.

The inner region would enclose any irregular boundaries and non-homogeneities (e.g. density and mean flow variations) which exist for the problem.

The sound field in this region can be adequately represented using either FD or FE techniques. In the case of a turbofan inlet, for example, the methods for predicting the sound field in the ducted sections include wave envelope weighted residual schemes, [8] ; FE schemes of various types, [9], [10] and transient finite difference schemes [11], [12], [13].

The propagation of sound in the outer region presents a more demanding computational problem. This outer region will require a radiation type boundary condition to be applied at some distant boundary. Also, none of the numerical schemes developed for the inner region may be conventionally applied to the outer region.

A brief summary of some methods which have been applied within the outer region is given below.

One method involves the application of boundary integral (B.I.) methods to the outer region. This approach models the outer field by a distribution of source functions over a control surface enclosing the radiating body. The impedance on this surface is then matched iteratively to the conventional FE or FD solutions of the inner region, [14], [15], [16]. The valid application of this method will demand a sufficiently large inner region so as to ensure uniform flow conditions within the outer region. A large inner region would be computationally expensive, so that in general this method is undesirable.

An alternative approach involves the modification of the shape and weighting functions within a standard Galerkin FE scheme in order to accommodate the fine harmonic detail of the solution in the outer region. This is done either through the use of infinite elements, [17], [18], [19] (which impose an exaggerated exponential decay on the outer solution) or by the use of wave envelope elements which incorporate the main features both of the asymptotic decay and of the harmonic variation within a large but finite outer domain, [20], [21]. The wave envelope elements have the advantage over infinite elements by directly predicting the far field solution. This method has also been successfully applied to two-dimensional and axisymmetric flow problems, [22].

A more detailed discussion of these solution schemes is given within section 3 of Chapter V.

The extension of these methods to the fully three dimensional case (necessary, for example, if the interaction of fan noise with neighbouring fuselage and wing surfaces is to be modelled) would be computationally unrealistic.

Several different approaches have been proposed for the three dimensional problem. Ray acoustical theory provides a high frequency approximation which has been applied with some success to problems with and without flow, [23]. Boundary integral formulations, over the whole exterior domain, are also readily applicable in the absence of flow, [24], [25]. However when flow is present B.I. formulations are no longer directly applicable. They may still be used to represent the acoustical field in the outer regions of uniform flow but must be matched to conventional numerical schemes in the inner region.

In the present study a transformed boundary element scheme is proposed for 'low' Mach number flows. A transformation of the temporal variable enables the problem with flow to be reformulated as the solution of an ordinary wave equation in the transformed variables, [7], [26]. The transformation includes the effects of non-uniform mean flow and may be applied to any irrotational mean flow for which the velocity potential has been calculated. It will be demonstrated later that this transformation is valid within the high frequency limit, thus ensuring its applicability to most aeroacoustic problems.

The principal advantage of transforming the flow problem into an analogous no-flow formulation lies in the potential which then exists for the use of established techniques in the solution of the ordinary wave equation. The resulting solution of this problem must then be transformed back into the original variables to give physically meaningful results. One of the most obvious numerical schemes which is applicable within the transformed problem is the boundary element method. It is the implementation of this approach which will be discussed in the remainder of this work.

The boundary element method arises from the discretization of the analytic boundary integral formulations. Initially three classical integral formulations will be proposed for obtaining approximate solutions of the external steady-state transformed problem. That is:-

(a) the simple-source formulation, adapted from potential theory, [27], [28]

(b) the surface Helmholtz integral formulation, [29]

(c) the interior Helmholtz integral formulation, [30], [31]

These methods will be discussed in detail later. A review of their relative merits can also be found in reference [32]. The usual problems associated with the surface integral representation of external wave solutions will also exist in the transformed problem.

Therefore, for certain critical wavenumbers, it will be shown that no solution of the simple-source formulation exists and that there is no unique solution of the surface Helmholtz integral formulation. The interior Helmholtz integral formulation is subject to similar difficulties and has undesirable computational characteristics.

These difficulties can be resolved in a number of ways. A brief outline of available alternative methods is presented below.

In 1967, Schenk [24] proposed the combined Helmholtz integral equation formulation (CHIEF). This method combines the surface integral and interior integral formulations. The basic concept is that only one of the surface solutions will also satisfy the interior integral equation at the critical wavenumbers.

Burton and Miller,[33], initiated a method which linearly combines the surface integral equation and its normal derivative with respect to a field point. This method relies on the two implicit methods having only one solution in common at the critical wavenumbers. This method has been further modified by Meyer et al.[34],[25].

In 1973, Ursell,[35],described a method analogous to the surface Helmholtz method which utilizes a modified fundamental solution. Although theoretically straightforward this method leads to an infinite series which converges rapidly for low frequencies but slowly for high frequencies. A modification of this method has been given by Jones,[36], whereby the infinite series is replaced by a finite one. However this modification introduces bounds on the values of wavenumber for which it can be applied.

The null field method,[37], has also been applied to this radiation problem.

Recently a combined surface integral and exterior integral scheme has been introduced by Piaszczyk and Klosner,[32]. This method involves an iterative overdetermination procedure.

None of the above approaches is entirely without disadvantage, or pre-eminently reliable. The first two alternative methods appear to offer reliable solutions for the present case and have in fact been applied to the untransformed no-flow problem in various forms,[24],[25]. Both these two methods have been considered in the present analysis.

This work is divided into six chapters. The proceeding chapter contains a derivation of the linearized acoustic field equation followed by an approximation and a transformation that will reduce the field equation to the ordinary wave equation. Solution methods relevant to the no-flow wave equation are discussed in Chapter Three. Chapter Four discusses the numerical implementation of two boundary integral solution methods. The fifth chapter specifies two test case vibrations for a simple sphere; the remainder of this chapter compares the computed results (arising from the boundary element implementation) against exact solutions and alternative numerical results for the pulsating or juddering sphere of a uniform low Mach number flow. Finally the conclusions of this analysis are given in Chapter Six.

II ANALYSIS

In this chapter a description of the problem to be investigated is outlined. An acoustical equation relevant to this problem is derived from governing equations of Mass conservation, Momentum conservation and an equation of state. The formulation of a general linearized boundary condition relevant to an acoustically vibrating body within a perturbed flow is described. The remaining sections of the chapter deal with an approximation and a transformation that, in precise circumstances, can be applied to the derived acoustic equation in order to reduce it to the ordinary wave equation within a no-flow problem.

1. THE PROBLEM

The problem under investigation throughout this study is that of determining the acoustical field generated by a vibrating or reflecting body immersed in a mean flow. This problem is a simple case of the class of problem mentioned in the introduction. Although apparently simple this configuration will incorporate most of those features which would be modelled in the more general case. Of particular interest is the interaction of the sound field with the perturbed mean flow, the interaction with vibrating and reflecting boundaries within the flow and radiation into an infinite domain.

The model problem, initially stated with very few assumptions, will ultimately involve a steady, isentropic, irrotational mean flow of low Mach number. It will also be shown that the ratio of a characteristic length scale for the acoustic disturbance to a characteristic length scale for the mean flow will play an important part in determining the validity of the methods used to solve the problem.

2. GEOMETRY

Figure 1 shows the geometry of the problem. An arbitrary three dimensional body lies within a perturbed mean flow which approaches an adverse uniform flow in the farfield. The boundary of the body is denoted by the surface S which is of finite area. Let D_- denote the interior domain of the body, bounded externally by S. Denote the infinite exterior domain by D_+, where D_+ is the complement of $D_- \cup S$.

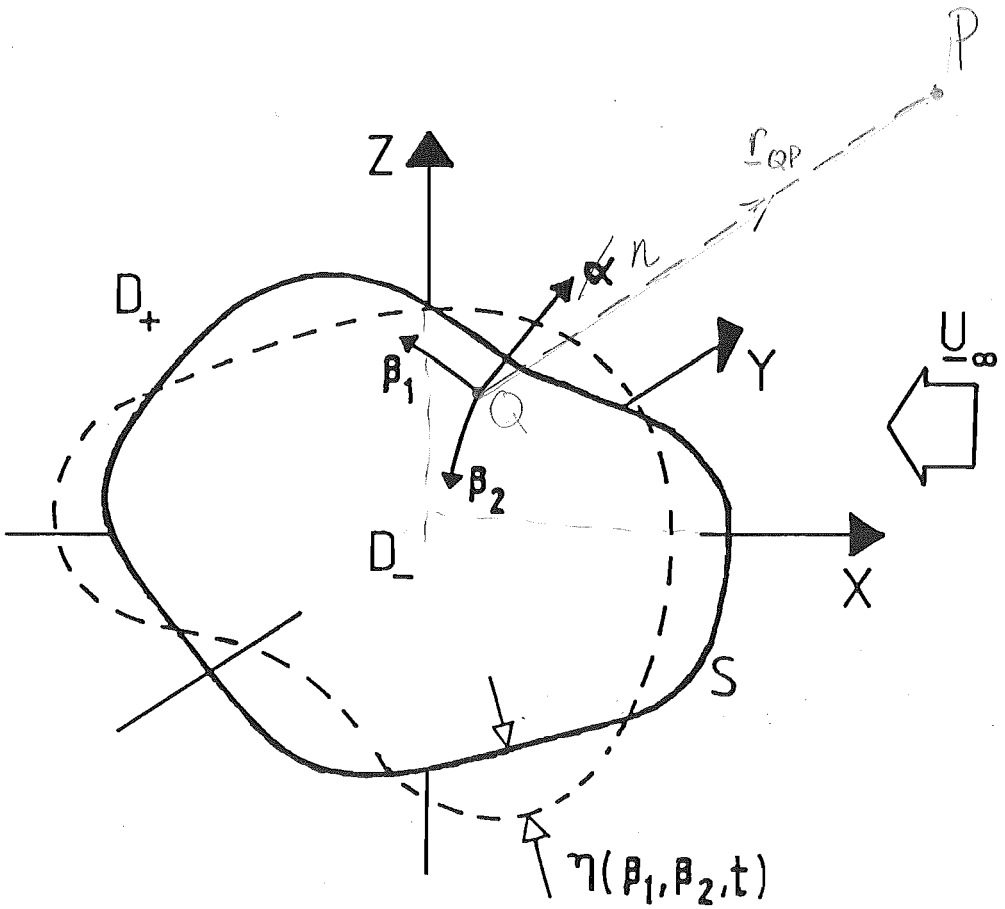

Figure 1. Geometry

The boundary S oscillates with a displacement $\eta(\beta_1,\beta_2,t)$ normal to the surface of the body. (β_1 & β_2 are curvilinear coordinates on the surface S, as shown in Fig. 1; see Myer [38]).

This vibration of S causes an acoustical disturbance to propagate in the infinite exterior domain D_+. At large distances from the body the acoustical field must be entirely radiative. Since it is assumed that there are no distant sources, this 'radiation condition' implies the non-existence of any reflected waves from infinity.

3. ACOUSTIC EQUATIONS

This section contains a derivation of the acoustic field equation relevant to the problem. This derivation is similar to a derivation given by Vaidya [39] . The field equations are first derived for a more general problem, where it is initially assumed that:

1. the fluid medium is non-heat conducting with constant specific heats;
2. all processes involved are isentropic;
3. the perfect gas law applies.

It will be shown, under more specific conditions, that two field equations can be combined to produce a linearized, irrotational, non-viscous acoustic equation in terms of the acoustic velocity potential.

Under the initial assumptions above, the governing field equations are the constitutive equations for a Newtonian fluid (see Batchelor [40] and Hunter [41]).

Note as much as possible all equations will be expressed in vector form.

3A GOVERNING EQUATIONS

The governing equations are:

Mass conservation:

$$\frac{\partial \rho}{\partial t} + \underline{\nabla}.(\rho \underline{V}) = 0 \qquad (2.3.1)$$

ρ is the total fluid density and $\underline{V}$ is the total velocity in the flow field.

Momentum conservation:

$$\rho \frac{D\underline{V}}{Dt} = \rho \underline{b} - \underline{\nabla} p + \mu \nabla^2 \underline{V} + (\xi + 1/3\mu)\underline{\nabla}(\underline{\nabla}.\underline{V}) \qquad (2.3.2)$$

where $\frac{D\underline{V}}{Dt} \equiv \frac{\partial \underline{V}}{\partial t} + (\underline{V}.\underline{\nabla})\underline{V}$

$\underline{b}$ represents an external body force, p the fluid pressure, ξ is the coefficient of bulk viscosity and μ is the coefficient of shear viscosity.

Sound speed:

$$c^2 = \frac{dp}{d\rho} = \frac{\gamma p}{\rho} \tag{2.3.3}$$

for constant entropy.
c is the sound speed and γ is the ratio of specific heats.

Equation (2.3.3) gives:

$$\frac{p}{p_r} = \left(\frac{\rho}{\rho_r}\right)^{\gamma} \tag{2.3.4}$$

$$\frac{c^2}{c_r^2} = \left(\frac{\rho}{\rho_r}\right)^{\gamma-1} \tag{2.3.5}$$

where p_r, c_r, ρ_r are reference values of pressure, sound speed and density relevant to some reference state.

Using the vector identities:-

(i) $\nabla^2\underline{V} = \underline{\nabla}(\underline{\nabla}.\underline{V}) - \underline{\nabla} \times (\underline{\nabla} \times \underline{V})$

(ii) $(\underline{V}.\underline{\nabla})\underline{V} = \tfrac{1}{2}\underline{\nabla}(\underline{V}.\underline{V}) - \underline{V} \times (\underline{\nabla} \times \underline{V})$

equation (2.3.2) is rearranged to yield:-

$$\frac{\partial \underline{V}}{\partial t} + \tfrac{1}{2}\underline{\nabla}(\underline{V}.\underline{V}) - \underline{V} \times (\underline{\nabla} \times \underline{V}) - \theta\nabla^2\underline{V} + (\nu - \theta)\underline{\nabla} \times (\underline{\nabla} \times \underline{V}) + \underline{b} + \frac{1}{\rho}\underline{\nabla}p = 0 \tag{2.3.6}$$

where $\theta = \frac{1}{\rho}\left(\frac{4}{3}\mu + \xi\right)$, $\nu = \frac{\mu}{\rho}$.

3B VELOCITY POTENTIAL FORMULATION

The flow field will now be restricted to irrotational motion in the absence of external body forces. Irrotational motion is curl free, and this condition is ensured when the fluid velocity is expressed as the gradient of a velocity potential. i.e.

$$\underline{V} = \underline{\nabla}\overset{*}{\phi} \tag{2.3.7}$$

$\overset{*}{\phi}$ is the total velocity potential of the flow field.
So (2.3.6) becomes:

$$\frac{\partial(\underline{\nabla}\overset{*}{\phi})}{\partial t} + \tfrac{1}{2}\underline{\nabla}\left[(\underline{\nabla}\overset{*}{\phi}).(\underline{\nabla}\overset{*}{\phi})\right] - \theta\nabla^2(\underline{\nabla}\overset{*}{\phi}) + \frac{1}{\rho}\underline{\nabla}p = 0 \qquad (2.3.8)$$

and can be written as:-

$$\underline{\nabla}\left[\frac{\partial\overset{*}{\phi}}{\partial t} + \tfrac{1}{2}|\underline{\nabla}\overset{*}{\phi}|^2 - \theta\nabla^2\overset{*}{\phi} + \frac{\overset{*}{c}^2}{\gamma-1}\right] = 0 \qquad (2.3.9)$$

where, using (2.3.3), (2.3.4) and (2.3.5)

$$\frac{1}{\rho}\underline{\nabla}p = \underline{\nabla}\left[p_r\,\rho_r^{-\gamma}\,\frac{\gamma}{\gamma-1}\,\rho^{\gamma-1}\right] = \underline{\nabla}\left(\frac{\overset{*}{c}^2}{\gamma-1}\right) \qquad (2.3.10)$$

$\overset{*}{c}$ is the total speed of sound.
If the reference conditions are taken to be stagnation conditions then (2.3.9) becomes:

$$\frac{\partial\overset{*}{\phi}}{\partial t} + \tfrac{1}{2}|\underline{\nabla}\overset{*}{\phi}|^2 - \theta\nabla^2\overset{*}{\phi} + \frac{\overset{*}{c}^2}{\gamma-1} = \frac{c_o^2}{\gamma-1} \qquad (2.3.11)$$

where c_o is the speed of sound at the stagnation state. This equation will be referred to as the first field equation.

The conservation of mass equation (2.3.1) can be stated as:-

$$\frac{1}{\rho}\frac{D\rho}{Dt} + \underline{\nabla}.\underline{V} = 0 \qquad (2.3.12)$$

and with $\underline{V} = \underline{\nabla}\overset{*}{\phi}$ becomes,

$$\frac{D}{Dt}\ln\rho + \nabla^2\overset{*}{\phi} = 0 \qquad (2.3.13)$$

Equation (2.3.5) gives:

$$\overset{*}{c}^2 = c_r^2\,\rho_r^{-(\gamma-1)}\,\rho^{\gamma-1} \qquad (2.3.14)$$

and so,

$$\frac{D\overset{*}{c}^2}{Dt} = \overset{*}{c}^2(\gamma-1)\frac{D}{Dt}\ln\rho \qquad (2.3.15)$$

Hence using (2.3.15), equation (2.3.13) can be written as:

$$\frac{Dc^{*2}}{Dt} = -c^{*2}(\gamma-1)\nabla^2\phi^* \tag{2.3.16}$$

This equation will be referred to as the second field equation. The two field equations (2.3.11) and (2.3.16) are now combined by eliminating c^{*2} between them.

Rearranging (2.3.11) gives:

$$c^{*2} = c_o^2 - (\gamma-1)\left[\phi^*_t + \tfrac{1}{2}|\underline{\nabla}\phi^*|^2 - \theta\nabla^2\phi^*\right] \tag{2.3.17}$$

and substituting (2.3.17) into (2.3.16) yields:

$$-(\gamma-1)\phi^*_{tt} - \tfrac{1}{2}(\gamma-1)\frac{\partial}{\partial t}|\underline{\nabla}\phi^*|^2 + (\gamma-1)\theta\frac{\partial}{\partial t}(\nabla^2\phi^*) - (\gamma-1)\underline{\nabla}\phi^*.\left[\frac{\partial}{\partial t}(\underline{\nabla}\phi^*)\right]$$

$$-\tfrac{1}{2}(\gamma-1)\underline{\nabla}\phi^*.\underline{\nabla}|\underline{\nabla}\phi^*|^2 + \theta(\gamma-1)\underline{\nabla}\phi^*.\underline{\nabla}(\nabla^2\phi^*) = -c_o^2(\gamma-1)\nabla^2\phi^* + (\gamma-1)^2(\nabla^2\phi^*)\phi^*_t$$

$$+ \tfrac{1}{2}(\gamma-1)^2(\nabla^2\phi^*)|\nabla\phi^*|^2 - \theta(\gamma-1)^2(\nabla^2\phi^*)^2 \tag{2.3.18}$$

The fluid is now specified to be non-viscous, i.e. $\theta=0$. Hence dividing through by $(\gamma-1)$ and noting that

$$\underline{\nabla}\phi^*.\left[\frac{\partial}{\partial t}(\underline{\nabla}\phi^*)\right] = \tfrac{1}{2}\frac{\partial}{\partial t}|\underline{\nabla}\phi^*|^2$$

equation (2.3.18) is rewritten:-

$$c_o^2\nabla^2\phi^* - \phi^*_{tt} = (\gamma-1)(\nabla^2\phi^*)\phi^*_t + \frac{\partial}{\partial t}|\underline{\nabla}\phi^*|^2 + \tfrac{1}{2}(\gamma-1)(\nabla^2\phi^*)|\underline{\nabla}\phi^*|^2 + \tfrac{1}{2}\underline{\nabla}\phi^*.\underline{\nabla}|\underline{\nabla}\phi^*|^2 \tag{2.3.19}$$

This combined field equation relates the total velocity potential and stagnation sound speed within an irrotational, inviscid flow field.

3C THE PERTURBED EQUATION

The assumption that the acoustic quantities consist of small perturbations superimposed on a time invariant mean flow is now introduced.

The total velocity potential and total density are split into a steady part, representative of the mean flow, and a perturbed part.

That is:

$$\overset{*}{\phi} = \bar{\phi} + \phi \tag{2.3.20}$$

$$\rho = \bar{\rho} + \delta \tag{2.3.21}$$

where $\bar{\phi}$ and $\bar{\rho}$ are the velocity potential and density of the steady mean flow. The local mean flow velocity, $\underline{U}$, is given by:

$$\underline{U} = \underline{\nabla}\bar{\phi} , \tag{2.3.22}$$

δ represents the perturbed density and ϕ is the true acoustic velocity potential.

Substituting (2.3.20) into (2.3.19) yields:-

$$c_o^2\nabla^2\phi - \phi_{tt} + c_o^2\underline{\nabla}.\underline{U} = T_1 + T_2 + T_3 + T_4 \tag{2.3.23}$$

T_1, T_2, T_3 and T_4 are the resulting four terms corresponding to the four terms on the right of equation (2.3.19); such that,

$$T_1 = (\gamma-1)\phi_t\nabla^2\phi + (\gamma-1)\phi_t\underline{\nabla}.\underline{U} \tag{2.3.24}$$

$$T_2 = \frac{\partial}{\partial t}\left[|\underline{\nabla}\phi|^2 + |\underline{U}|^2 + 2\underline{U}.\underline{\nabla}\phi\right] = 2\underline{\nabla}\phi_t.\underline{\nabla}\phi + 2\underline{U}.\underline{\nabla}\phi_t \tag{2.3.25}$$

$$\begin{aligned} T_3 &= \frac{(\gamma-1)}{2}(\nabla^2\phi + \underline{\nabla}.\underline{U})\left[|\underline{\nabla}\phi|^2 + |\underline{U}|^2 + 2\underline{U}.\underline{\nabla}\phi\right] \\ &= \frac{(\gamma-1)}{2}\left[|\underline{\nabla}\phi|^2\nabla^2\phi + |\underline{U}|^2\nabla^2\phi + 2\underline{U}.\underline{\nabla}\phi(\nabla^2\phi) + |\underline{\nabla}\phi|^2\underline{\nabla}.\underline{U}\right. \\ &\quad \left. + |\underline{U}|^2\underline{\nabla}.\underline{U} + 2\underline{U}.\underline{\nabla}\phi(\underline{\nabla}.\underline{U})\right] \end{aligned} \tag{2.3.26}$$

$$\begin{aligned} T_4 &= \tfrac{1}{2}\left[\underline{\nabla}\phi.\underline{\nabla}|\underline{\nabla}\phi|^2 + \underline{\nabla}\phi.\underline{\nabla}|\underline{U}|^2 + 2\underline{\nabla}\phi.\underline{\nabla}(\underline{U}.\underline{\nabla}\phi) + \underline{U}.\underline{\nabla}|\underline{\nabla}\phi|^2\right. \\ &\quad \left. + \underline{U}.\underline{\nabla}|\underline{U}|^2 + 2\underline{U}.\underline{\nabla}(\underline{U}.\underline{\nabla}\phi)\right] \end{aligned} \tag{2.3.27}$$

Equation (2.3.23) contains terms without ϕ, terms with the first power of ϕ and terms of higher powers of ϕ. The terms without ϕ contain steady mean flow quantities.

The steady flow quantities will satisfy the field equations (2.3.11) and (2.3.12) by themselves, hence;

$$c^2 = c_o^2 - \frac{(\gamma-1)}{2} |\underline{U}|^2 \tag{2.3.28}$$

and

$$\underline{U} \cdot \left(\frac{\underline{\nabla}\bar{\rho}}{\bar{\rho}} \right) + \underline{\nabla}.\underline{U} = 0 \tag{2.3.29}$$

for nonviscous flow, where c is the local sound speed of the mean flow.

To eliminate $\bar{\rho}$ from (2.3.29) consider the gradient of equation (2.3.5). Thus;

$$\underline{\nabla}\bar{\rho} = \frac{\bar{\rho}}{\gamma-1} \frac{\underline{\nabla}c^2}{c^2} \tag{2.3.30}$$

and using the gradient of (2.3.28) gives:

$$\frac{1}{\bar{\rho}} \underline{\nabla}\bar{\rho} = -\tfrac{1}{2} \frac{\underline{\nabla}|\underline{U}|^2}{c^2} \tag{2.3.31}$$

Substituting (2.3.31) into equation (2.3.29) gives:

$$c^2 \underline{\nabla}.\underline{U} = \tfrac{1}{2}\underline{U}.\underline{\nabla}|\underline{U}|^2 \tag{2.3.32}$$

Equations (2.3.28) and (2.3.32) show that the terms without ϕ in equation (2.3.23) can be equated out. This can be explained by realizing that for small acoustic perturbations the acoustic interaction with the mean flow will not produce significant changes in the mean flow.

From the initial assumption that the acoustic quantities consist of small perturbations superimposed on a mean flow, the true acoustic velocity potential can be expanded:

$$\phi = \varepsilon\phi_1 + \varepsilon^2\phi_2 + \ldots \tag{2.3.33}$$

where ε is a small dimensionless parameter characterizing the magnitude of the acoustic disturbances.

Therefore all those terms with second powers of ϕ or higher will be of order ε^2. So because the acoustic perturbations are assumed small the linear approximation of equation (2.3.23) will contain only those terms with first powers of ϕ.

Thus,

$$c^2\nabla^2\phi - 2\underline{U}.\nabla\phi_t - \tfrac{1}{2}\nabla\phi.\nabla|\underline{U}|^2 - \phi_{tt} - (\gamma-1)\phi_t\nabla.\underline{U} - (\gamma-1)(\underline{U}.\nabla\phi)(\nabla.\underline{U}) - \underline{U}.\nabla(\underline{U}.\nabla\phi) = 0 \tag{2.3.34}$$

where

$$c^2 = c_o^2 - \frac{(\gamma-1)}{2}|\underline{U}|^2 \tag{2.3.35}$$

Equation (2.3.34) is a linearized, irrotational, nonviscous equation describing the sound-mean flow interaction.

At infinity the mean flow is assumed steady and uniform, so the steady, inviscid form of (2.3.17) at infinity is:

$$c_\infty^2 = c_o^2 - \frac{(\gamma-1)}{2}|\underline{U}_\infty|^2 \tag{2.3.36}$$

where c_∞ and $\underline{U}_\infty$ are the sound speed and flow velocity at infinity. Combining equations (2.3.35) and (2.3.36) yields the equation:

$$c^2 = c_\infty^2 - \frac{(\gamma-1)}{2}\left[\,|\underline{U}|^2 - |\underline{U}_\infty|^2\right] \tag{2.3.37}$$

This equation states the relationship of the local sound speed and mean flow velocity with their corresponding reference values at infinity. Equations (2.3.34) and (2.3.37) are the two main results of this section. Note that in the absence of a mean flow equation (2.3.34) will reduce to the ordinary wave equation.

In its present form equation (2.3.34) is still a complicated equation to solve for ϕ. After first formulating a boundary condition, the remaining sections of this chapter introduce techniques that may be used in order to reduce (2.3.34) to a simpler, readily solvable equation.

4. THE BOUNDARY CONDITION

The boundary condition on the acoustic perturbation velocity at the impermeable surface, S, in a perturbed mean flow, is considered for the case in which the surface generates a sound field by vibration.

From the continuum theory of fluid motion the boundary condition, (which must be satisfied at each point of the moving surface) demands that the total velocity component of the fluid and that of a neighbouring point on the surface in the direction normal to the surface are equal.

Both Myer[38] and Taylor[7] have derived the same boundary condition for a vibrating surface in a perturbed mean flow by starting from this initial assumption.

The derivation of the boundary condition given by Myer is conceptually very straightforward while not losing any generality. It is based on the ability of the perturbed quantities to be expanded in a series about some base value. For example it is assumed the motion of the surface is a small perturbation about a stationary mean surface, and the fluid velocity field is a small perturbation about a mean flow. These series are expanded in powers of a small dimensionless parameter characterizing the magnitude of the acoustic disturbances. The expansions are then substituted into an equation that expresses the initial assumption stated at the beginning of this section. Then after truncating this equation to the leading order of the small dimensionless parameter and after further rearranging, the following boundary condition results:

$$\underline{\nabla}\phi.\hat{\underline{n}} = \left(\frac{\partial}{\partial t} + \underline{U}.\underline{\nabla}\right)\frac{\eta}{|\underline{\nabla}\alpha|} - \left(\frac{\eta}{|\underline{\nabla}\alpha|}\right)\hat{\underline{n}}.\left[(\hat{\underline{n}}.\underline{\nabla})\underline{U}\right] , \qquad (2.4.1)$$

on some mean stationary surface S_0; where ϕ is the acoustic velocity potential, $\hat{\underline{n}}$ is an outward unit normal to S_0, α is a curvilinear coordinate fixed on the surface S_0 pointing in the direction of $\hat{\underline{n}}$ and η is given in section 2, as the surface displacement normal to the surface of the body.

Equation (2.4.1) is the linearized boundary condition governing the acoustic perturbation velocity at an impermeable surface within a mean flow. As indicated, this boundary condition is applied on the mean position, S_0, of the moving surface. Hence the boundary condition on an impermeable vibrating body in a mean flow can be represented by a certain volume flow across the mean position of the surface.

This boundary condition has also been derived by Taylor using a similar method. Equation (2.4.1) is the form of the boundary condition that will be applied throughout this study.

5. A LOW MACH NUMBER APPROXIMATION

The acoustic field equation (2.3.34) is given in section 3 as:

$$c^2\nabla^2\phi - 2\underline{U}.\underline{\nabla}\phi_t - \phi_{tt} - \tfrac{1}{2}\underline{\nabla}\phi.\underline{\nabla}|\underline{U}|^2 - (\gamma-1)\phi_t\underline{\nabla}.\underline{U} - (\gamma-1)(\underline{U}.\underline{\nabla}\phi)(\underline{\nabla}.\underline{U}) - \underline{U}.\underline{\nabla}(\underline{U}.\underline{\nabla}\phi) = 0 \qquad (2.5.1)$$

with

$$c^2 = c_\infty^2 - \frac{(\gamma-1)}{2}\left(|\underline{U}|^2 - |\underline{U}_\infty|^2\right) \quad . \qquad (2.5.2)$$

Putting $\underline{U} = c_r\underline{M}$,
where c_r is a reference value for the sound speed and $\underline{M}$ is the non-dimensional vector Mach number defined by:-

$$\underline{M} = \frac{\underline{U}}{c_r}$$

equation (2.5.1) becomes:

$$c^2\nabla^2\phi - 2c_r\underline{M}.\underline{\nabla}\phi_t - \phi_{tt} - \tfrac{1}{2}\underline{\nabla}\phi.\underline{\nabla}|\underline{M}|^2 c_r^2 - (\gamma-1)\phi_t c_r(\underline{\nabla}.\underline{M})$$

$$- (\gamma-1)(\underline{M}.\underline{\nabla}\phi)c_r^2(\underline{\nabla}.\underline{M}) - c_r^2\,\underline{M}.\underline{\nabla}(\underline{M}.\underline{\nabla}\phi) = 0 \qquad (2.5.3)$$

The first three terms of (2.5.3) above are of lower order with respect to Mach number than the remaining terms. The quantity $(\underline{\nabla}.\underline{M})$ will be shown later to be of order M^3.

The basis of a low Mach number approximation is that for low Mach numbers the higher order terms may be discarded leaving a relatively simple equation to solve.

Taylor[7] has used a low Mach number approximation for equation (2.5.1) above. In his approximation the terms are ranked purely on the basis of Mach number order alone. This is not entirely valid since the magnitudes of the various terms in equation (2.5.1) are also dependent upon the non-dimensional ratio of the lengthscales associated with the mean flow and the acoustical disturbance. So this approximation must be applied cautiously to ensure that the discarded terms of higher order Mach number have smaller magnitudes than all remaining terms.

Before beginning the analysis of the individual terms within equation (2.5.3) some more substitutions are made. The reference value of sound speed c_r is taken to be the far field sound speed c_∞, and

$$c^2 = c_\infty^2 - c_\infty^2\,\frac{(\gamma-1)}{2}\left(|\underline{M}|^2 - |\underline{M}_\infty|^2\right)$$

so that (2.5.3) becomes:

$$c_\infty^2\nabla^2\phi - \phi_{tt} - 2c_\infty \underline{M}.\underline{\nabla}\phi_t - \frac{(\gamma-1)}{2} c_\infty^2(|\underline{M}|^2 - |\underline{M}_\infty|^2)\nabla^2\phi - \tfrac{1}{2}\underline{\nabla}\phi.\underline{\nabla}|\underline{M}|^2 c_\infty^2$$

$$- c_\infty(\gamma-1)\phi_t(\underline{\nabla}.\underline{M}) - (\gamma-1)(\underline{M}.\underline{\nabla}\phi)c_\infty^2(\underline{\nabla}.\underline{M}) - c_\infty^2\underline{M}.\underline{\nabla}(\underline{M}.\underline{\nabla}\phi) = 0 \qquad (2.5.4)$$

An expression for $(\underline{\nabla}.\underline{M})$ is now derived. When the steady mean flow and the acoustical perturbation are assumed to be inviscid, irrotational and isentropic, the mass conservation equation (2.3.1) for the mean flow is:

$$\underline{\nabla}.(\rho\underline{U}) = 0 \qquad (2.5.5)$$

Using equation (2.3.5) with the reference values taken at infinity i.e.

$$\frac{c^2}{c_\infty^2} = \left(\frac{\rho}{\rho_\infty}\right)^{\gamma-1} \qquad (2.5.6)$$

(2.5.6) and (2.5.2) give:

$$\rho = \rho_\infty\left[1 - \frac{(\gamma-1)}{2}(|\underline{M}|^2 - |\underline{M}_\infty|^2)\right]^{1/(\gamma-1)} \qquad (2.5.7)$$

where $\underline{M} = \dfrac{\underline{U}}{c_\infty}$, $\underline{M}_\infty = \dfrac{\underline{U}_\infty}{c_\infty}$

$\underline{U}$ and ρ denote the velocity and density of the mean flow while $\underline{U}_\infty$ and ρ_∞ are their reference values at infinity.

Equations (2.5.5) and (2.5.7) can be combined to obtain an expression for $\underline{\nabla}.\underline{M}$ (see Appendix (A) for details). i.e.

$$\underline{\nabla}.\underline{M} = \frac{\tfrac{1}{2}\underline{M}.\underline{\nabla}(|\underline{M}|^2)}{1 - \frac{(\gamma-1)}{2}(|\underline{M}|^2 - |\underline{M}_\infty|^2)} \qquad (2.5.8)$$

Equation (2.5.4) can now be separated out into five groups. That is:

$$c_\infty^2\nabla^2\phi - \phi_{tt} \qquad (a)$$

$$-2c_\infty\underline{M}.\underline{\nabla}\phi_t \qquad (b)$$

$$-\frac{(\gamma-1)}{2} c_\infty^2(|\underline{M}|^2 - |\underline{M}_\infty|^2)\nabla^2\phi - c_\infty^2\,\underline{M}.\left[(\underline{M}.\underline{\nabla})\underline{\nabla}\phi\right] \qquad (c)$$

$$-c_\infty^2\,\underline{M}.\left[(\underline{\nabla}\phi.\underline{\nabla})\underline{M}\right] - \tfrac{1}{2}\underline{\nabla}\phi.\underline{\nabla}|\underline{M}|^2 c_\infty^2 \qquad (d)$$

$$-\frac{(\gamma-1)}{2} c_\infty\underline{M}.\underline{\nabla}(|\underline{M}|^2)\left[\phi_t + c_\infty\underline{M}.\underline{\nabla}\phi\right] \Big/ \left[1 - \frac{(\gamma-1)}{2}(|\underline{M}|^2 - |\underline{M}_\infty|^2)\right] \qquad (e)$$

$$= 0 \qquad (2.5.9)$$

In order to compare the relative magnitudes of the terms in (2.5.9), the typical magnitudes of the individual quantities are required.

For the mean flow a characteristic lengthscale, L_M, is defined. The lengthscale L_M is typically taken as the geometric lengthscale of the reflecting body. For the acoustic disturbance both a characteristic lengthscale, L_A, and a corresponding characteristic time scale, T, need to be defined.

The characteristic timescale is defined by the relation

$$T = \frac{L_A}{c_\infty}$$

The characteristic lengthscale, L_A, of the acoustic disturbance is typically defined to be the characteristic wavelength, λ, of the disturbance, although it will be shown later that in some cases this may be misleading.

A typical reference value of ϕ will be denoted by Φ. With these characteristic values it is now possible to deduce the magnitudes of the terms in equation (2.5.9).

The groups (a), (b), (c), (d) of (2.5.9) are of order

$$\left[\frac{\Phi}{T^2}\right], \quad \left[\frac{\Phi}{T^2}\right]M_\infty, \quad \left[\frac{\Phi}{T^2}\right]M_\infty^2, \quad \left[\frac{\Phi}{T^2}\right]M_\infty^2 \frac{L_A}{L_M}$$

respectively, and group (e) contains two terms of orders

$$\left[\frac{\Phi}{T^2}\right]M_\infty^3 \frac{L_A}{L_M} \quad \text{and} \quad \left[\frac{\Phi}{T^2}\right]M_\infty^4 \frac{L_A}{L_M}$$

The first three terms given in groups (a) and (b) are obviously much larger than the remaining terms provided $M_\infty^2 << M_\infty$ and $M_\infty^2 \frac{L_A}{L_M} << M_\infty$.

The truncated equation containing only the terms of (a) and (b) is therefore valid only if both conditions are satisfied. That is, provided

(i) M_∞ is small

and

(ii) $M_\infty \frac{L_A}{L_M}$ is small. (2.5.10)

The first of the above conditions is simply a requirement that the Mach number be small. The second condition, however, requires in general that the characteristic lengthscale, L_M, of the mean flow is of the same order as or larger than the characteristic length scale of the disturbance.

If the characteristic lengthscale, L_A, is given by the characteristic wavelength, λ, of the acoustic disturbance then the second condition will clearly be satisfied in the high frequency (short wavelength) limit. It may not, however, be satisfied for low frequency (long wavelength) disturbances.

From this it appears that the validity of the low Mach number approximation is restricted to a high frequency limit and/or a large geometric lengthscale.

Note that the above conditions for the validity of the low Mach number approximation depend on the magnitude of the lengthscale, L_A. The geometric lengthscale of a typical problem is usually intuitively obvious but the interpretation of a characteristic lengthscale for the acoustic disturbance is not so obvious, particularly in the low frequency (long wavelength) limit.

Consider the extreme case of an acoustically 'compact' reflecting body. The reflected wavelength will be large compared with the geometric dimensions of the body and the reflected waveform will not be totally dissimilar from that of an incident wave. So in this case the question arises whether the characteristic lengthscale of the disturbance should be taken as the wavelength of the disturbance or as a lengthscale representative of the change in waveform undergone by the reflected wave. This latter lengthscale for the 'compact' situation would be a great deal smaller than the wavelength.

Note that for an intermediate wavelength the interpretation will become more complex. Therefore the application of a low Mach number approximation to any problem must also involve the careful consideration of the characteristic lengthscales.

Within the context of most aeroacoustic problems the low Mach number approximation is readily applicable since the characteristic lengthscales are generally small compared with geometrical lengthscales.

Under conditions that make the low Mach number approximation valid equation (2.5.9) may be written in the simplified form

$$c_\infty^2 \nabla^2 \phi - \phi_{tt} - 2c_\infty \underline{M}.\underline{\nabla}\phi_t = 0 \qquad (2.5.11)$$

Note that the linearized boundary condition equation (2.4.1) remains unaltered through the application of a low Mach number approximation. So the condition (2.4.1) can be applied as the appropriate boundary condition for the simplified equation (2.5.11).

6. THE TRANSFORMED PROBLEM

The application of the low Mach number approximation, under proper circumstances, produces the simplified equation

$$c_\infty^2 \nabla^2 \phi - \phi_{tt} - 2c_\infty \underline{M}.\nabla\phi_t = 0 \qquad (2.6.1)$$

and the unaltered boundary condition

$$\underline{\nabla}\phi.\hat{\underline{n}} = \left(\frac{\partial}{\partial t} + \underline{U}.\underline{\nabla}\right)\frac{n}{|\underline{\nabla}\alpha|} - \left(\frac{n}{|\underline{\nabla}\alpha|}\right)\hat{\underline{n}}.\left[(\hat{\underline{n}}.\underline{\nabla})\underline{U}\right] \qquad (2.6.2)$$

The simplified equation (2.6.1) represents the governing equation for the acoustic velocity potential in a steady, isentropic, potential flow at low Mach number applied within a region where the low Mach number approximation is valid.

The purpose of this section is to describe a transformation in time which reduces equation (2.6.1) to an ordinary wave equation. This is the same transformation that is given by Taylor [7],[26].

The application of this transformation effectively converts the problem of acoustic propagation within a mean flow to an analogous no-flow problem. In the transformed space the ordinary wave equation is applicable and it is known that a unique solution to this external radiation problem always exists (see Appendix (D)). There are also a large number of techniques that can be employed to solve this problem, and some of these will be discussed in the next chapter.

The temporal transformation proposed by Taylor is now derived for the purpose of clarifying the assumptions that are necessary for its accurate implementation.

The physical problem involves the presence of an isentropic, irrotational, mean flow over an arbitrary body. The mean flow being generated by an adverse uniform flow at infinity. Define c_∞, U_∞ and M_∞ as the sound speed, flow speed and Mach number respectively at infinity.

Note that since the mean flow is adverse at infinity the quantities U_∞ and M_∞ are considered constant.

The total velocity potential is split into a true acoustic potential plus a potential representative of the steady flow. Thus,

$$\underline{\nabla}\overset{*}{\phi} = \nabla\phi + \underline{U} \tag{2.6.3}$$

ϕ is the true acoustical potential and $\underline{U}$ is the local mean flow velocity.

Now define a velocity potential, $\hat{\phi}$, such that $\hat{\phi}$ is the steady state velocity potential divided by the flow speed at infinity

i.e. $$\hat{\phi} = \frac{\overline{\phi}}{U_\infty} \quad , \quad \underline{U} = \underline{\nabla}\overline{\phi} \tag{2.6.4}$$

hence $$\underline{\nabla}\hat{\phi} = \frac{\underline{U}}{U_\infty} \quad \text{and} \quad \underline{M} = M_\infty \underline{\nabla}\hat{\phi} \tag{2.6.5}$$

$\hat{\phi}$ also has the property:-

$$\hat{\phi} \sim - x \qquad \text{as } x \to \infty \tag{2.6.6}$$

This condition ensures that the flow tends to an adverse mean flow, of Mach number M_∞, at infinity. Note the negative sign in (2.6.6) is just a convention representing the direction of the mean flow.

Taylor's transformation is now introduced. The independent variables x, y, z and t are replaced by X, Y, Z and T where

$$(X,Y,Z,T) = (x,y,z,t + \frac{M_\infty}{c_\infty}\hat{\phi}) \tag{2.6.7}$$

and $$\phi(X,Y,Z,T) = \phi(x,y,z,t) \tag{2.6.8}$$

That is, ϕ, the acoustic velocity potential in the transformed space, is identical to the acoustic potential in the original space.

Before substituting these transformed-space variables into equation (2.6.1), the derivatives with respect to these variables are calculated.

Using $(X,Y,Z) = (x,y,z)$ and $T = t + \frac{M_\infty}{c_\infty}\hat{\phi}$

so $$\frac{\partial}{\partial t} = \frac{\partial T}{\partial t} \cdot \frac{\partial}{\partial T} \qquad \text{and} \qquad \frac{\partial}{\partial x} = \frac{\partial X}{\partial x}\frac{\partial}{\partial X} + \frac{\partial T}{\partial x}\frac{\partial}{\partial T}$$

hence $$\underline{\nabla} = (\underline{\nabla}_X + M_\infty \underline{\nabla}\hat{\phi} \frac{\partial}{c_\infty \partial T}) = (\underline{\nabla}_X + \frac{\underline{M}}{c_\infty} \frac{\partial}{\partial T}) \qquad (2.6.9)$$

and so

$$\nabla^2 = \underline{\nabla}.\underline{\nabla} = \underline{\nabla}_X^2 + \frac{2}{c_\infty} \underline{M}.\underline{\nabla}_X(\frac{\partial}{\partial T}) + \frac{1}{c_\infty}(\underline{\nabla}_X.\underline{M})\frac{\partial}{\partial T} + \frac{1}{c_\infty^2} |\underline{M}|^2 \frac{\partial^2}{\partial T^2} \qquad (2.6.10)$$

Thus equation (2.6.1), rewritten in terms of X,Y,Z and T, is:

$$c_\infty^2 \underline{\nabla}_X^2\phi - \phi_{TT} + c_\infty \underline{\nabla}_X.\underline{M}\phi_T - |\underline{M}|^2 \phi_{TT} = 0 \qquad (2.6.11)$$

The magnitudes of the four terms in equation (2.6.11) are now estimated in terms of the same length and time scales defined in the preceding section. (Noting that the time scale T is not related to the variable, T, of the above transformation).

The orders of the four terms in (2.6.11) are:

$$\left[\frac{\Phi}{T^2}\right], \quad \left[\frac{\Phi}{T^2}\right], \quad \left[\frac{\Phi}{T^2}\right] M_\infty^3 \frac{L_A}{L_M} \quad \text{and} \quad \left[\frac{\Phi}{T^2}\right] M_\infty^2$$

respectively. So if both M_∞ is small and $M_\infty^2 \frac{L_A}{L_M}$ is small the last two terms may be neglected. This is consistent with the order of approximation already established in the derivation of equation (2.6.1) above. Discarding the last two terms of equation (2.6.11) will yield an approximate transformed equation:-

$$c_\infty^2 \underline{\nabla}_X^2\phi - \phi_{TT} = 0 \qquad (2.6.12)$$

It must be noted again that an approximation of this type should be applied with caution. The validity of the approximation depending on the relative magnitudes of the lengthscales associated with the particular problem. As before, if a typical aeroacoustic problem is considered, where in general $\frac{L_A}{L_M} << 1$ then the approximate transformed equation (2.6.12) can readily be applied.

The derivation of Taylor's transformation requires the existence of a steady potential $\hat{\phi}$, which in turn requires that the body surface be stationary. This apparent discrepancy does not necessarily restrict Taylor's transformation to non-vibrating bodies. This is discussed below.

The boundary condition appropriate to a vibrating impermeable surface is that the total velocity component of the fluid and that of a neighbouring point on the surface in the direction normal to the surface are equal. Starting from this assumption both Myer[38] and Taylor[7] have derived the same boundary condition in terms of the acoustic velocity potential at the body surface. Their results imply that the effect of an acoustic vibration can be represented by a certain volume flow per unit area across some convenient stationary surface. The form of the boundary condition is:

$$\underline{\nabla}\phi.\hat{\underline{n}} = v(x,y,z,t) \qquad \text{on the surface } S_o$$

ϕ is the acoustic velocity potential, $\hat{\underline{n}}$ is an outward unit normal at the surface and v is the volume flow per unit area across the stationary surface S_o. This statement of the boundary condition, as shown by Myer, can only be obtained when the body is vibrating acoustically.

Therefore in the case of an acoustic disturbance the vibrating body surface can be assumed stationary (at some mean position) and the application of Taylor's transformation will be valid.

Having shown the validity of the transformation, it must now be applied to the boundary condition (2.4.1).

It can be seen that the effect of the transformation on (2.4.1) will be to replace the term $\underline{\nabla}\phi.\hat{\underline{n}}$ on the left by $\underline{\nabla}_X\phi.\hat{\underline{n}}$ and that the right hand side must be regarded as a function of curvilinear coordinates, and a time T of the transformed space.

It has now been shown that by first transforming the approximate acoustic equation (2.6.1) and then applying a valid low Mach number approximation to the transformed equation, an ordinary wave equation will result in the transformed-space, i.e. equation (2.6.12).

The wave equation along with a transformed boundary condition are used to obtain a unique solution of the external domain within the transformed space. The methods that are used to try and obtain this solution are now discussed.

III THE SOLUTION METHOD

Having reduced the acoustical field equation, applicable within a mean flow, to the simple wave equation of a no-flow problem, consideration will now be given to solving this simple wave equation.

1. THE HELMHOLTZ EQUATION AND NEUMANN BOUNDARY CONDITION

This section reduces the problem to that of solving the spatial Helmholtz equation with a Neumann boundary condition.

It is now assumed that the acoustical disturbance is a superposition of time harmonic components. By specifying the time dependence, the problem is reduced to finding the steady spatial portion of the solution.

In the original space the solution is assumed to have the form:

$$\phi(\underline{x},t) = \Phi(\underline{x})e^{i\omega t} \tag{3.1.1}$$

where $\underline{x} = (x,y,z)$ and ω is the harmonic frequency. In the transformed space this becomes:

$$\phi(\underline{X},T) = \Phi(\underline{X})e^{i\omega\left[T - \frac{M_\infty}{C_\infty}\hat{\phi}\right]} \tag{3.1.2}$$

where $\underline{X} = (X,Y,Z)$.

That is;

$$\phi(\underline{X},T) = \Psi(\underline{X})e^{i\omega T} \tag{3.1.3}$$

where $\Psi(\underline{X}) = \Phi(\underline{X})e^{-ikM_\infty\hat{\phi}}$ and $k = \frac{\omega}{C_\infty}$ (3.1.4)

In the transformed space a solution is now sought in the form given by (3.1.3). Using this formulation equation (2.6.12) of the previous chapter is reduced to the classical Helmholtz equation:

$$\nabla_X^2 \Psi + k^2\Psi = 0 \tag{3.1.5}$$

For the original problem the boundary condition on S can be written:

$$\underline{\nabla}\phi.\underline{\hat{n}} = f\, e^{i\omega t} \qquad \text{on S} \tag{3.1.6}$$

where f is a known function.

Thus the steady boundary condition in the transformed problem will be:

$$\underline{\nabla}_x \Psi . \hat{\underline{n}} = F \qquad \text{on } S \qquad (3.1.7)$$

where $F = fe^{-ikM_\infty \hat{\phi}}$.

The problem expressed by (3.1.5) and (3.1.7) represents a classical Neumann problem for the three dimensional Helmholtz equation in the exterior domain D_+.

It is useful at this stage to introduce the free-space Green's function G(P,Q). The Green's function, G(P,Q) is a fundamental solution of the inhomogeneous Helmholtz equation:

$$(\nabla^2 + k^2)G(P,Q) + \delta(P - Q) = 0 \qquad (3.1.8)$$

where δ is the Dirac delta function and G(P,Q) represents the sound field at a point P due to a point source located at Q. In three dimensions it has the form:

$$G(P,Q) = \frac{e^{-ikr}}{4\pi r} \qquad (3.1.9)$$

where r is the distance between points P and Q.

Before discussing the methods available for solving the above problem, it must be stated that if the acoustic field is entirely radiative at infinity then this radiation problem has at most one solution in D_+.

This uniqueness condition is now stated formally in a theorem: (see Smirnov[28] Vol. 4, Art. 228).

THEOREM 1

If a function Ψ satisfies outside a closed surface S both the Helmholtz equation (3.1.5), the Sommerfeld radiation principle at infinity and a homogeneous boundary condition on the surface then Ψ is identically zero in D_+.

The Sommerfeld radiation principle is a mathematical formulation of the radiation condition previously mentioned. In three dimensional space it can be written:

$$\Psi = O(R^{-1}) \quad , \quad \frac{\partial \Psi}{\partial R} + ik\Psi = o(R^{-1}) \quad \text{as } R \to \infty \qquad (3.1.10)$$

where R is the radius of a large sphere enclosing S with centre in D_+.

A proof of Theorem 1 and the Sommerfeld radiation principle (3.1.10) is given in Appendices (D) and (B) respectively.

2. THE BOUNDARY INTEGRAL METHOD

This section considers the possible solution methods. The boundary integral (B.I.) method is chosen and its application to the present problem is discussed.

All the solution methods mentioned within Chapter One can be considered for this no-flow problem. However, the arbitrary geometry of the vibrating body is invariant under Taylor's transformation so that any analytic separation of variables technique is still unfavourable. The computational disadvantages of the finite element (FE) and finite difference (FD) methods within an infinite domain still exist in the absence of a mean flow. Although for this special case of zero mean flow the application of B.I. methods is now valid.

The essential feature of B.I. methods is that the governing differential equation of the problem under consideration is transformed into an integral equation on the boundary. So in principle, B.I. formulations appear attractive as they:-

(i) eliminate the need to consider the infinite domains characteristic of FE and FD methods;
(ii) reduce the dimensionality of the problem by one;
(iii) are readily applicable to arbitrary geometries and boundary conditions.

From these considerations, the B.I. formulation will be the chosen method of solution for the Helmholtz equation with a Neumann boundary condition.

There are essentially two distinct derivations of the B.I. equations applicable to this radiation problem. These two formulations are discussed below.

2A THE SOURCE LAYER FORMULATION

This B.I. formulation for the Helmholtz equation is in close analogy with the Potential theory methods for solution of Laplace's equation. This is due to the fact that the singularity in the Green's function for Helmholtz' equation is of the same character as that displayed by the Green's function ($1/4\pi r$) of Potential theory.

The Source layer formulation is based on the initial assumption that the acoustic potential in the field surrounding the radiating body has been produced by a layer of either monopole or dipole sources of unknown density distribution on the surface.

If $\Psi(P)$ is the unknown potential at an exterior point, P, then for a single-layer potential:

$$\Psi(P) = \int_S \sigma(Q)G(P,Q)dS_q \qquad P\varepsilon D_+ , \quad Q\varepsilon S \tag{3.2.1}$$

or a double-layer potential

$$\Psi(P) = \int_S \mu(Q) \frac{\partial}{\partial n_q} G(P,Q)dS_q \qquad P\varepsilon D_+ , \quad Q\varepsilon S \tag{3.2.2}$$

where $\frac{\partial}{\partial n_q}$ denotes differentiation along the outward normal at Q.

G(P,Q) is the free-space Green's function and in analogy to potential theory σ and μ are termed the densities of the monopole and dipole source distributions respectively.

Equations (3.2.1) and (3.2.2) both satisfy Helmholtz' equation and the radiation condition for arbitrary density functions. In order to solve for the potential at the exterior point P the surface source density distribution needs to be determined. The surface, S, will be assumed to satisfy the Lyapunov smoothness conditions (see Pogorzelski [42], p.231 and Appendix (E)).

In complete analogy to Potential theory the following results apply: (see Kellogg[43] pp160-172; Mikhlin [44] ; Smirnov[28] §193,§195 and§231).

THEOREM 2

If the density σ of the monopole distribution is continuous at η on the surface then

(i) the single-layer potential given by equation (3.2.1) is continuous for all $P\varepsilon \underline{D} \cup S \cup D_+$ *i.e. continuous across the surface* S.

(ii) the normal derivative of the single layer potential $\Psi(P)$ *approaches limits as* P *approaches* η *along the normal to* S *at* η *from either side. The limiting value of* $\Psi(P)$ *as* P *approaches* S *from the outside is:*

$$\lim_{P\to\eta_+} \frac{\partial\Psi}{\partial n}(P) \equiv \frac{\partial\Psi(\eta)}{\partial n_+} = -\tfrac{1}{2}\sigma(\eta) + \int_S \sigma(\xi)\frac{\partial}{\partial n_\eta} G(\eta,\xi)dS_\xi \tag{3.2.3}$$

and the limit from the inside is

$$\lim_{P\to\eta_-} \frac{\partial\Psi(P)}{\partial n} \equiv \frac{\partial\Psi(\eta)}{\partial n_-} = \tfrac{1}{2}\sigma(\eta) + \int_S \sigma(\xi)\frac{\partial}{\partial n_\eta} G(\eta,\xi)dS_\xi \qquad (3.2.4)$$

The normal derivatives are therefore discontinuous across the surface.

THEOREM 3

If the density μ *of the dipole distribution is continuous at* η *on* S *then*

(i) the normal derivative of the double layer potential, $\Psi(P)$ *in (3.2.2), is continuous for all* $P\in D_-\cup S\cup D_+$; *i.e. the normal derivative is continuous across* S.

(ii) the double-layer potential, $\Psi(P)$, *approaches limits as* P *approaches* η *along the normal to* S *at* η *from either side.*

These limits are:

$$\lim_{P\to\eta_+} \Psi(P) \equiv \Psi(\eta)_+ = \tfrac{1}{2}\mu(\eta) + \int_S \mu(\xi)\frac{\partial}{\partial n_\xi} G(\eta,\xi)dS_\xi \qquad (3.2.5)$$

$$\lim_{P\to\eta_-} \Psi(P) \equiv \Psi(\eta)_- = -\tfrac{1}{2}\mu(\eta) + \int_S \mu(\xi)\frac{\partial}{\partial n_\xi} G(\eta,\xi)dS_\xi \qquad (3.2.6)$$

so that the double layer potential is discontinuous across S.

The above discontinuities or 'jump' relations at the surface S arise from the singularity in the normal derivative of the Green's function.

With these results it is now possible to determine the density distribution. In the present problem the potential Ψ satisfies a Neumann boundary condition on S; that is:

$$\frac{\partial\Psi}{\partial n} = F \qquad \text{on S} \qquad (3.2.7)$$

where F is known.

Applying theorem 2 and the Neumann boundary conditions, equation (3.2.3) can be solved for the density distribution σ on the surface. That is:

$$\frac{\partial\Psi(\eta)}{\partial n_+} = F = -\tfrac{1}{2}\sigma(\eta) + \int_S \sigma(\xi)\frac{\partial}{\partial n_\eta} G(\eta,\xi)dS_\xi \qquad (3.2.8)$$

The equations (3.2.1) and (3.2.8) represent the two phase solution procedure characteristic of B.I. methods. This method of solution of Helmholtz' equation is typically called the simple source method due to the initial assumption that the boundary surface is represented by an unknown distribution of monopole sources.

2B THE HELMHOLTZ INTEGRAL FORMULATION

The Helmholtz integral formulation, unlike the Source layer formulation, does not require an initial assumption about the form of the solution.

This formulation expresses the acoustic potential explicitly at any field point external to the boundary as an integral in terms of the surface velocity potential and its normal derivative. This normal derivative of the velocity potential on the surface is given by the Neumann boundary condition (3.2.7), hence the problem is reduced to finding the velocity potential on the surface. This represents the two phase method of solution for the Helmholtz integral formulation.

This formulation is derived below:

Define a domain D_+ to be bounded internally by the surface S and externally by a large sphere S_R of radius R. Let Ψ be a solution of:

$$(\nabla^2 + k^2)\Psi = 0 \tag{3.2.9}$$

whose first and second order partial derivatives are continuous outside and on the closed surface S. The function Ψ is defined to satisfy the Sommerfeld radiation conditions. Let G be the free-space Green's function satisfying:

$$(\nabla^2 + k^2)G + \delta(P) = 0 \tag{3.2.10}$$

In this case G represents the field at some point in D_+ due to a point source located at P.

Using a vector identity, $G(\nabla^2\Psi + k^2\Psi)$ is written as:

$$\begin{aligned} G(\nabla^2\Psi + k^2\Psi) &= \underline{\nabla}.(G\underline{\nabla}\Psi) - \underline{\nabla}G.\underline{\nabla}\Psi + k^2G\Psi \\ &= \underline{\nabla}.(G\underline{\nabla}\Psi - \Psi\underline{\nabla}G) + \Psi\nabla^2G + k^2G\Psi \end{aligned} \tag{3.2.11}$$

Integrating (3.2.11) over the domain D_+:

$$\int_{D_+} G(\nabla^2\Psi + k^2\Psi)dD_+ = \int_{D_+} \underline{\nabla}.(G\underline{\nabla}\Psi - \Psi\underline{\nabla}G)dD_+ + \int_{D_+} \Psi(\nabla^2G + k^2G)dD_+ \tag{3.2.12}$$

and using Green's theorem gives:

$$\begin{aligned} \int_{D_+} G(\nabla^2\Psi + k^2\Psi)dD_+ - \int_{D_+} \Psi(\nabla^2G + k^2G)dD_+ &= \int_S (G\underline{\nabla}\Psi - \Psi\underline{\nabla}G).\hat{\underline{n}}_i dS \\ &\quad + \int_{S_R} (G\underline{\nabla}\Psi - \Psi\underline{\nabla}G).\hat{\underline{n}}_R\, dS_R \end{aligned} \tag{3.2.13}$$

where the direction of the normal $\hat{n}_i$ is pointing out of D_+ into D_- and $\hat{n}_R$ is pointing out of D_+ towards infinity. The integral over the surface of the large sphere will vanish as $R \to \infty$. This results from the requirement that the Sommerfeld radiation condition be satisfied. The proof of this is given in Appendix (B).

Denote $\hat{n}_0$ as the normal opposite to $\hat{n}_i$, outward from S into D_+, hence:

$$\int_{D_+} \left[G(\nabla^2\Psi + k^2\Psi) - \Psi(\nabla^2 G + k^2 G) \right] dD_+ = \int_S (\Psi \underline{\nabla} G.\hat{n}_0 - G\underline{\nabla}\Psi.\hat{n}_0) dS \qquad (3.2.14)$$

If the singularity point P lies outside the domain of integration; that is if $P \varepsilon D_-$ then clearly (3.2.14) becomes:

$$\int_S (\Psi \underline{\nabla} G.\hat{n}_0 - G\underline{\nabla}\Psi.\hat{n}_0) dS = 0 \quad , \qquad P \varepsilon D_- \qquad (3.2.15)$$

If the point P lies within D_+, then G will become singular in the neighbourhood of P. To remove this singularity from the original integral (3.2.12) the point P is first surrounded by a small sphere of surface area σ and radius ε (see Fig. 2). Now equation (3.2.12) can be written as:

$$\int_{D'_+} \left[G(\nabla^2\Psi + k^2\Psi) - \Psi(\nabla^2 G + k^2 G) \right] dD'_+ = \int_{D'_+} \underline{\nabla}.(G\underline{\nabla}\Psi - \Psi\underline{\nabla}G) dD_+ \qquad (3.2.16)$$

where the domain D'_+ is just D_+ minus the small sphere. Since there exists no singularity within D'_+, the integral on the left of (3.2.16) will vanish. Therefore using Green's theorem equation (3.2.16) becomes:

$$\int_S (G\underline{\nabla}\Psi - \Psi\underline{\nabla}G).\hat{n}_i dS + \int_\sigma (G\underline{\nabla}\Psi - \Psi\underline{\nabla}G).\hat{n}_\nu \, d\sigma = 0 \qquad (3.2.17)$$

since the integral over the large sphere S_R will vanish as before. The normals $\hat{n}_i$ and $\hat{n}_\nu$ point out of D'_+ and into S and σ respectively (see Fig. 2). Equation (3.2.17) can be written as:

$$\int_S (\Psi \underline{\nabla} G.\hat{n}_0 - G\underline{\nabla}\Psi.\hat{n}_0) dS = \int_\sigma (G\underline{\nabla}\Psi.\hat{n}_\varepsilon - \Psi\underline{\nabla}G.\hat{n}_\varepsilon) d\sigma \qquad (3.2.18)$$

where the normals $\hat{n}_0$ and $\hat{n}_\varepsilon$ point into D'_+ from S and σ respectively.

Before letting $\varepsilon \to 0$ in equation (3.2.18) consider the form of the free-space Green's function G.

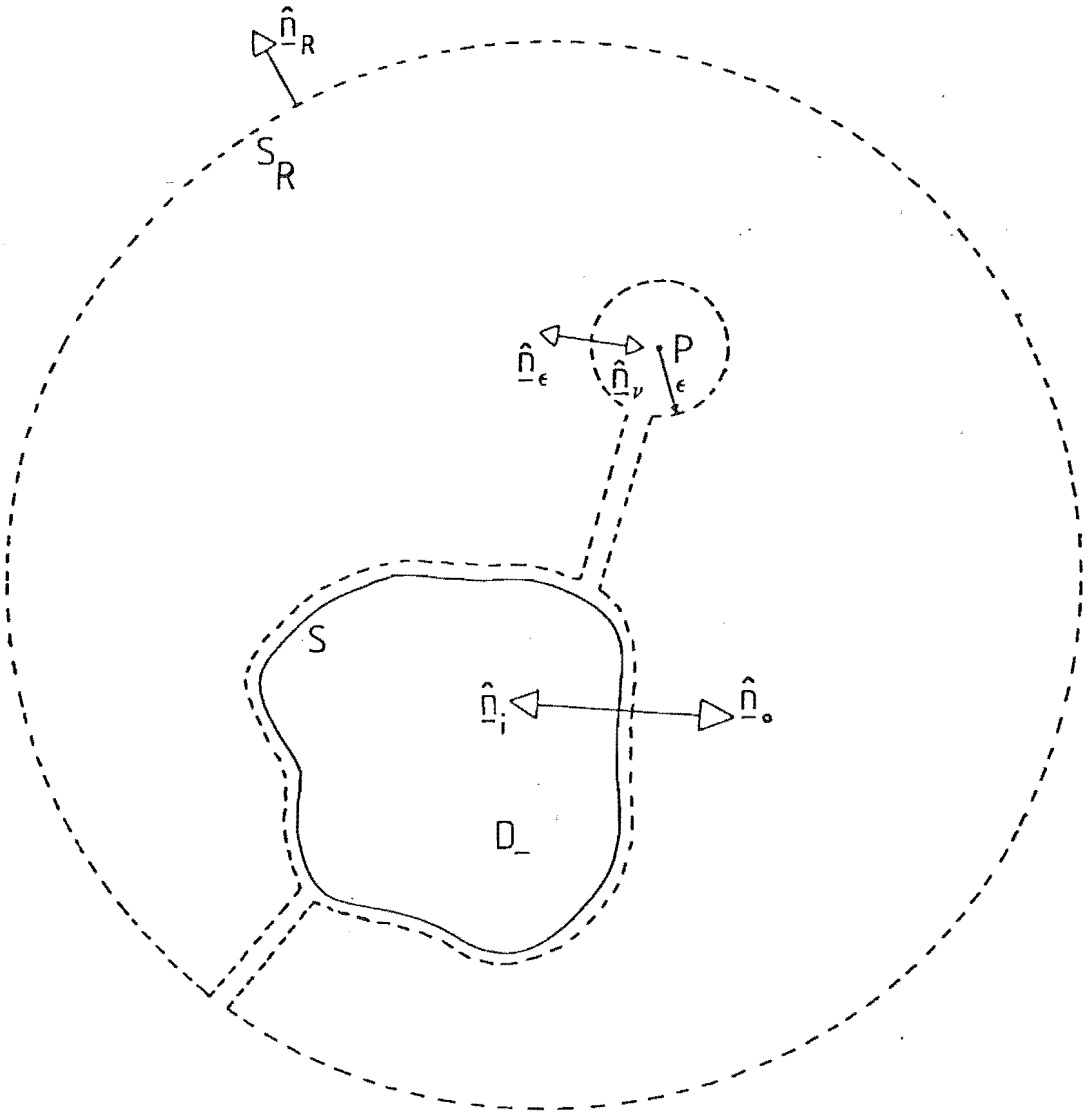

Figure 2. The integration surface for the point P

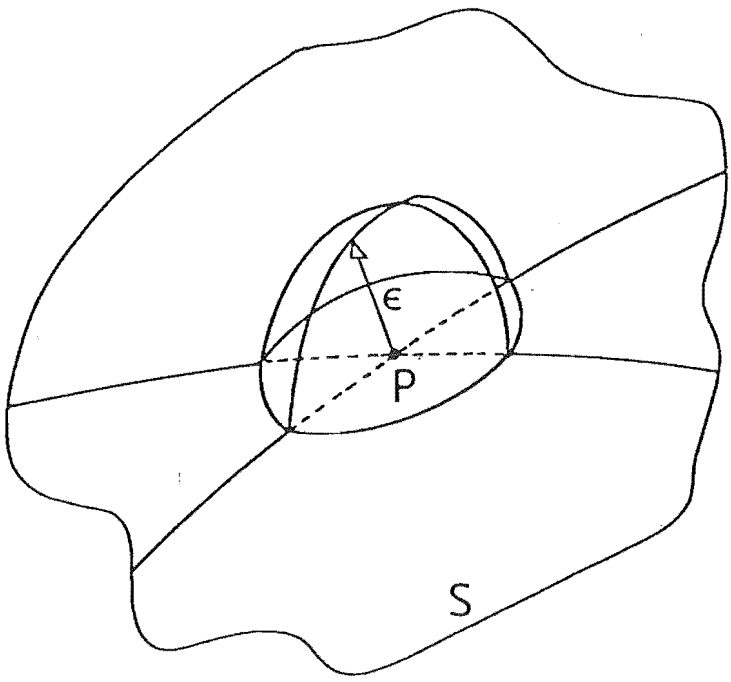

Figure 3. Hemispherical approximation

In this case G is written

$$G = \frac{e^{-ikr}}{4\pi r} \quad , \quad r = |\underline{r} - \underline{r}_p| \tag{3.2.19}$$

Substituting (3.2.19) into the equation (3.2.18), the limit, as $\varepsilon \to 0$, of the right hand side is:

$$\lim_{\varepsilon \to 0} \tfrac{1}{4\pi} \int_{\sigma} \left\{ \frac{e^{-ik\varepsilon}}{\varepsilon} \frac{\partial \Psi}{\partial \varepsilon} + \Psi \frac{e^{-ik\varepsilon}}{\varepsilon} (ik + \frac{1}{\varepsilon}) \right\} d\sigma \tag{3.2.20}$$

since $\hat{\underline{n}}_{\varepsilon}$ and the small radius ε have identical directions. Now Ψ and $\frac{\partial \Psi}{\partial \varepsilon}$ are continuous at P and an element of surface on σ is given as:

$$d\sigma = \varepsilon^2 \sin\theta \, d\theta \, d\phi \tag{3.2.21}$$

where θ and ϕ are spherical surface coordinates on σ; so that equation (3.2.20) is essentially;

$$\lim_{\varepsilon \to 0} \tfrac{1}{4\pi} \int_0^{2\pi} \int_0^{\pi} \Psi \sin\theta \, d\theta \, d\phi = \Psi(P) \tag{3.2.22}$$

Hence for $P \epsilon D_+$, equation (3.2.18) is:

$$\int_S (\Psi \underline{\nabla} G . \hat{\underline{n}}_0 - G \underline{\nabla} \Psi . \hat{\underline{n}}_0) dS = \Psi(P) \quad , \quad P \epsilon D_+ \tag{3.2.23}$$

Consider now the case when the source point P is on the surface S. In this case the surface integral equation is not as easily derived (see Pogorzelski [42] . The general concept of the proof is mentioned only.

A small sphere, centred at P is introduced again.

As the radius, ε, tends to zero that part of the sphere within D_+ will tend to a hemisphere (see Fig. 3). From this it might be expected that the right hand side of (3.2.18) would be one half the limit given in equation (3.2.20), i.e. $\frac{1}{2}\Psi(P)$.

When the surface S is sufficiently smooth, this is in fact the case. So for $P \epsilon S$, equation (3.2.18) can be written as:

$$\int_S (\Psi \underline{\nabla} G . \hat{\underline{n}}_0 - G \underline{\nabla} \Psi . \hat{\underline{n}}_0) dS = \tfrac{1}{2}\Psi(P) \quad , \quad P \epsilon S \tag{3.2.24}$$

The Helmholtz integral formulation can be expressed as one equation.

$$\int_S (\Psi(Q)\underline{\nabla}G(P,Q).\hat{\underline{n}}_q - G(P,Q)\underline{\nabla}\Psi(Q).\hat{\underline{n}}_q)dS_q = \begin{cases} \Psi(P) \text{ if } P\varepsilon D_+ \\ \tfrac{1}{2}\Psi(P) \text{ if } P\varepsilon S \\ 0 \text{ if } P\varepsilon D_- \end{cases} \qquad (3.2.25)$$

where Q is a point on the surface S and $\frac{\partial}{\partial n_q}$ denotes differentiation along the outward normal at Q.

Equation (3.2.25) can be used to solve for the acoustic velocity potential at an exterior field point $P\varepsilon D_+$, hence

$$\Psi(P) = \int_S \left[\Psi(Q) \frac{\partial G(P,Q)}{\partial n_q} - G(P,Q) \frac{\partial \Psi(Q)}{\partial n_q}\right] dS_q \; ; \; P\varepsilon D_+, \; Q\varepsilon S \qquad (3.2.26)$$

Consider the terms on the right of (3.2.26). $\frac{\partial \Psi(Q)}{\partial n_q}$ represents the boundary condition (3.2.7) on the surface and is already known, i.e. $\frac{\partial \Psi}{\partial n} = F$ on S. Therefore the problem is reduced to finding the distribution of the velocity potential $\Psi(Q)$ on the surface.

This second phase of solution can be solved by employing one of two distinct methods. It has become common to refer to these methods as 'the Surface Helmholtz integral method' and 'the Interior Helmholtz integral method'. These second phase solution methods are introduced below.

2B1 THE SURFACE HELMHOLTZ INTEGRAL METHOD

This method of solving for the surface potential employs the Helmholtz integral formulation with the source point P on the boundary S. So from equation (3.2.25)

$$\tfrac{1}{2}\Psi(P) = \int_S \left[\Psi(Q) \frac{\partial G(P,Q)}{\partial n_q} - G(P,Q) \frac{\partial \Psi(Q)}{\partial n_q}\right] dS_q \; ; \; P,Q\varepsilon S \qquad (3.2.27)$$

This integral equation is solved for Ψ on the surface.

2B2 THE INTERIOR HELMHOLTZ INTEGRAL METHOD

This method also uses the Helmholtz integral formulation; this time for the case of an interior source point, i.e. $P\varepsilon D_-$, hence

$$0 = \int_S \left[\Psi(Q) \frac{\partial G(P,Q)}{\partial n_q} - G(P,Q) \frac{\partial \Psi(Q)}{\partial n_q}\right] dS_q \; ; \; P\varepsilon D_- \; , \; Q\varepsilon S \qquad (3.2.28)$$

Both equations (3.2.27) and (3.2.28) can be used to determine the distribution of the velocity potential on the surface; once this is known, equation (3.2.26) can be solved explicitly for the potential at some exterior field point.

In summary, the solution procedure for the Helmholtz equation can be described by essentially three methods. That is;

(a) the Simple source method from the Source-layer formulation;

(b) the Surface Helmholtz integral method from the Helmholtz integral formulation;

(c) the Interior Helmholtz integral method also from the Helmholtz integral formulation.

Now it is well known that at particular distinct frequencies the above methods will not yield a reliable solution. A discussion of why and where these methods break down is presented within the next section.

3. PROBLEMS WITH THE SOLUTION METHODS

This section introduces the general theory of Fredholm integral equations in order to explain the inconsistencies of the three classical solution procedures, i.e.

(a) the simple source method
(b) the surface Helmholtz integral method
(c) the interior Helmholtz integral method.

In the application of B.I. methods to the problem of acoustic radiation, the very process of reduction from the exterior domain D_+ to the boundary S may give rise to difficulties of non-uniqueness which are not inherent in the physical problem.

At a particular non-trivial set of eigenfrequencies, characteristic of the vibrating surface S, the simple source solution will in general not exist, the surface Helmholtz integral solution will suffer non-uniqueness and the interior Helmholtz integral solution will be at least unreliable.

To understand this more fully some classical theorems for Fredholm integral equations of the second kind are presented. The results given below are based on those proved by Smirnov[28] and Smithies[45].

Fredholm integral equations of the second kind are characterised by nonvariable integration limits and the occurrence of the unknown function both under the sign of integration and elsewhere in the equation.

The general inhomogeneous equation of the second kind is defined as:

$$x(\eta) - \lambda \int_S K(\eta,\xi)x(\xi)dS_\xi = f(\eta) \qquad (3.3.1)$$

and the associated homogeneous equation as:

$$x_o(\eta) - \lambda \int_S K(\eta,\xi)x_o(\xi)dS_\xi = 0 \qquad (3.3.2)$$

The adjoint equation for (3.3.1) is:

$$y(\eta) - \lambda^* \int_S \left[K(\xi,\eta)\right]^* y(\xi)dS_\xi = g(\eta) \qquad (3.3.3)$$

and the adjoint homogeneous equation is:

$$y_o(\eta) - \lambda^* \int_S \left[K(\xi,\eta)\right]^* y_o(\xi)dS_\xi = 0 \qquad (3.3.4)$$

where x and y are the unknown functions, the function K is called the kernel of the integral equation and the asterisk above is used to denote the complex conjugate.

The homogeneous equation (3.3.2) has an obvious solution, $x_o(\eta) = 0$, this is referred to as the trivial solution. The values $\lambda = \lambda_o$ for which (3.3.2) has a non-trivial solution are called the eigenvalues of the kernel $K(\eta,\xi)$; while every non-trivial solution of

$$x_o(\eta) = \lambda_o \int_S K(\eta,\xi)x_o(\xi)dS_\xi \qquad (3.3.5)$$

is called an eigenfunction corresponding to the eigenvalue $\lambda = \lambda_o$. When the homogeneous equations have only trivial solutions the parameter λ is called a regular value of the kernel $K(\eta,\xi)$. Four classical Fredholm theorems are now stated.

THEOREM 4

If λ is a regular value of $K(\eta,\xi)$ then λ^* is a regular value of $\left[K(\xi,\eta)\right]^*$.

THEOREM 5

If λ is a regular value of $K(\eta,\xi)$ then both homogeneous equations (3.3.2) and (3.3.4) will have only trivial solutions and the inhomogeneous equations (3.3.1) and (3.3.3) will have unique solutions for any continuous functions $f(\eta)$ and $g(\eta)$.

THEOREM 6

If λ *is an eigenvalue of* $K(\eta,\xi)$ *then* λ^* *is an eigenvalue of* $\left[K(\xi,\eta)\right]^*$ *and the homogeneous equations (3.3.2) and (3.3.4) will have non-trivial solutions.*

THEOREM 7

If λ *is an eigenvalue, the necessary and sufficient condition for the inhomogeneous equation (3.3.1) to be solvable is that the function* $f(\eta)$ *be orthogonal to every solution of the adjoint homogeneous equation, i.e. if*

$$\int_S \left[y_o(\xi)\right]^* f(\xi) dS_\xi = 0 \qquad (3.3.6)$$

If this condition is satisfied then the inhomogeneous equation has an infinite set of solutions; since any multiple of $x_o(\xi)$ *can be added to a particular solution of equation (3.3.1).*

A proof of condition (3.3.6) as a necessary condition is shown in Appendix (F).

The three classical solution methods of the Helmholtz equation are now discussed with reference to the above theorems.

3A NON EXISTENCE AND THE SIMPLE SOURCE METHOD

Equation (3.2.8) of the simple source method can be written as:

$$-2\frac{\partial \Psi(\eta)}{\partial n_+} = \sigma(\eta) - 2\int_S \sigma(\xi)\frac{\partial}{\partial n_\eta} G(\eta,\xi) dS_\xi \; ; \quad \eta, \xi \in S \qquad (3.3.7)$$

and this equation is of the same form as equation (3.3.1), where

$$x(\eta) = \sigma(\eta) \; ; \quad f(\eta) = \frac{-2\partial \Psi(\eta)}{\partial n} \; ; \quad \lambda = +1 \text{ and}$$

$$K(\eta,\xi) = \frac{2\partial}{\partial n_\eta}\left[G(\eta,\xi)\right]$$

Since $K(\eta,\xi)$ is a function of wavenumber k, each k will have a set of eigenvalues for $K(\eta,\xi)$. Any k that includes $\lambda = +1$ in its set of eigenvalues is called an eigenwavenumber and is denoted by k_o.

Therefore by theorems (5) and (7) a unique solution of (3.3.7) exists unless $k = k_o$. For the eigenwavenumbers $k = k_o$ a solution will not exist unless the condition,

$$\int_S [\sigma_o(\xi)]^* \frac{\partial \Psi(\xi)}{\partial n} \, dS_\xi = 0 \qquad (3.3.8)$$

holds for all $\sigma_o(\xi)$ which satisfy the adjoint homogeneous equation,

$$0 = \sigma_o(\eta) - 2\int_S \sigma_o(\xi) \frac{\partial}{\partial n_\xi} [\, G(\xi,\eta)]^* \, dS \qquad (3.3.9)$$

In general, condition (3.3.8) will not be satisfied; and in the special cases where it is, the solution would not be unique.

Therefore at certain eigenwavenumbers the simple source solution will generally not exist, hence this equation cannot be relied upon to solve the Helmholtz equation. It must be noted that this general non-existence of solutions does not correspond to any physical situation. It is a result of the failure of equation (3.3.7) to accurately represent the solution on the surface at certain eigenwavenumbers.

3B NON-UNIQUENESS AND THE SURFACE HELMHOLTZ INTEGRAL METHOD

Equation (3.2.27) of the surface Helmholtz integral method can be written as:

$$\Psi(\eta) - 2\int_S \Psi(\xi) \frac{\partial G(\eta,\xi)}{\partial n_\xi} \, dS_\xi = 2\int_S G(\eta,\xi) \frac{\partial \Psi(\xi)}{\partial n_\xi} \, dS_\xi \qquad (3.3.10)$$

which is of the same form as (3.3.1) where

$$x(\eta) = \Psi(\eta), \quad f(\eta) = 2\int_S G(\eta,\xi) \frac{\partial \Psi(\xi)}{\partial n_\xi} \, dS_\xi, \quad \lambda = +1$$

and

$$K(\eta,\xi) = \frac{2\partial G(\eta,\xi)}{\partial n_\xi}$$

Similar to the simple source method, equation (3.3.10) will have a unique solution except at wavenumbers $k = k_o$. For these eigenwavenumbers no solution exists unless the orthogonality condition,

$$\int_S [\Psi_o(\xi)]^* \left\{ \int_S G(\xi,\mu) \frac{\partial \Psi(\mu)}{\partial n_\mu} \, dS_\mu \right\} dS_\xi = 0 \qquad (3.3.11)$$

holds for all $\Psi_o(\xi)$ that satisfy the adjoint homogeneous equation:-

$$\Psi_o(\eta) - 2\int_S \Psi_o(\xi) \frac{\partial}{\partial n_\eta} [\, G(\xi,\eta)]^* \, dS_\xi = 0 \qquad (3.3.12)$$

Now unlike the simple source method, condition (3.3.11) will always be satisfied (see Appendix (G) for proof). However the solution will still not be determined uniquely. Therefore at certain eigenwavenumbers the surface Helmholtz integral method will suffer non-uniqueness.

Before proceeding with the interior Helmholtz integral method it is convenient at this stage to look at the critical wavenumbers of these representations in more detail.

The above critical wavenumbers are the eigenwavenumbers of the standing waves that satisfy the Helmholtz equation throughout the interior domain D_- while vanishing on the boundary S. Therefore the eigenfrequencies corresponding to the eigenwavenumbers are the resonant frequencies of the interior Dirichlet problem (see Chertock[46] , Kleiman and Roach[47]).

Copley[31] demonstrates that the simple source and surface Helmholtz integral methods do break down at the eigenwavenumbers of the interior Dirichlet problem. It must be remembered that for a truly arbitrary body these internal eigenwavenumbers will not be known *a priori*. Now consider:-

3C UNRELIABILITY OF THE INTERIOR HELMHOLTZ INTEGRAL METHOD

In the formulation of this method, the position of the interior source point, P, is completely arbitrary. However when the interior source point lies on a nodal surface of the interior standing wave for the homogeneous Dirichlet problem the solution will not be unique. Incidentally the method will also break down if the interior point lies on a nodal surface corresponding to the interior standing wave for the homogeneous Neumann problem, (see Chertock[46]).

Therefore if the internal source point does not lie on any of the above mentioned nodal surfaces, then the solution of equation (3.2.28) for the surface velocity potential will be unique at all wavenumbers.

In summary, this method is comparatively 'better' than the previous two, since it is possible - with 'careful' positioning of the interior point - to obtain a unique solution at the critical wavenumbers.

However, as the wavenumber, k, increases the density of the critical eigenwavenumbers also increases ,[46], and hence the spacing between the nodal surfaces of the standing wave within S likewise decreases. So, for sufficiently high k, it becomes impractical to solve for the surface potential $\Psi(Q)$ by any of the above three methods.

The following sections involve formulations that were proposed in order to remove the unreliability of the above methods at internal eigenfrequencies.

4. TWO IMPROVED FORMULATIONS

This section introduces two B.I. formulations that were devised in order to eliminate the problems associated with the previous three integral methods. These methods are the CHIEF method devised by Schenk[24] and a formulation devised by Burton and Miller[33].

4A CHIEF

The Combined Helmholtz Integral Equation Formulation (CHIEF) was proposed by Schenk in order to overcome the non-uniqueness problems of the surface Helmholtz integral method at critical wavenumbers.

This formulation is based on the fact that, for any wavenumber k, only one of the solutions of the surface integral equation (3.2.27) can also satisfy the interior integral equation (3.2.28), (see Appendix (H)).

Therefore in Schenk's CHIEF method the interior integral equation (3.2.28) is used to supplement the surface equation (3.2.27) in order to remove the indeterminant part of the solution to equation (3.2.27).

4B THE BURTON AND MILLER FORMULATION (BMF)

This formulation proposed by Burton and Miller also involves the combination of two integral equation methods. The BMF method is based on the formation of a linear combination of the surface Helmholtz integral equation (3.2.27) and its normal derivative with respect to the field point P.

The surface Helmholtz integral equation is written as:

$$\tfrac{1}{2}\Psi(P) = \int_S \left[\Psi(Q) \frac{\partial G(P,Q)}{\partial n_q} - G(P,Q) \frac{\partial \Psi(Q)}{\partial n_q} \right] dS_q \qquad (3.4.1)$$

and its normal derivative with respect to P is:

$$\tfrac{1}{2}\frac{\partial \Psi(P)}{\partial n_p} = \int_S \left[\Psi(Q) \frac{\partial^2 G(P,Q)}{\partial n_p \, \partial n_q} - \frac{\partial G(P,Q)}{\partial n_p} \frac{\partial \Psi(Q)}{\partial n_q} \right] dS_q \qquad (3.4.2)$$

Taken by itself, equation (3.4.2) will suffer non-uniqueness at a particular set of resonant wavenumbers that correspond to the homogeneous interior Neumann problem.

Linearly combining (3.4.1) and (3.4.2) gives the Burton and Miller formulation:

$$\int_S \left[\Psi(Q)\frac{\partial G(P,Q)}{\partial n_q} - G(P,Q)\frac{\partial \Psi}{\partial n_q}\right] dS_q + \alpha \int_S \left[\Psi(Q)\frac{\partial^2 G(P,Q)}{\partial n_p \partial n_q} - \frac{\partial G(P,Q)}{\partial n_p}\frac{\partial \Psi(Q)}{\partial n_q}\right] dS_q$$

$$= \tfrac{1}{2}\left(\Psi(P) + \alpha \frac{\partial \Psi(P)}{\partial n_p}\right) \qquad (3.4.3)$$

where α is a complex coupling constant.

Equations (3.4.1) and (3.4.2) both have a set of eigenwavenumbers at which a unique solution cannot be obtained. However, it can be shown (see Appendix (I), Burton and Miller[33]) that the uniqueness of the solution for the combined integral equation (3.4.3) can be ensured by a suitable choice of the complex coupling constant α.

The restrictions on α are discussed in more detail within the next section.

5. PROBLEMS WITH CHIEF AND BMF

This section discusses the problems associated with the CHIEF and BMF methods.

5A PROBLEMS WITH CHIEF

The numerical implementation of CHIEF involves writing the N-by-N system of equations resulting from the surface Helmholtz integral equation (3.2.27), and then overdetermining the solution with additional equations based on the interior Helmholtz integral equation (3.2.28) for 'strategically' placed interior points. Of these additional equations, there must be a sufficient number that correspond to non-nodal interior points.

It is the above implementation process that introduces the problems associated with CHIEF.

The first problem is that of determining the number of additional equations that must be employed in order to 'extract' the proper solution

from the set of possible solutions of the non-unique surface integral equation. This immediately introduces a second problem concerned with the placement of the interior points. If the body is truely arbitrary there is no way of knowing whether or not the interior points lie on a nodal surface.

Recalling that at high frequencies the spacing between the nodal surfaces becomes small; the implementation of CHIEF at such frequencies is just as impractical as it is for the original three methods.

5B PROBLEMS WITH BMF

The Burton and Miller formulation (3.4.3) involves the integral

$$\int_S \psi(Q)\, \frac{\partial^2 G(P,Q)}{\partial n_p\, \partial n_q}\, dS_q \tag{3.5.1}$$

In its present form the kernel of (3.5.1) is highly singular as the point Q approaches the point P on the surface. That is, as the distance, r, between points P and Q approaches zero

$$\frac{\partial^2 G(P,Q)}{\partial n_p\, \partial n_q} = O(r^{-3}) \tag{3.5.2}$$

in three dimensions, where $G(P,Q) = \frac{e^{-ikr}}{4\pi r}$

and where an element of surface, dS, is proportional to r^2. As it stands (3.5.1) cannot be integrated numerically. The kernel must be transformed so as to reduce the strength of the singularity. A representation derived by Maue [48] involves tangential rather than normal derivatives at the surface (see Appendix (J), Maue[48] , Mitzner[49]). That is:

$$\int_S \psi(Q)\, \frac{\partial^2 G(P,Q)}{\partial n_p\, \partial n_q}\, dS_q = \int_S \left[\underline{n}_q \times \underline{\nabla}_q \psi(Q)\right] \cdot \left[\underline{n}_p \times \underline{\nabla}_p G(P,Q)\right] dS_q + \int_S \psi(Q) k^2 (\underline{n}_p \cdot \underline{n}_q) G(P,Q)\, dS_q \qquad P,Q \in S \tag{3.5.3}$$

where $\underline{n}_p$ and $\underline{n}_q$ are outward unit normals at the surface points P and Q respectively; while $\underline{\nabla}_p$ and $\underline{\nabla}_q$ are the gradient operators at these points.

Equation (3.5.3) expresses (3.5.1) as the sum of two regular integrals. However (3.5.3) does not lend itself to immediate numerical implementation.

Meyer et al.[34] have further modified equation (3.5.3) such that, (see Appendix (J));

$$\int_S \psi(Q)\,\frac{\partial^2 G(P,Q)}{\partial n_p\,\partial n_q}\,dS_q = \int_S \left[\psi(Q) - \psi(P)\right] \underline{n}_q \cdot \underline{\nabla}_q \times \left[\underline{n}_p \times \underline{\nabla}_p G(P,Q)\right] dS_q + \int_S \psi(Q)(\underline{n}_p \cdot \underline{n}_q) k^2 G(P,Q)\,dS_q \qquad (3.5.4)$$

and this can still further be modified to give:

$$\int_S \psi(Q)\,\frac{\partial^2 G(P,Q)}{\partial n_p\,\partial n_q}\,dS_q = \int_S \left[\psi(Q) - \psi(P)\right] \frac{\partial^2 G(P,Q)}{\partial n_p\,\partial n_q}\,dS_q + \psi(P) \int_S (\underline{n}_p \cdot \underline{n}_q) k^2\, G(P,Q)\,dS_q \qquad (3.5.5)$$

Equation (3.5.5) expresses the strongly singular integral (3.5.1) as two regular integrals which are amenable to numerical implementation.

Burton and Miller have shown that to ensure a unique solution of equation (3.4.3), the coupling constant α must have a non-zero imaginary part. This is the only restriction Burton and Miller place on α. However, consider the two terms on the right of equation (3.5.5). Both these terms are of order k^2. Therefore at higher wavenumbers the terms of order k^2 will dominate, hence equation (3.4.2) will dominate equation (3.4.3). So when k is sufficiently high and close to one of the eigenwavenumbers associated with equation (3.4.2) the combined equation (3.4.3) would be expected to become ill-conditioned.

It will be demonstrated later that a marked improvement in accuracy of the computed solution is seen at high k, when α is modified to be inversely proportional to the wavenumber. This is also shown by Meyer et al,[25].

In summary, the reliability of the BMF method will:

(i) depend on the accurate representation of the highly singular integral (3.5.1);
(ii) become sensitive to the choice of the coupling constant in the high frequency limit.

In the chapters that follow, the solution for the surface potential will be considered using both the CHIEF and BMF methods.

IV NUMERICAL IMPLEMENTATION

The numerical implementation of the CHIEF and BMF boundary integral methods is to be discussed within this chapter.

In both these methods an integral equation, (3.2.27), (3.2.28) or (3.4.3), is to be applied on the surface of the body under consideration.

The first step in the numerical analysis will involve an approximation of the integral equation over the surface S. A boundary element scheme will be used to carry out this approximation.

1. THE BOUNDARY ELEMENT TECHNIQUE

The boundary element (BE) technique consists of subdividing the boundary of the body under consideration into a series of elements.

This discretization of the boundary permits the unknown functions within the integral equation to be approximated at a finite number of points (nodes) over the surface. Therefore the numerical approximation of the surface integral will be expressed in the form of a finite summation.

In three dimensions the discretized boundary can be represented by either a faceted surface, consisting of planar elements, or a curved surface made up of curvilinear elements.

For an arbitrarily shaped three dimensional body, triangular boundary elements are capable of producing a close approximation to the body surface. The defined variation of the unknown function within each element will determine the type of boundary element to be considered.

If the unknown function is assumed constant over each element then its value over an element will be given by its value at some nodal point within that element. In this case the boundary elements will be planar and for a triangular facet the nodal point is typically taken at the centroid.

If the function is defined to vary linearly over each triangular element then the nodal points are usually positioned at the three vertices of each triangle. The boundary elements will again be planar.

It is also possible to assume that the unknown function will display a higher order variation over each element. In this case the element will be curved and the nodal points of the triangular element will typically be positioned at the three vertices and the midpoints of the three sides.

In order to explain the numerical implementation of the BE technique it will be convenient to consider a particular formulation. The surface Helmholtz integral method is implicit within both the CHIEF and BMF methods, and so will be chosen as a relevant formulation.

Recalling the surface Helmholtz integral method; the first phase of solution involves the calculation of the velocity potential on the surface using equation (3.2.27), i.e.

$$-\tfrac{1}{2}\Psi(P) + \int_S \Psi(Q)\,\frac{\partial G(P,Q)}{\partial n_q}\,dS_q = \int_S G(P,Q)\,\frac{\partial \Psi(Q)}{\partial n_q}\,dS_q \qquad (4.1.1)$$

where P and Q are points on the surface s. The boundary condition, $\frac{\partial \Psi}{\partial n}$ is known on s and the surface velocity potential Ψ is unknown.

The boundary is now discretized into N elements. Therefore the discretized surface integral equation will be:

$$-\tfrac{1}{2}\Psi(P_i) + \sum_{j=1}^{N} \int_{S_j} \Psi(Q)\,\frac{\partial G(P_i,Q)}{\partial n_q}\,dS_q = \sum_{j=1}^{N} \int_{S_j} \frac{\partial \Psi(Q)}{\partial n}\,G(P_i,Q)\,dS_q \qquad i=1,\ldots,N \qquad (4.1.2)$$

where this equation applies to a particular node, P_i. The nodal points P_i are where the velocity potential is to be evaluated, they are also called singularity points. The points Q within the integrals are referred to as integration points. This terminology will become obvious later.

First assume that the functions Ψ and $\frac{\partial \Psi}{\partial n}$ are constant over each element S_j, (j=1, ...,N), and are denoted by:

$$\Psi_j \text{ and } \left(\frac{\partial \Psi}{\partial n}\right)_j$$

Therefore (4.1.2) will be:

$$-\tfrac{1}{2}\Psi_i + \sum_{j=1}^{N} \Psi_j \int_{S_j} \frac{\partial G(P_i,Q)}{\partial n_q}\,dS_q = \sum_{j=1}^{N} \left(\frac{\partial \Psi}{\partial n}\right)_j \int_{S_j} G(P_i,Q)\,dS_q \qquad (4.1.3)$$

where i runs from 1 to N.

The integrals within equation (4.1.3) are to be evaluated over each triangular element s_j. The numerical evaluation of these weakly singular integrals will be discussed later.

Equation (4.1.3) can be written for each node i, resulting in a system of N algebraic equations: i.e.

$$\sum_{j=1}^{N} H_{ij} \Psi_j = \sum_{j=1}^{N} G_{ij} \left(\frac{\partial \Psi}{\partial n}\right)_j \quad ; \quad i=1,\ldots,N \tag{4.1.4}$$

where

$$H_{ij} = \int_{s_j} \frac{\partial G(P_i,Q)}{\partial n_q} \, dS_q - \tfrac{1}{2}\delta_{ij} \tag{4.1.5}$$

$$G_{ij} = \int_{s_j} G(P_i,Q) \, dS_q \tag{4.1.6}$$

and δ_{ij} is the kronecker delta.

In matrix notation (4.1.4) will be:

$$[H]\{\Psi\} = [G]\left\{\frac{\partial \Psi}{\partial n}\right\} \tag{4.1.7}$$

and because the boundary condition is known on the surface, (4.1.7) can be written as:

$$[H]\{\Psi\} = \{M\} \tag{4.1.8}$$

where

$$M_i = \sum_{j=1}^{N} G_{ij} F_j \quad , \text{ since } \left(\frac{\partial \Psi}{\partial n}\right)_j = F_j \text{ on } s .$$

It is now a simple matter to solve the matrix equation of (4.1.8) for the surface velocity potential. i.e.

$$\{\Psi\} = [H]^{-1}\{M\} \tag{4.1.9}$$

if $[H]^{-1}$ exists. The solution of (4.1.8) is typically calculated using a Gauss reduction method.

Once the acoustic velocity potential is known on the whole boundary, i.e. over all the elements s_j, then it is possible to calculate the potential at any exterior field point using an identical discretization on equation (3.2.26).

Thus,

$$\psi(P_i) = \sum_{j=1}^{N} A_{ij}\,\psi_j - \sum_{j=1}^{N} G_{ij}\,F_j \qquad (4.1.10)$$

or

$$\{\psi\} = ([A][H]^{-1} - [I])\{M\} \qquad (4.1.11)$$

where

$$A_{ij} = \int_{S_j} \frac{\partial}{\partial n_q} G(P_i,Q)\, dS_q$$

P_i is a point in the exterior domain D_+ and I is the NxN identity matrix.

The functions ψ and $\frac{\partial\psi}{\partial n}$ can also be assumed to have a linear or higher order variation over each element S_j. The first stage in the study of these elements is to introduce a local coordinate system on the surface S.

For the case of triangular elements, the local coordinates ξ_1 and ξ_2 will have their origin at an element vertex and will point along the two edges which meet at this vertex.

Therefore a variation, whether linear or higher order, over the triangular face can be expressed in terms of variations along the local coordinates ξ_1 and ξ_2. So for these elements the values of Ψ and $\frac{\partial\Psi}{\partial n}$ at any point on the element can be defined in terms of its nodal values and some interpolation functions acting along ξ_1 and ξ_2 (see [50] and [51]).

The Jacobian of the transformation from global to local surface coordinates, ξ_1 and ξ_2, is given as the magnitude of the normal $\underline{\nu}$:

$$\underline{\nu} = \frac{\partial \underline{R}}{\partial \xi_1} \times \frac{\partial \underline{R}}{\partial \xi_2}$$

where $\underline{R}$ is the position vector, from the global origin, to the origin of ξ_1 and ξ_2.

It might be expected that the linear or higher order elements would always be preferred over the more crude constant planar elements.

However computational difficulties arise when using linear elements. In this case care has to be taken when positioning the nodal points on the triangle. If these points are placed on the triangle vertices or edges then their normals will not be clearly defined. This is important because the normals describe the general shape of the surface and hence the approximate smoothness of the surface. Remembering that the formulation of the boundary integral in this problem stipulates that the surface be

smooth, it is possible that a poor approximation of a normal might suggest a surface with sharp corners. This problem could be removed by placing the nodes within the triangular element; however, this scheme would require the use of complicated interpolation functions whose form might not be immediately obvious.

The higher order elements will have similar problems. The constant planar elements have another numerical advantage over higher order elements. In the case when the singularity point and integration points are in the same element, the normal derivative of the Green's function, with respect to these points, will vanish. This will simplify the formulation of the matrices.

The approximation of a surface by constant planar elements will be employed in the numerical implementation of the CHIEF and BMF methods. However, before considering these methods the numerical integration of the weakly singular Green's function and derivatives over these elements is discussed.

A comprehensive list of the available literature relating to boundary element methods has been given by Tanaka [52].

2. NUMERICAL INTEGRATION

In the previous section, if the unknown functions were assumed constant over each element they were taken outside the integral signs of the discretized equation.

For the surface Helmholtz integral method the kernels that still require to be integrated over each element will be the free-space Green's function and its normal derivative.

A similar situation occurs when considering constant elements for the CHIEF and BMF methods. The Green's function and its normal derivatives will be implicit within the kernels of both the CHIEF and BMF methods. It is these functions, which are both oscillatory and singular, that demand the most attention when integrating numerically.

The quadrature formulas for numerical integration of a function, f, over a triangle of area, A, all have the form;

$$\int_{\Delta} f \, dA = A \sum_{k=1}^{M} w_k f(\nu_{k,1}, \nu_{k,2}) + E \qquad (4.2.1)$$

where the points $\underline{\nu}_k = (\nu_{k,1}, \nu_{k,2})$ $k=1,\ldots,M$, are the integration points that lie in the two dimensional triangular domain; w_k is the weight or coefficient associated with the k-th integration point and E is the error in the numerical approximation.

The integration points $\underline{\nu}_k$ are usually positioned, in an optimal manner within the domain, so as to minimize the magnitude of the error E.

In the present problem the integration of Green's function, for example, is performed over each element for a finite number of singularity points P_i. The integration over each element can be approximated by first choosing a finite number of integration points, Q_k, within each element. The value of the Green's function, $G(P_i,Q)$, at each of these discrete points is then calculated for all the singularity points P_i, i = 1, ..., N. Each of these values is then multiplied by a weighting factor w_k and summed over the M integration points. This final value represents a numerical approximation to the integration of Green's function over an element (see Fig. 4).

Before making a choice as to which integration scheme to apply, the behaviour of the kernel functions over each element will be investigated.

When integrating over the i-th element the kernels will become singular at the singularity point, P_i, within this element. So obviously an integration point, Q_k, of the i-th element cannot correspond to the singularity point P_i of the same element.

In the case where the integration points, Q_k, are in the neighbourhood of a singularity point, P_i, the value of the kernel functions will display a large variation due to the singularity. The element that contains P is typically taken to represent the size of this large variation neighbourhood.

All the integrals are regular, therefore a better approximation to this large variance could be obtained by increasing the number of integration points around the singularity point in question.

At this stage it would appear more convenient to apply two separate integration schemes over the discretized surface. A higher order integration scheme could be introduced to an element whenever the singularity and integration point were both present in the same element.

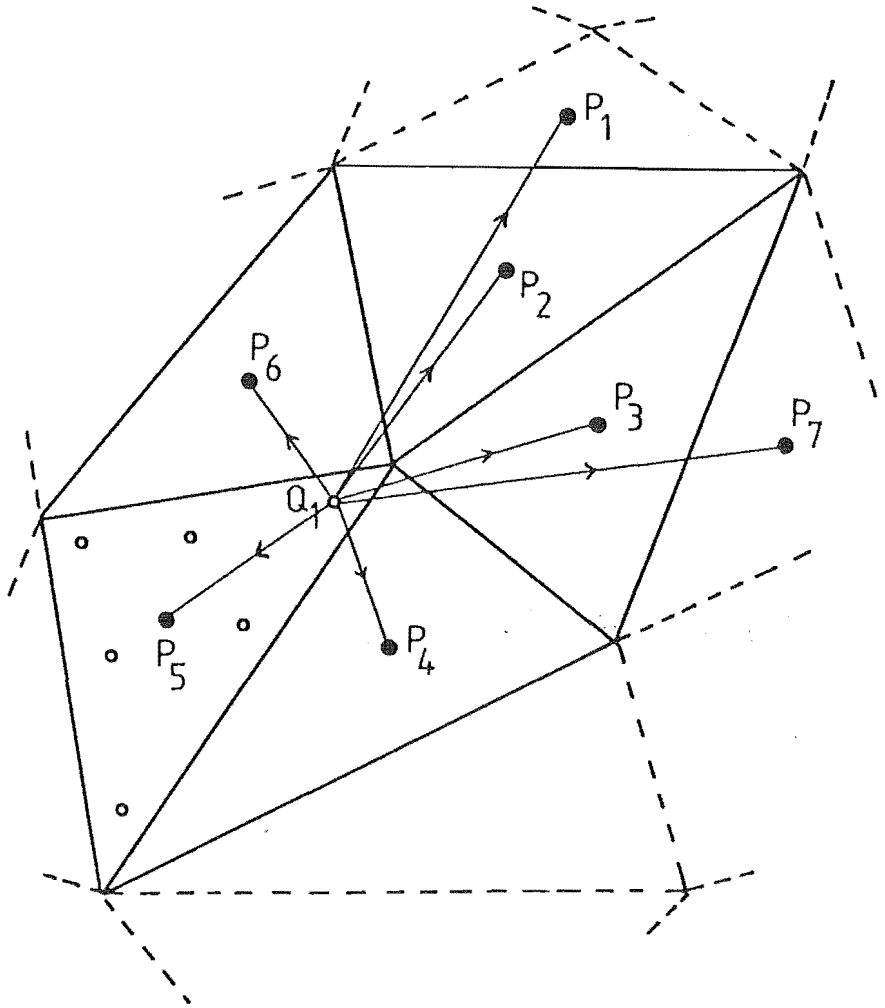

Figure 4. Numerical integration over a triangular element

The integrals relate the i-th singularity point to the j-th element, hence the composition of the NxN integration matrices is now more obvious. The integration over the i-th element, when that element contains the i-th singularity point, will now be referred to as a 'diagonal' integration.

An integration scheme of high order will not be required for the 'off-diagonal' integrations. In this case the kernel functions will not become singular and so their variance over each element will be less dramatic.

The 'diagonal' integrations, however, will require a larger number of integration points positioned around the singularity in order to obtain a reasonable approximation. In this case no integration point will be allowed to correspond to the triangle centroid as this is typically the position of the singularity point P_i.

Even after the above restrictions there is still a large number of integration schemes available (see [53]).
However from a computational viewpoint it would be advantageous to choose the most efficient.

Suitable integration schemes have been developed by Silvester[54], Irons[55], Hammer, Marlowe and Stroud[56] and Cowper[57].

The quadrature formulas of Silvester have the advantage of simple coefficients and complete symmetry with respect to the three triangle vertices, but they are of the Newton-Cotes type and so will be relatively inefficient compared with Gaussian formulas. The formulas of Irons are commonly referred to as the conical product formulas. These formulas are based on the successive application of Gauss and Radau one dimensional quadrature rules over a quadrilateral. The triangle is then treated as a degenerate case of a quadrilateral with two coincident vertices. These formulas are highly efficient but as expected will have the unappealing feature that the sampling points will not be arranged symmetrically within the triangle (see Fig. 5).

From the viewpoint of numerical efficiency and symmetry, the formulas of Hammer, Marlow and Stroud are comparatively better. They are of the Gaussian type and are fully symmetric with respect to the three triangle vertices.

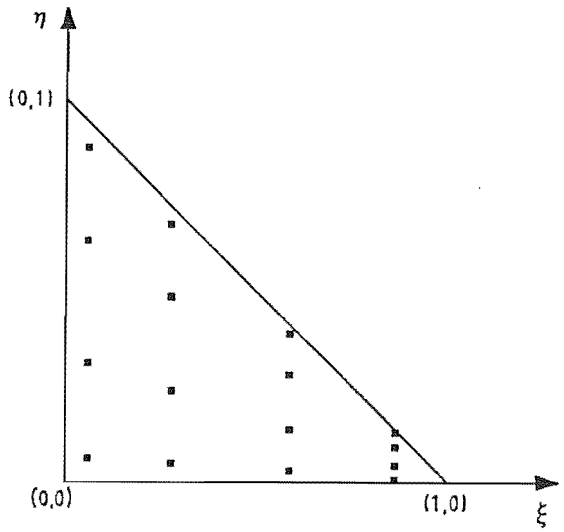

Figure 5. A 16-point, degree-7 simplex quadrature rule

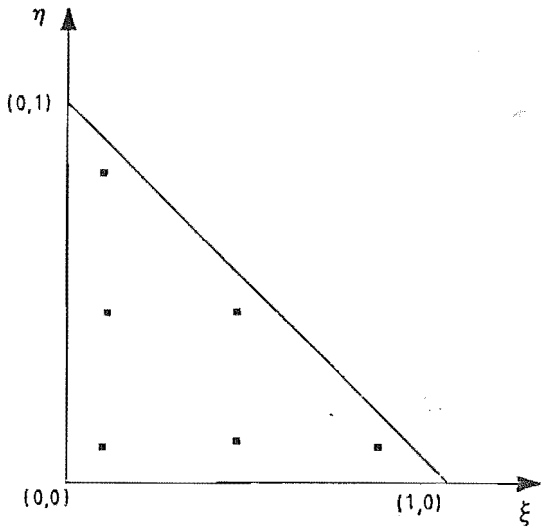

Figure 6. A 6-point, degree-4 simplex quadrature rule

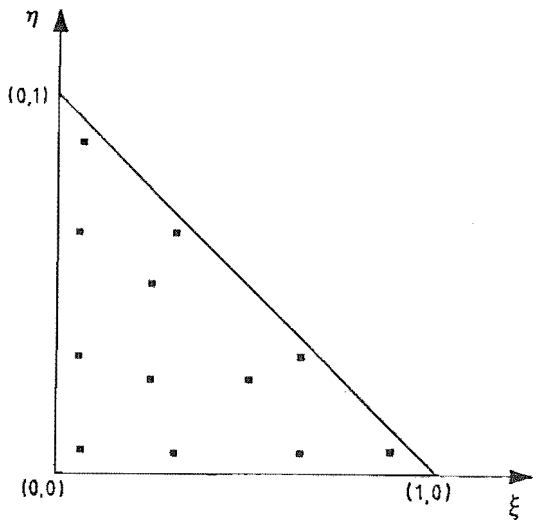

Figure 7. A 12-point, degree-6 simplex quadrature rule

TABLE 1

Quadrature points and weights for a 6-point, degree-4 simplex integration rule

k	ξ_k	η_k	W_k
1	0.8168480	0.0915760	0.1099520
2	0.0915760	0.8168480	0.1099520
3	0.0915760	0.0915760	0.1099520
4	0.1081030	0.4459480	0.2233810
5	0.4459480	0.1081030	0.2233810
6	0.4459480	0.4459480	0.2233810

TABLE 2

Quadrature points and weights for a 12-point, degree-6 simplex integration rule

k	ξ_k	η_k	W_k
1	0.8738220	0.0630890	0.0508449
2	0.0630890	0.8738220	0.0508449
3	0.0630890	0.0630890	0.0508449
4	0.5014265	0.2492867	0.1167863
5	0.2492867	0.5014265	0.1167863
6	0.2492867	0.2492867	0.1167863
7	0.6365025	0.3103524	0.0828511
8	0.6365025	0.0531450	0.0828511
9	0.3103524	0.6365025	0.0828511
10	0.3103524	0.0531450	0.0828511
11	0.0531450	0.6365025	0.0828511
12	0.0531450	0.3103524	0.0828511

TABLE 3

Quadrature points and weights for a 16-point, degree-7 simplex integration rule

k	ξ_k	η_k	W_k
1	0.0571042	0.0654670	0.0471367
2	0.2768430	0.0502101	0.0707761
3	0.5835904	0.0289121	0.0451681
4	0.8602401	0.0097038	0.0108465
5	0.0571042	0.3111646	0.0883702
6	0.2768430	0.2386487	0.1326885
7	0.5835904	0.1374191	0.0846794
8	0.8602401	0.0461221	0.0203345
9	0.0571042	0.6317312	0.0883702
10	0.2768430	0.4845083	0.1326885
11	0.5835904	0.2789905	0.0846794
12	0.8602401	0.0936378	0.0203345
13	0.0571042	0.8774288	0.0471367
14	0.2768430	0.6729468	0.0707761
15	0.5835904	0.3874975	0.0451681
16	0.8602401	0.1300561	0.0108465

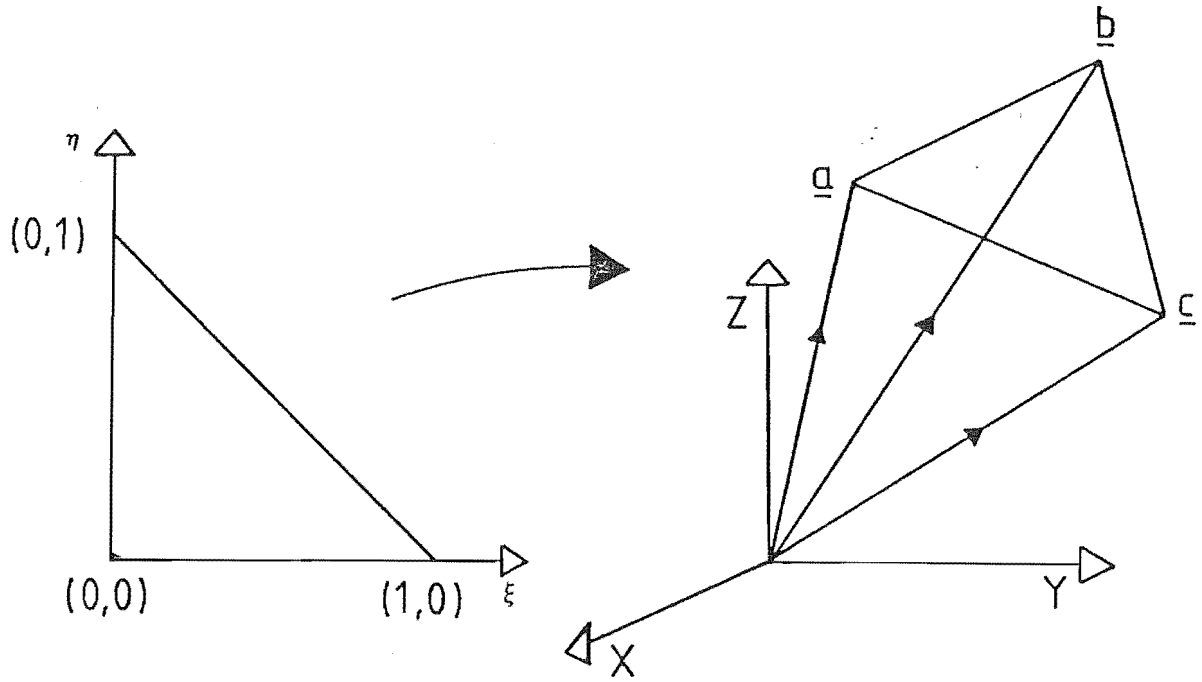

Figure 8. Transformation to an arbitrary triangular element

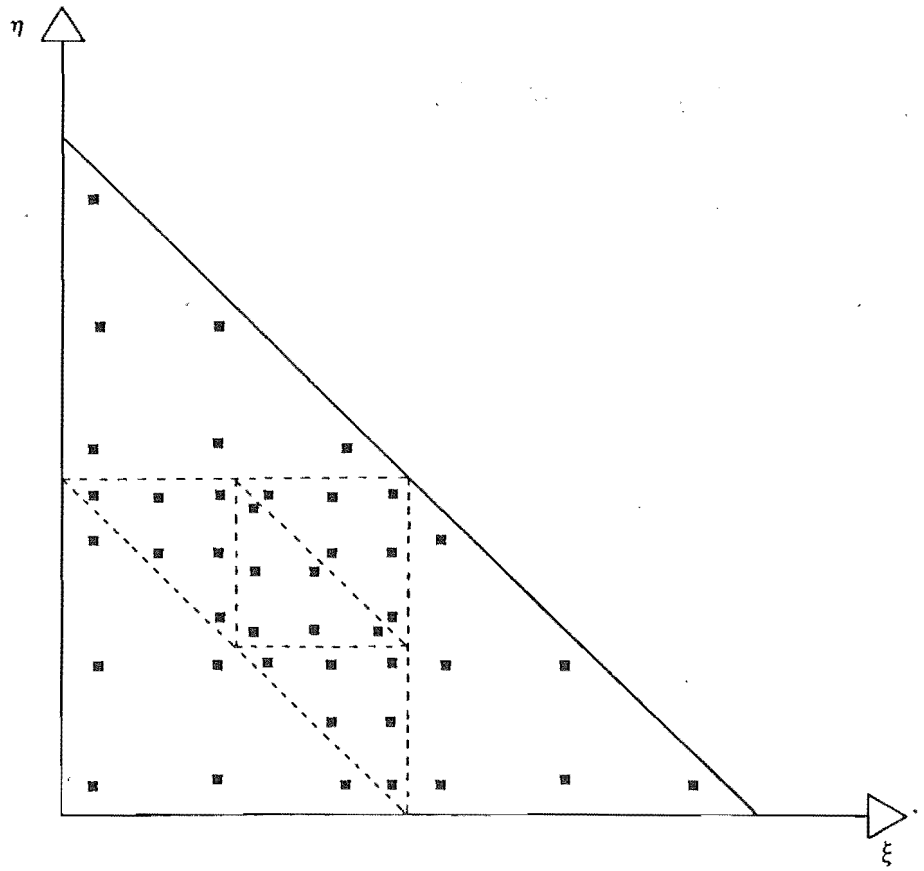

Figure 9. A 42-point simplex quadrature rule (consisting of seven 6-point rules)

Cowper introduces some new higher order formula that are also of the Gaussian type as well as being fully symmetric (see Fig.6,7). It is these formulas due to Cowper which will be used within the present problem.

It will be shown later that Cowper's 12-point, 6-th degree rule will produce similar results to a 16-point, 7-th degree rule due to Irons.

The task of positioning the integration points within each triangular element of an arbitrary body can be simplified by first positioning them within a standard base triangle. A linear transformation is then used to map this base triangle onto an element of the faceted surface.

The positions of the integration points within the base triangle are usually given in terms of three area coordinates.

However, it is simpler to consider the base triangle defined to be an isoceles right triangle in the ξ,η plane with vertices: (0,0), (0,1), (1,0). Any two of the three area coordinates will represent the coordinates of an integration point within the ξ,η domain. The remaining integration points are found by considering all possible permutations of the three area coordinates.

Now each point, (ξ,η), of the base triangle can be transformed onto a point, $\underline{q} = (q_1,q_2,q_3)$ of some triangular surface element. Therefore:

$$\underline{q} = \left[1 - (\xi + \eta)\right]\underline{a} + \xi\underline{b} + \eta\underline{c} \qquad (4.2.2)$$

where $\underline{a}$, $\underline{b}$ and $\underline{c}$ are the three vertices of the triangular element that contains the point $\underline{q}$ (see Fig. 8)

The Jacobian of this transformation will be twice the area of the triangular element on the body since the area of the base triangle is ½.

For the 'diagonal' integrations, where the singularity and integration points are within the same element, another scheme can be derived that recognizes the singular behaviour of the kernels within these elements.

This integration scheme involves first subdividing the original triangle into four smaller triangles, the central triangle that contains the centroid is then subdivided once more. This process of successively subdividing each central triangle into four smaller triangles will result in a concentration of integration points about the centroid (see Fig. 9).

The only restriction to the choice of integration points for each small triangle will be given to the final central triangle, which must not have an integration point on the centroid.

The degree of improvement due to the introduction of this specialised scheme for the 'diagonal' integrations will be demonstrated later.

The next two sections apply the discretization procedure to the CHIEF and BMF methods.

3. THE CHIEF METHOD

This method utilizes both the surface Helmholtz integral equation (3.2.27) and the interior Helmholtz integral equation (3.2.28). It is based on the concept that there exists only one solution common to both formulations.

To implement this method the body surface is first discretized into N triangular elements. If the unknown functions are assumed constant over each element then for the surface integral method there will exist N singularity points P_i, i=1,..,N. These singularity points will be positioned at the centroid of each planar element.

For the interior method the need to decide on the number of interior nodes required is removed by simply choosing one interior point for each element. The position of the i-th interior point, corresponding to the i-th element, is chosen to be at a distance γ_i along the inward normal from the i-th centroid (see Fig. 10). The distance γ_i of the point P_i from the surface element is arbitrary. However, in this problem γ_i is chosen to have a value characteristic of the dimensions of the i-th triangular element.

Although the placement of interior points inside the body surface is arbitrary, the above scheme chooses a set of points that will bear some relation to the shape of the three dimensional body.

The numerical implementation process will first involve discretizing the two integral equations, (3.2.27) and (3.2.28), for the case of constant elements.

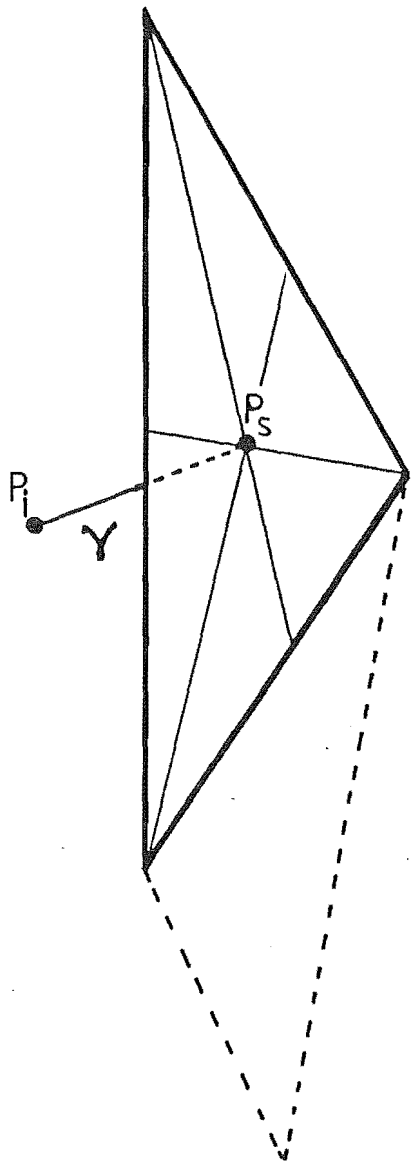

Figure 10. Position of the surface and internal singularity points for the CHIEF method

P_i = internal singularity, $P_i \in D_-$

P_s = surface singularity, $P_s \in S$

$$\text{i.e.}\quad -\tfrac{1}{2}\Psi(P_i) + \sum_{j=1}^{N} \Psi_j \int_{S_j} \frac{\partial G(P_i,Q)}{\partial n_q}\, dS_q = \sum_{j=1}^{N} \left(\frac{\partial \Psi}{\partial n}\right)_j \int_{S_j} G(P_i,Q)\, dS_q \qquad (4.3.1)$$

where $P_i,\ Q \varepsilon S; \quad S = S_1 \cup S_2 \ldots \cup S_N$

and

$$\sum_{j=1}^{N} \Psi_j \int_{S_j} \frac{\partial G(P_i,Q)}{\partial n_q}\, dS_q = \sum_{j=1}^{N} \left(\frac{\partial \Psi}{\partial n}\right)_j \int_{S_j} G(P_i,Q)\, dS_q \qquad (4.3.2)$$

where $P_i \varepsilon D_-$, $Q \varepsilon S$ and $i=1,\ldots,N$

Now define:

$$A_{ij} = \int_{S_j} \frac{\partial G(P_i,Q)}{\partial n_q}\, dS_q - \tfrac{1}{2}\delta_{ij} \qquad P_i \varepsilon S \qquad (4.3.3)$$

$$B_{ij} = \int_{S_j} \frac{\partial G(P_i,Q)}{\partial n_q}\, dS_q \qquad P_i \varepsilon D_- \qquad (4.3.4)$$

$$C_{ij} = \int_{S_j} G(P_i,Q)\, dS_q \qquad P_i \varepsilon S \qquad (4.3.5)$$

$$D_{ij} = \int_{S_j} G(P_i,Q)\, dS_q \qquad P_i \varepsilon D_- \qquad (4.3.6)$$

hence (4.3.1) and (4.3.2) can be written as:

$$\sum_{j=1}^{N} A_{ij} \Psi_j = \sum_{j=1}^{N} C_{ij} \left(\frac{\partial \Psi}{\partial n}\right)_j \qquad i=1,\ldots,N \qquad (4.3.7)$$

$$\sum_{j=1}^{N} B_{ij} \Psi_j = \sum_{j=1}^{N} D_{ij} \left(\frac{\partial \Psi}{\partial n}\right)_j \qquad i=1,\ldots,N \qquad (4.3.8)$$

It must be noted that the choice of 'diagonal' integration scheme for the interior integral method is not as critical as it is for the surface integral method. This is because the distance from an internal node to an integration point will be bounded below by the value of γ_i.

In matrix notation, equations (4.3.7) and (4.3.8) become:

$$\underset{N\times N}{[A]}\ \underset{N\times 1}{\{\Psi\}} = \underset{N\times 1}{\{G\}} \qquad (4.3.9)$$

$$\underset{N\times N}{[B]}\ \underset{N\times 1}{\{\Psi\}} = \underset{N\times 1}{\{H\}} \qquad (4.3.10)$$

where

$$G_i = \sum_{j=1}^{N} C_{ij}\left(\frac{\partial \Psi}{\partial n}\right)_j \tag{4.3.11}$$

$$H_i = \sum_{j=1}^{N} D_{ij}\left(\frac{\partial \Psi}{\partial n}\right)_j \tag{4.3.12}$$

since the boundary condition $\left(\frac{\partial \Psi}{\partial n}\right)_j$ is assumed known over each element of the surface.

Equations (4.3.9) and (4.3.10) represent two N-by-N systems of equations. The problem is now over specified, there being 2N equations for the N unknown values of Ψ. Therefore these equations cannot be solved simultaneously. However, this overdetermined system can be solved approximately by using a residual least-squares procedure.

This procedure initially defines a residual χ of the form

$$\chi = \alpha|[A]\{\Psi\} - \{G\}|^2 + (1-\alpha)|[B]\{\Psi\} - \{H\}|^2 \tag{4.3.13}$$

where α is a real constant such that $0 < \alpha < 1$.

The approximate solution to equations (4.3.9) and (4.3.10) will result from minimizing the residual χ with regard to the components of Ψ. This minimization procedure will give the following matrix equation for the surface potential ψ: (see Appendix K for derivation).

i.e.
$$\underset{N\times N}{[K]}\underset{N\times 1}{\{\psi\}} = \underset{N\times 1}{\{M\}} \tag{4.3.14}$$

where
$$K = \alpha[A]^{*T}[A] + (1-\alpha)[B]^{*T}[B] \tag{4.3.15}$$

and
$$\{M\} = \alpha[A]^{*T}\{G\} + (1-\alpha)[B]^{*T}\{H\} \tag{4.3.16}$$

The superscripts * and T denote a complex conjugate and transpose respectively. The NxN coefficient matrix $[K]$ will be complex, Hermitian and full.

It is this equation (4.3.14) that has to be solved in order to obtain the surface velocity potential ψ within each boundary element.

The value of the constant α determines the relative weighting of the surface and interior formulations. For example, if $\alpha = 1$ the

solution of (4.3.14) will be identical to that of (4.3.9), i.e. the surface Helmholtz integral equation. If $\alpha = 0$ the solution will correspond to that of the interior Helmholtz integral equation (4.3.10) and if $\alpha = \frac{1}{2}$ then equal weighting will be given to both formulations.

The results of this numerical implementation will be presented later.

4. THE BMF METHOD

This method is based on the concept that the surface Helmholtz integral equation (3.4.1) and its normal derivative at the surface (3.4.2) will have only one solution in common. The formulation of this method consists of linearly combining the surface equation and its normal derivative.

The initial discretization process is similar to that employed for the CHIEF method. The body surface is discretized into N elements and the unknown functions are assumed constant over each element. The surface singularity points P_i correspond to the centroids of the triangular elements. The normal derivative of the surface integral equation is to be taken with respect to these surface singularity points.

The combined equation of the BMF method can be written as:

$$\int_S \Psi(Q)\,\frac{\partial G(P,Q)}{\partial n_q}\,dS_q + \alpha\int_S \left[\Psi(Q) - \Psi(P)\right]\frac{\partial^2 G(P,Q)}{\partial n_p \partial n_q}\,dS_q$$

$$+ \alpha\Psi(P)\int_S (\underline{n}_p \cdot \underline{n}_q)k^2 G(P,Q)\,dS_q - \tfrac{1}{2}\Psi(P) = \int_S G(P,Q)\frac{\partial \Psi(Q)}{\partial n_q}\,dS_q$$

$$+ \alpha\int_S \frac{\partial G(P,Q)}{\partial n_p}\frac{\partial \Psi(Q)}{\partial n_q}\,dS_q + \tfrac{1}{2}\alpha\frac{\partial \Psi(P)}{\partial n_p} \qquad (4.4.1)$$

where $P,Q \in S$ and $\mathrm{Im}(\alpha) \neq 0$.

Discretizing (4.4.1) yields:

$$-\tfrac{1}{2}\Psi_i + \sum_{j=1}^{N} \Psi_j \int_{S_j} \frac{\partial G(P_i,Q)}{\partial n_q}\,dS_q + \alpha \sum_{j=1}^{N} (\Psi_j - \Psi_i)\int_{S_j} \frac{\partial^2 G(P_i,Q)}{\partial n_p \partial n_q}\,dS_q$$

$$+ \alpha\Psi_i \sum_{j=1}^{N} \int_{S_j} (\underline{n}_{P_i} \cdot \underline{n}_q)k^2 G(P_i,Q)\,dS_q$$

$$= \sum_{j=1}^{N} \left(\frac{\partial \Psi}{\partial n}\right)_j \int_{S_j} G(P_i,Q)\,dS_q + \alpha \sum_{j=1}^{N} \left(\frac{\partial \Psi}{\partial n}\right)_j \int_{S_j} \frac{\partial G(P_i,Q)}{\partial n_p}\,dS_q + \tfrac{1}{2}\alpha\frac{\partial \Psi_i}{\partial n_p} \qquad (4.4.2)$$

where $P_i, Q \in S$, $S = S_1 \cup S_2 \cup \ldots \cup S_N$ and $i=1, \ldots, N$.

Now define

$$A_{ij} = \int_{S_j} \frac{\partial G(P_i,Q)}{\partial n_q} dS_q - \tfrac{1}{2}\delta_{ij} \tag{4.4.3}$$

$$B_{ij} = \alpha \int_{S_j} \frac{\partial^2 G(P_i,Q)}{\partial n_p \partial n_q} dS_q \tag{4.4.4}$$

$$C_{ij} = \alpha \int_{S_j} (\underline{n}_{P_i} \cdot \underline{n}_q) k^2 G(P_i,Q) dS_q \tag{4.4.5}$$

$$D_{ij} = \int_{S_j} G(P_i,Q) dS_q \tag{4.4.6}$$

$$E_{ij} = \alpha \int_{S_j} \frac{\partial G(P_i,Q)}{\partial n_p} dS_q + \tfrac{1}{2}\alpha\delta_{ij} \tag{4.4.7}$$

hence (4.4.2) can be written as:

$$\sum_{j=1}^{N} A_{ij}\Psi_j + \sum_{j=1}^{N} B_{ij}\Psi_j - \Psi_i \sum_{j=1}^{N} B_{ij} + \Psi_i \sum_{j=1}^{N} C_{ij}$$

$$= \sum_{j=1}^{N} D_{ij}\left(\frac{\partial \Psi}{\partial n}\right)_j + \sum_{j=1}^{N} E_{ij}\left(\frac{\partial \Psi}{\partial n}\right)_j \qquad i=1,\ldots,N \tag{4.4.8}$$

In matrix form this will be:

$$([A] + [B] - [\hat{B}] + [\hat{C}])\{\Psi\} = ([D] + [E])\{\frac{\partial \Psi}{\partial n}\} \tag{4.4.9}$$

where $[\hat{B}]$ and $[\hat{C}]$ are diagonal matrices of the form:

$$\hat{B}_{ij} = \begin{cases} \sum_{q=1}^{N} B_{iq} , & i = j \\ 0 , & i \neq j \end{cases} \tag{4.4.10}$$

and similarly for $\hat{C}_{ij}$.

Because the boundary condition $\left(\frac{\partial \Psi}{\partial n}\right)_j$ is known over each surface element, equation (4.4.9) can be written as:

$$\underset{N\times N}{[K]}\underset{N\times 1}{\{\Psi\}} = \underset{N\times 1}{\{M\}} \tag{4.4.11}$$

where $[K] = [A] + [B] - [\hat{B}] + [\hat{C}]$ (4.4.12)

and $\{M\} = ([D] + [E])\{\frac{\partial \Psi}{\partial n}\}$ (4.4.13)

The matrix equation (4.4.11) can now be solved for the unknown surface velocity potential Ψ within each boundary element.

5. THE MEAN FLOW SOLUTION

The preceeding two sections have explained the numerical implementation procedure for both the CHIEF and BMF methods. Both methods result in a matrix equation, i.e. (4.3.15) or (4.4.11), whose solution represents the N nodal values of Ψ over each of the N surface elements.

Once these nodal values of the surface potential Ψ have been determined they can be converted into the surface values of the velocity potential ϕ for the mean flow problem.

The value of the acoustic velocity potential on the j-th surface element in the mean flow problem will be given by the discretized form of (3.1.1), i.e.

$$\phi_j = \Phi_j e^{i\omega t} \tag{4.5.1}$$

where $$\Phi_j = \Psi_j e^{-ikM\hat{\phi}} \tag{4.5.2}$$

The results presented in the following chapter, for the CHIEF and BMF methods, were derived using equation (4.5.1) along with the solutions, Ψ_j, of the matrix equations (4.3.15) and (4.4.11).

V TEST CASES AND RESULTS

A specific body shape is now selected in order to assess the solution procedure discussed so far.

The vibration of a perfect sphere within a uniform mean flow will be the model considered throughout the rest of this chapter.

Aside from the obvious computational advantages that exist for a fully symmetric sphere it is also advantageous, in this case, to be able to compare the resulting solutions with;

(i) the 'exact' analytic solutions of reference [7].
(ii) the results from an alternative numerical formulation, see [22].

The following section will derive the specific boundary conditions and the form of the final solution for two test case vibrations.

1. THE TEST CASES

The two test case vibrations are assumed to vibrate about a mean spherical surface of radius, r=a. This mean spherical surface will represent the stationary surface at which the boundary condition is to be applied.

The general Neumann boundary condition on this surface, within a mean flow, is given by equation (2.4.1). That is;

$$\underline{\nabla}\phi.\hat{\underline{n}} = \left(\frac{\partial}{\partial t} + \underline{U}.\underline{\nabla}\right)\frac{\eta}{|\underline{\nabla}\alpha|} - \frac{\eta}{|\underline{\nabla}\alpha|}\,\hat{\underline{n}}.\left[\,(\hat{\underline{n}}.\underline{\nabla})\underline{U}\,\right] \qquad (5.1.1)$$

where ϕ is the acoustic velocity potential, $\underline{U}$ is the mean flow velocity and η is the displacement of the boundary (normal to the surface) due to some vibration and α is a curvilinear co-ordinate at the surface, in the direction of $\hat{\underline{n}}$.

For the present case the spherical surface is centred at the origin of a spherical coordinate system, hence $\hat{\underline{n}}$ and α will lie along the radial coordinate, r.

In the case of an arbitrary vibration the surface displacement, η, will be a function of the spherical coordinates, θ and ψ as well as the time, t.

At low Mach numbers the mean flow may be approximated by an incompressible flow about a spherical surface of radius, a, (see Batchelor [40] §3.6). The mean flow velocity potential will then be:

$$\bar{\phi}(r,\theta) = -U_\infty(r + \frac{a^3}{2r^2})\cos\theta \qquad (5.1.2)$$

where U_∞ is the speed of the uniform flow at infinity and the negative sign indicates the flow direction. The velocity of the mean flow will be given by:

$$\underline{U} = \underline{\nabla}\bar{\phi}(r,\theta) \qquad (5.1.3)$$

Therefore boundary condition (5.1.1), at the spherical surface r=a, will reduce to:

$$\frac{\partial\phi}{\partial r} = (\frac{\partial}{\partial t} + \frac{U_\theta}{a}\frac{\partial}{\partial\theta})\eta(\theta,\psi,t) - \eta(\theta,\psi,t)\frac{\partial U_r}{\partial r} \quad , \quad \text{at } r=a \qquad (5.1.4)$$

where U_r and U_θ are the spherical polar components of the mean flow velocity.

From equation (5.1.2) these velocity components will be:

$$U_r = -M_\infty C_\infty(1 - \frac{a^3}{r^3})\cos\theta \qquad (5.1.5)$$

$$U_\theta = M_\infty C_\infty(1 + \frac{a^3}{2r^3})\sin\theta \qquad (5.1.6)$$

The boundary condition (5.1.4) can now be written in the form:

$$\frac{\partial\phi}{\partial r} = (\frac{\partial}{\partial t} + \frac{3}{2}M_\infty C_\infty\sin\theta\frac{\partial}{\partial\theta})\eta(\theta,\psi,t) - \eta(\theta,\psi,t)\left[\frac{3M_\infty C_\infty}{a}\cos\theta\right] \quad , \text{ at } r=a \qquad (5.1.7)$$

Equation (5.1.7) is the form of the general boundary condition (5.1.1) to be applied in the cases that follow. The two test case vibrations are now presented.

1A THE 'PULSATING' SPHERE

A 'pulsating' sphere is taken to be one whose centre remains fixed while its radius oscillates about the mean value r=a. In this case the surface displacement, η, will have no directional preference, and so will be a function of time only.

If the amplitude of the radial vibration is $a\varepsilon$ then the surface displacement, $\eta(t)$, can be written as: (see Fig. 11)

$$\eta(t) = a\varepsilon e^{i\omega t} \tag{5.1.8}$$

The equation of the 'pulsating' body surface being:

$$r = a + \eta(t) \tag{5.1.9}$$

Substituting equation (5.1.8) into the boundary condition (5.1.7) yields:

$$\frac{\partial\phi}{\partial r} = \varepsilon C_\infty \left[ika + 3M_\infty \cos\theta\right] e^{i\omega t} \quad , \quad \text{at } r=a \tag{5.1.10}$$

where $k = \frac{\omega}{C_\infty}$.

Equation (5.1.10) represents the boundary condition on a pulsating sphere within a mean flow.

Consider the boundary condition (5.1.10) written in the form:

$$\frac{\partial\phi}{\partial r} = f(\theta)e^{i\omega t} \quad , \quad \text{at } r=a \tag{5.1.11}$$

where $f(\theta) = \varepsilon C_\infty \left[ika + 3M_\infty \cos\theta\right]$ (5.1.12)

This condition can be converted to a no-flow boundary condition using Taylor's transformation:

$$(r_x, \theta_x, \psi_x, T) = \left(r, \theta, \psi, t + \frac{M_\infty}{C_\infty}\hat{\phi}\right)$$

Therefore

$$\frac{\partial\phi}{\partial r_x} = F(\theta_x)e^{i\omega T} \quad , \quad \text{at } r_x=a \tag{5.1.13}$$

where, with $\hat{\phi} \equiv \frac{\bar{\phi}}{U_\infty} = -\frac{3}{2} a \cos\theta_x$ at $r_x=a$; (5.1.14)

$$F(\theta_x) = f(\theta_x)\, e^{(3/2)ikaM_\infty \cos\theta_x} \tag{5.1.15}$$

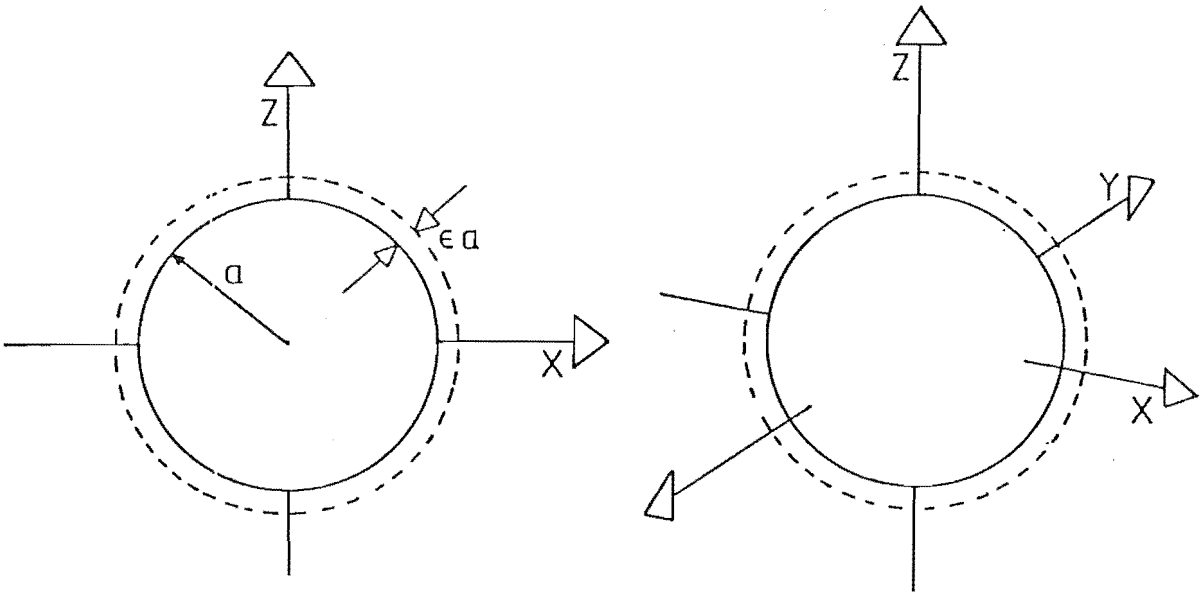

Figure 11. The pulsating sphere

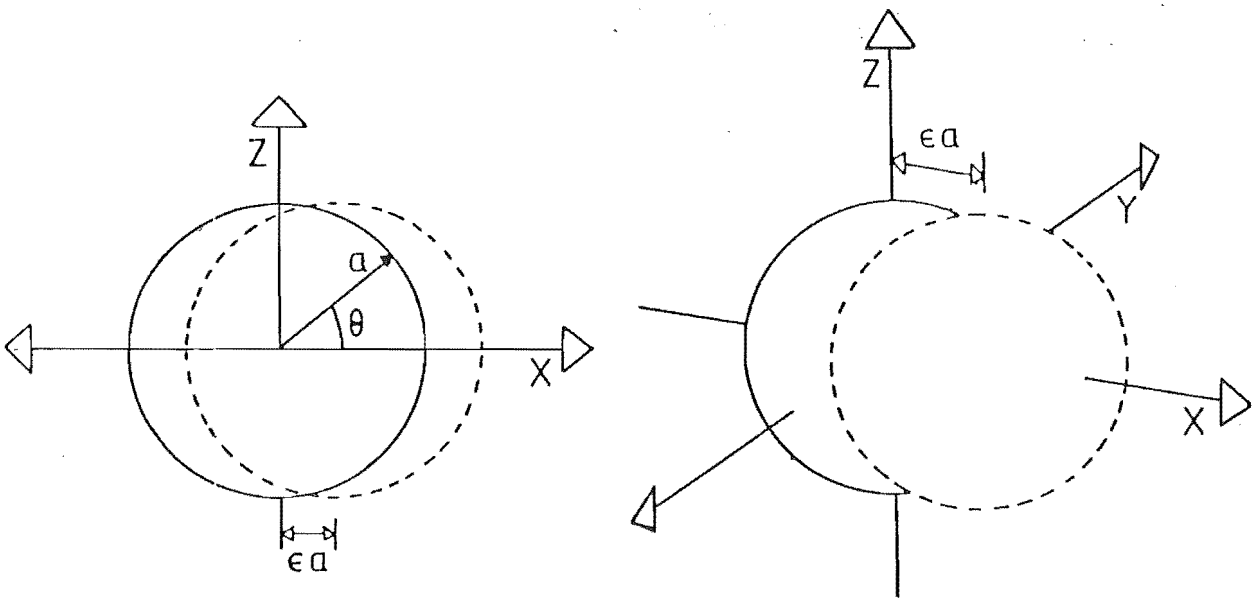

Figure 12. The juddering sphere

Using (5.1.12), equation (5.1.15) can be written as:

$$F(\theta_x) = \varepsilon C_\infty \left[ika + 3M_\infty \cos\theta_x\right] e^{(3/2)ikaM_\infty \cos\theta_x} \quad , \text{ at } r_x=a \qquad (5.1.16)$$

Equations (5.1.13) and (5.1.16) together represent the boundary condition to be applied on a pulsating sphere within a zero mean flow. This no-flow problem will reduce to solving the Helmholtz equation with boundary condition (5.1.16) alone.

Consider now the second test case vibration.

1B THE 'JUDDERING' SPHERE

A 'juddering' sphere is taken to be one whose radius remains fixed while its centre oscillates about the origin in the x coordinate direction.

If $a\varepsilon$ is the amplitude of the vibration along the x axis, then the normal surface displacement, $\eta(\theta,t)$, can be written as: (see Fig. 12)

$$\eta(\theta,t) = a\varepsilon \cos\theta \, e^{i\omega t} \qquad (5.1.17)$$

The equation of the juddering body surface being:

$$r = a + \eta(\theta,t) \qquad (5.1.18)$$

Substituting (5.1.17) into the boundary condition (5.1.7) gives:

$$\frac{\partial\phi}{\partial r} = \varepsilon C_\infty \left[ika\cos\theta - \frac{3}{2}M_\infty \sin^2\theta + 3M_\infty \cos^2\theta\right] e^{i\omega t} \quad , \text{ at } r=a \qquad (5.1.19)$$

Equation (5.1.19) represents the boundary condition on a juddering sphere within a mean flow.

As in the pulsating case this boundary condition can be written in the form:

$$\frac{\partial\phi}{\partial r} = f(\theta)e^{i\omega t} \quad , \text{ at } r=a \qquad (5.1.20)$$

$$\text{where } f(\theta) = \varepsilon C_\infty \left[ika\cos\theta - \frac{3}{2}M_\infty \sin^2\theta + 3M_\infty \cos^2\theta\right] \qquad (5.1.21)$$

The transformation of this boundary condition to a no-flow problem yields:

$$\frac{\partial \phi}{\partial r_x} = F(\theta_x)e^{i\omega T} \qquad \text{at } r_x = a \qquad (5.1.22)$$

where

$$F(\theta_x) = \varepsilon C_\infty \left[ika\cos\theta_x - \frac{3}{2}M_\infty \sin^2\theta_x + 3M_\infty \cos^2\theta_x \right] e^{(3/2)ikaM_\infty \cos\theta_x}$$

$$\text{at } r_x = a \qquad (5.1.23)$$

Thus, equations (5.1.22) and (5.1.23) together represent the boundary condition on a juddering sphere in a zero flow. As for the pulsating case, this problem will reduce to solving Helmholtz' equation with (5.1.23) being the Neumann boundary condition on the sphere.

From equations (2.1.3) and (2.1.4) the solution for the acoustic velocity potential on the surface of a vibrating sphere is:-

$$\phi = \Psi\, e^{(-3/2)ikaM_\infty \cos\theta}\, e^{i\omega t} \qquad (5.1.24)$$

where the function Ψ is a solution of the exterior Helmholtz equation, which satisfies one of the boundary conditions (5.1.16) and (5.1.23).

The solution of Ψ on the surface of a vibrating sphere is obtained using a boundary integral method. The CHIEF and BMF methods are the two methods chosen to solve for Ψ. The results of their numerical implementation (over a discretized sphere) will be presented in comparison with two alternative solution methods.

A brief outline of these alternative methods is given within the following two sections.

2. AN ANALYTIC SOLUTION

An 'exact' analytic solution for both the pulsating and juddering test cases has been given by Taylor[7].

This analytic solution, however, is valid for only a restricted range of frequencies.

In order to explain the deficiencies of Taylor's 'exact' solution a brief outline of its derivation, for time harmonic vibrations, is presented. The full details of the derivation for both a pulsating and juddering sphere are given in Appendix (L).

Taylor begins his derivation by introducing the surface displacement of a general vibration about a mean spherical surface of radius a. If the vibration is assumed to be time harmonic, the surface displacement will take the form:

$$\eta(\theta,\psi,t) = a\, e^{i\omega t} \sum_{n=0}^{\infty} \sum_{m=-n}^{n} E_n^m P_n^m(\cos\theta) e^{im\psi} \qquad (5.2.1)$$

where E_n^m is constant and P_n^m is the Legendre function of the first kind, m-th order and n-th degree. Equation (5.2.1) represents the form of a general solution to the spherical wave equation. The surface displacement given by (5.2.1) is then substituted into the boundary condition given by (5.1.7). The boundary condition, at r=a, will be of the form:

$$\frac{\partial \phi}{\partial r} = \frac{\partial \Phi}{\partial r} e^{i\omega t} \quad , \text{ at } r=a \qquad (5.2.2)$$

where, after some rearrangement,

$$\frac{\partial \Phi}{\partial r} = C_\infty \sum_{n=0}^{\infty} \sum_{m=-n}^{n} E_n^m \left[ika\, P_n^m(\cos\theta) - \frac{3M_\infty}{2(2n+1)} A_n^m(\cos\theta) \right] e^{im\psi}, \text{ at } r=a \qquad (5.2.3)$$

with $A_n^m(\cos\theta) \equiv (n-1)(n+m)P_{n-1}^m(\cos\theta) - (n+2)(n-m+1)P_{n+1}^m(\cos\theta)$

The problem is now converted to a no-flow problem using the transformation:

$$(r_x,\theta_x,\psi_x,T) = (r,\theta,\psi,t + \frac{M_\infty}{C_\infty}\hat{\phi}) \, .$$

Therefore, noting $\hat{\phi} = \frac{-3}{2} a \cos\theta_x$ on $r_x=a$, equation (5.2.2) becomes:

$$\frac{\partial \phi}{\partial r_x} = \frac{\partial \Phi}{\partial r_x} e^{(3/2)ikaM_\infty \cos\theta_x} e^{i\omega t}, \quad \text{at } r_x=a \qquad (5.2.4)$$

At this stage Taylor linearizes the boundary condition (5.2.4) with respect to the Mach number, M_∞. It is within this linearization process that inconsistencies first become apparent. In order to demonstrate the deficiencies of the analytic solution, the boundary condition (5.2.4) will be expanded up to terms containing M_∞^2.

The expansion of the exponential term in (5.2.4) implies the following boundary condition:

$$\frac{\partial\phi}{\partial r_x} = C_\infty e^{i\omega T} \sum_{n=0}^{\infty} \sum_{m=-n}^{n} E_n^m \Bigg[ika\, P_n^m(\cos\theta_x) \qquad \text{(a)}$$

$$- \frac{3M_\infty}{2(2n+1)} A_n^m(\cos\theta_x) \qquad \text{(b)}$$

$$- \frac{3}{2}(ka)^2 M_\infty \cos\theta_x\, P_n^m(\cos\theta_x) \qquad \text{(c)}$$

$$- \frac{9}{4} \frac{ikaM_\infty^2}{(2n+1)} \cos\theta_x\, A_n^m(\cos\theta_x) \qquad \text{(d)}$$

$$- \frac{9}{8}(ka)^3 M_\infty^2 \cos^2\theta_x\, P_n^m(\cos\theta_x) \Bigg] e^{im\psi x} \qquad \text{(e)}$$

$$+ \text{(terms containing higher powers of } M_\infty) \qquad (5.2.5)$$

The linearization process used by Taylor simply ranks the terms with respect to Mach number order alone. So that in the above equation (5.2.5), Taylor discards all the terms except those given by (a), (b) and (c). The magnitude of each term in (5.2.5) is now considered more closely.

If P_n^m denotes a typical reference value for the Legendre functions, then the terms (a), (b), (c), (d) and (e) will be of order:

$$\left[P_n^m\right](ka), \quad \left[P_n^m\right]M_\infty, \quad \left[P_n^m\right]M_\infty(ka)^2, \quad \left[P_n^m\right]M_\infty^2(ka)$$

and $\left[P_n^m\right]M_\infty^2(ka)^3$ respectively.

Therefore, the truncated equation containing terms (a), (b) and (c) will be valid only if the following conditions are satisfied:

$$\begin{aligned} &\text{(i)} && M_\infty^2 << 1 \\ &\text{(ii)} && M_\infty(ka) << 1 \\ &\text{(iii)} && M_\infty/(ka) << 1 \\ &\text{(iv)} && M_\infty(ka)^3 << 1 \end{aligned} \qquad (5.2.6)$$

The first condition, above, is just a requirement that the Mach number, M_∞, be small. The second and third conditions require both $M_\infty(ka)$ and $M_\infty/(ka)$ to be small. This will effectively exclude both large and small values of (ka). The third condition is equivalent to the condition used in the derivation of the original low Mach number approximation. Since the requirement that $M_\infty/(ka)$ be small will translate into the requirement that $M_\infty(\lambda/L_M)$ must be small (because λ is equal to $2\pi/k$ and L_M, the geometrical lengthscale is chosen as the sphere radius).

Therefore after considering the fourth condition, the truncation used by Taylor will be valid only if M_∞ is small and if (ka) is of order 1.

The truncated form of (5.2.5) will be implicit within the derivation of the analytic solution, hence the validity of this solution will also be restricted by the above conditions.

If it is assumed that the truncation of (5.2.5) is valid then the boundary condition can be written as:

$$\frac{\partial \psi}{\partial r_x} = \frac{\partial \Psi}{\partial r_x} e^{i\omega T} \qquad \text{on } r_x=a \tag{5.2.7}$$

where

$$\frac{\partial \Psi}{\partial r_x} = C_\infty \sum_{n=0}^{\infty} \sum_{m=-n}^{n} E_n^m \left[ikaP_n^m(\cos\theta_x) - \frac{3M_\infty}{2(2n+1)} A_n^m(\cos\theta_x) \right.$$

$$\left. - \frac{3}{2}(ka)^2 M_\infty \cos\theta_x P_n^m(\cos\theta_x) \right] e^{im\psi_x} \text{ , on } r_x=a \tag{5.2.8}$$

The function, Ψ, besides satisfying the boundary condition (5.2.8) at $r_x=a$, will also satisfy the exterior Helmholtz equation:-

$$(\nabla_x^2 + k^2)\Psi = 0 \tag{5.2.9}$$

Therefore the function Ψ can be written in the general form:

$$\Psi = \sum_{n=0}^{\infty} \sum_{m=-n}^{n} B_n^m h_n^{(2)}(kr_x) P_n^m(\cos\theta_x) e^{im\psi_x} \tag{5.2.10}$$

where B_n^m is constant and $h_n^{(2)}$ is the spherical Hankel function of the second kind and n-th order.

From equations (5.2.8) and (5.2.10) it is possible to solve for the constants B_n^m and hence eventually obtain a restricted solution for the acoustic field generated within a mean flow.

For the case of a pulsating sphere the analytic solution for the acoustic velocity potential is:-

$$\phi = \varepsilon \frac{C_\infty}{k} e^{-ikM_\infty(r+(a^3/2r^2))\cos\theta}\left[ika\frac{h_o^{(2)}(kr)}{h_o^{(2)'}(ka)} + \frac{3M_\infty}{2}(2-k^2a^2)\frac{h_1^{(2)}(kr)}{h_1^{(2)'}(ka)}\cos\theta\right]e^{i\omega t} \qquad (5.2.11)$$

For a juddering sphere the velocity potential is:-

$$\phi = \varepsilon \frac{C_\infty}{k} e^{-ikM_\infty(r+(a^3/2r^2))\cos\theta}\left[-\tfrac{1}{2}M_\infty k^2a^2\frac{h_o^{(2)}(kr)}{h_o^{(2)'}(ka)} + ika\frac{h_1^{(2)}(kr)}{h_1^{(2)'}(ka)}\cos\theta + \frac{M_\infty}{2}(3-k^2a^2)\frac{h_2^{(2)}(kr)}{h_2^{(2)'}(ka)}(3\cos^2\theta-1)\right]e^{i\omega t} \qquad (5.2.12)$$

Equations (5.2.11) and (5.2.12) are in fact the complex conjugates - with an opposite flow direction - of equations (47) and (64) of reference [7]. This arises from the initial assumption of time harmonic behaviour in the form $e^{+i\omega t}$ instead of $e^{-i\omega t}$.

In equation (64) of reference [7], the oscillation amplitude is given by the parameter, ε, while in (5.2.12) above this amplitude is given by $a\varepsilon$. This accounts for the extra a in the denominator of equation (64) within reference [7].

The complete derivation of equations (5.2.11) and (5.2.12) is given in appendix (L).

The following section describes another solution method.

3. AN ALTERNATIVE METHOD

The alternative method presented here is a modified finite element (FE) scheme.

The general problems associated with FE schemes and wave radiation in an infinite domain are summarised below.

The implementation of a conventional FE scheme to an unbounded domain presents immediate computational problems. In practice any computational domain must be of finite size. This will imply the existence of an outer surface S_R which must be completely absorbing. This requirement would be satisfied with the application of a Sommerfeld type radiation condition on S_R. However the Sommerfeld condition is valid only if the outer boundary

is a large distance from the radiating surface. In effect this outer boundary must be many wavelengths from the vibrating body. So any solution domain will contain many spatial wavelength variations. This will imply a fine mesh if the local wavelike nature of the solution is to be captured.

The implementation of a conventional FE scheme over this domain would be possible to implement two different schemes, one for each subregion. This is the usual FE procedure for modelling wave radiation into an unbounded domain.

Within the inner region a conventional FE scheme would be a logical choice. The scheme to be applied outside this inner region is, however, not so obvious. A discussion of the schemes applicable in the outer region is given below.

3A THE BOUNDARY INTEGRAL METHOD

This scheme involves the application of boundary integral methods within the outer region. In this case the outer field will be modelled by a distribution of source functions over a control surface which encloses the vibrating body. The impedance on this surface is then matched iteratively to the conventional FE solution in the inner region.

This method is fairly restrictive especially when a non-zero mean flow is assumed. In this case the control surface must be extended a sufficient distance from the body to ensure uniformity in the outer region. This is necessary for the valid application of the B.I. method within this region. So the use of a conventional FE scheme in this larger inner region will again be computationally impractical [15],[16]

3B THE 'INFINITE ELEMENT' METHOD

The infinite element scheme divides the outer region into a single layer of elements. The outer boundary is moved to infinity so that the elements will become infinite. This scheme includes the assumption of an exponentially decaying, outward travelling, wave-like variation in the shape functions. The assumption of exponential decay will ensure that the integrals involved in calculating the stiffness terms will be finite over an infinite domain. However this same assumption will violate the known asymptotic behaviour of the radiation at large distances from the vibrating body. Therefore the 'infinite element' method will be unreliable in predicting the far field radiation[21].

3C THE 'WAVE ENVELOPE' METHOD

In this case the outer region is subdivided into one or more layers of large but finite elements. In the outer region the basic functions are defined so as to incorporate a reciprocal decay and a wave-like variation corresponding to a locally outward travelling wave.

This scheme will incorporate the advantages of the infinite element method as well as providing accurate information in the far field.

Of the outer region schemes discussed above the 'wave envelope' method compares the most favourably. It is this 'wave envelope' scheme which has also been applied to the problem of radiation within a mean flow[22].

It must be noted that in the implementation of this method the full linearized acoustic field equation is used. There exist no low Mach number approximations apart from that of the initial linearization. This scheme will not exhibit any of the problems that are associated with B.I. methods at interior resonances.

The attractive advantages stated above are immediately overshadowed by the computational increase within three dimensional applications. The three-dimensional examples discussed in the references above are all axisymmetric, and so effectively represent a two dimensional example.

In conclusion the 'wave envelope' scheme will serve as a good comparison to the axisymmetric sphere used in this study. However the extension of the scheme to an arbitrary three-dimensional body would be computationally clumsy.

4. THE COMPUTED SOLUTION

This section will describe a specialisation of the boundary element method to the surface of a sphere. This is presented in the form of:

(i) a description of the discretization procedure;
(ii) a comment on the final appearance of the computed results.

The final part of this section will develop a modification of the 'exact' analytical solution. This modification is introduced in order to obtain a 'justifiable' comparison with the computed results. This is explained in more detail later.

4A DISCRETIZATION OF A SPHERE

For any body surface there will exist an infinite number of possible discretizations. In the present spherical test case an 'optimal' type of discretization has been generated. This 'optimal' surface is used purely for the assessment of the general solution method.

Obviously for the case of an arbitrary body there exist no rules for defining an 'optimal' discretization. However, in the case of a sphere, the discretization will be termed 'optimal' if:

(i) all the triangular elements are approximately equilateral and of similar size;
(ii) the variation in the radial distance to the nodal points from the model centre is a minimum.

A crude model which satisfies the above 'optimal' conditions exactly is the icosahedron (see [58] and Fig. 13).

4A.1 THE ICOSAHEDRON

The icosahedron has 20 equilateral faces of identical size. The 20 centroids or nodes corresponding to these faces are at the same radial distance from the model centre.

For an icosahedron the exact 'optimal' conditions are offset by the relative crudeness in its spherical approximation. Therefore a further discretization of the icosahedron is proposed.

At this stage it is convenient to define the centre of the discretized model as the origin of a spherical coordinate system. Thus, it is possible to define:

(i) the 'vertex radius' as the distance from the origin to the model's vertices;
(ii) the 'nodal radius' as the distance from the origin to a nodal point.

Two distinct refinements to the icosahedron are now presented.

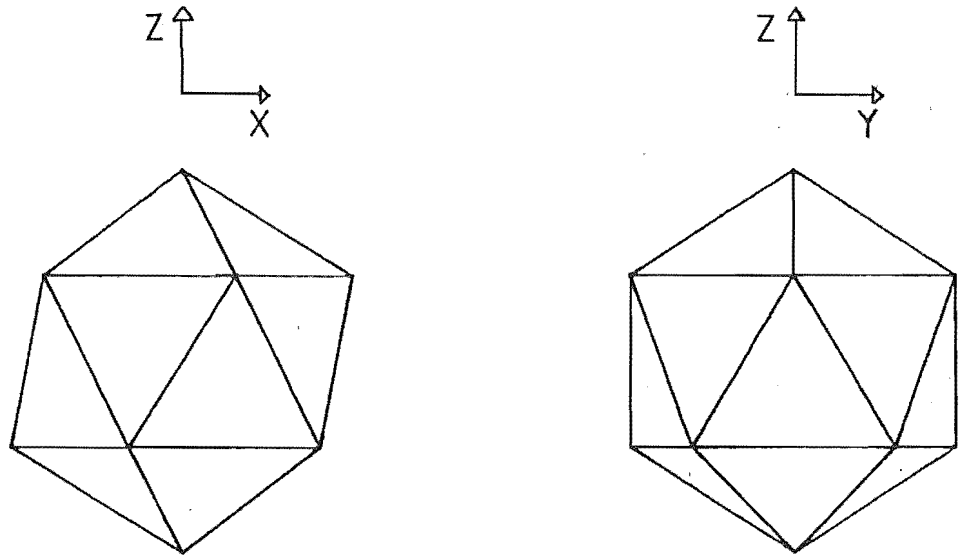

Figure 13. The icosahedron (20 elements)

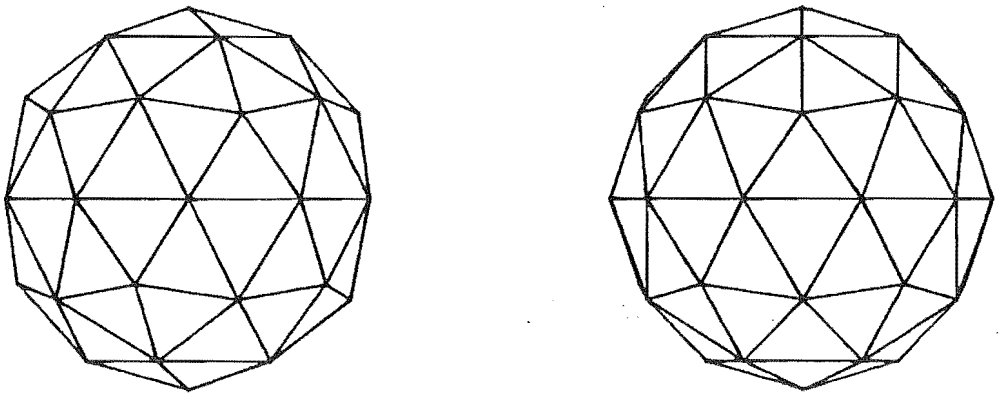

Figure 14. The '2-segment' discretization (80 elements)

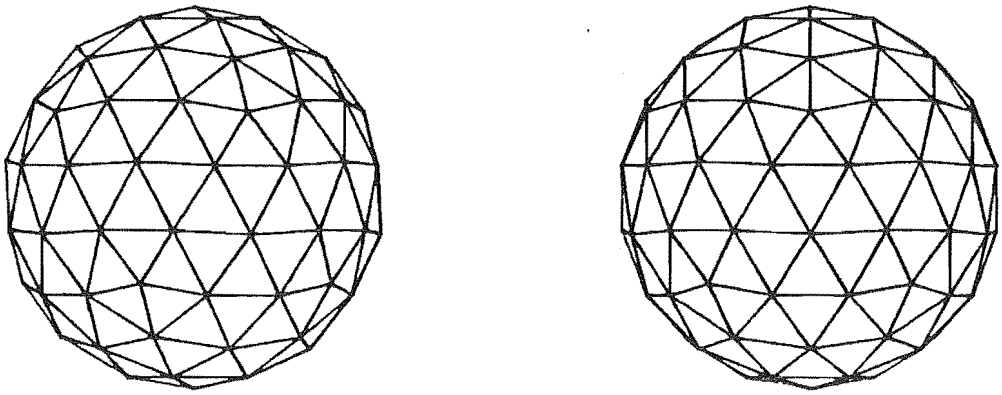

Figure 15. The '3-segment' discretization (180 elements)

4A.2 THE '2-SEGMENT' SUBDIVISION

In this refinement the edges of each face are divided into two equal lengths. The division point - the edge midpoint - is then projected radially outwards until its distance from the origin is equivalent to the icosahedron vertex radius.

Therefore each face of the icosahedron will be 'blown out' into 4 smaller triangles, 1 equilateral and 3 isoceles, (see Fig. 16a). These triangles will be of similar size and shape.

The resulting model will have 80 faces and hence 80 nodal points. Each of these nodal points will be at one of two possible radii. The two different radii correspond to the two different triangular elements.

If the nodal radius is non-dimensionalized with respect to the vertex radius then the two nodal radii will be given approximately as:

(i) $\hat{R}_1 \doteq 0.934172$, for the equilateral nodes
(ii) $\hat{R}_2 \doteq 0.944024$, for the isoceles nodes

These can be compared favourably with the nondimensional nodal radius, $\hat{R} = 0.794655$, of the icosahedron.

The change in mean nodal radius between the two models gives an indication of the improvement in the surface discretization (see Fig. 16).

In order to obtain a more accurate discretization it is possible to keep successively subdividing each new element into 4 smaller triangles. However one more '2-segment' subdivision would result in the number of surface elements increasing from 80 to 320. This number of elements would be computationally expensive and unnecessary.

A different refinement is now presented which subdivides each face of the icosahedron into 9 smaller triangles. A 180 element model results which is relatively inexpensive to implement.

4A.3 THE '3-SEGMENT' SUBDIVISION

In this refinement the edges of the icosahedron are subdivided into three lengths. The two division points are then projected outwards until their distance from the origin equals the vertex radius.

The subdivision can be performed by two methods; either

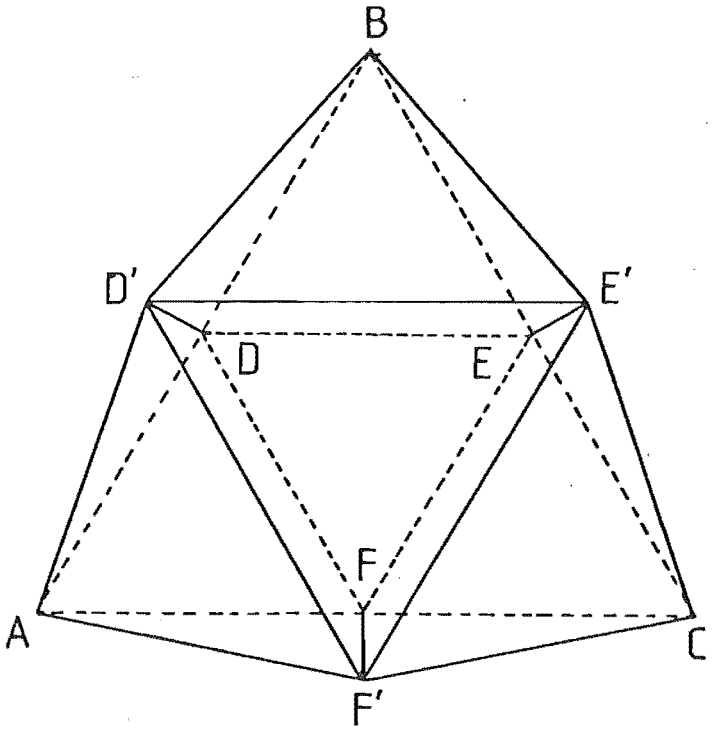

Figure 16(a). The '2-segment' subdivision of an icosahedron face, ΔABC

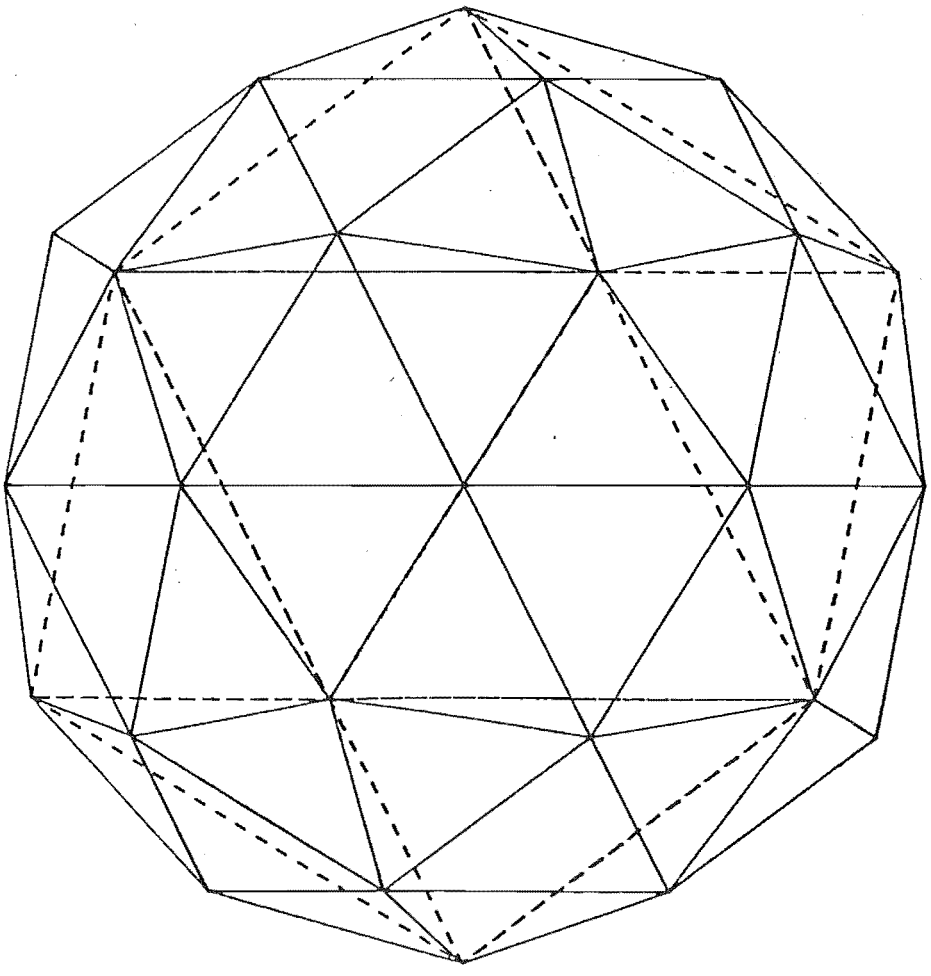

Figure 16(b). The '2-segment' model

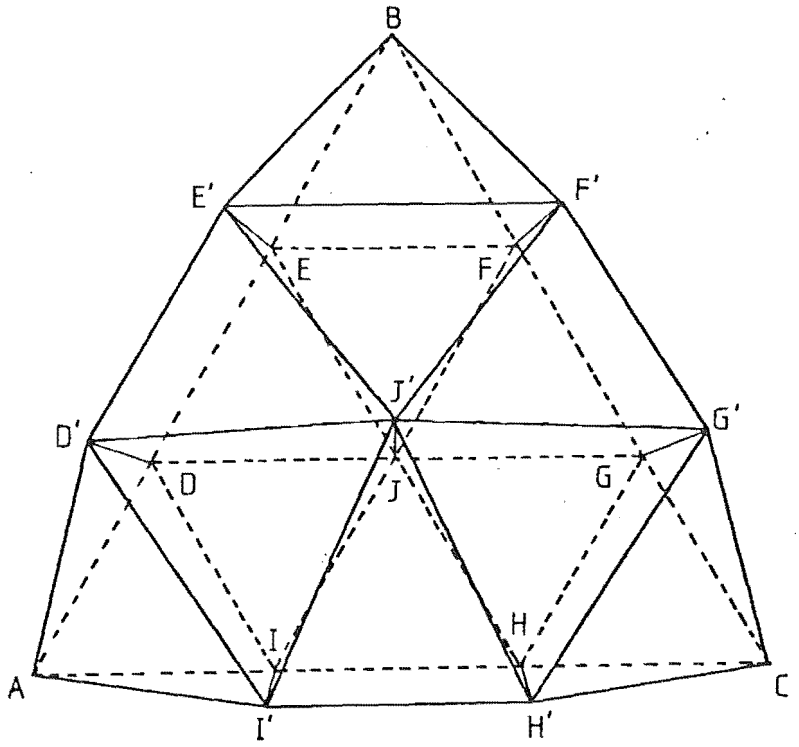

Figure 17(a). The '3-segment' subdivision of an icosahedron face, ΔABC

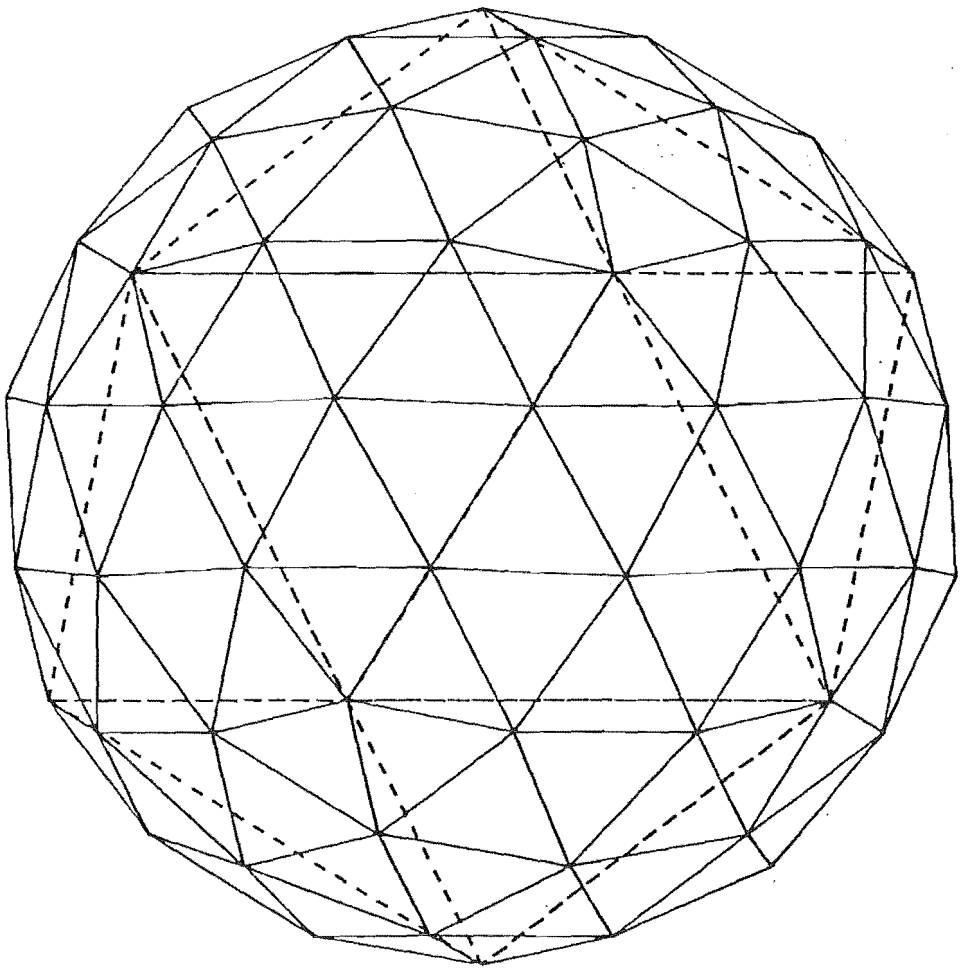

Figure 17(b). The '3-segment' model

(i) the edge is broken into 3 equal lengths, or

(ii) the edge is broken such that the 3 lengths represent equal spacing of the θ coordinate down the icosahedron edge.

Method (i) will result in a greater variation of triangle size rather than triangle shape, while method (ii) will have the reverse effect, [59].

Therefore in order to preserve the general triangular shape, method (i) will be the method applied here.

In this refinement each icosahedron face is subdivided into 9 smaller triangles, (see Fig. 15 and Fig. 17).

Of the 180 nodal points, there will only be 2 different nodal radii corresponding to 2 distinct isoceles triangles.

In non-dimensional form these can be written approximately as:

(i) $\hat{R}_1 \doteq 0.971653$, for the 6 inner triangles of Fig.17a

(ii) $\hat{R}_2 \doteq 0.977189$, for the 3 remaining corner triangles of Fig.17a

The relative effect of the above three surface discretizations will be demonstrated in a later section.

4B THE FORM OF THE SOLUTION

The acoustic potential on a vibrating sphere within a mean flow is given by equation (5.1.24). In discretized form this equation will be (after suppressing the time harmonic term);

$$\phi_j = \Psi_j \, e^{(-3/2)ika_jM_\infty\cos\theta_j} \quad , j=1,\ldots,N \qquad (5.4.1)$$

where the subscript j indicates the j-th nodal point. The values a_j and θ_j being the spherical polar coordinates of the j-th node. The spherical coordinates, (r,θ,ψ) are defined so that;

$$\begin{aligned} x &= r\cos\theta \\ y &= r\sin\theta\cos\psi \\ z &= r\sin\theta\sin\psi \ . \end{aligned} \qquad (5.4.2)$$

Ψ_j represents the nodal values of the function Ψ. This function Ψ satisfies the Helmholtz equation as well as a boundary condition at each nodal point.

It has been stated earlier and is reinforced by (5.4.2) that the mean flow propagates along the x axis towards negative infinity. This now raises the question regarding the orientation of the model with respect to the mean flow. The orientation becomes important when considering the variation in the computed solution over the surface. In this case it would be desirable to orientate the model in such a way so as to ensure an optimum number of nodes with a different θ value. Thus resulting in an optimum number of distinct solutions over the surface.

For the discretizations described above a maximum number of distinct solutions will be obtained when the axis of 'greatest symmetry' is perpendicular to the flow. This orientation is given in Figures 13, 14 and 15.

Now before discussing the presentation of the computed results, the following subsection will introduce a modification to the analytic solution.

4C A MODIFIED ANALYTIC SOLUTION

The surface discretizations mentioned above are typically assumed to represent a sphere of radius equal to the vertex radius. The analytic solution is usually evaluated on this modelled spherical surface. The computed results are evaluated, using equation (5.4.1), at discrete nodal points on the discretized surface. These nodal points can be thought of as approximating an inner sphere of radius equal to the mean nodal radius.

A discrepancy now becomes obvious. It is difficult to justify a comparison between the computed results, evaluated at the nodal points, and the analytic results, evaluated at corresponding positions above the nodal points.

A method of resolving this discrepancy is described below. The basic idea consists of equating the volume velocities (at each node) of both the discrete surface and the inner surface, on which the analytic solution is evaluated.

The procedure involves first solving for the analytic solution on the inner sphere. The non-dimensional (ND) vibration amplitude of this sphere is equated to the ND vibration amplitude of the discretized surface at the nodal points.

The volume velocity of a vibrating sphere can be written as the product of the vibration amplitude and the spherical surface area. Therefore in order that the inner sphere have the same volume velocity as the discrete model, the ND vibration amplitude of the inner sphere is multiplied by a ratio of surface areas. That is:

$$\varepsilon = \frac{S_d}{4\pi a^2} \varepsilon_N \qquad (5.4.3)$$

where a is the mean nodal radius representing the radius of the inner sphere, S_d is the total surface area of the discretized model and the ND vibration amplitude ε_N is the ND vibration amplitude of both the nodal points and the inner sphere.

Therefore after evaluating the analytic solution on the surface of the inner sphere, it is then multiplied by the ratio of surface areas given in (5.4.3).

5. THE PRESENTATION OF RESULTS

Once the nodal values of the acoustic velocity potential have been computed their presentation will take the form of:

(a) plots of the real, imaginary and absolute values of $\frac{\phi}{\varepsilon C_\infty}$ at the surface. These values are plotted against the coordinate θ, where θ is defined in equation (5.4.2).

The boundary element solutions will be plotted at discrete points corresponding to distinct nodal positions. The 'wave envelope' solutions and the adjusted analytic solutions will be plotted as continuous curves.

(b) contours of $|\frac{\phi}{\varepsilon C_\infty}|$ plotted over the surface of the discretized model. These contour lines will be plotted at equal increments.

The first type of plot, i.e. (a) above, will give a concise comparison between the computed values and those values obtained from alternative methods. The second type of presentation will serve to illustrate the nature of the solution over the discretized surface.

The procedure by which the contour plots are generated is outlined below.

The first step of the procedure is to shift the absolute values of the potentials from the nodal points to the vertices. This is done by assigning to each vertex an average potential. This potential represents the average of those elements that surround the vertex in question.

Each triangular element will therefore have three absolute values represented at its three vertices. These three values, and hence the three vertices, are now ranked in order of magnitude. At this stage the contour increments are chosen. Each increment is considered with regard to the three potential values of each triangular element. If the increment lies between two of the three potentials then two triangle edges will be cut and the contour will travel through the element.

Having decided whether or not a contour will cut an edge it is then necessary to compute the position of the cut. This point of intersection can be evaluated by interpolating linearly over the edge in question.

When the above procedure has been carried out over each element for each incremental value a plot of contour lines will be generated over the discretized surface.

6. THE RESULTS

6A INTRODUCTORY COMMENT

This section presents solutions for the acoustical field generated by a pulsating or juddering sphere in a uniform mean flow. Two different boundary integral formulations have been used to obtain these results.

The CHIEF boundary integral method is presented as a particular case of the residual least-squares procedure defined in Chapter 4 and Appendix K. This least-squares procedure is to be applied for three different values of the weighting factor, α. The value of this factor determines the relative weighting of the surface and interior formulations. In this case the values $\alpha=0$, $\alpha=\frac{1}{2}$ and $\alpha=1$ represent three different weightings of the matrix equation (4.3.14). If $\alpha=0$ the solution of (4.3.14) will be identical to the solution of the interior Helmholtz integral equation. If $\alpha=1$ the solution will correspond to that of the surface integral equation and if $\alpha=\frac{1}{2}$ equal weighting will be given to both formulations.

In the present application the interior points are located a distance γ_i along the inward normal from the centroid of the i-th element. The value of γ_i is taken as one half the distance from the i-th centroid to one of the vertices of the same element. Since the triangular elements are all nearly equilateral in shape this value of γ_i is approximately one third the height of each triangle. This choice of γ_i was found to produce good results, as will be shown later.

The other formulation for which results are obtained is the formulation due to Burton and Miller (BMF).

The BMF method is represented by equation (4.4.1) as

$$\int_S \Psi(Q) \frac{\partial G(P,Q)}{\partial n_q} dS_q + \alpha \int_S [\Psi(Q) - \Psi(P)] \frac{\partial^2 G(P,Q)}{\partial n_p \partial n_q} dS_q$$

$$+ \alpha\Psi(P) \int_S (\underline{n}_p . \underline{n}_q) k^2 G(P,Q) dS_q - \tfrac{1}{2}\Psi(P)$$

$$= \int_S G(P,Q) \frac{\partial \Psi(Q)}{\partial n_q} dS_q + \alpha \int_S \frac{\partial G(P,Q)}{\partial n_p} \frac{\partial \Psi(Q)}{\partial n_q} dS_q + \tfrac{1}{2}\alpha \frac{\partial \Psi(P)}{\partial n_p} \qquad (5.6.1)$$

If the free-space Green's function, G(P,Q) is written in the form:

$$G(P,Q) = \frac{e^{-ikr}}{4\pi r} \qquad (5.6.2)$$

where $r \equiv r(P,Q)$ is the distance between points P and Q, then the double derivative within the second integral of equation (5.6.1) can be written as; (see appendix M)

$$\frac{\partial^2 G(P,Q)}{\partial n_p \partial n_q} = \frac{e^{-ikr}}{4\pi r} \left\{ \left[(ik)^2 + \frac{3ik}{r} + \frac{3}{r^2} \right] \frac{\partial r}{\partial n_p} \frac{\partial r}{\partial n_q} + \frac{1}{r}(ik + \frac{1}{r})(\underline{n}_p . \underline{n}_q) \right\} \qquad (5.6.3)$$

Therefore substituting (5.6.3) into (5.6.1) yields:-

$$-\tfrac{1}{4\pi} \int_S \Psi(Q) \frac{e^{-ikr}}{r}(ik + \frac{1}{r}) \frac{\partial r}{\partial n_q} dS_q - \alpha \frac{\Psi(P)}{4\pi} \int_S (\underline{n}_p . \underline{n}_q)(ik)^2 \frac{e^{-ikr}}{r} dS_q$$

$$- \tfrac{1}{2}\Psi(P) + \frac{\alpha}{4\pi} \int_S [\Psi(Q) - \Psi(P)] \frac{e^{-ikr}}{r} \left\{ \left[(ik)^2 + \frac{3ik}{r} + \frac{3}{r^2} \right] \frac{\partial r}{\partial n_p} \frac{\partial r}{\partial n_q} \right.$$

$$\left. + \frac{1}{r}(ik + \frac{1}{r})(\underline{n}_p . \underline{n}_q) \right\} dS_q = \tfrac{1}{4\pi} \int_S \frac{\partial \Psi(Q)}{\partial n_q} \frac{e^{-ikr}}{r} dS_q$$

$$- \frac{\alpha}{4\pi} \int_S \frac{\partial \Psi(Q)}{\partial n_q} \frac{e^{-ikr}}{r} (ik + \frac{1}{r}) \frac{\partial r}{\partial n_p} dS_q + \tfrac{1}{2}\alpha \frac{\partial \Psi(P)}{\partial n_p} \qquad (5.6.4)$$

This equation represents the form of the BMF method to be applied in the present problem. In this application the values of Ψ are assumed constant over each plane element, hence the third integral of equation (5.6.4) will conveniently vanish whenever the singularity and integration points are within the same element.

Equation (5.6.4) is effectively the same as that used by Meyer et al. [34], the only difference being in the representation of the Green's function. However, it must be noted that although Meyer et al. start from the same boundary integral equation their method of numerical implementation is very different.

In reference [34], Meyer et al. start with the 80 element (2-segment) discretization inscribed within a unit sphere. Unlike a boundary element scheme, where the singularity and integration points lie in the plane of the faceted elements, Meyer et al. project these points on to the spherical surface. In this case three quarters of the singularity points will be offset from the centroid of each curved triangular element, (see Fig. 16).

It has been stated earlier (and proved in Appendix I) that if equation (5.6.4) is to yield a unique solution then the complex coupling constant α must have a non-zero imaginary part. This is the only formal restriction imposed on the choice of the complex coupling constant. Thus the value of α is often taken as simply the complex number i. However, as mentioned within section 5 of Chapter 3, some of the terms which contain the coupling constant α are of order k^2. This implies that for large values of wavenumber, k, equation (5.6.4) would be at risk of becoming weighted in favour of the normal derivative formulation. This weighting would be particularly undesirable in the case when the wavenumber corresponds to an eigenwavenumber of the same implicit formulation. This problem can be resolved by setting $\alpha = \frac{i}{k}$, this is in fact the coupling constant used by Meyer et al. in reference [25].

In the BMF method used here both values of the coupling constant (i.e. $\alpha = i$ and $\alpha = \frac{i}{k}$) will be utilized.

In comparison with the residual least-squares procedure, the BMF equation, (5.6.4), is more demanding in its implementation. This is because some of the integrations in (5.6.4) will require the value of the normal vector at each singularity point. The residual least-squares procedure is, however, computationally more expensive. This arises from the fact that the final matrix equation must be reformulated for each weighting factor.

The use of three weighting factors is necessary to check the validity of the CHIEF method. For example, if the interior points are 'safely' positioned the interior method will produce results of the same accuracy as the CHIEF method.

Results are presented below for the cases ka = 3.1 (for the pulsating sphere) and ka = 4.5 (for the juddering sphere). These values are close to resonance for monopole and dipole interior fields (interior resonances are given by ka = π and ka = 4.493 respectively). Each of these cases will be considered for mean flows of Mach number, 0.0, 0.1 and 0.3.

The results will be compared with the adjusted analytic solution described in Chapter 5. As discussed earlier this analytic solution will be valid only when M_∞ is small and the parameter (ka) is of order 1. For the pulsating and juddering sphere solutions presented in this section the value of $M_\infty(ka)$ ranges from 0 to 1.35. For values of $M_\infty(ka)$ greater than approximately 0.5 the computed results and the analytic solution will be shown to diverge significantly. This does not suggest, however, that the boundary element scheme is giving poor results at these values. The requirement that $M_\infty(ka)$ be small is purely a condition imposed during the derivation of the analytic solution. The validity of the boundary element scheme at these higher frequencies is in fact strongly indicated by a comparison with results obtained from an alternative numerical scheme. This alternative scheme is based on a combined finite element, wave envelope formulation which makes no assumption about the Mach number or frequency. It will be demonstrated below that at the higher values of $M_\infty(ka)$ good agreement still exists between the boundary element results and those of the alternative numerical scheme.

A quantitative comparison between the computed results and the analytic solution is given as an average percentage error. This percentage error is calculated using the following formula:

$$\text{Percentage error} = 100 \times \left[\frac{\sum_{i=1}^{N} \left| Z_i^A - Z_i^C \right|}{\sum_{i=1}^{N} \left| Z_i^A \right|} \right] \qquad (5.6.5)$$

where Z_i^A is the value of the analytic solution at the i-th node

Z_i^C is the computed boundary element solution at the i-th node,

and both these values are complex. N is the total number of elements or nodes.

The boundary element solutions are obtained using two distinct integration schemes over each triangular facet. One scheme being applied to the 'off-diagonal' integrations and the other to the more critical 'diagonal' integrations. The two schemes chosen initially are both due to Cowper [57]. A 6-point, 4-th degree rule is applied to the 'off-diagonal' integrations (see table 1 and Fig. 6), while a 12-point, 6-th degree rule is applied to the 'diagonal' integrations, (see table 2 and Fig. 7). For the triangular elements and the frequencies considered in the present problem the above integration schemes will be shown to yield adequate results. A specific integration scheme that accounts for the singularity within each 'diagonal' integration is also presented. This scheme contains 42 points and will produce improved results. However for the formulations considered in this problem the results indicate that the introduction of this specialized scheme will be unnecessary.

Initially results will be considered for the 80 element (2-segment) discretization of the spherical surface. This is the same model which has been considered by both Chen and Schweikert [27] and Meyer et al. [34]. The 180 element (3-segment) discretization will be introduced later in order to demonstrate the expected convergence of results due to the surface refinement. This will be presented for the specific case of ka = 4.5 and M_∞ = 0.3

6B DISCUSSION OF RESULTS

The zero-Mach number problem is presented first. A pulsating sphere is considered for ka = 3.1 and M_∞ = 0.0. In this case good agreement exists between the analytic solution and both the CHIEF and BMF methods. (see Figures 18a, b and c). The relative errors between the analytic solution and the computed results are given in table 4 . Both the CHIEF and BMF (α=i) methods appear more accurate than the BMF ($\alpha=\frac{i}{k}$) method.

A 16-point 'diagonal' integration rule due to Irons [55] was found to produce an error comparable to Cowper's 12-point rule (see table 4). To test the relative improvement expected from a more refined 'diagonal' integration rule, a 42 point scheme (see Fig. 9 and table 4) was introduced to the BMF ($\alpha=\frac{i}{k}$) method. The scheme resulted in the percentage error decreasing from 5.7% to 3.5%. The error now becoming comparable with that of CHIEF.

The results for the conventional surface integral formulation (see Fig 18a) are obviously in error, as might be expected given that the frequency for which these results are obtained is close to an interior resonance. For the case of a juddering sphere at ka = 4.5 and M_∞ = 0.0 similar conclusions can be drawn.

The BMF method is considered for the case of low Mach number flow i.e. M_∞ = 0.1. The percentage errors for the cases of a pulsating sphere (ka = 3.1) and a juddering sphere (ka = 4.5) are given in table 6 . For this low Mach number flow the plotted results are still close to the analytic solution (see Figures 20 and 21). In the juddering sphere problem (M_∞(ka) = 0.45) the error is reduced from 18% to 12% when the coupling constant α=i is replaced by $\alpha=\frac{i}{k}$. For this higher wavenumber case the BMF($\alpha=\frac{i}{k}$) method would be preferred over the BMF(α=i) method.

For the relatively high Mach number case, i.e. M_∞ = 0.3, both the BMF and the CHIEF boundary element formulations produce results which are in poor agreement with the analytic solution (see Figures 22 and 23).

For the pulsating and juddering spheres the values of M_∞(ka) are 0.93 and 1.35 respectively. Both these values are outside the small parameter limit required by the analytic solution. It is significant, therefore, that the 'equal weighting' CHIEF method corresponds closely with the finite element solutions, (see Figures 22a and 23a). For the pulsating sphere, (ka = 3.1), the CHIEF method follows the finite element, wave envelope solution very closely. Both the BMF (α=i) and BMF ($\alpha=\frac{i}{k}$) methods also give reasonable solutions (see Figures 22b and c). In the case of the juddering sphere (ka = 4.5) the BMF ($\alpha=\frac{i}{k}$) method shows a marked improvement over the BMF (α=i) method (see Figures 23c and 23d). The CHIEF method again follows the finite element solution closely.

For the present 80 element discretization with M_∞ = 0.3 the BMF ($\alpha=\frac{i}{k}$) method is used to produce contour plots of $|\frac{\phi}{\varepsilon C_\infty}|$ over the surface of the model, (see Figures 24 and 25).

The 180 element (3-segment) discretization is now introduced as a final check on the convergence of both methods. The relatively high frequency, high Mach number problem (ka = 4.5, M_∞ = 0.3) is considered. The plots of the BMF ($\alpha=\frac{i}{k}$) results converge, as expected, towards the CHIEF results and for this discretization both the BMF ($\alpha=\frac{i}{k}$) and CHIEF solutions follow the finite element solution very closely, (see Figure 26). A contour plot over the 180 element surface is given for the BMF ($\alpha=\frac{i}{k}$) method (see Figure 27).

VI CONCLUSIONS

A boundary element technique has been applied to the acoustical radiation problem in a non-uniform, low Mach number flow.

The analysis and results presented in this work indicate, for low Mach number flows, that a transformed boundary element scheme will offer a relatively simple and computationally inexpensive formulation for the prediction of acoustical radiation in non-uniform flows. A comparison of computed results with those from analytic solutions, where applicable, and an alternative numerical (FE) scheme confirm the validity and accuracy of the present approach. The transformation of the problem, prior to analysis, into an analogous no-flow problem is shown to be valid in the short wavelength limit hence lending itself to aeroacoustic applications.

The two boundary integral formulations considered were the CHIEF and BMF methods. The CHIEF method appears to give the more accurate results for the present choice of interior points. However, in order to check the validity of this method it must be applied as part of a less efficient residual least-squares procedure. The Burton and Miller formulation, with coupling constant $\alpha = \frac{i}{k}$, is shown to produce consistently good results for the wavenumbers considered. This method - although presently not as accurate as CHIEF - is computationally less expensive than the residual least-squares procedure and does not rely on the 'safe' positioning of the interior points. Overall the BMF ($\alpha = \frac{i}{k}$) method appears to be the most reliable and efficient boundary integral scheme for high frequency aeroacoustic applications. For both methods the computed results converge on introducing more refined numerical integrations and higher order surface discretizations.

Although demonstrated only for a simple spherical test case the above approach may clearly be applied to an arbitrarily shaped body without incurring a significant increase in computational cost.

TABLE 4

Pulsating sphere: ka = 3.1, M_∞ = 0.0

(i) Integration scheme:
'off-diagonal' : 6-point, 4-th degree (see Fig. 6, Table 1)
'diagonal' : 12-point, 6-th degree (see Fig. 7, Table 2)

Method	Coupling Constant	Percentage Error
BMF	$\alpha = i$	5.7310
	$\alpha = \frac{i}{k}$	3.9742
	Weighting factor	
Interior	$\alpha = 0$	3.3725
CHIEF	$\alpha = \frac{1}{2}$	3.1507
Surface	$\alpha = 1$	70.9098

(ii) Integration scheme:
'off-diagonal' : 6-point, 4-th degree
'diagonal' : 16-point, 7-th degree (see Fig. 5, Table 3)

Method	Coupling Constant	Percentage Error
BMF	$\alpha = \frac{i}{k}$	5.1012

(iii) Integration scheme:
'off-diagonal' : 6-point, 4-th degree
'diagonal' : 42-point, (see Fig. 9, Table 1)

Method	Coupling Constant	Percentage Error
BMF	$\alpha = \frac{i}{k}$	3.5030

TABLE 5

Juddering sphere : ka = 4.5, M_∞ = 0.0

(i) Integration scheme

'off-diagonal' : 6-point, 4-th degree

'diagonal' : 12-point, 6-th degree

Method	Coupling Constant	Percentage Error
BMF	$\alpha = i$	6.4180
	$\alpha = \frac{i}{k}$	9.1809
	Weighting Factor	
Interior	= 0	4.6437
CHIEF	= ½	4.5440
Surface	= 1	*

* Percentage error greater than or equal to 1000

TABLE 6

Pulsating sphere : ka = 3.1, M_∞ = 0.1

Integration scheme:
'off-diagonal' : 6-point, 4-th degree
'diagonal' : 12-point, 6-th degree

Method	Coupling Constant	Percentage Error
BMF	$\alpha = i$	4.2547
	$\alpha = \frac{i}{k}$	5.7332

TABLE 7

Juddering sphere : ka = 4.5, M_∞ = 0.1

Integration scheme:
'off-diagonal' : 6-point, 4-th degree
'diagonal' : 12-point, 6-th degree

Method	Coupling Constant	Percentage Error
BMF	$\alpha = i$	18.4328
	$\alpha = \frac{i}{k}$	12.0514

In the surface potential plots which follow, a circle represents the absolute value, a square the real part and a diamond the imaginary part of $\frac{\Phi}{\varepsilon C_\infty}$.

The thin line drawn on all plots represents the adjusted analytic solution. The dashed line drawn on the relatively high Mach number plots represents the finite element, wave envelope solution.

Figure 18. Surface potential, pulsating sphere, ka = 3.1, M_∞ = 0.0

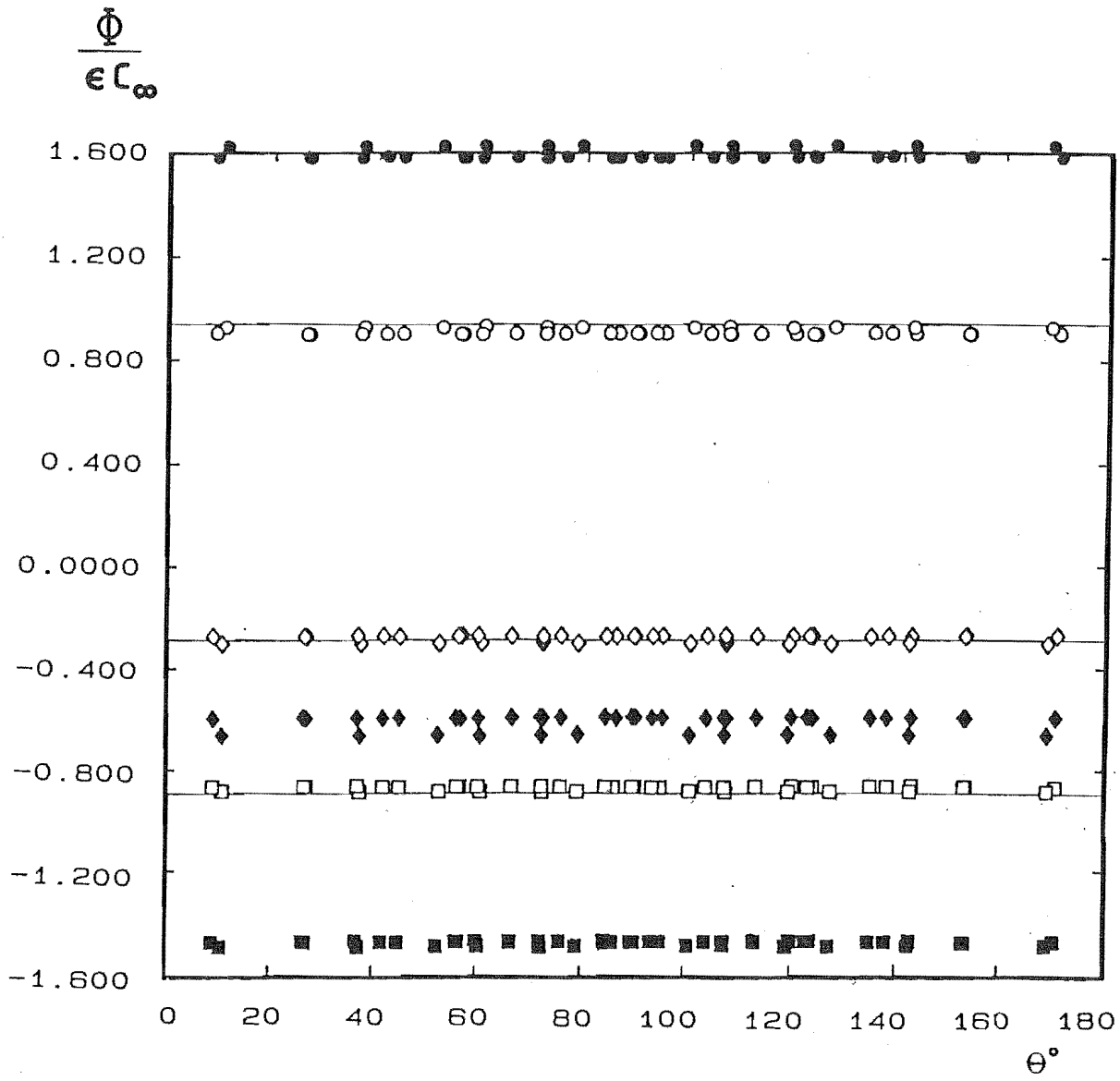

Figure 18(a). The surface Helmholtz and CHIEF solutions

- ○ - absolute value (CHIEF)
- □ - real part (CHIEF)
- ◇ - imaginary part (CHIEF)
- ● - absolute value (surface Helmholtz)
- ■ - real part (surface Helmholtz)
- ◆ - imaginary part (surface Helmholtz)

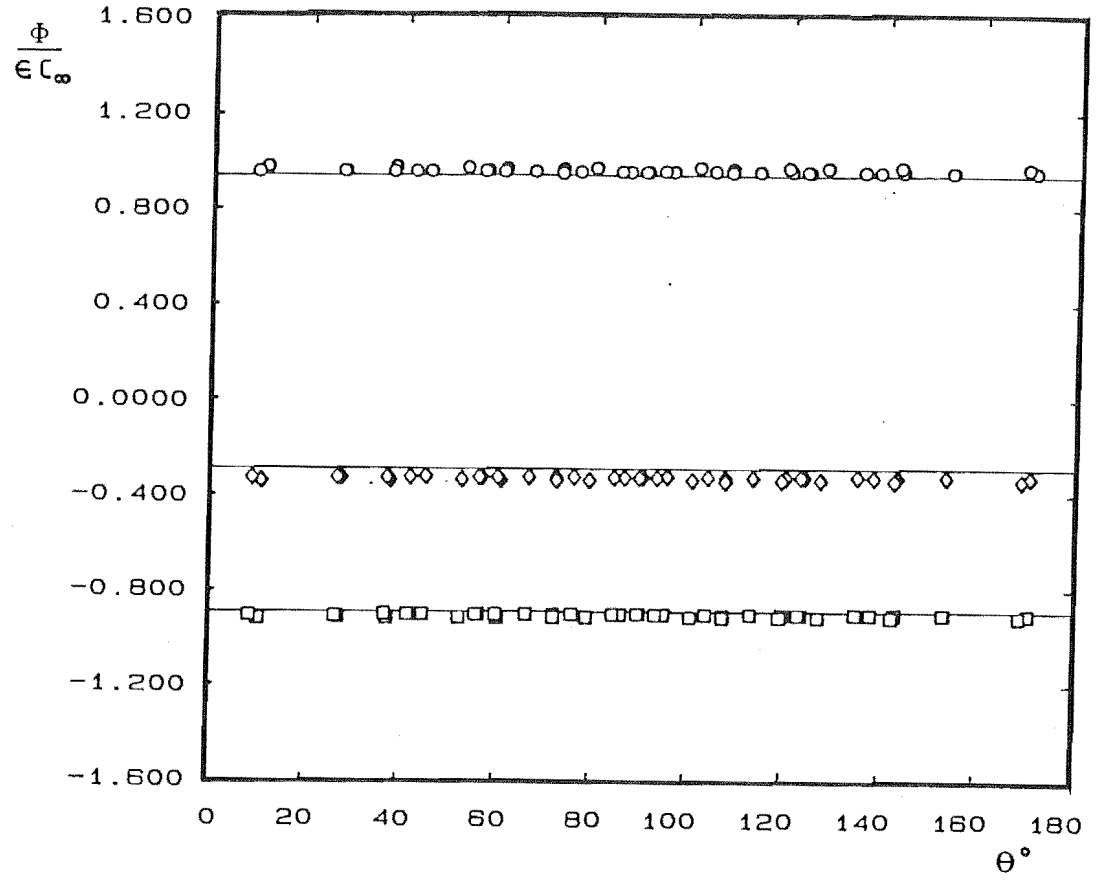

Figure 18(b). The BMF solutions, coupling constant $\alpha = i$

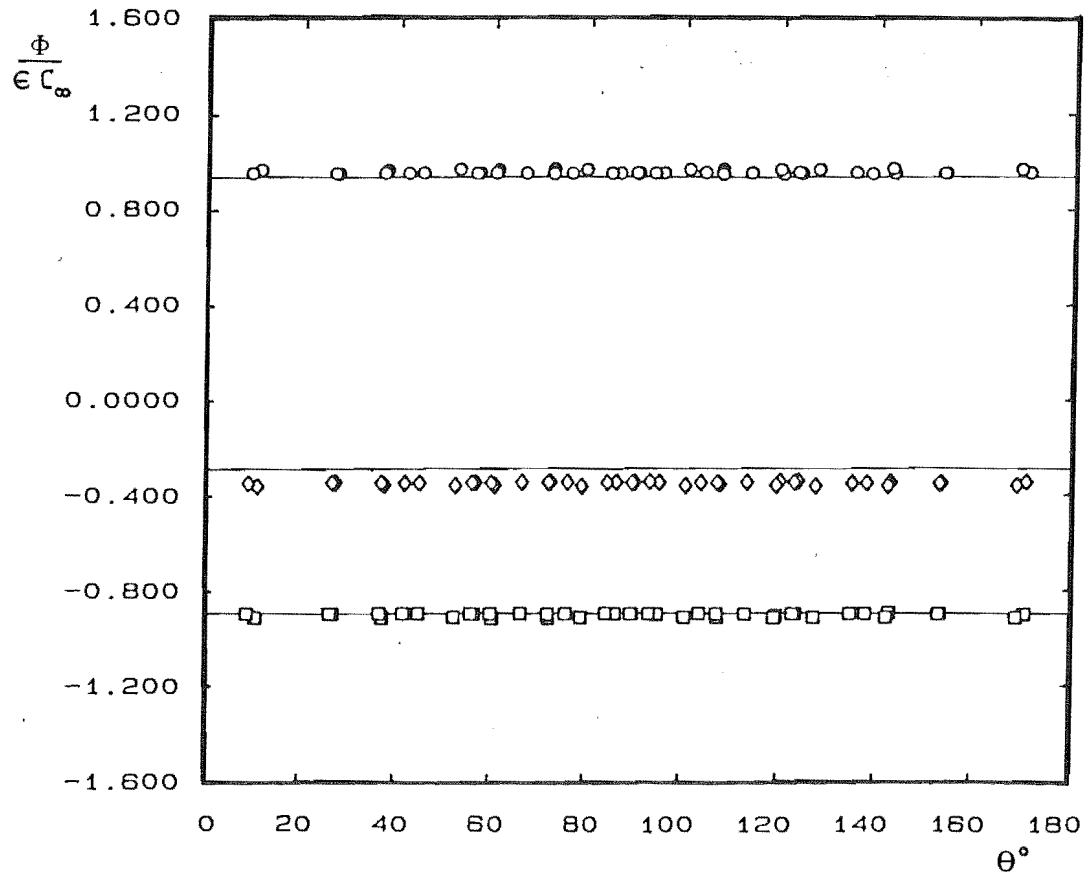

Figure 18(c). The BMF solutions, coupling constant $\alpha = \frac{i}{k}$

Figure 19. Surface potential, juddering sphere, ka = 4.5, M_∞ = 0.0

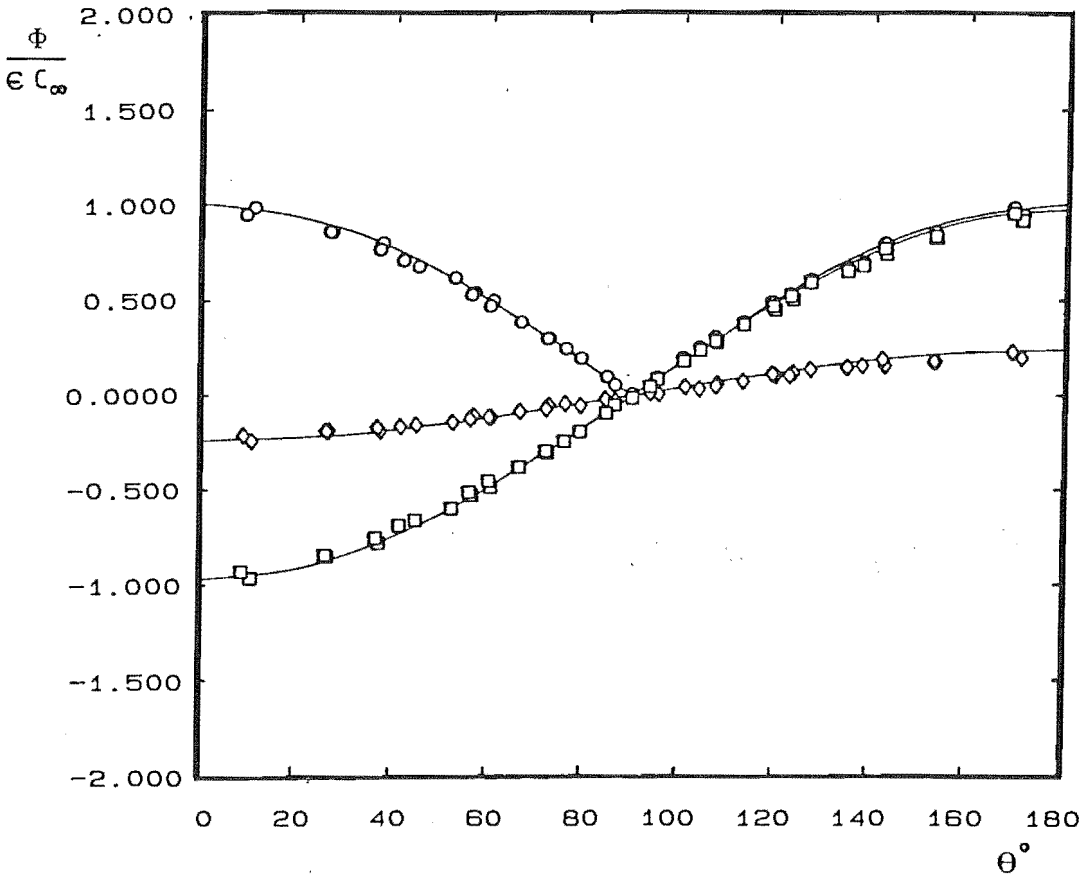

Figure 19(a). The CHIEF solutions

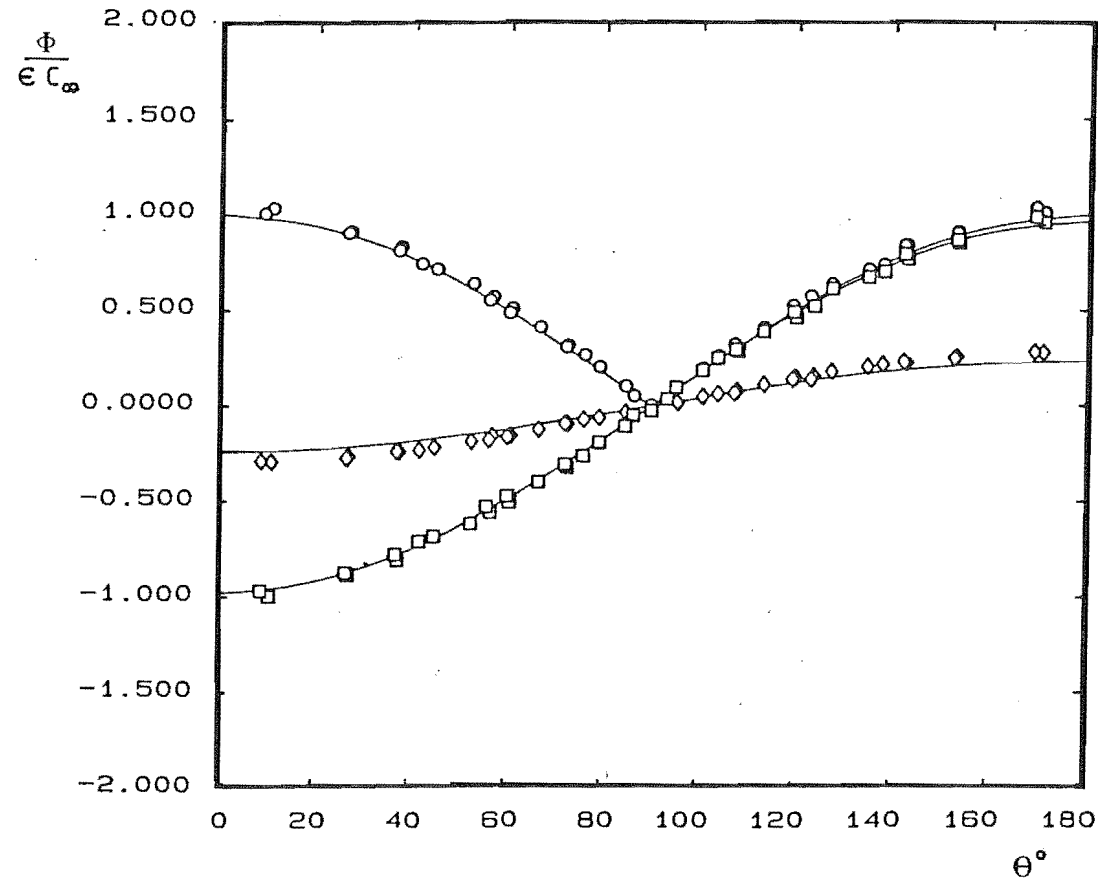

Figure 19(b). The BMF solutions, coupling constant $\alpha = i$

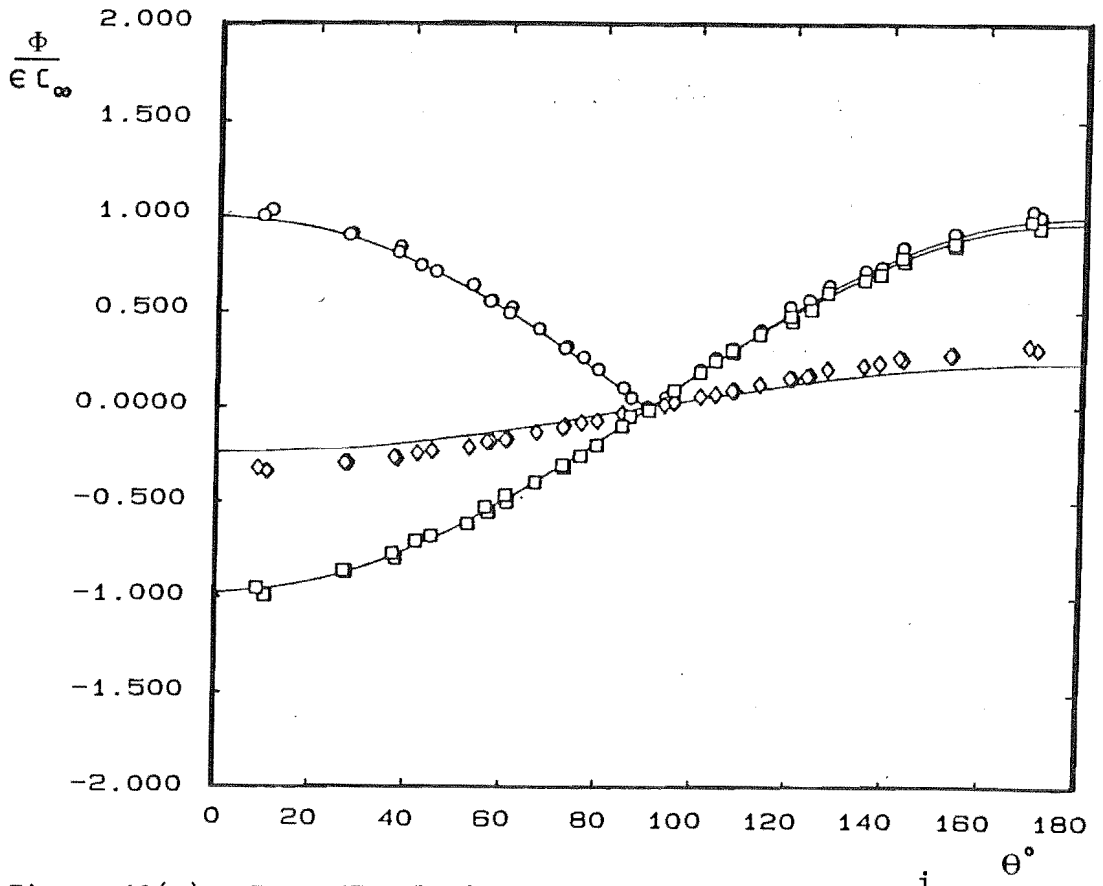

Figure 19(c). The BMF solutions, coupling constant $\alpha = \frac{i}{k}$

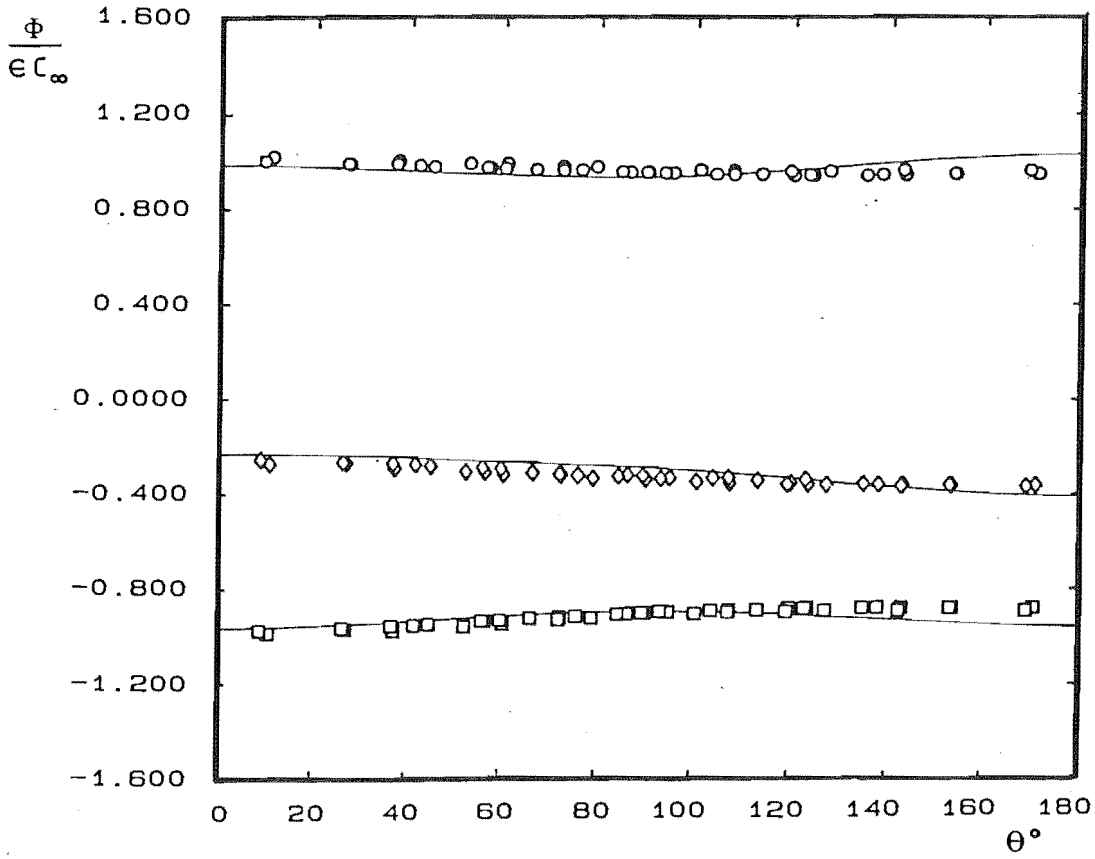

Figure 20. Surface potential, pulsating sphere, ka = 3.1, M_∞ = 0.1
20(a). The BMF solutions α = i

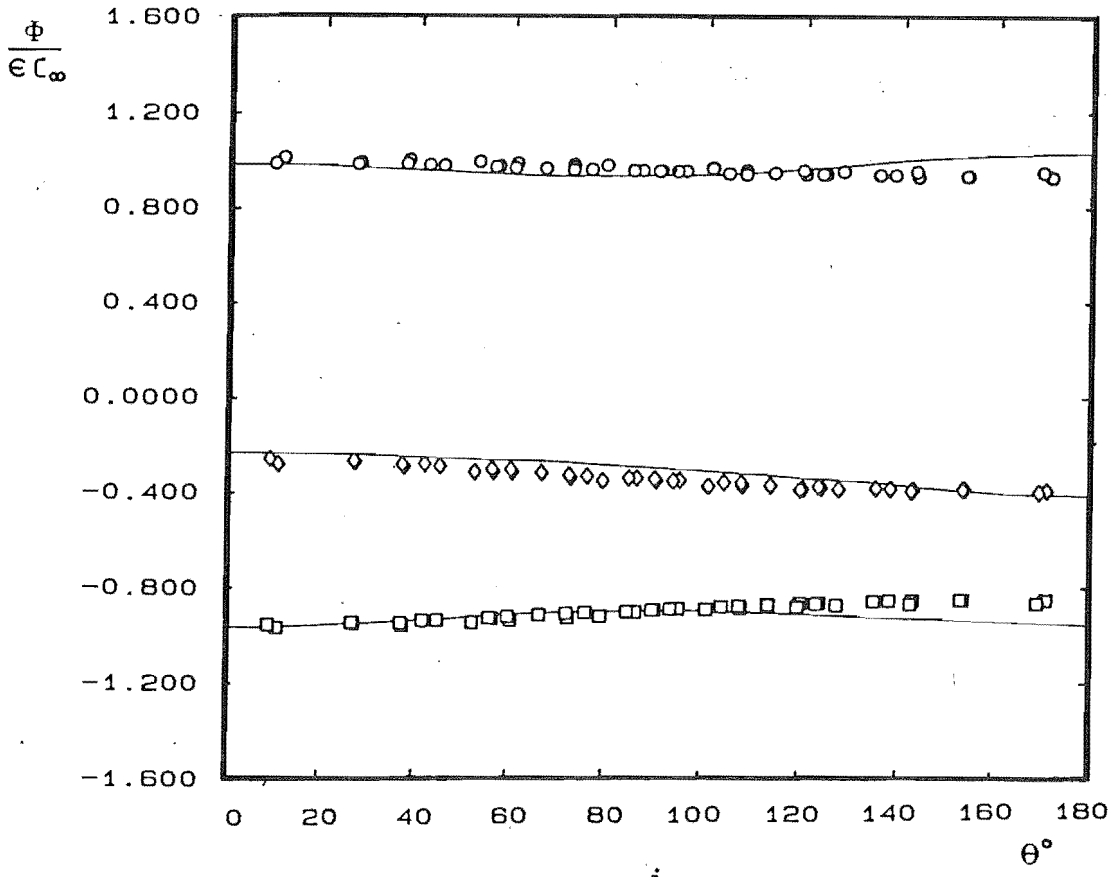

Figure 20(b). The BMF solutions $\alpha = \frac{i}{k}$

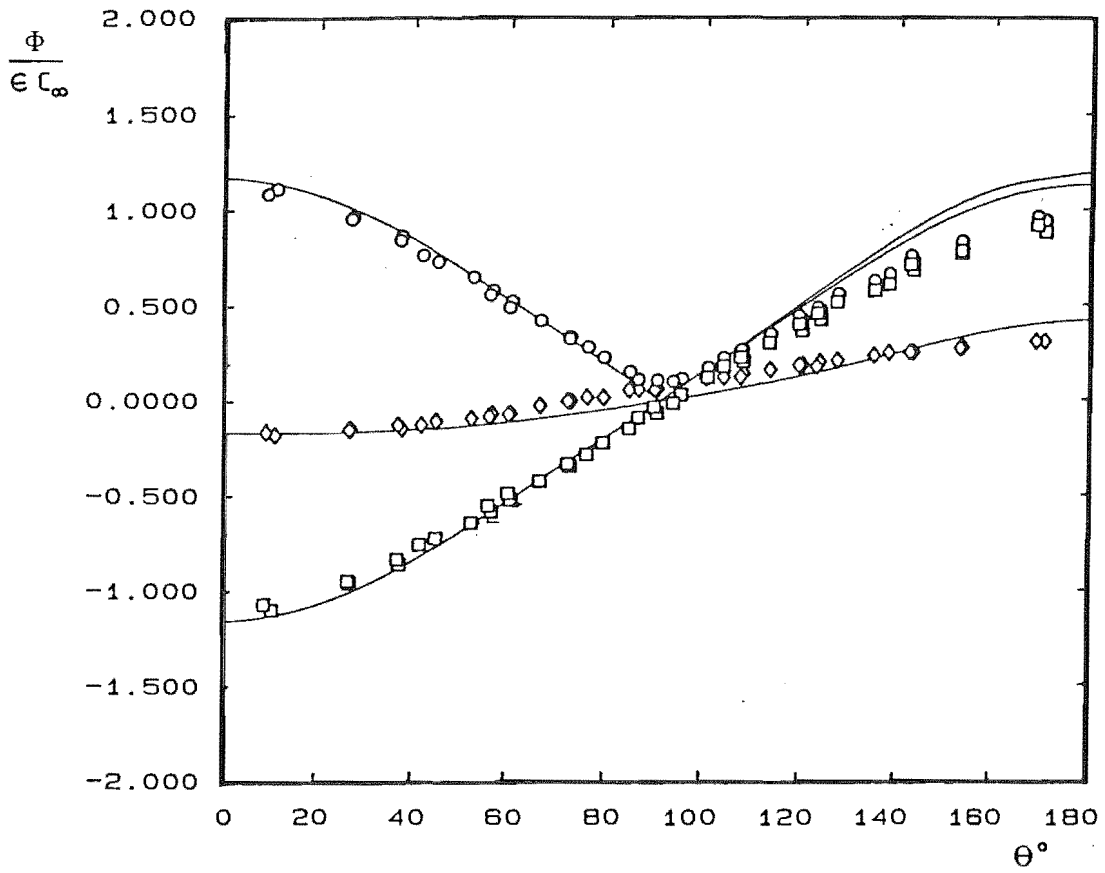

Figure 21. Surface potential, juddering sphere, ka = 4.5, M_∞ = 0.1
21(a). The BMF solutions α = i

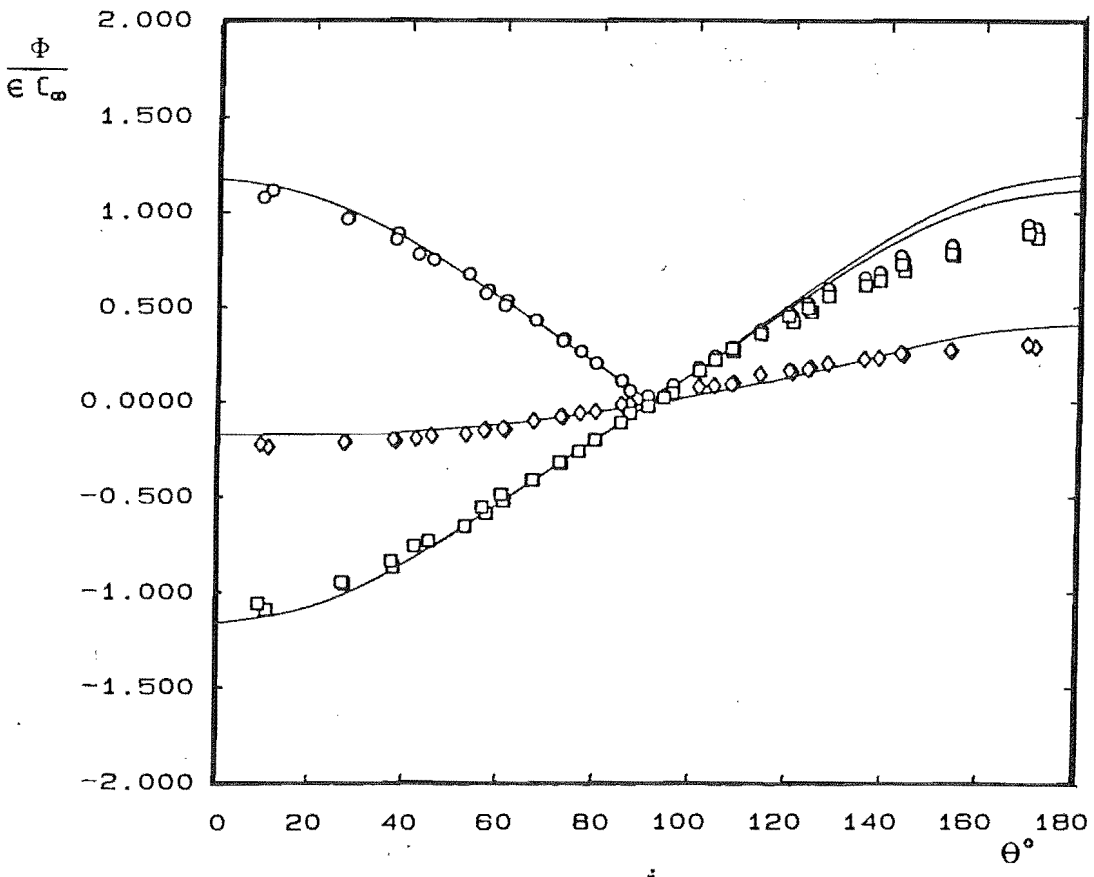

Figure 21(b). The BMF solutions $\alpha = \frac{i}{k}$

Figure 22. Surface potential, pulsating sphere, ka = 3.1, M_∞ = 0.3

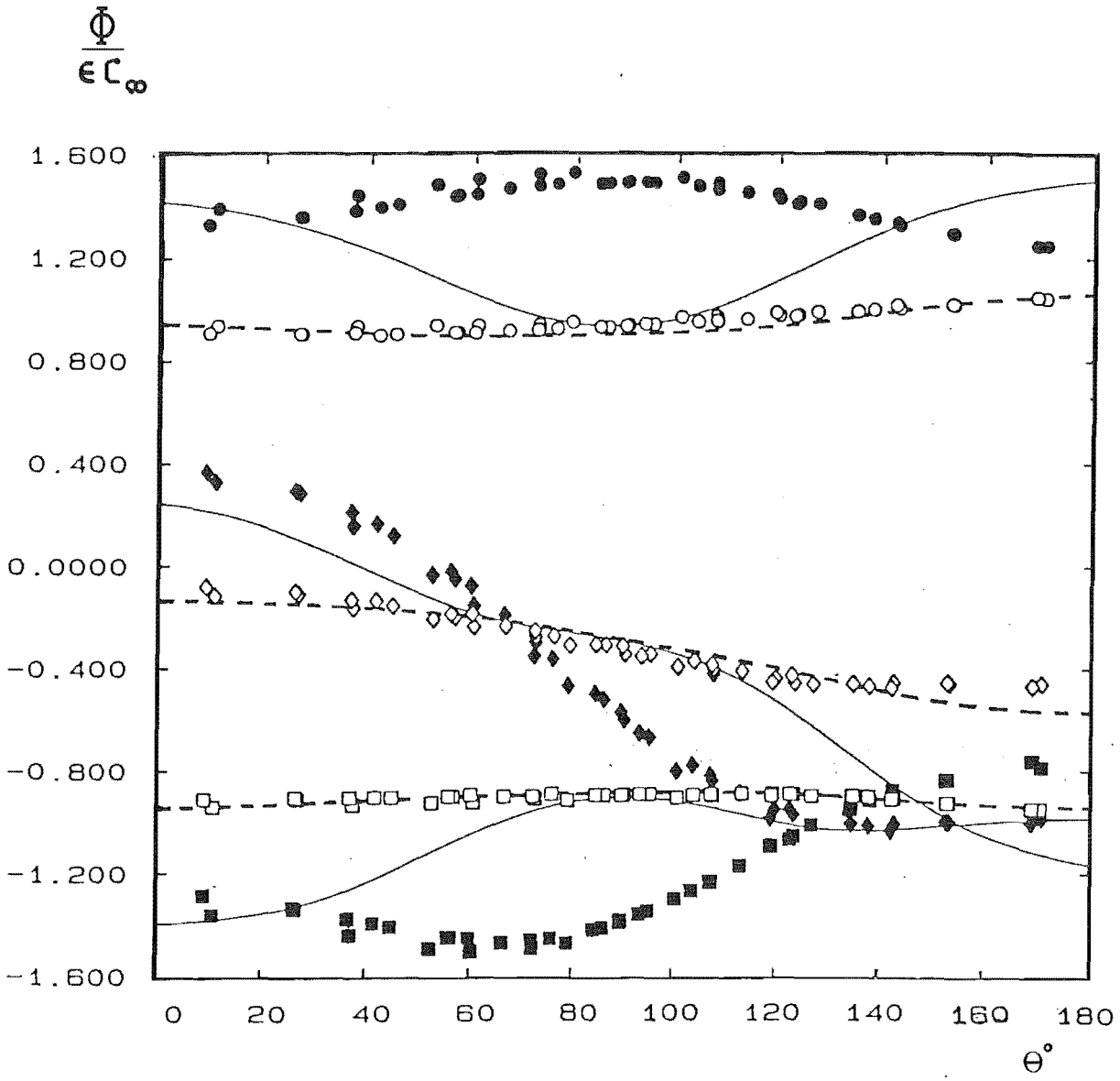

Figure 22(a). The surface Helmholtz and CHIEF solutions

○ - Absolute value (CHIEF)

□ - Real part (CHIEF)

◇ - Imaginary part (CHIEF)

● - Absolute value (surface Helmholtz)

■ - Real part (surface Helmholtz)

◆ - Imaginary part (surface Helmholtz)

--- - Finite element solution

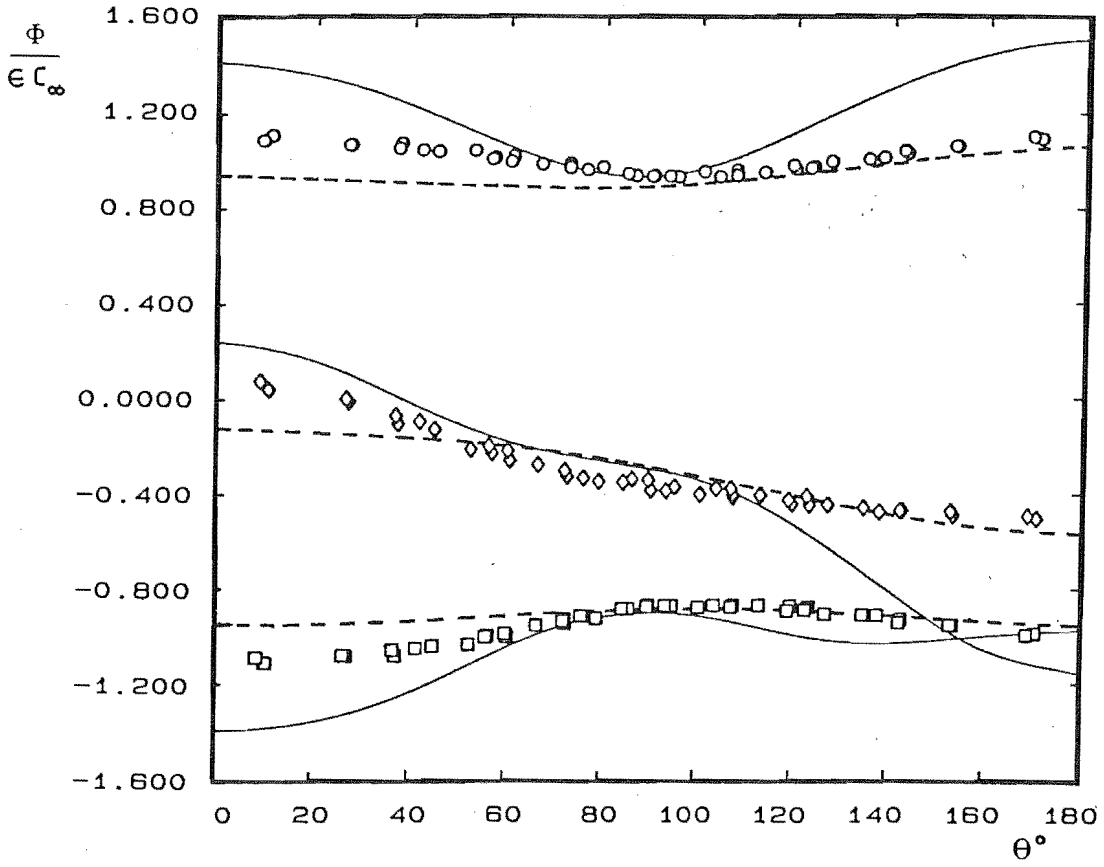

Figure 22(b). The BMF solutions $\alpha = i$

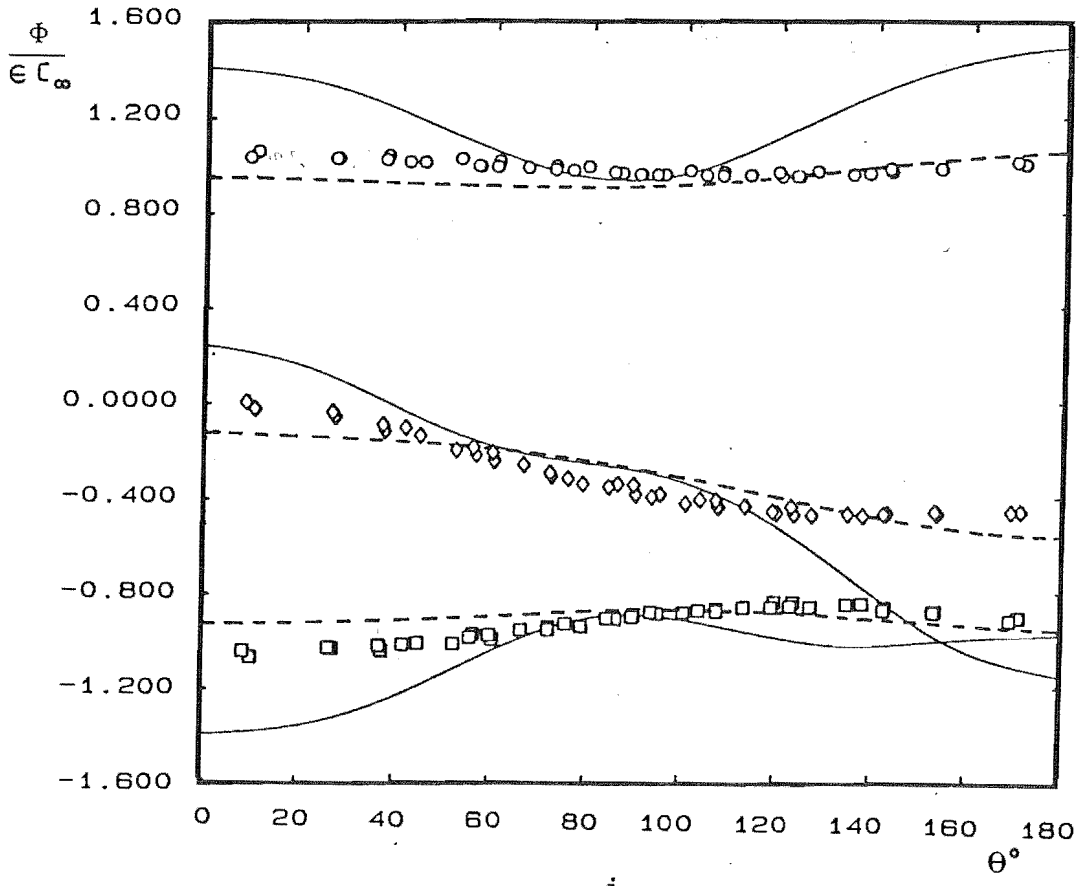

Figure 22(c). The BMF solutions $\alpha = \frac{i}{k}$

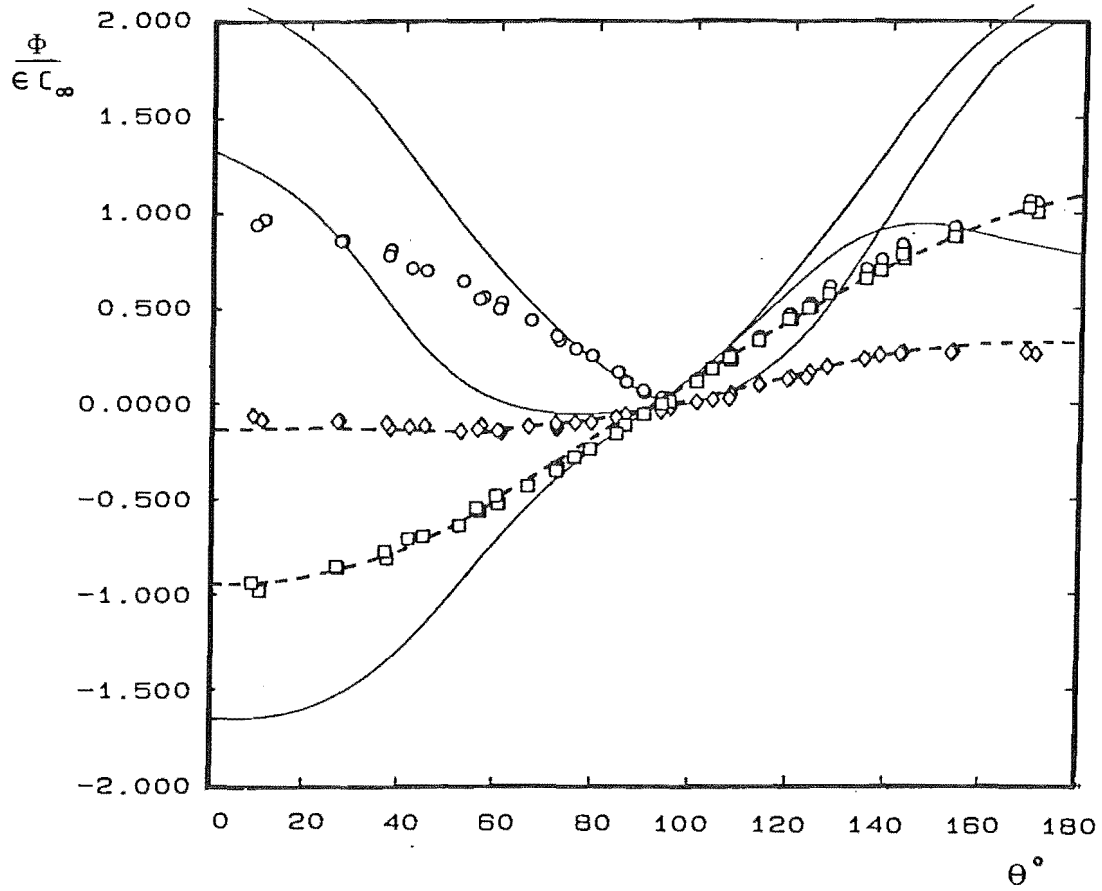

Figure 23. Surface potential, juddering sphere, ka = 4.5, M_∞ = 0.3
23(a). The CHIEF solutions

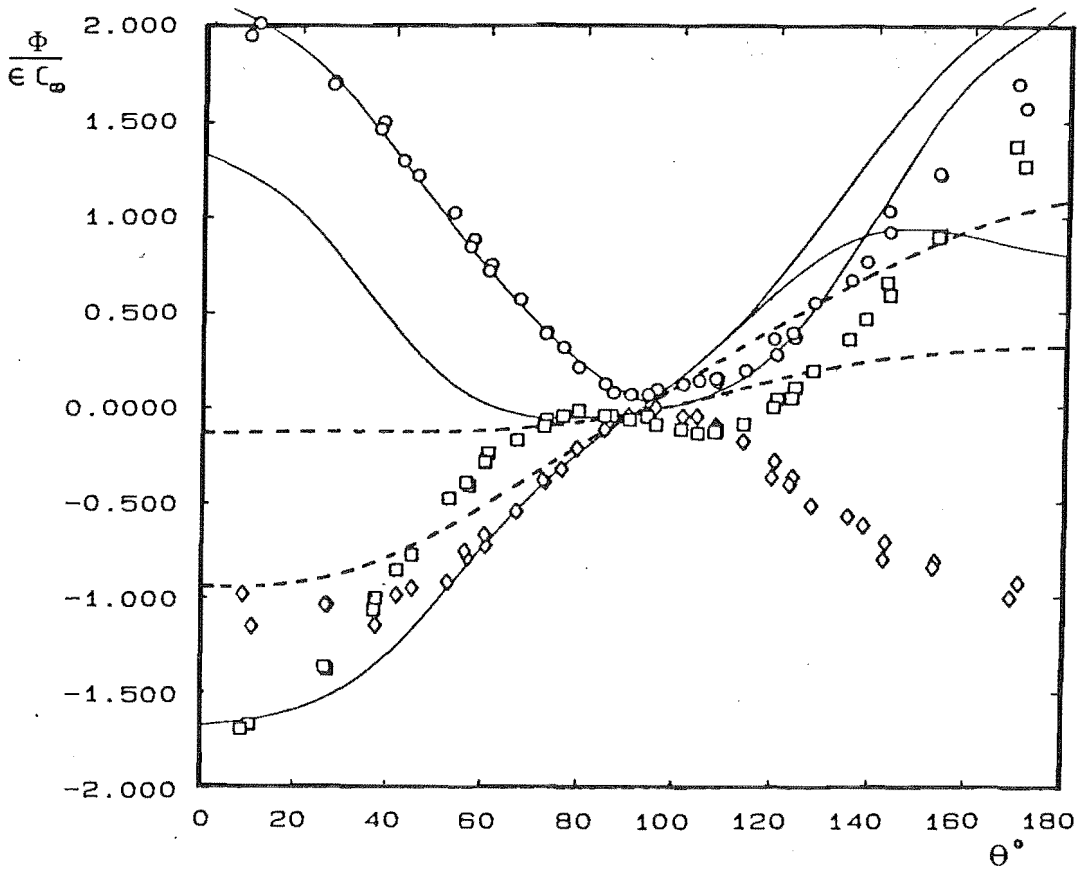

Figure 23(b). The surface Helmholtz solutions

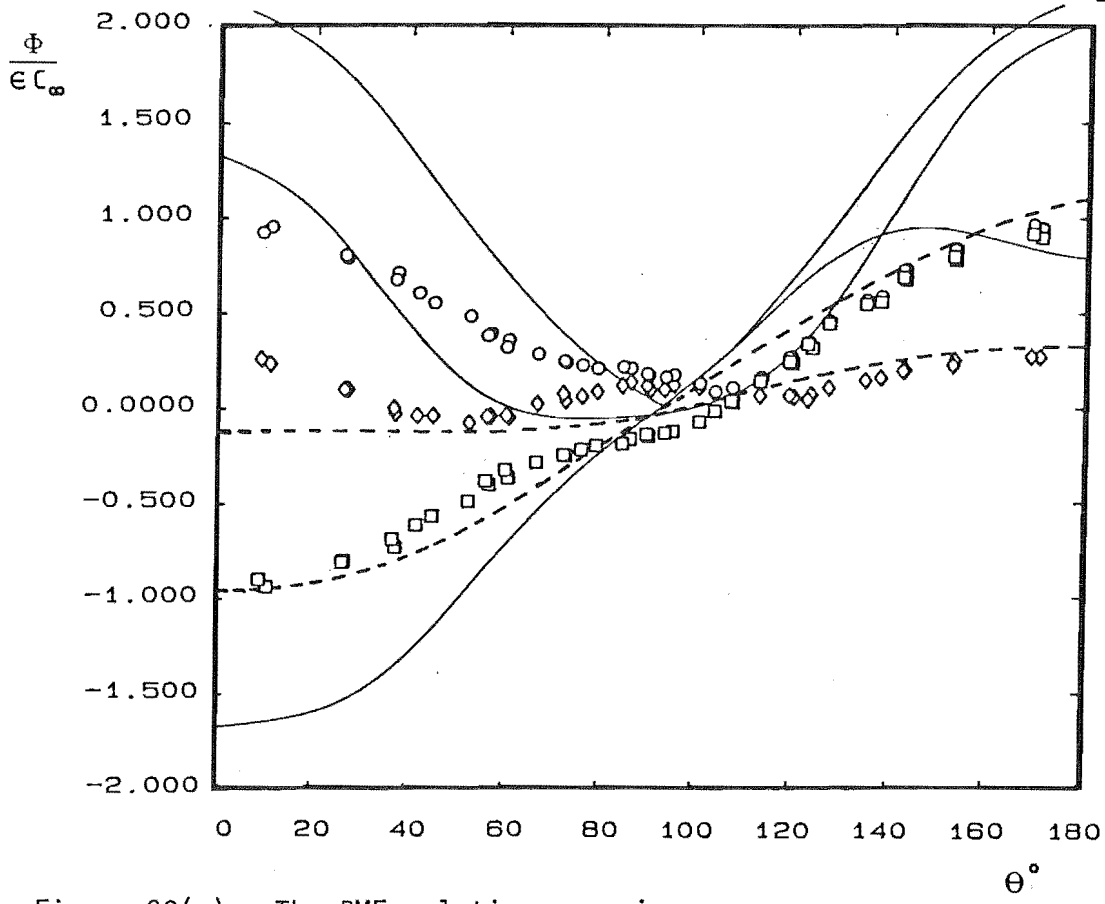

Figure 23(c). The BMF solutions $\alpha = i$

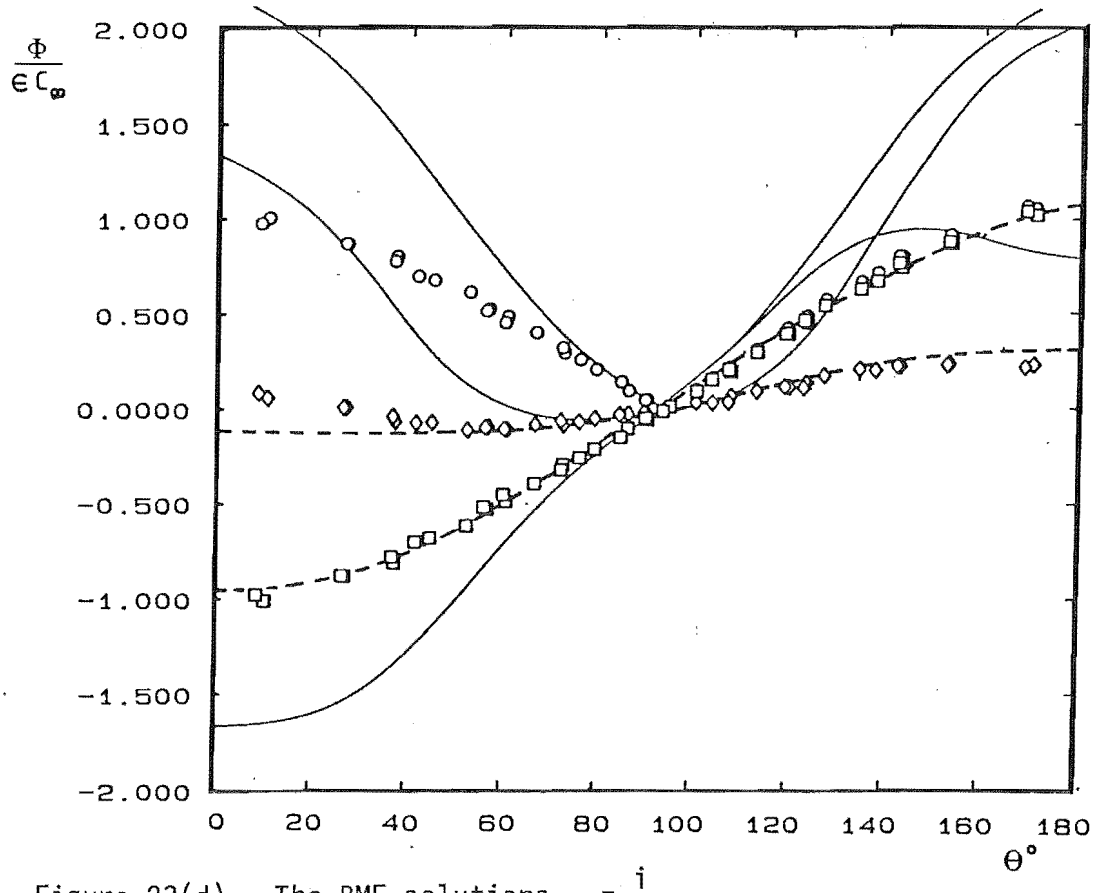

Figure 23(d). The BMF solutions $\alpha = \frac{i}{k}$

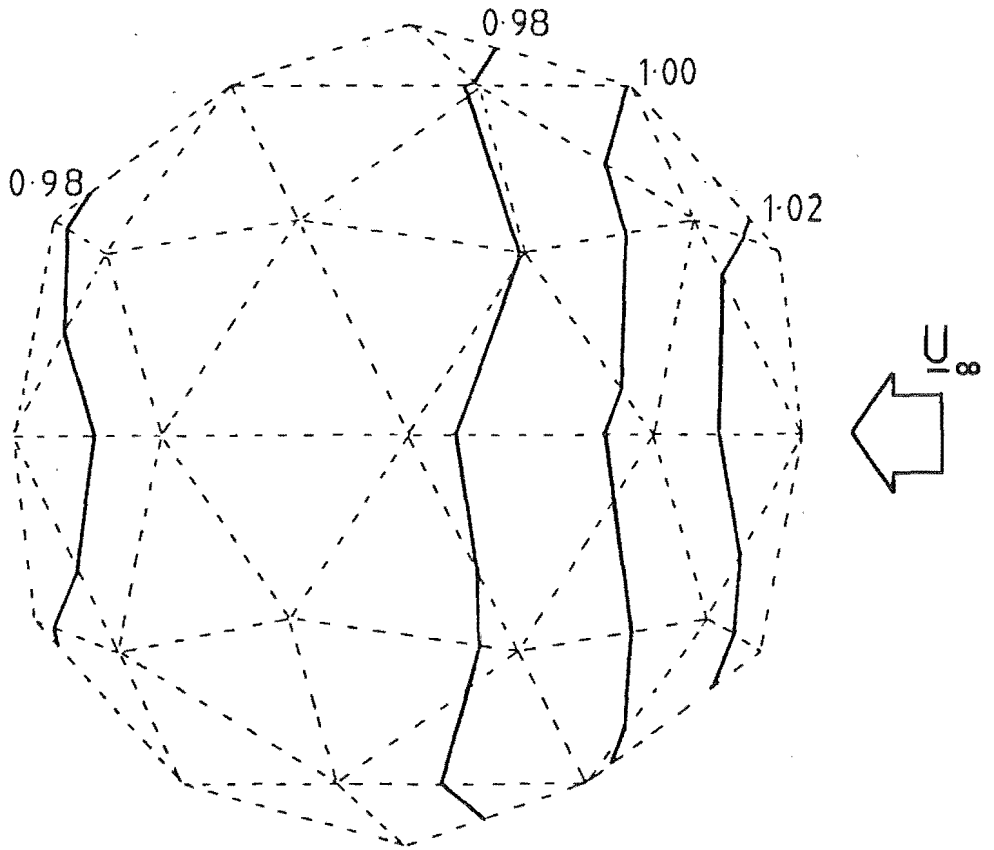

Figure 24. Contour plots of the absolute surface potential; pulsating sphere ka = 4.5, M_∞ = 0.3 - BMF ($\alpha = \frac{i}{k}$) method

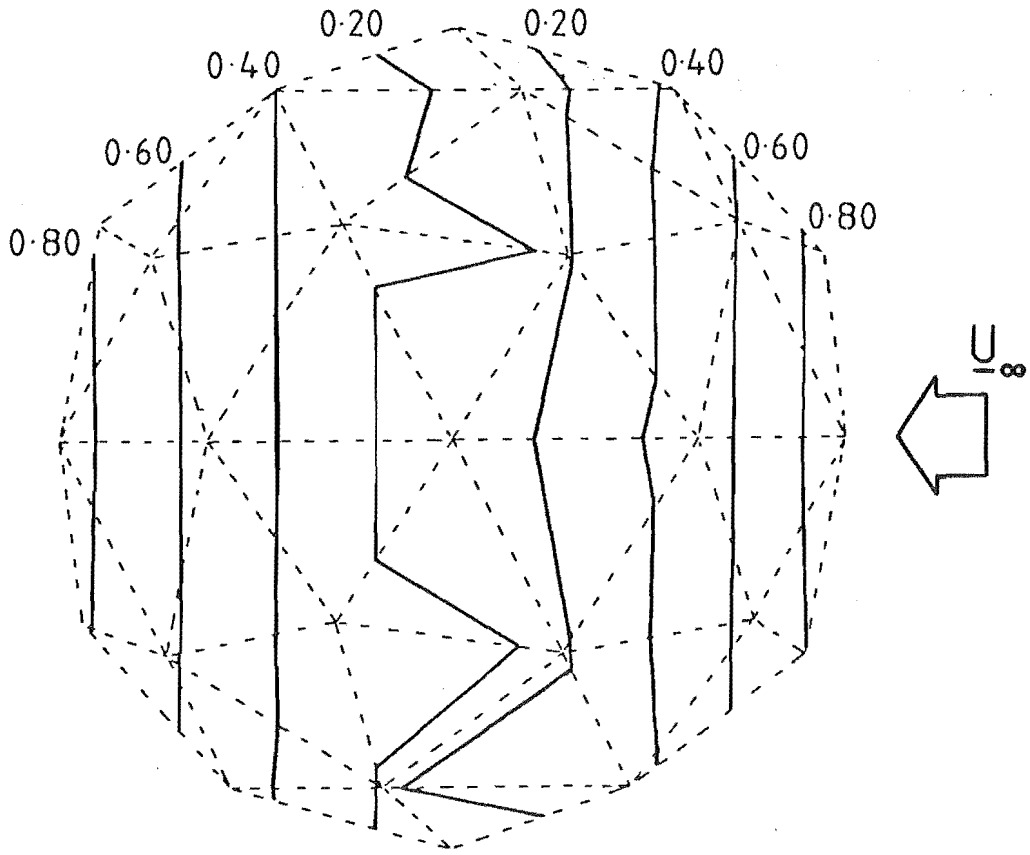

Figure 25. Contour plots of the absolute surface potential, juddering sphere ka = 4.5, M_∞ = 0.3 - BMF ($\alpha = \frac{i}{k}$) method

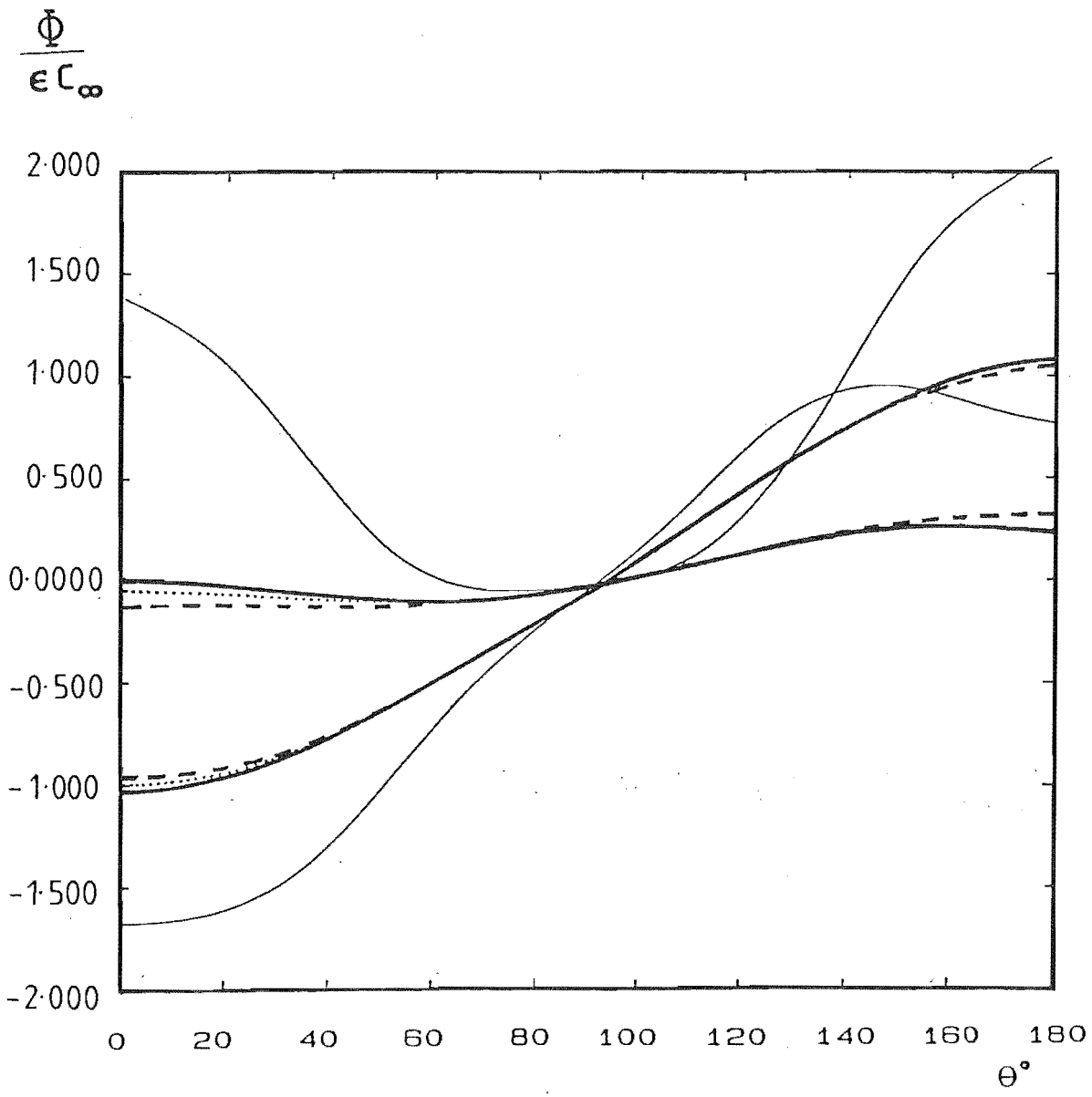

Figure 26. Surface potential, juddering sphere, ka = 4.5, M_∞ = 0.3
A '3-segment' discretization.

BMF ($\alpha = \frac{i}{k}$)
Finite element
CHIEF
Analytic

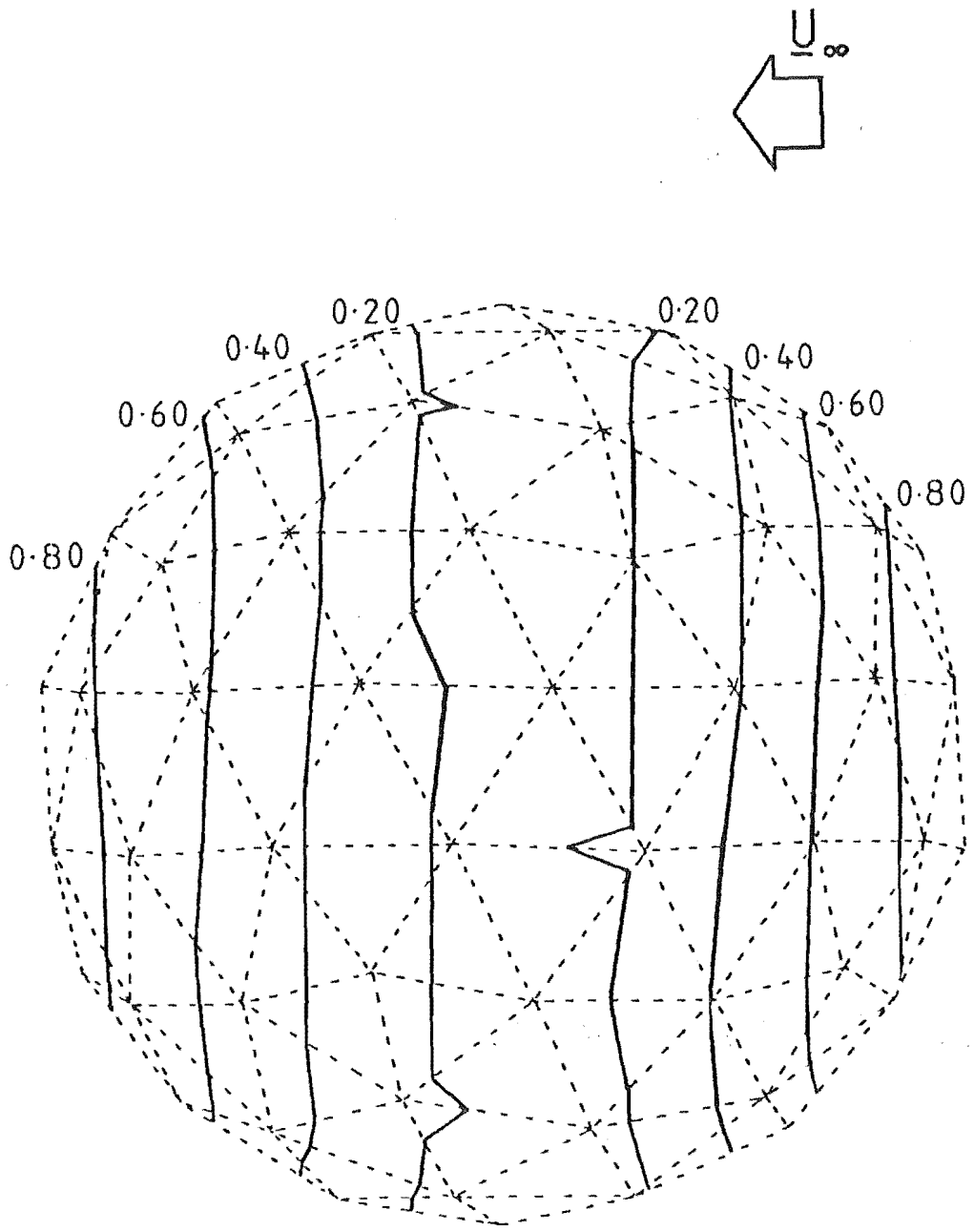

Figure 27. Contour plots of the absolute surface potential; juddering sphere ka = 4.5, M_∞ = 0.3 - BMF ($\alpha = \frac{i}{k}$) method

REFERENCES

[1] Lord Rayleigh. The Theory of Sound, Vol. 2, 1878. Re-issued Dover Publications, 1945.

[2] Y.C. Cho, "Sound Radiation from a Hyperboloidal Inlet Duct". AIAA Paper 79-0677 (1979).

[3] H. Levine and J. Schwinger, "On the Radiation of Sound from an Unflanged Circular Pipe". Physical Review, 73(4) pp.383-406 (1948).

[4] L.A. Weinstein. Theory of Diffraction and the Factorization Method, (Generalized Weiner-Hopf Technique). Boulder, Colorado: Golem Press, 1969.

[5] G.F. Homicz and J.A. Lordi, "A Note on the Directivity of Duct Acoustic Modes". Journal of Sound and Vibration, 41 pp.283-290 (1975).

[6] A. Dowling, "Convective Amplification of Real Simple Sources". Journal of Fluid Mechanics, 74(3) pp.529-546 (1976).

[7] K. Taylor, "Acoustic Generation by Vibrating Bodies in Homentropic Potential Flow at Low Mach Number". Journal of Sound and Vibration, 65(1) pp.125-136, (1979).

[8] A.H. Nayfeh, B.S. Shaker and J.E. Kaiser, "Transmission of Sound through Non-uniform Circular Ducts with Compressible Mean Flow", AIAA Journal 18 pp.515-525 (1980).

[9] R.K. Sigman, R.K. Majjigi and B.T. Zinn, "Determination of Turbofan Inlet Acoustics using Finite Elements". AIAA Journal 16(11) pp.1139-1145 (1978).

[10] R.J. Astley and W. Eversman, "Acoustic Transmission in Lined Ducts with Flow, Part 2: The Finite Element Method". Journal of Sound and Vibration, 74(1) pp.103-121 (1981).

[11] K.J. Baumeister, "Time Dependent Difference Theory for Noise Propagation in a Two-Dimensional Duct". AIAA Journal, 18 pp.1470-1476 (1980).

[12] A. Cabelli, "Duct Acoustics - A Time Dependent Difference Approach for Steady State Solutions", Journal of Sound and Vibration, 85(4) pp.423-434 (1982).

[13] K.J. Baumeister, "Transient Finite Difference Solutions of the Inhomogeneous Wave Equation: Simulation of the Green's Function". AIAA Paper 83-0667, April 1983.

[14] S.J. Horowitz, R.K. Sigman and B.T. Zinn, "An Iterative Finite Element - Integral Technique for Predicting Sound Radiation from Turbofan Inlets". AIAA Paper 81-1987.

[15] S.J. Horowitz, R.K. Sigman and B.T. Zinn, "An Iterative Finite Element - Integral Technique for Predicting Sound Radiation from Turbofan Inlets in Steady Flight", AIAA Paper 82-0124.

[16] R.K. Sigman, S.J. Horowitz and B.T. Zinn, "Optimization of Acoustic Liners by the Hybrid Finite Element Integral Approach". AIAA Paper 83-0670, April 1983.

[17] P. Bettess, "Infinite Elements". International Journal for Numerical Methods in Engineering, 11, pp.53-64 (1977).

[18] P. Bettess and O.C. Zienkiewicz, "Diffraction and Refraction of Surface Waves using Finite and Infinite Elements". International Journal for Numerical Methods in Engineering, 11, pp.1271-1290 (1977).

[19] R.J. Astley and W. Eversman, "Finite Element Formulations for Acoustical Radiation", Journal of Sound and Vibration, 88(1) pp.47-64 (1983).

[20] R.J. Astley and W. Eversman, "A Note on the Utility of a Wave Envelope Approach in Finite Element Duct Transmission Studies". Journal of Sound and Vibration, 76(4) pp.595-601 (1981).

[21] R.J. Astley, "Wave Envelope and Infinite Elements for Acoustical Radiation", International Journal for Numerical Methods in Fluids, 3 pp.507-526 (1983).

[22] R.J. Astley, "A Finite Element, Wave Envelope Formulation for Acoustical Radiation in Moving Flows". Journal of Sound and Vibration, 101(4) (1985).

[23] A.J. Kempton, "Ray-Theory and Mode-Theory Predictions of Intake-Linear Performance. A Comparison with Engine Measurements". AIAA Paper 83-0711.

[24] H.A. Schenk, "Improved Integral Formulation for Acoustic Radiation Problems". Journal of the Acoustical Society of America, 44(1) pp.41-58 (1968).

[25] W.L. Meyer, W.A. Bell, M.P. Stallybrass and B.T. Zinn, "Prediction of the Sound Field Radiated from Axisymmetric Surfaces". Journal of the Acoustical Society of America, 65(3) pp.631-638 (1979).

[26] K. Taylor, "A Transformation of the Acoustic Equation with Implications for Wind-Tunnel and Low-Speed Flight Tests". Proceedings of the Royal Society of London, A363, pp.271-281 (1978).

[27] L.H. Chen and D.G. Schweikert, "Sound Radiation from an Arbitrary Body". Journal of the Acoustical Society of America, 35(10) pp.1626-1632 (1963).

[28] V.I. Smirnov. A Course of Higher Mathematics, Volume 4 (Pergamon Press, 1964).

[29] G. Chertock, "Sound Radiation from Vibrating Surfaces". Journal of the Acoustical Society of America, 36(7) pp.1305-1313 (1964).

[30] L.G. Copley, "Integral Equation Method for Radiation from Vibrating Bodies". Journal of the Acoustical Society of America, 41(4) pp.807-816 (1967).

[31] L.G. Copley, "Fundamental Results Concerning Integral Representations in Acoustic Radiation". Journal of the Acoustical Society of America 44(1) pp.28-32 (1968).

[32] C.M. Piaszczyk and J.M. Klosner, "Acoustic Radiation from Vibrating Surfaces at Characteristic Frequencies". Journal of the Acoustical Society of America, 75(2) pp.363-375 (1984).

[33] A.J. Burton and G.F. Miller, "The Application of Integral Equation Methods to the Numerical Solution of some Exterior Boundary-Value Problems". Proceedings of the Society of London, A323, pp.201-210 (1971).

[34] W.L. Meyer, W.A. Bell, B.T. Zinn and M.P. Stallybrass, "Boundary Integral Solutions of Three Dimensional Acoustic Radiation Problems". Journal of Sound and Vibration, 59(2) pp.245-262 (1978).

[35] F. Ursell, "On the Exterior Problems of Acoustics". Proceedings of the Cambridge Philosophical Society, 74 pp.117-125 (1973).

[36] D.S. Jones, "Integral Equations for the Exterior Acoustic Problem". Quarterly Journal of Mechanics and Applied Mathematics, XXVII Part I pp.129-142 (1974).

[37] P.C. Waterman, "New Formulation of Acoustic Scattering". Journal of the Acoustical Society of America" 45 pp.1417-1429 (1969).

[38] M.K. Myers, "On the Acoustic Boundary Condition in the Presence of Flow". Journal of Sound and Vibration, 71(3) pp.429-434 (1980).

[39] P.G. Vaidya, "Propagation of Sound in Flows Containing Mean Flow Gradients". AIAA Paper 81-1987.

[40] G.K. Batchelor. An Introduction to Fluid Dynamics (Cambridge University Press, 1967).

[41] S.C. Hunter. Mechanics of Continuous Media. (Ellis Horwood, 1976).

[42] W. Pogorzelski. Integral Equations and their Applications, Vol. I (Pergamon Press, 1966).

[43] O.D. Kellogg. Foundations of Potential Theory (Dover Publications Inc., 1953).

[44] S.G. Mikhlin. Linear Equations of Mathematical Physics (Holt, Rinehart and Winston, Inc., 1967).

[45] F. Smithies. Integral Equations (Cambridge University Press, 1958).

[46] G. Chertock, "Solutions for Sound-Radiation Problems by Integral Equations at the Critical Wave Numbers". Journal of the Acoustical Society of America", 47(1) pp.387-388 (1970).

[47] R.E. Kleinman and G.F. Roach, "Boundary Integral Equations for the Three Dimensional Helmholtz Equation", SIAM Review, 16(2) pp.214-236 (1974).

[48] A.W. Maue, "Zur Formulierung eines Allgemeinen Beugungsproblems durch eine Integralgleichung". Zeitschrift für Physik, 126 pp.601-618 (1949).

[49] K.M. Mitzner, "Acoustic Scattering from an Interface between Media of Greatly Different Density". Journal of Mathematical Physics, 7 pp.2053-2060 (1966).

[50] C.A. Brebbia and S. Walker. Boundary Element Techniques in Engineering (London, Newnes-Butterworths, 1980).

[51] C.A. Brebbia (ed.). New Developments in Boundary Element Methods; Proceedings of the Second International Seminar on Recent Advances in Boundary Element Methods, (1980) C.M.L. Publications.

[52] Masataka Tanaka, "Some Recent Advances in Boundary Element Methods", Applied Mechanics Reviews, 36(5) pp.627-634 (1983).

[53] A.H. Stroud. Approximate Calculation of Multiple Integrals. (Prentice-Hall, Inc., 1977).

[54] P. Silvester, "Symmetric Quadrature Formulae for Simplexes". Mathematical Tables and Other Aids to Computation, 24 pp.95-100 (1970).

[55] B.M. Irons, "Engineering Applications of Numerical Integration in Stiffness Methods". AIAA Journal 4(11) pp.2035-2037 (1966).

[56] P.C. Hammer, O.J. Marlowe and A.H. Stroud, "Numerical Integration over Simplexes" 10(55) pp.130-137 (1956).

[57] G.R. Cowper, "Gaussian Quadrature Formulas for Triangles", International Journal for Numerical Methods in Engineering, 7(3) pp.405-408, (1973).

[58] H.S.M. Coxeter. Regular Polytopes. (Dover Publications, 1973).

[59] H. Kenner. Geodesic Math and how to use it (University of California Press, 1976).

[60] B.B. Baker and E.T. Copson. The Mathematical Theory of Huyghens' Principle (The Clarendon Press, Oxford, 1950).

[61] R. Leis, "Über das Neumannsche Randwertproblem für die Helmholtzsche Schwingungsgleichung", Archives of Rational Mechanics and Analysis, 2, pp.101-113 (1958).

APPENDIX A

Derivation of an expression for $\underline{\nabla}.\underline{M}$:

$$\underline{\nabla}.\underline{M} = \frac{\frac{1}{2}\underline{M}.\underline{\nabla}(|\underline{M}|^2)}{1 - \frac{(\gamma-1)}{2}(|\underline{M}|^2 - |\underline{M}_\infty|^2)}$$

PROOF:

Consider equations (2.5.5) and (2.5.7), i.e.

$$\underline{\nabla}.(\rho\underline{U}) = 0 \tag{1}$$

$$\rho = \rho_\infty\left[1 - \frac{(\gamma-1)}{2}(|\underline{M}|^2 - |\underline{M}_\infty|^2)\right]^{1/(\gamma-1)} \tag{2}$$

Equation (1) can be written as:

$$\underline{\nabla}.(\rho\underline{M}) = 0 \quad , \qquad \underline{M} = \frac{\underline{U}}{C_\infty} \tag{3}$$

and using the identity: $\underline{\nabla}.(\rho\underline{M}) = (\underline{\nabla}\rho).\underline{M} + \rho(\underline{\nabla}.\underline{M})$, (3) becomes:-

$$\underline{\nabla}.\underline{M} = \frac{-1}{\rho}(\underline{\nabla}\rho).\underline{M} \tag{4}$$

The gradient of mean flow density, eq. (2) is:

$$\underline{\nabla}\rho = \rho_\infty\,\sigma^{1/(\gamma-1)} \quad \text{where } \sigma = \frac{c^2}{c_\infty^2} \tag{5}$$

hence

$$\underline{\nabla}\rho = \frac{\rho_\infty}{(\gamma-1)}\,\frac{\sigma^{1/(\gamma-1)}}{\sigma}\,\underline{\nabla}\sigma \tag{6}$$

and

$$\underline{\nabla}\sigma = \underline{\nabla}\left[1 - \frac{(\gamma-1)}{2}(|\underline{M}|^2 - |\underline{M}_\infty|^2)\right]$$

$$= \frac{-(\gamma-1)}{2}\,\underline{\nabla}(|\underline{M}|^2) \tag{7}$$

hence

$$\underline{\nabla}.\underline{M} = \tfrac{1}{2}\underline{\nabla}(|\underline{M}|^2).\left[\frac{\underline{M}}{\sigma}\right] \tag{8}$$

so

$$\underline{\nabla}.\underline{M} = \frac{\frac{1}{2}\underline{M}.\underline{\nabla}(|\underline{M}|^2)}{1 - \frac{(\gamma-1)}{2}(|\underline{M}|^2 - |\underline{M}_\infty|^2)} \tag{9}$$

which was to be shown.

APPENDIX B

Derivation of the Sommerfeld radiation principle in three-dimensions.

This appendix derives the mathematical form of the radiation principle:

$$\text{i.e. } \Psi = O(R^{-1}) \text{ and } \frac{\partial \Psi}{\partial R} + ik\Psi = o(R^{-1}) \text{ as } R \to \infty \qquad (1)$$

Define a domain D_+ to be bounded internally by the surface S and externally by a spherical surface S_R of radius R, centred at a point $P \varepsilon D_+$.

Define Ψ to be a solution of Helmholtz' equation in the domain D_+:

$$\text{i.e. } \nabla^2\Psi + k^2\Psi = 0 \quad , \quad \Psi \varepsilon D_+ \qquad (2)$$

where k is real such that $k = \frac{\omega}{c}$.

Define $G(P,Q) = \frac{e^{-ikr}}{4\pi r}$ as the fundamental solution of the inhomogeneous Helmholtz equation:

$$(\nabla^2 + k^2)G + \delta(P) = 0 \qquad (3)$$

where G represents the sound field at some point in D_+ due to a point source located at P.

Let the singularity point P within D_+ be surrounded by a small sphere of surface area σ and radius ε. Applying Green's theorem to equation (3.2.12) yields:

$$\int_{D_+'} \left[G(\nabla^2\Psi + k^2\Psi) - \Psi(\nabla^2 G + k^2 G)\right] dD_+$$
$$= \int_S (G\underline{\nabla}\Psi - \Psi\underline{\nabla}G).\hat{\underline{n}}_i dS + \int_\sigma (G\underline{\nabla}\Psi - \Psi\underline{\nabla}G).\hat{\underline{n}}_\nu d\sigma + \int_{S_R} (G\underline{\nabla}\Psi - \Psi\underline{\nabla}G).\hat{\underline{n}}_R dS_R \qquad (4)$$

where the domain D_+' is just D_+ minus the small sphere. The normals $\hat{\underline{n}}_i$, $\hat{\underline{n}}_\nu$ and $\hat{\underline{n}}_R$ all point out of D_+ from the surfaces S, σ and S_R respectively. Since there are no singularities in D_+', the left hand side of (4) will vanish, and it can be shown that the integral over σ is just $-\Psi(P)$ (see equations (3.2.20) and (3.2.22)).

Therefore (4) above can be written as:

$$\Psi(P) = \int_S (G\underline{\nabla}\Psi - \Psi\underline{\nabla}G).\hat{\underline{n}}_i dS + \int_{S_R} (G\underline{\nabla}\Psi - \Psi\underline{\nabla}G).\hat{n}_R dS_R \qquad (5)$$

The Sommerfeld radiation principle requires that the contribution to $\Psi(P)$ arising from the integral over S_R vanishes as that surface recedes to infinity.

Therefore it is required to show:

$$\int_{S_R} (G\underline{\nabla}\Psi - \Psi\underline{\nabla}G).\hat{\underline{n}}_R \, dS_R \to 0 \quad \text{as } R\to\infty \qquad (6)$$

The integral of equation (6) can be rewritten as:

$$\frac{1}{4\pi}\int_{S_R} \frac{e^{-ikR}}{R}\left(\frac{\partial\Psi}{\partial R} + ik\Psi\right)dS_R + \frac{1}{4\pi}\int_{S_R} \Psi \frac{e^{-ikR}}{R^2} \, dS_R \qquad (7)$$

Introducing spherical coordinates θ and ϕ over the surface S_R yields:

$$\frac{1}{4\pi}\int_{S_R} e^{-ikR}\left[R\left(\frac{\partial\Psi}{\partial R} + ik\Psi\right)\right]\sin\theta \, d\theta \, d\phi + \frac{1}{4\pi}\int_{S_R} \Psi \, e^{-ikR} \sin\theta \, d\theta \, d\phi \qquad (8)$$

The second integral of equation (8) will tend to zero if $\Psi\to 0$ as $R\to\infty$, uniformly with respect to the coordinates θ and ϕ. In particular this integral will tend to zero if:

$$|\Psi| < \frac{K}{R} \qquad \text{as } R\to\infty \qquad (9)$$

where K is some positive constant. That is, $|R\Psi|$ will be bounded as $R\to\infty$, and so equation (9) can be written as:

$$\Psi = O(R^{-1}) \qquad \text{as } R\to\infty \qquad (10)$$

The first integral tends to zero if:

$$R\left(\frac{\partial\Psi}{\partial R} + ik\Psi\right) \to 0 \qquad \text{as } R\to\infty \qquad (11)$$

uniformly with respect to θ and ϕ. Equation (11) can be written as:

$$\left(\frac{\partial\Psi}{\partial R} + ik\Psi\right) = o(R^{-1}) \quad \text{as } R\to\infty \qquad (12)$$

The equations (10) and (12) ensure the vanishing of the integral in equation (6). These equations define the Sommerfeld radiation principle. (see Baker and Copson [60], Smirnov [28] vol. 4 Art. 228).

APPENDIX C

This appendix contains the derivation of an important Lemma. A similar lemma has been proved by Leis [61].

Denote the limiting value of a function U(P), as P approaches the surface S from the outside as:

$$\lim_{P \to Q_+} U(P) = U_+(Q) \quad , \quad Q \epsilon S$$

Initially assume that k is complex. Therefore $k = k_1 + ik_2$ where $k_1 = \mathrm{Re}(k)$ and $k_2 = \mathrm{Im}(k)$.

LEMMA

If a function U(P) satisfies outside a closed surface, S, both the Helmholtz equation and the radiation principle at infinity and if its boundary values and those of its normal derivative exist then

$$\mathrm{Im} \int_S U_+(Q) \left[\frac{\partial U_+(Q)}{\partial n_q} \right]^* dS_q = C \, \mathrm{Re}(k) \; ; \quad C \geq 0 \qquad (1)$$

where C is an arbitrary constant and C = 0 if and only if U(P) vanishes identically in the exterior domain D_+. The asterisk denotes a complex conjugate.

PROOF

Apply Green's theorem to U and its complex conjugate U^* within the domain D_+. The domain D_+ is bounded internally by the surface S and externally by the surface S_R.

Therefore:

$$\int_{D_+} (U \nabla^2 U^* - U^* \nabla^2 U) dD_+ = -\int_S (U_+ \frac{\partial U_+^*}{\partial n_o} - U_+^* \frac{\partial U}{\partial n_o}) dS + \int_{S_R} (U \frac{\partial U^*}{\partial n} - U^* \frac{\partial U}{\partial n}) dS_R \qquad (2)$$

where $\frac{\partial}{\partial n_o}$ denotes differentiation along the normal pointing into D_+ from S, hence the negative sign. Rearranging (2) gives:

$$\int_S (U_+ \frac{\partial U_+^*}{\partial n_o} - U_+^* \frac{\partial U_+}{\partial n_o}) dS = -\int_{D_+} (U \nabla^2 U^* - U^* \nabla^2 U) dD_+ + \int_{S_R} (U \frac{\partial U^*}{\partial n} - U^* \frac{\partial U}{\partial n}) dS_R \qquad (3)$$

Consider the Helmholtz equation:

$$\nabla^2 U + k^2 U = 0 \quad ; \quad k = k_1 + ik_2 \tag{4}$$

and the Sommerfeld radiation conditions in the form:

$$U = O(R^{-1}) \quad \text{and} \quad \frac{\partial U}{\partial n} = -ikU + o(R^{-1}) \quad \text{as } R\to\infty \tag{5}$$

Substituting equations (4) and (5) into the right hand side of (3) yields:

$$\int_S (U_+ \frac{\partial U_+^*}{\partial n} - U_+^* \frac{\partial U_+}{\partial n_o})dS = (k^{*2} - k^2)\int_{D_+} |U|^2 \, dD_+ + i(k^* + k)\int_{S_R} |U|^2 dS_R + o(1) \tag{6}$$

That is:

$$\int_S (U_+ \frac{\partial U_+^*}{\partial n_o} - U_+^* \frac{\partial U_+}{\partial n_o})dS = -4ik_1k_2\int_{D_+} |U|^2 \, dD_+ + 2ik_1\int_{S_R} |U|^2 \, dS_R + o(1) \tag{7}$$

The left hand side of equation (7) can be written as:

$$\int_S (U_+ \frac{\partial U_+^*}{\partial n_o} - \left[U_+ \frac{\partial U_+^*}{\partial n_o}\right]^*)dS = 2i\,\mathrm{Im}\int_S U_+ \frac{\partial U_+^*}{\partial n_o} dS \tag{8}$$

Combining equations (7) and (8) gives:

$$\mathrm{Im}\int_S U_+ \frac{\partial U_+^*}{\partial n_o} dS = -2k_1k_2\int_{D_+} |U|^2 \, dD_+ + k_1\int_{S_R} |U|^2 \, dS_R + o(1) \tag{9}$$

k is now specified to be real, i.e. $k_2 = 0$. So that equation (9) is now:

$$\mathrm{Im}\int_S U_+ \frac{\partial U_+^*}{\partial n_o} dS = k_1\int_{S_R} |U|^2 \, dS_R + o(1) \tag{10}$$

An element of surface on the sphere S_R can be given by:

$$dS_R = R^2 \sin\theta \; d\theta \, d\phi \tag{11}$$

where θ and ϕ are spherical surface coordinates on S_R. So the kernel on the right of equation (10) will be of the form:

$$|RU|^2 \sin\theta \tag{12}$$

The radiation condition of equation (5) requires $|RU|$ to be bounded as $R\to\infty$. That is,

$$|RU| < K \qquad \text{as } R\to\infty \tag{13}$$

where K is some positive constant. The integral on the right of (10) will therefore be bounded above. Equation (10) will now become:

$$\mathrm{Im}\int_S U_+ \frac{\partial U_+^*}{\partial n_o}\, dS = k_1 C \quad , \qquad C \geq 0 \tag{14}$$

where C is a constant given by:

$$C = \int_{S_R} |U|^2 \, dS_R + o(1) \tag{15}$$

Therefore C will vanish if and only if U(P) vanishes identically in the exterior domain D_+.

APPENDIX D

A solution of the Helmholtz equation outside a closed surface, S, which also satisfies the Sommerfeld radiation condition, will be unique, [21].

THE UNIQUENESS THEOREM

If a function Ψ satisfies outside a closed surface, S, both the Helmholtz equation, the radiation principle at infinity and a homogeneous boundary condition on the surface S i.e. $\Psi(\xi) = 0$ or $\frac{\partial \Psi}{\partial n}(\xi) = 0$ for $\xi \epsilon S$, then Ψ is identically zero.

PROOF

The proof of this theorem follows immediately from the lemma of appendix (C). In this case equation (1) of appendix (C) is written as:

$$\mathrm{Im} \int_S \Psi(\xi)_+ \left[\frac{\partial \Psi_+(\xi)}{\partial n}\right]^* dS_\xi = C\ \mathrm{Re}(k) \quad , \quad C > 0$$

Due to the homogeneous boundary conditions, C must vanish and so from the lemma, Ψ will be identically zero.

APPENDIX E

This appendix states the Lyapunov conditions that ensure sufficient smoothness of a surface S (see Pogorzelski [42], p.231).

THE LYAPUNOV CONDITIONS

1. The surface S has a tangent plane at every point P and the angle ν_{PQ} between the normals to the surface at two arbitrary points P and Q, satisfies the inequality

$$|\nu_{PQ}| < C\, r_{PQ}^{\alpha} \qquad (0 < \alpha < 1)$$

where r_{PQ} denotes the distance between the points P and Q, the exponent α is a positive number not exceeding unity, and C is a known positive coefficient.

2. There exists a number δ so small that a sphere of radius δ and centre $P \epsilon S$ cuts out in the neighbourhood of every point $P \epsilon S$, a part of the surface, such that an arbitrary line parallel to the normal at P intersects this part at most one point.

APPENDIX F

Theorem 7 states: If λ is an eigenvalue, the necessary and sufficient condition for the equation

$$x(\eta) = f(\eta) + \lambda \int_S K(\eta,\xi)x(\xi)dS_\xi \tag{1}$$

to be solvable is that the function $f(\eta)$ satisfy the condition,

$$\int_S [y_o(\eta)]^* f(\eta)\, dS_\eta = 0 \tag{2}$$

where $y_o(\eta)$ is any eigenfunction of the adjoint homogeneous equation:

$$y_o(\eta) = \lambda^* \int_S [K(\xi,\eta)]^*\, y_o(\xi)\, dS_\xi \tag{3}$$

This appendix will show that equation (2) is a necessary condition for equation (1) to be solvable when λ is an eigenvalue.

First take the adjoint of equation (3). That is,

$$[y_o(\eta)]^* = \lambda \int_S K(\eta,\xi)[y_o(\xi)]^*\, dS_\xi \tag{4}$$

Now multiply both sides of equation (1) by the solution $[y_o(\eta)]^*$ of equation (4) and integrate with respect to η. Thus:

$$\int_S x(\eta)[y_o(\eta)]^*\, dS_\eta = \int_S f(\eta)[y_o(\eta)]^*\, dS_\eta + \int_S \left(\lambda \int_S K(\eta,\xi)[y_o(\eta)]^* dS_\eta\right) x(\xi) dS_\xi \tag{5}$$

which is equivalent to:

$$\int_S x(\eta)[y_o(\eta)]^* dS_\eta = \int_S f(\eta)[y_o(\eta)]^* dS_\eta + \int_S x(\xi)[y_o(\xi)]^* dS_\xi \tag{6}$$

and this yields:

$$\int_S f(\eta)[y_o(\eta)]^*\, dS_\eta = 0$$

as a necessary condition.

A proof for equation (2) to be a sufficient condition can be found in [28], [42], and [45]

APPENDIX G

This appendix demonstrates the compatibility of the orthogonality condition (3.3.6) for the surface Helmholtz integral method.

Thus when the wavenumber, k, is an eigenwavenumber the orthogonality condition:

$$\int_S \left[\Psi_o(\xi)\right]^* \left\{\int_S G(\xi,\mu)\, \frac{\partial \Psi(\mu)}{\partial n_\mu}\, dS_\mu\right\} dS_\mu = 0 \qquad (1)$$

will hold for all $\Psi_o(\xi)$ that satisfy the adjoint homogeneous equation:

$$\Psi_o(\eta) - 2\int_S \Psi_o(\xi)\, \frac{\partial \left[G(\xi,\eta)\right]^*}{\partial n_\eta}\, dS_\xi = 0 \qquad (2)$$

The proof presented below is based on a proof given by Schenk[24].

PROOF:

Consider the Helmholtz integral equation analogous to equation (3.2.26) but for an interior problem. That is:

$$\Psi^I(P) = -\int_S \left[\Psi^I(\xi)\, \frac{\partial G(P,\xi)}{\partial n_\xi} - G(P,\xi)\, \frac{\partial \Psi^I(\xi)}{\partial n_\xi}\right] dS \quad , \quad \xi \epsilon S \qquad (3)$$

where the superscript I denotes an interior quantity and the point P is contained within the 'interior' domain which is bounded externally by the surface S.

Using equation (3.2.4) of theorem 2, the normal derivative of (3) at $\eta \epsilon S$ will be:

$$\frac{\partial \Psi^I}{\partial n_\eta} = -\left\{\frac{\partial}{\partial n_\eta}\int_S \Psi^I(\xi)\, \frac{\partial G(\eta,\xi)}{\partial n_\xi}\, dS_\xi - \left[\tfrac{1}{2}\, \frac{\partial \Psi^I(\eta)}{\partial n_\eta} + \int_S \frac{\partial \Psi^I(\xi)}{\partial n_\xi}\, \frac{\partial G(\eta,\xi)}{\partial n_\xi}\, dS_\xi\right]\right\} \qquad (4)$$

and rearranging (4) yields:

$$-\tfrac{1}{2}\, \frac{\partial \Psi^I(\eta)}{\partial n_\eta} + \int_S \frac{\partial \Psi^I(\xi)}{\partial n_\xi}\, \frac{\partial G(\eta,\xi)}{\partial n_\xi}\, dS_\xi = \frac{\partial}{\partial n_\eta}\int_S \Psi^I(\xi)\, \frac{\partial G(\eta,\xi)}{\partial n_\xi}\, dS_\xi \qquad (5)$$

Consider now the homogeneous Dirichlet problem in which $\Psi^I(\xi) = 0$ on the surface S, and let the wavenumber k be an eigenwavenumber k_o.

Therefore equation (5) becomes:

$$-\tfrac{1}{2}\frac{\partial\Psi^I(n)}{\partial n_n} + \int_S \frac{\partial\Psi^I(\xi)}{\partial n_\xi}\frac{\partial G(n,\xi)}{\partial n_n}\,dS_\xi = 0 \tag{6}$$

Now take the complex conjugate of equation (3.3.12), which is the adjoint homogeneous equation for the exterior problem;

$$\left[\Psi_o(n)\right]^* - 2\int_S\left[\Psi_o(\xi)\right]^*\frac{\partial G(\xi,n)}{\partial n_n}\,dS_\xi = 0 \tag{7}$$

and rearranging;

$$-\tfrac{1}{2}\left[\Psi_o(n)\right]^* + \int_S\left[\Psi_o(\xi)\right]^*\frac{\partial G(\xi,n)}{\partial n_n}\,dS_\xi = 0 \tag{8}$$

Note that equation (8) is identical in form to equation (6).

Therefore the set $\{\frac{\partial\Psi^I(n)}{\partial n_n}\}$ of solutions that satisfy (6) is the same as the set $\{\Psi_o(n)^*\}$ of solutions which satisfy (8).

Consider again equation (3) and let the interior point P approach S. Using equation (3.2.6) of theorem 3 yields

$$\begin{aligned}\Psi^I(n) &= \lim_{P\to n}\Psi^I(P)\\ &= -\left\{\left[-\tfrac{1}{2}\Psi^I(n) + \int_S \Psi^I(\xi)\frac{\partial G(n,\xi)}{\partial n_\xi}\,dS_\xi\right] - \int_S G(n,\xi)\frac{\partial\Psi^I(\xi)}{\partial n_\xi}\right\}\end{aligned} \tag{9}$$

Rearranging (9) gives:

$$\tfrac{1}{2}\Psi^I(n) + \int_S \Psi^I(\xi)\frac{\partial G(n,\xi)}{\mu n_\xi}\,dS_\xi = \int_S G(n,\xi)\frac{\partial\Psi^I(\xi)}{\partial n_\xi}\,dS_\xi \tag{10}$$

Therefore for the homogeneous case in which $\Psi^I(\xi) \equiv 0$ on S and for $k = k_o$, equation (10) implies that:

$$\int_S G(n,\xi)\frac{\partial\Psi^I(\xi)}{\partial n_\xi}\,dS_\xi = 0 \tag{11}$$

Remembering the equivalence between the sets of solutions of equations (6) and (8), equation (11) will imply:

$$\int_S G(n,\xi)\left[\Psi_o(\xi)\right]^*\,dS_\xi = 0 \tag{12}$$

Now interchanging the order of integration in the orthogonality condition, equation (1) above, yields

$$\int_S \frac{\partial \Psi(\mu)}{\partial n_\mu} \left\{ \int_S \left[\Psi_o(\xi)\right]^* G(\xi,\mu)\, dS_\xi \right\} dS_\mu = 0 \qquad (13)$$

So from equation (12), equation (13) will be satisfied for any $\frac{\partial \Psi(\mu)}{\partial n_\mu}$.

APPENDIX H

The surface Helmholtz integral equation (3.2.27) and the interior Helmholtz integral equation (3.2.28) will have only one solution that is common to both.

The proof given below is based on a proof given by Schenk[24].

Let $\Psi_1(\xi)$ be a solution of the surface Helmholtz integral equation that also satisfies the interior Helmholtz integral equation for $k = k_o$ (k_o is an eigenwavenumber of the associated interior Dirichlet problem) and the given boundary condition $\frac{\partial \Psi(\xi)}{\partial n_\xi}$.

Therefore

$$\tfrac{1}{2}\Psi_1(\eta) - \int_S \left[\Psi_1(\xi) \frac{\partial G(\eta,\xi)}{\partial n_\xi} - G(\eta,\xi) \frac{\partial \Psi(\xi)}{\partial n_\xi}\right] dS_\xi = 0; \quad \eta \varepsilon S \tag{1}$$

$$\int_S \left[\Psi_1(\xi) \frac{\partial G(P,\xi)}{\partial n_\xi} - G(P,\xi) \frac{\partial \Psi(\xi)}{\partial n_\xi}\right] dS_\xi = 0; \quad P \varepsilon D_- \tag{2}$$

Any other solution of the surface integral equation (3.2.27)is of the form:

$$\Psi_2(\xi) = \Psi_1(\xi) + A\Psi_o(\xi) \tag{3}$$

where A is an arbitrary constant and $\Psi_o(\xi)$ is a nontrivial solution of the homogeneous form of the surface equation; i.e.

$$\tfrac{1}{2}\Psi_o(\eta) - \int_S \Psi_o(\xi) \frac{\partial G(\eta,\xi)}{\partial n_\xi} dS_\xi = 0 \tag{4}$$

If it is required that $\Psi_2(\xi)$ also satisfy the interior Helmholtz integral equation, then;

$$\int_S \left\{\left[\Psi_1(\xi) + A\Psi_o(\xi)\right] \frac{\partial G(P,\xi)}{\partial n_\xi} - G(P,\xi) \frac{\partial \Psi(\xi)}{\partial n_\xi}\right\} dS_\xi = 0 \tag{5}$$

From equation (2) this yields:

$$A \int_S \Psi_o(\xi) \frac{\partial G(P,\xi)}{\partial n_\xi} dS_\xi = 0 \qquad P \varepsilon D \tag{6}$$

If it can be shown that the integral in equation (6) does not vanish identically in D_-, then equation (6) will imply that $A = 0$ and hence, that $\Psi_1(\xi) = \Psi_2(\xi)$.

Consider now a function $U(P)$ defined by:

$$U(P) \equiv \int_S \Psi_o(\xi) \frac{\partial G(P,\xi)}{\partial n} dS_\xi \tag{7}$$

where P denotes a point in either D_- or D_+.

Note that equation (7) is the form of a double layer potential. Therefore, from equation (3.2.6) of theorem 3, the limiting value of $U(P)$ as P approaches S from the inside is:

$$\lim_{P\to\eta_-} U(P) \equiv U_- = -\tfrac{1}{2}\Psi_o(\eta) + \int_S \Psi_o(\xi) \frac{\partial G(\eta,\xi)}{\partial n_\xi} dS_\xi; \qquad \eta\epsilon S \tag{8}$$

hence equations (4) and (8) imply that:

$$U_- = 0 \tag{9}$$

The limit as P approaches S from the outside is:

$$\lim_{P\to\eta_+} U(P) \equiv U_+ = \tfrac{1}{2}\Psi_o(\eta) + \int_S \Psi_o(\xi) \frac{\partial G(\eta,\xi)}{\partial n_\xi} dS_\xi ; \quad \eta\epsilon S \tag{10}$$

hence using equation (4)

$$U_+ = \Psi_o(\eta) \tag{11}$$

In order to complete the proof the lemma of appendix (C) is needed. That is:
If $U(P)$ satisfies the Helmholtz equation, the Sommerfeld radiation condition and if its boundary values and those of its normal derivative exist then;

$$\mathrm{Im} \int_S U_+(\xi) \left[\frac{\partial U_+(\xi)}{\partial n_\xi}\right]^* dS_\xi = kC \qquad C \geq 0 \tag{12}$$

where C is an arbitrary constant and $C = 0$ if and only if $U(P)$ vanishes identically in D_+.

Now assume:

$$\frac{\partial U_-(\xi)}{\partial n_\xi} = 0 \tag{13}$$

From theorem 3 the normal derivative of a double-layer potential will remain continuous as the point P passes through the surface S.

Therefore, it follows that:

$$\frac{\partial U_+(\xi)}{\partial n_\xi} = 0 \tag{14}$$

and furthermore that:

$$\left[\frac{\partial U_+(\xi)}{\partial n_\xi}\right]^* = 0 \tag{15}$$

Substituting (15) into (12) gives C = 0 and hence that:

$$U(x) \equiv 0 \qquad x \varepsilon D_+ \tag{16}$$

and, in particular;

$$\lim_{x \to \eta_+} U(x) = U_+ = 0 \tag{17}$$

However equation (17) is in direct contradiction with equation (11) since $\Psi_0(\eta) \neq 0$ by definition, and so the original assumption, (13), must be false. That is:

$$\frac{\partial U_-(\xi)}{\partial n_\xi} \neq 0 \tag{18}$$

Because $U_- = 0$ by (9) and its rate of change as it moves toward the surface from the inside is non-zero by (18), then U(P) cannot vanish identically for all $P \varepsilon D_-$.

This result implies that A = 0 in equation (6) and, hence, that only one of the solutions of the surface Helmholtz integral equation can also satisfy the interior Helmholtz integral equation.

APPENDIX I

Proof of uniqueness of the BMF solution.

The Burton and Miller formulation involves the following equation applied on the surface:

$$\int_S \left[\Psi(\xi)\,\frac{\partial G(\eta,\xi)}{\partial n_\xi} - G(\eta,\xi)\,\frac{\partial \Psi(\xi)}{\partial n_\xi}\right] dS_\xi + \alpha \int_S \left[\Psi(\xi)\,\frac{\partial^2 G(\eta,\xi)}{\partial n_\eta \partial n_\xi} - \frac{\partial G(\eta,\xi)}{\partial n_\eta}\,\frac{\partial \Psi(\xi)}{\partial n_\xi}\right] dS_\xi$$

$$= \tfrac{1}{2}\left(\Psi(\eta) + \alpha\,\frac{\partial \Psi(\eta)}{\partial n_\eta}\right) \qquad ; \qquad \eta,\xi \in S \tag{1}$$

where α is a complex coupling constant. For the Neumann boundary-value problem the value of $\frac{\partial \Psi(\xi)}{\partial n_\xi}$ is given on the surface.

From theorem (5), the uniqueness of the solution of equation (1) will follow if it can be shown that the corresponding homogeneous equation:

$$\tfrac{1}{2}\Psi(\eta) - \int_S \Psi(\xi)\,\frac{\partial G(\eta,\xi)}{\partial n_\xi}\, dS_\xi - \alpha \int_S \Psi(\xi)\,\frac{\partial^2 G(\eta,\xi)}{\partial n_\eta \partial n_\xi}\, dS_\xi = 0 \tag{2}$$

has only the trivial solution $\Psi = 0$.

The proof that follows is based on a proof given by Burton and Miller[33].

Consider the double-layer Helmholtz potential function

$$U(P) = \int_S \Psi(\xi)\,\frac{\partial G(P,\xi)}{\partial n_\xi}\, dS_\xi \tag{3}$$

where P denotes a point in either D_- or D_+.

Theorem (3) gives the following limits as P approaches the surface from either side. When P approaches the surface from the inside then:

$$\lim_{P\to\eta_-} U(P) \equiv U_- = -\tfrac{1}{2}\Psi(\eta) + \int_S \Psi(\xi)\,\frac{\partial G(\eta,\xi)}{\partial n_\xi}\, dS_\xi \qquad ; \quad \eta\epsilon S \tag{4}$$

and from the outside:

$$\lim_{P\to\eta_+} U(P) \equiv U_+ = \tfrac{1}{2}\Psi(\eta) + \int_S \Psi(\xi)\,\frac{\partial G(\eta,\xi)}{\partial n_\xi}\, dS_\xi \qquad ; \quad \eta\epsilon S \tag{5}$$

The normal derivatives are continuous as P passes through the surface S, hence;

$$\frac{\partial U_-}{\partial n} = \frac{\partial U_+}{\partial n} = \frac{\partial U}{\partial n} \tag{6}$$

Now using equations (4) and (6) it is possible to express equation (2) as a relationship between the interior boundary values of U and $\frac{\partial U}{\partial n}$.

That is;

$$-U_- - \alpha\left(\frac{\partial U_-}{\partial n}\right) = 0 \tag{7}$$

Applying Green's theorem to U and its complex conjugate U^* within the exterior domain D_+ gives

$$\int_{D_+} (U\nabla^2 U^* - U^*\nabla^2 U)dD_+ = -\int_S (U_- \frac{\partial U_-^*}{\partial n} - U_-^* \frac{\partial U_-}{\partial n})dS \tag{8}$$

where U(P) satisfies the Helmholtz equation in D_+ as well as the Sommerfeld radiation condition at infinity. Using the Helmholtz equation in the left-hand side of equation (8) along with equation (7) in the right-hand side yields:

$$(\alpha - \alpha^*)\int_S \left|\frac{\partial U}{\partial n}\right|^2 dS = 0 \tag{9}$$

or, with $\alpha = \alpha_1 + i\alpha_2$,

$$2i\alpha_2 \int_S \left|\frac{\partial U}{\partial n}\right|^2 dS = 0 \tag{10}$$

Now provided that $\alpha_2 \neq 0$ it follows that $\frac{\partial U}{\partial n}$ will vanish on the surface S. Therefore equation (7) implies that $U_- = 0$.

With the result that $\frac{\partial U}{\partial n}$ vanishes on S, it follows from the uniqueness of the solution of the exterior problem (see Appendix (D)) that $U_+ \equiv 0$

Now with $U_+ = 0$ and $U_- = 0$, equations (4) and (5) imply that $\Psi = 0$ on the surface.

So the solution of equation (1) will be unique provided that α is chosen such that $\alpha_2 \equiv \mathrm{Im}(\alpha) \neq 0$

APPENDIX J

The strongly singular integral of the Burton and Miller formulation can be expressed as the sum of two weakly singular integrals, i.e.

$$\int_S \Psi(Q)\,\frac{\partial^2 G(P,Q)}{\partial n_p \partial n_q}\,dS_q = \int_S \left[\Psi(Q) - \Psi(P)\right]\,\frac{\partial^2 G(P,Q)}{\partial n_p \partial n_q}\,dS_q - \Psi(P)\int_S (\underline{n}_p.\underline{n}_q)(ik)^2\,G(P,Q)\,dS_q \qquad (1)$$

where G(P,Q) is the free-space Green's function, with P and Q points on the surface S.

PROOF:

First consider the singular part of the kernel.

$$\frac{\partial^2 G(P,Q)}{\partial n_p \partial n_q} = \underline{n}_q.\underline{\nabla}_q(\underline{n}_p.\underline{\nabla}_p G(P,Q))$$

$$= -\,\underline{n}_q.\underline{\nabla}_q(\underline{n}_p.\underline{\nabla}_q G(P,Q))$$

since $\underline{\nabla}_p G(P,Q) = -\underline{\nabla}_q G(P,Q)$.

Using the identity:

$$(\underline{a} \times \underline{b}).(\underline{c} \times \underline{d}) = (\underline{a}.\underline{c})(\underline{b}.\underline{d}) - (\underline{a}.\underline{d})(\underline{b}.\underline{c})$$

$$-(\underline{n}_q.\underline{\nabla}_q)(\underline{n}_p.\underline{\nabla}_q)G = (\underline{n}_q \times \underline{\nabla}_q).(\underline{n}_p \times \underline{\nabla}_q)G - (\underline{n}_q.\underline{n}_p)(\underline{\nabla}_q.\underline{\nabla}_q)G$$

$$= -(\underline{n}_q \times \underline{\nabla}_q).(\underline{n}_p \times \underline{\nabla}_p)G - (\underline{n}_p.\underline{n}_q)\nabla_q^2 G$$

$$= -\underline{n}_q.\underline{\nabla}_q \times (\underline{n}_p \times \underline{\nabla}_p G) + k^2(\underline{n}_p.\underline{n}_q)G \qquad (2)$$

since $\nabla_q^2 G = -k^2 G$ and using $(\underline{a} \times \underline{b}).\underline{c} = \underline{a}.(\underline{b} \times \underline{c})$

Hence:

$$\int_s \Psi(Q)\,\frac{\partial^2 G(P,Q)}{\partial n_p \partial n_q}\,dS_q = \int_s \Psi(Q)k^2(\underline{n}_p.\underline{n}_q)G(P,Q)dS_q - \int_s \Psi(Q)\underline{n}_q.\underline{\nabla}_q \times (\underline{n}_p \times \underline{\nabla}_p G(P,Q))dS_q$$

$$= I_1 + I_2 \tag{3}$$

The integral I_1 is weakly singular but I_2 is not. Consider I_2 by itself.

Let $\underline{\sigma} = (\underline{n}_p \times \underline{\nabla}_p G)$; hence

$$I_2 = -\int_s \Psi \underline{n}_q.\underline{\nabla}_q \times \underline{\sigma}\, dS_q$$

$$= -\int_s \underline{n}_q.\Psi\underline{\nabla}_q \times \underline{\sigma}\, dS_q \tag{4}$$

Apply the identity: $\underline{\nabla} \times (\Psi\underline{\sigma}) = \Psi(\underline{\nabla} \times \underline{\sigma}) + \underline{\nabla}\Psi \times \underline{\sigma}$, so

$$I_2 = -\int_s \underline{n}_q.\underline{\nabla}_q \times \Psi\underline{\sigma}\, dS_q + \int_s \underline{n}_q.\underline{\nabla}_q\Psi \times \underline{\sigma}\, dS_q \tag{5}$$

$$= -\int_{D_+} \underline{\nabla}_q.(\underline{\nabla}_q \times \Psi\underline{\sigma})\, dD_+ + \int_s \underline{n}_q.\underline{\nabla}_q\Psi \times \sigma\, dS_q \tag{6}$$

after using Green's theorem.

Noting that the divergence of a curl vanishes, equation (6) becomes:

$$I_2 = \int_s \underline{n}_q.\underline{\nabla}_q\Psi \times \underline{\sigma}\, dS_q = \int_s (\underline{n}_q \times \underline{\nabla}_q\Psi).\underline{\sigma}\, dS_q \tag{7}$$

since $\underline{a}.(\underline{b} \times \underline{c}) = \underline{c}.(\underline{a} \times \underline{b})$.

The integral I_2 is now expressed as a weakly singular integral. That is:

$$-\int_s \Psi(Q)\underline{n}_q.\underline{\nabla}_q \times (\underline{n}_p \times \underline{\nabla}_p G(P,Q))dS_q = \int_s \left[\underline{n}_q \times \underline{\nabla}_q\Psi(Q)\right].\left[\underline{n}_p \times \underline{\nabla}_p G(P,Q)\right] dS_q \tag{8}$$

Equation (3) can now be written as:

$$\int_s \Psi\,\frac{\partial^2 G}{\partial n_p \partial n_q}\,dS_q = \int_s \Psi k^2(\underline{n}_p.\underline{n}_q)G\, dS_q + \int_s (\underline{n}_q \times \underline{\nabla}_q\Psi).(\underline{n}_p \times \underline{\nabla}_p G)dS_q \tag{9}$$

This is the form given by Maue[48] and Burton[33], but as it stands this formulation (9) is difficult to implement numerically.

Returning to the integral I_2, as given on the left of (8), then;

$$I_2 = -\int_S \left[\Psi(Q) - \Psi(P)\right] \underline{n}_q \cdot \underline{\nabla}_q \times \left[\underline{n}_p \times \underline{\nabla}_p G(P,Q)\right] dS_q$$

$$- \Psi(P) \int_S \underline{n}_q \cdot \underline{\nabla}_q \times (\underline{n}_p \times \underline{\nabla}_p G(P,Q)) dS_q \qquad (10)$$

The second integral in (10) will vanish identically by putting $\Psi(Q) = 1$ in equation (8).

Thus:

$$\int_S \Psi(Q) \frac{\partial^2 G(P,Q)}{\partial n_p \partial n_q} dS_q = \int_S \Psi(Q) k^2 (\underline{n}_p \cdot \underline{n}_q) G(P,Q) \, dS_q$$

$$- \int_S \left[\Psi(Q) - \Psi(P)\right] \underline{n}_q \cdot \underline{\nabla}_q \times (\underline{n}_p \times \underline{\nabla}_p G(P,Q)) dS_q \qquad (11)$$

Now set $\Psi(Q) = 1$ in equation (11), so that

$$\int_S \frac{\partial^2 G(P,Q)}{\partial n_p \partial n_q} dS_q = \int_S (\underline{n}_p \cdot \underline{n}_q) k^2 \, G(P,Q) \, dS_q \qquad (12)$$

Noting that the left hand side of (11) can be given as:

$$\int_S \Psi(Q) \frac{\partial^2 G(P,Q)}{\partial n_p \partial n_q} dS_q = \int_S \left[\Psi(Q) - \Psi(P)\right] \frac{\partial^2 G(P,Q)}{\partial n_p \partial n_q} dS_q + \Psi(P) \int_S \frac{\partial^2 G(P,Q)}{\partial n_p \partial n_q} dS_q \qquad (13)$$

Employing equation (12) yields:

$$\int_S \Psi(Q) \frac{\partial^2 G(P,Q)}{\partial n_p \partial n_q} dS_q = \int_S \left[\Psi(Q) - \Psi(P)\right] \frac{\partial^2 G(P,Q)}{\partial n_p \partial n_q} dS_q - \Psi(P) \int_S (\underline{n}_p \cdot \underline{n}_q)(ik)^2 G(P,Q) dS_q \qquad (14)$$

which was to be shown.

APPENDIX K

The residual least squares procedure.

Consider the residuals R_1 and R_2 such that

$$\begin{aligned} R_1 &= [A]\{\Psi\} - \{G\} \\ R_2 &= [B]\{\Psi\} - \{H\} \end{aligned} \tag{1}$$

Define a residual χ given by

$$\chi = \alpha R_1^T R_1^* + (1-\alpha) R_2^T R_2^* \tag{2}$$

or

$$\chi = \alpha[\Psi^T A^T - G^T][A^*\Psi^* - G^*] + (1-\alpha)[\Psi^T B^T - H^T][B^*\Psi^* - H^*] \tag{3}$$

where α is a real constant $(0 < \alpha < 1)$ and the matrix brackets have been dropped for clarity.

The residual χ can now be written as:

$$\chi = \Psi^T[\alpha A^T A^* + (1-\alpha)B^T B^*]\Psi^* - \Psi^T[\alpha A^T G^* + (1-\alpha)B^T H^*] - \Psi^{*T}[\alpha A^{*T} G + (1-\alpha)B^{*T} H]$$

$$+ [\alpha G^T G^* + (1 -)H^T H^*] \tag{4}$$

noting that $[\alpha G^T A^* + (1-\alpha)H^T B^*]\Psi^* = \Psi^{*T}[\alpha A^{*T} G + (1-\alpha)B^{*T} H]$.

Now define

$$K_A^* = A^T A^* \quad , \quad K_B^* = B^T B^*$$

$$M^* = \alpha A^T G^* + (1-\alpha)B^T H^* \rightarrow M = \alpha A^{T*} G + (1-\alpha)B^{T*} H$$

$$E = \alpha G^T G^* + (1-\alpha)G^T G^*$$

and let $K^* = K_A^* + (1-\alpha)K_B^*$

Therefore equation (4) is:

$$\chi = \Psi^T K^* \Psi^* - \Psi^T M^* - \Psi^{*T} M + E \tag{5}$$

or

$$\chi = \Psi^{*T} K \Psi - \Psi^T M^* - \Psi^{*T} M + E \tag{6}$$

hence $$\{\frac{\partial \chi}{\partial \Psi}\} = K^{*}\Psi^{*} - M^{*} \tag{7}$$

$$\{\frac{\partial \chi}{\partial \Psi^{*}}\} = K\Psi - m \tag{8}$$

Now writing:

$$\begin{aligned} \Psi &= \Psi_R + i\Psi_I \\ \Psi^{*} &= \Psi_R - i\Psi_I \end{aligned} \tag{9}$$

where the subscripts R and I indicate real and imaginary parts respectively. Thus

$$\frac{\partial \chi}{\partial \Psi_R} = \frac{\partial \chi}{\partial \Psi} + \frac{\partial \chi}{\partial \Psi^{*}} \tag{10}$$

$$\frac{\partial \chi}{\partial \Psi_I} = i(\frac{\partial \chi}{\partial \Psi} + \frac{\partial \chi}{\partial \Psi^{*}}) \tag{11}$$

and equations (10) and (11) give

$$\frac{\partial \chi}{\partial \Psi_R} + i\,\frac{\partial \chi}{\partial \Psi_I} = 2\,\frac{\partial \chi}{\partial \Psi^{*}} \tag{12}$$

So letting $\frac{\partial \chi}{\partial \Psi^{*}} = 0$ implies that the equation:

$$\left[K\right]\{\Psi\} = \{M\} \tag{13}$$

will give a least-squares solution.

APPENDIX L

Derivation of an analytic solution.

This appendix derives a restricted analytic solution for the acoustic velocity potential in the case of both a pulsating and juddering sphere within a mean flow.

The derivation presented here is based on a derivation given in reference [7]. Without loss of generality, the surface vibration will be specified as time harmonic.

In three dimensions, the general surface displacement, η, of a time harmonic vibration can be expressed in the form:

$$\eta(\theta,\psi,t) = a\, e^{i\omega t} \sum_{n=0}^{\infty} \sum_{m=-n}^{n} E_n^m P_n^m (\cos\theta) e^{im\psi} \qquad (1)$$

where, a is the radius of the mean position of the sphere, E_n^m is a constant and P_n^m is the Legendre function of the first kind, m-th order n-th degree. Equation (1) is of the same form as the general solution of the spherical wave equation.

If the mean position of the vibrating body is a sphere of radius, $r = a$ and if the mean flow has a low Mach number then the boundary condition at r=a is given by equation (5.1.7). That is:

$$\frac{\partial\phi}{\partial r} = \left[\frac{\partial}{\partial t} + \frac{3}{2}\frac{M_\infty}{a} C_\infty \sin\theta \frac{\partial}{\partial\theta}\right]\eta(\theta,\psi,t) + \eta(\theta,\psi,t)\left[\frac{3M_\infty}{a} C_\infty \cos\theta\right] \text{ at } r = a \qquad (2)$$

Substituting the surface displacement of (1) in the boundary conditon (2) yields:

$$\frac{\partial\phi}{\partial r} = C_\infty e^{i\omega t} \sum_{n=0}^{\infty} \sum_{m=-n}^{n} E_n^m \left[ika\, P_n^m(\cos\theta)\right.$$

$$\left. - \frac{3}{2} M_\infty \left\{ P_n^{m'}(\cos\theta)\sin^2\theta - 2P_n^m(\cos\theta)\cos\theta \right\}\right] e^{im\psi}, \text{ at } r = a \qquad (3)$$

Consider the following recurrence relations for Legendre functions:

$$(1-z^2)P_n^{m'}(z) = (n+1)zP_n^m(z) - (n-m+1)P_n^m(z) \qquad (i)$$

$$(2n+1)zP_n^m(z) = (n-m+1)P_{n+1}^m(z) + (n+m)P_{n-1}^m(z) \qquad (ii)$$

Using both relations (i) and (ii) equation (3) can be written as:

$$\frac{\partial\phi}{\partial r} = C_\infty e^{i\omega t} \sum_{n=0}^{\infty} \sum_{m=-n}^{n} E_n^m \left[ika\, P_n^m(\cos\theta) - \frac{3M_\infty}{2(2n+1)} \left\{ (n-1)(n+m)P_{n-1}^m(\cos\theta) - (n+2)(n-m+1)P_n^m(\cos\theta)\cos\theta \right\} \right] e^{im\psi}$$

$$\text{at } r = a \qquad (4)$$

Taylor's transformation (2.6.7) is now applied to the problem in the form:

$$(r_x, \theta_x, \psi_x, T) = (r, \theta, \psi, t + \frac{M_\infty}{C_\infty}\hat{\phi})$$

$$\phi(r_x, \theta_x, \psi_x, T) = \phi(r, \theta, \psi, t) \qquad (5)$$

where $\hat{\phi} = \frac{\bar{\phi}}{U_\infty} = -(r + \frac{a^3}{2r^2})\cos\theta$

Letting:

$$A_n^m(\cos\theta) = (n-1)(n+m)P_{n-1}^m(\cos\theta) - (n+2)(n-m+1)P_{n+1}^m(\cos\theta) \qquad (6)$$

the transformed boundary condition can be written as:

$$\frac{\partial\phi}{\partial r_x} = C_\infty e^{i\omega T} e^{(3/2)ikaM_\infty\cos\theta_x} \sum_{n=0}^{\infty} \sum_{m=-n}^{n} \left[ika\, P_n^m(\cos\theta_x) - \frac{3M_\infty}{2(2n+1)} A_n^m(\cos\theta_x) \right] e^{im\psi_x}$$

$$\text{at } r_x = a \qquad (7)$$

where $\hat{\phi} = \frac{-3}{2} a \cos\theta_x$ at $r_x = a$.

At this stage of the derivation the term:

$$e^{(3/2)ikaM_\infty\cos\theta_x}$$

is expanded as an exponential series.

Therefore equation (7) can be written in an expanded form as:

$$\frac{\partial\phi}{\partial r_x} = C_\infty e^{i\omega T} \sum_{n=0}^{\infty} \sum_{m=-n}^{n} E_n^m \left[ikaP_n^m(\cos\theta_x) - \frac{3M_\infty}{2(2n+1)} A_n^m(\cos\theta_x) - \frac{3}{2}(ka)^2 M_\infty \cos\theta_x P_n^m(\cos\theta_x) - \frac{9}{4}\frac{ika}{(2n+1)} M_\infty^2 \cos\theta_x A_n^m(\cos\theta_x) - \frac{9}{8}(ka)^3 M_\infty^2 \cos^2\theta_x P_n^m(\cos\theta_x) \right] e^{im\psi} + (\text{terms containing higher powers of } M_\infty),$$

$$\text{at } r_x = a \qquad (8)$$

In the derivation of reference [7], equation (8) is truncated by removing all those terms that contain the second or higher powers of M_∞. After considering equation (8) in more detail this linearization procedure will be valid only if the following conditions are satisfied:

i.e. (i) $M_\infty^2 \ll 1$

(ii) $M_\infty(ka) \ll 1$

(iii) $M_\infty/(ka) \ll 1$

(iv) $M_\infty(ka)^3 \ll 1$

This implies validity only where the Mach number, M_∞, is small and the frequency parameter (ka) is of order 1.

Assuming the above conditions are satisfied, the truncated equation will be:

$$\frac{\partial\phi}{\partial r_x} = C_\infty e^{i\omega T} \sum_{n=0}^{\infty} \sum_{m=-n}^{n} E_n^m \left[ikaP_n^m(\cos\theta_x) - \frac{3M_\infty}{2(2n+1)} A_n^m(\cos\theta_x) - \frac{3}{2}(ka)^2 M_\infty \cos\theta_x P_n^m(\cos\theta_x) \right] e^{im\psi_x} \quad , \quad \text{at } r_x = a \tag{9}$$

Using the recurrence relations again gives:-

$$\frac{\partial\phi}{\partial r_x} = C_\infty e^{i\omega T} \sum_{n=0}^{\infty} \sum_{m=-n}^{n} E_n^m \left[ikaP_n^m(\cos\theta_x) - \frac{3M_\infty}{2(2n+1)} A_n^m(\cos\theta_x) - \frac{3(ka)^2}{2(2n+1)} M_\infty \left\{ (n-m+1)P_{n+1}^m(\cos\theta_x) + (n+m)P_{n-1}^m(\cos\theta_x) \right\} \right] e^{im\psi_x} \quad \text{at } r_x = a \tag{10}$$

Equation (10) can be further rearranged to give:

$$\frac{\partial\phi}{\partial r_x} = C_\infty e^{i\omega T} \sum_{n=0}^{\infty} \sum_{m=-n}^{n} E_n^m \left[ikaP_n^m(\cos\theta_x) - \frac{3M_\infty}{2(2n+1)} (n+m)(n-1+k^2a^2)P_{n-1}^m(\cos\theta_x) + \frac{3M_\infty}{2(2n+1)} (n-m+1)(n+2-k^2a^2)P_{n+1}^m(\cos\theta_x) \right] e^{im\psi_x} \quad , \text{ at } r_x = a \tag{11}$$

Now equation (11) can be written in the form:

$$\frac{\partial\phi}{\partial r_x} = \frac{\partial\Psi}{\partial r_x} e^{i\omega T} \qquad \text{at } r_x = a \tag{12}$$

where the function Ψ satisfies the Helmholtz equation:

$$(\nabla_x^2 + k^2)\Psi = 0 \tag{13}$$

Therefore the problem reduces to solving equation (13) for Ψ which also satisfies the boundary condition given by:

$$\frac{\partial \Psi}{\partial r_x} = C_\infty \sum_{n=0}^{\infty} \sum_{m=-n}^{n} E_n^m \left[\frac{-3M_\infty}{2(2n+1)} (n+m)(n-1+k^2a^2) P_{n-1}^m(\cos\theta_x) + ika P_n^m(\cos\theta_x) \right.$$

$$\left. + \frac{3M_\infty}{2(2n+1)} (n-m+1)(n+2-k^2a^2) P_{n+1}^m(\cos\theta_x) \right] e^{im\psi_x} \quad \text{at } r_x = a \qquad (14)$$

The general solution of equation (13) can be written in the form:

$$\Psi = \sum_{n=0}^{\infty} \sum_{m=-n}^{n} B_n^m h_n^{(2)}(kr_x) P_n^m(\cos\theta_x) e^{im\psi_x} \qquad (15)$$

where B_n^m is constant and $h_n^{(2)}$ is the spherical Hankel function of the second kind and n-th order.

The constants B_n^m can be evaluated from the requirement that Ψ must also satisfy the boundary condition (14) at $r_x = a$. Therefore, equation (15) will become:

$$\Psi = \frac{C_\infty}{k} \sum_{n=0}^{\infty} \sum_{m=-n}^{n} E_n^m \left[\frac{-3M_\infty}{2(2n+1)} (n+m)(n-1+k^2a^2) \frac{h_{n-1}^{(2)}(kr_x)}{h_{n-1}^{(2)'}(ka)} P_{n-1}^m(\cos\theta_x) \right.$$

$$+ ika \frac{h_n^{(2)}(kr_x)}{h_n^{(2)'}(ka)} P_n^m(\cos\theta_x)$$

$$\left. + \frac{3M_\infty}{2(2n+1)} (n-m+1)(n+2-k^2a^2) \frac{h_{n+1}^{(2)}(kr_x)}{h_{n+1}^{(2)'}(ka)} P_{n+1}^m(\cos\theta_x) \right] e^{im\psi_x}, \text{ at } r_x = a \qquad (16)$$

The acoustic velocity potential, $\phi(r_x, \theta_x, \psi_x, T)$ is given by:

$$\phi(r_x, \theta_x, \psi_x, T) = \Psi e^{i\omega T} \qquad (17)$$

so that for the mean flow problem;

$$\phi(r, \theta, \psi, t) = \Psi e^{ikM_\infty \hat{\phi}} e^{i\omega t} \qquad (18)$$

since $$(r_x, \theta_x, \psi_x, T) = (r, \theta, \psi, t + \frac{M_\infty}{C_\infty} \hat{\phi})$$

Therefore the acoustic velocity potential, ϕ, in a mean flow due to a general time harmonic vibration about a mean spherical surface, r=a, is given by:

$$\phi = \frac{C_\infty}{k} e^{-ikM_\infty(r+(a^3/2r^2))\cos\theta} \sum_{n=0}^{\infty} \sum_{m=-n}^{n} E_n^m \left[ika \frac{h_n^{(2)}(kr)}{h_n^{(2)'}(ka)} P_n^m(\cos\theta) \right.$$

$$- \frac{3M_\infty}{2(2n+1)}(n+m)(n-1+k^2a^2) \frac{h_{n-1}^{(2)}(kr)}{h_{n-1}^{(2)'}(ka)} P_{n-1}^m(\cos\theta)$$

$$\left. + \frac{3M_\infty}{2(2n+1)}(n-m+1)(n+2-k^2a^2) \frac{h_{n+1}^{(2)}(kr)}{h_{n+1}^{(2)'}(ka)} P_{n+1}^m(\cos\theta) \right] e^{im\psi} e^{i\omega t} \qquad (19)$$

This equation is valid when the Mach number, M_∞, is small and the frequency parameter (ka) is of order 1. Consider now the specific case of a 'pulsating' sphere.

The surface displacement of a 'pulsating' sphere can be expressed in the form of equation (5.1.8), therefore equating this to the general surface displacement of equation (1) above gives:

$$a\varepsilon e^{i\omega t} = a \sum_{n=0}^{\infty} \sum_{m=-n}^{n} E_n^m P_n^m(\cos\theta) e^{im\psi} e^{i\omega t} \qquad (20)$$

Equation (20) implies that:

$$E_o^o = \varepsilon \quad \text{and} \quad E_n^m = 0 \text{ for all other values of m and n,}$$

hence for the case of a pulsating sphere, equation (19) will become:

$$\phi = \varepsilon \frac{C_\infty}{k} e^{-ikM_\infty(r+(a^3/2r^2))\cos\theta} \left[ika \frac{h_o^{(2)}(kr)}{h_o^{(2)'}(ka)} + \frac{3M_\infty}{2}(2-k^2a^2) \frac{h_1^{(2)}(kr)}{h_1^{(2)'}(ka)} \cos\theta \right] e^{i\omega t} \qquad (21)$$

Equation (21) expresses the form of the acoustic velocity potential due to a 'pulsating' sphere within a low Mach number mean flow.

For the case of a 'juddering' sphere the surface displacement given by equation (5.1.16) can be equated to the general surface displacement of equation (1) above. That is:

$$a\varepsilon\cos\theta\, e^{i\omega t} = a \sum_{n=0}^{\infty} \sum_{m=-n}^{n} E_n^m P_n^m(\cos\theta) e^{im\psi} e^{i\omega t} \qquad (22)$$

This implies that:

$$E_1^o = \varepsilon \quad \text{and} \quad E_n^m = 0 \quad \text{for all other values of m and n,}$$

so for the case of a 'juddering' sphere within a low Mach number mean flow of the acoustic velocity potential is given by:

$$\phi = \varepsilon \frac{C_\infty}{k} e^{-ikM_\infty(r+(a^3/2r^2))\cos\theta} \left[-\tfrac{1}{2}M_\infty k^2a^2 \frac{h_o^{(2)}(kr)}{h_o^{(2)'}(ka)} \right.$$

$$\left. + ika \frac{h_1^{(2)}(kr)}{h_1^{(2)'}(ka)} \cos\theta + \frac{M_\infty(3-k^2a^2)}{2} \frac{h_2^{(2)}(kr)}{h_2^{(2)'}(ka)} (3\cos^2\theta-1) \right] e^{i\omega t} \qquad (23)$$

Both equations (21) and (23) will be valid only in the case of a low Mach number mean flow and a frequency parameter (ka) of order 1.

APPENDIX M

If the free-space Green's function in three dimensional space is:

$$G(P,Q) = \frac{e^{-ikr(P,Q)}}{4\pi r(P,Q)}$$

where $r = r(P,Q)$ is the distance between points P and Q then

$$\frac{\partial^2 G(P,Q)}{\partial n_p \partial n_q} = \frac{e^{-ikr}}{4\pi r}\left\{\left[(ik)^2 + \frac{3(ik)}{r} + \frac{3}{r^2}\right]\frac{\partial r}{\partial n_p}\frac{\partial r}{\partial n_q} + \frac{1}{r}(ik + \frac{1}{r})(\underline{n}_p.\underline{n}_q)\right\} \qquad (1)$$

$\underline{n}_p$ and $\underline{n}_q$ are unit normal vectors directed outward from points P and Q respectively.

$\underline{r}_{PQ}$ is the vector from point P to point Q on the surface S.

So $\underline{r}_{QP} = -\underline{r}_{PQ}$, and $\hat{\underline{r}}_{PQ} = \underline{r}_{PQ}/r$, is the unit vector in the direction of $\underline{r}_{PQ}$.

Also

$$\frac{\partial r(P,Q)}{\partial n_q} = \underline{\nabla}_q r(P,Q).\underline{n}_q = \hat{\underline{r}}_{PQ}\cdot\underline{n}_q$$

$$\frac{\partial r(P,Q)}{\partial n_q} = \underline{\nabla}_p r(P,Q).\underline{n}_p = \hat{\underline{r}}_{QP}\cdot\underline{n}_p = -\hat{\underline{r}}_{PQ}\cdot\underline{n}_p$$

Now let $G(P,Q) = H(r)$ where $r = r(P,Q)$ then,

(i) $$\frac{\partial G}{\partial n_q} = H'(r)\frac{\partial r}{\partial n_q} = H'(r)(\hat{\underline{r}}_{PQ}\cdot\underline{n}_q) \qquad (2)$$

(ii) $$\frac{\partial^2 G}{\partial n_p \partial n_q} = \frac{\partial}{\partial n_p}\left(\frac{\partial G}{\partial n_q}\right) = \frac{\partial}{\partial n_p}\frac{1}{r}H'(r)(\underline{r}_{PQ}\cdot\underline{n}_q)$$

$$= \frac{\partial}{\partial n_p}\frac{1}{r}H'(r)\,(\underline{r}_{PQ}\cdot\underline{n}_q) + \frac{1}{r}H'(r)\frac{\partial}{\partial n_p}(\underline{r}_{PQ}\cdot\underline{n}_q)$$

$$= \frac{1}{r}H''(r) - \frac{1}{r^2}H'(r)\,(\underline{r}_{QP}\cdot\underline{n}_p)(\underline{r}_{PQ}\cdot n_q)$$

$$+ \frac{1}{r}H'(r)\frac{\partial}{\partial n_p}(\underline{r}_{PQ}\cdot\underline{n}_q) \qquad (3)$$

The term $\frac{\partial}{\partial n_p}(\underline{r}_{PQ}\cdot n_q)$ of (3) is simplified by differentiating from first principles.

Let $\delta\underline{r} = \delta r.\underline{n}_p$ where δr is the infinitesimal distance between points P and P' on the normal vector outward from P.

Therefore:

$$\frac{\partial}{\partial n_p}(\underline{r}_{PQ}\cdot\underline{n}_q) = \frac{-\partial}{\partial n_p}(\underline{r}_{QP}\cdot\underline{n}_q)$$

$$= -\lim_{\delta r\to 0}\left[\frac{\underline{r}_{QP'}\cdot\underline{n}_q - \underline{r}_{QP}\cdot\underline{n}_q}{\delta r}\right]$$

$$= -\lim_{\delta r\to 0}\left[\frac{(\delta r\ \underline{n}_p)\cdot\underline{n}_q}{\delta r}\right]$$

$$= -(\underline{n}_p\cdot\underline{n}_q) \qquad (4)$$

So equation (3) becomes:

$$\frac{\partial^2 G}{\partial n_p \partial n_q} = \left[\frac{1}{r}H''(r) - \frac{1}{r^2}H'(r)\right](\hat{\underline{r}}_{QP}\cdot\underline{n}_p)(\underline{r}_{PQ}\cdot\underline{n}_q) - \frac{1}{r}H'(r)(\underline{n}_p\cdot\underline{n}_q)$$

$$= \left[H''(r) - \frac{1}{r}H'(r)\right](\hat{\underline{r}}_{QP}\cdot\underline{n}_p)(\hat{\underline{r}}_{PQ}\cdot\underline{n}_q) - \frac{1}{r}H'(r)(\underline{n}_p\cdot\underline{n}_q) \qquad (5)$$

Now $$H(r) = \frac{e^{-ikr}}{4\pi r}$$

$$H'(r) = \frac{-e^{-ikr}}{4\pi r}\left(ik + \frac{1}{r}\right)$$

$$H''(r) = \frac{e^{-ikr}}{4\pi r}\left[(ik)^2 + \frac{2ik}{r} + \frac{2}{r^2}\right]$$

Thus equation (5) can be written as:

$$\frac{\partial^2 G(P,Q)}{\partial n_p \partial n_q} = \frac{e^{-ikr}}{4\pi r}\left\{\left[(ik)^2 + \frac{3ik}{r} + \frac{3}{r^2}\right]\frac{\partial r}{\partial n_p}\frac{\partial r}{\partial n_q} + \frac{1}{r}\left(ik + \frac{1}{r}\right)(\underline{n}_p\cdot\underline{n}_q)\right\}$$

which was to be shown.

```
C                       APPENDIX N.
C
C
C
C     THIS APPENDIX CONTAINS THE FORTRAN LISTINGS OF THE BOUNDARY
C     ELEMENT PROCEDURE DISCUSSED IN THE PRESENT STUDY.
C     BOTH THE CHIEF AND BMF METHODS ARE CONSIDERED. HOWEVER AS THE
C     GENERAL IMPLEMENTATION OF THESE METHODS IS SIMILAR, MANY
C     SUBROUTINES WILL 'OVERLAP' HENCE IN THIS CASE ONLY ONE IS
C     PRESENTED.
C
C
C
C ********************************************************************
C *                                                                  *
C *   FORTRAN SOURCE FOR BOUNDARY ELEMENT PROG. FOR A PULSATING      *
C *   OR JUDDERING SPHERE IN A LOW MACH NO. MEAN FLOW.               *
C *                                                                  *
C *   USING THE CHIEF AND BMF BOUNDARY INTEGRAL METHODS              *
C *                                                                  *
C ********************************************************************
$RESET LIST
$SET AUTOBIND
$BIND=FROM PLOTA/=
$BINDER RESET LIST
C ********************************************************************
C *                                                                  *
C *       BMF       MAIN PROGRAM.                                    *
C *                                                                  *
C *       THIS REPRESENTS THE MAIN PROGRAM FOR THE BMF METHOD.       *
C *       THREE SUBROUTINES ARE CALLED.  THE SURFAC SUBROUTINE       *
C *       EFFECTIVELY GENERATES THE BOUNDARY ELEMENT SURFACE,        *
C *       THE SURFACE SINGULARITY PTS.  ( AND INTERIOR POINTS FOR    *
C *       CHIEF ) ARE COMPUTED IN THIS SUBROUTINE.                   *
C *       THE ASSEMB SUBROUTINE FORMULATES THE INTEGRATION MATRICES  *
C *       AND TO DO SO CALLS THE INTEG SUBROUTINE.                   *
C *       THE SOLVE SUBROUTINE SOLVES THE FINAL MATRIX EQUATION      *
C *       [ ZM ][ ZPHI ] = [ ZF ] FOR ZPHI AND OUTPUTS THE           *
C *       COMPUTED SOLUTION.                                         *
C *       THE ARRAYS AND VARIABLES ARE DESCRIBED WITHIN THE          *
C *       RELEVANT SUBROUTINES.                                      *
C *                                                                  *
C ********************************************************************
C
C
      IMPLICIT COMPLEX(Z)
      DIMENSION SS(550),TH(16),PH(16),IR(18),IS(18),IT(18),ZM(32400)
     1,ZMAS(32400),ZMBS(32400),ZMCS(32400),ZMDS(32400),ZQ(180),ZPHI(180)
      COMMON NF,XK,XM,N1,ID1,N2,ID2,NV
      SFAREA=0.0
C
      CALL SURFAC(SS,TH,PH,IR,IS,IT,MODE)
C
      CALL ASSEMB(SS,TH,PH,IR,IS,IT,ZMAS,ZMBS,ZMCS,ZMDS,ZM
     1,ZQ,SFAREA,MODE)
C
      CALL SOLVE(ZM,ZQ,TH,PH,IR,IS,IT,SS,ZPHI,ZMDS,SFAREA,MODE)
      RETURN
      END
C
```

```
C
C
C ***************************************************************
C *                                                             *
C *     BMF OR CHIEF                                            *
C *                                                             *
C *     SUBROUTINE SURFAC ( CALLED FROM MAIN PROGRAM )          *
C *                                                             *
C *     THIS SUBROUTINE POSITIONS THE SURFACE SINGULARITY PT.   *
C *     ( AND THE INTERIOR PT.  NECESSARY FOR CHIEF ) FOR EACH  *
C *     ELEMENT OF THE BOUNDARY ELEMENT DISCRETIZATION.         *
C *                                                             *
C *     THIS SUBROUTINE FIRST READS 8 CONTROL VARIABLES         *
C *     CONTROL VARIABLES READ:                                 *
C *                    NF - TOTAL NO. OF FACETS ( ELEMENTS )    *
C *                    N1 - NO. OF PTS. IN OFF-DIAGONAL INTEGRATION *
C *                    N2 - NO. OF PTS. IN DIAGONAL INTEGRATION *
C *                   ID1 - DEGREE OF OFF-DIAGONAL INTEG. SCHEME *
C *                   ID2 - DEGREE OF DIAGONAL INTEG SCHEME     *
C *                    XK - WAVENUMBER                          *
C *                    XM - FARFIELD MACH NO.                   *
C *                    NV - NO. OF VERTICES IN A CHARACTERISTIC *
C *                         SEGMENT (SEE BELOW)                 *
C *                  MODE - MODE OF VIBRATION                   *
C *                                                             *
C *     THE DISCRETIZED SURFACE IS GENERATED BY ROTATING        *
C *     THE KNOWN CHARACTERISTICS OF A SMALL SEGMENT OF THE     *
C *     MODEL AROUND THE SURFACE.                               *
C *     THIS SMALL SEGMENT IS 'DIAMOND' SHAPED IN THAT IT       *
C *     ORIGINATES FROM TWO FACES OF AN ICOSAHEDRON.            *
C *                                                             *
C *     THE DATA OF THIS CHARACTERISTIC SEGMENT IS READ IN THE   *
C *     FORM OF:                                                *
C *             - ARRAYS IR, IS, IT REPRESENTING THE SPECIFIC   *
C *               CONFIGURATION OF TRIANGULAR ELEMENTS WITHIN THE *
C *               SEGMENT.                                      *
C *             - ARRAYS TH, PH REPRESENTING THE CO-ORDS. OF THE *
C *               TRIANGLE VERTICES WITHIN THE SEGMENT.         *
C *                                                             *
C ***************************************************************
C *                                                             *
C *      ARRAYS ( NOT ALREADY MENTIONED ABOVE )                 *
C *       ( XS, YS, WS ) - CO-ORDS. OF EACH VERTEX              *
C *          SS          - THE SURFACE SINGULARITY PTS.         *
C *          SI          - THE INTERIOR POINTS ( CHIEF )        *
C *          RNP         - OUTWARD UNIT NORMAL AT THE SING. PT. P *
C *                                                             *
C *      VARIABLES ( NOT ALREADY MENTIONED ABOVE )              *
C *          NT    - NO. OF TRIANGLES IN THE SEGMENT            *
C *          IND   - INDICATES WHETHER SEGMENT IS IN THE UPPER  *
C *                  OR LOWER HEMISPHERE.                       *
C *          M     - POSITION OF SEGMENT WITHIN EACH HEMISPHERE *
C *                                                             *
C ***************************************************************
C
C
      SUBROUTINE SURFAC(SS, SI, TH, PH, IR, IS, IT, MODE)
      IMPLICIT COMPLEX(Z)
      DIMENSION SS(3, 1), SI(3, 1), TH(1), PH(1), XS(16), YS(16), WS(16)
     1, IR(1), IS(1), IT(1), RN(3), RNP(3)
      COMMON NF, XK, XM, N1, ID1, N2, ID2, NV
C
C  READ CONTROL VARIABLES
C
      READ(5, 100)NF, N1, ID1, N2, ID2, XK, XM, NV, MODE
  100 FORMAT(5I5, 2F10.4, 2I5)
      NT=NF/10
```

```
C
C  READ THE TRIANGLE CONFIGURATION FOR THE CHARACTERISTIC SEGMENT
C
      DO 1 I=1,NT
    1 READ(5,101)IR(I),IS(I),IT(I)
  101 FORMAT(3I3)
C
C  READ THE THETA AND PHI SPHERICAL CO-ORDS. FOR THE VERTICES OF THE
C  CHARACTERISTIC SEGMENT.
C
      DO 2 I=1,NV
    2 READ(5,102)TH(I),PH(I)
  102 FORMAT(2F10.7)
C
      XPI=3.1415926
      TAU=(SQRT(5.0)+1.0)/2.0
C
C  GENERATION OF SINGULARITY POINTS
C
C  LOOP FOR TOP & BOTTOM HALFS
      DO 10 IND=1,2
C
C  LOOP FOR 5 SEGMENTS IN EACH HALF
      DO 11 M=1,5
C
C  LOOP FOR (NV) VERTICES WITHIN EACH 'DIAMOND' SEGMENT
      DO 12 I=1,NV
C
C  GENERATE CO-ORDS. OF EACH VERTEX IN EACH SEGMENT
C
      A=TH(I)+(IND-1)*(XPI-2.0*TH(I))
      B=PH(I)+(2*M+IND-3)*XPI/5.0
C
      XS(I)=SIN(A)*COS(B)
      YS(I)=SIN(A)*SIN(B)
   12 WS(I)=COS(A)
C
C  POSITION SURFACE SINGULARTY PTS. AT THE CENTROID OF EACH ELEMENT
C
      DO 13 K=1,NT
      IA=IR(K)
      IB=IS(K)
      IC=IT(K)
      IE=NT*(M-1)+K+(IND-1)*NT*5
      SS(1,IE)=(XS(IA)+XS(IB)+XS(IC))/3.0
      SS(2,IE)=(YS(IA)+YS(IB)+YS(IC))/3.0
      SS(3,IE)=(WS(IA)+WS(IB)+WS(IC))/3.0
C
C  THE REMAINING PART OF THE SUBROUTINE COMPUTES THE POSITION OF EACH
C  INTERIOR POINT FOR THE CHIEF METHOD. THEREFORE THE SUBROUTINE
C  SURFAC FOR BMF STOPS HERE. ( AFTER COMPLETING LOOPS )
C
      RDC=SQRT(SS(1,IE)**2.0+SS(2,IE)**2.0+SS(3,IE)**2.0)
      X1=XS(IB)
      Y1=YS(IB)
      U1=WS(IB)
      X2=XS(IA)
      Y2=YS(IA)
      U2=WS(IA)
      X3=XS(IC)
      Y3=YS(IC)
      U3=WS(IC)
      XG1=SS(1,IE)-X1
      XG2=SS(2,IE)-Y1
      XG3=SS(3,IE)-U1
      XG=SQRT(XG1**2.0+XG2**2.0+XG3**2.0)
      RN(1)=(Y1-Y2)*(U1-U3)-(U1-U2)*(Y1-Y3)
      RN(2)=(U1-U2)*(X1-X3)-(X1-X2)*(U1-U3)
      RN(3)=(X1-X2)*(Y1-Y3)-(Y1-Y2)*(X1-X3)
      XNLEN=SQRT(RN(1)**2.0+RN(2)**2.0+RN(3)**2.0)
      ANG=RN(1)*SS(1,IE)+RN(2)*SS(2,IE)+RN(3)*SS(3,IE)
      IF (ANG.GE.0.0) GO TO 14
      XNLEN=-XNLEN
   14 RNP(1)=RN(1)/XNLEN
      RNP(2)=RN(2)/XNLEN
      RNP(3)=RN(3)/XNLEN
C
C  POSITIONING OF INTERIOR PTS. A DISTANCE (XG/2) ALONG THE INWARD
C  POINTING NORMAL ORIGINATING FROM THE ELEMENT CENTROID
C
      SI(1,IE)=SS(1,IE)-XG*RNP(1)/2.0
      SI(2,IE)=SS(2,IE)-XG*RNP(2)/2.0
      SI(3,IE)=SS(3,IE)-XG*RNP(3)/2.0
   13 CONTINUE
   11 CONTINUE
   10 CONTINUE
      RETURN
      END
```

TRIANGLE CONFIGURATION

80 ELEMENT SEGMENT

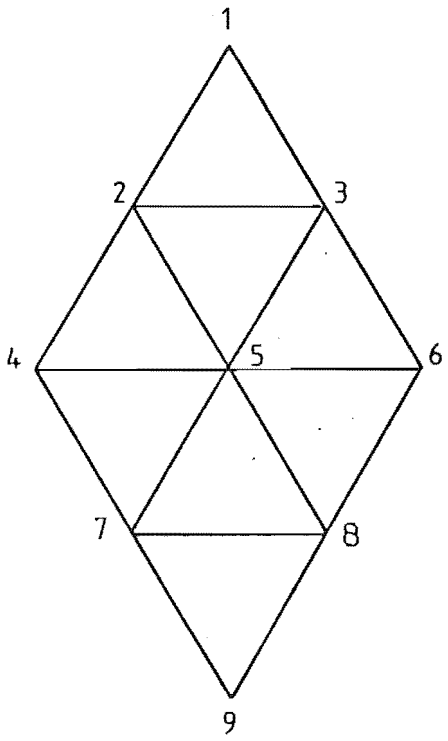

180 ELEMENT SEGMENT

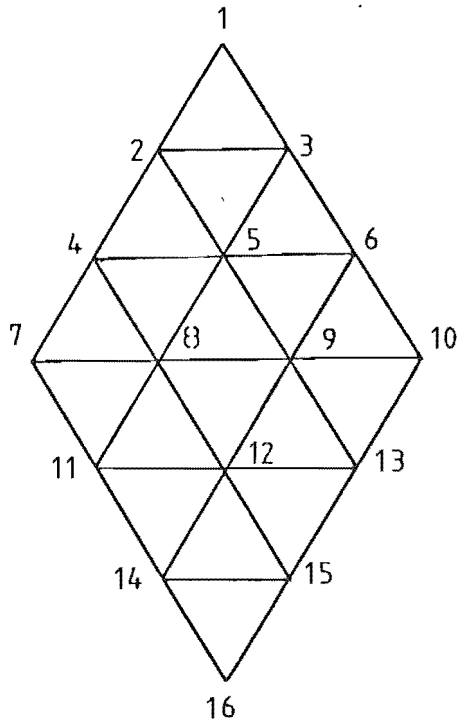

ICOSADATA/20

```
100       20     6     3    12     6    3.9010    0.0000    4    0
200      2  1  3
300      2  4  3
400     0.0000000 0.0000000
500     1.1071487 0.0000000
600     1.1071487 1.2566371
700     2.0344439 0.6283185
```

ICOSADATA/80

```
100       80     6     3    12     6    3.2924    0.3000    9    0
200      2  1  3
300      2  4  5
400      2  3  5
500      3  6  5
600      7  4  5
700      7  8  5
800      8  6  5
900      8  9  7
1000    0.0000000 0.0000000
1100    0.5535743 0.0000000
1200    0.5535743 1.2566371
1300    1.1071487 0.0000000
1400    1.0172220 0.6283185
1500    1.1071487 1.2566371
1600    1.5707963 0.3141593
1700    1.5707963 0.9424778
1800    2.0344439 0.6283185
```

ICOSADATA/180

```
100      180     6     3    12     6    4.6625    0.3000    16    1
200      2  1  3
300      2  5  4
400      2  5  3
500      3  5  6
600      4  7  8
700      4  5  8
800      8  5  9
900      9  5  6
1000     9 10  6
1100    11  7  8
1200    11 12  8
1300     8 12  9
1400     9 12 13
1500     9 10 13
1600    11 12 14
1700    14 12 15
1800    15 12 13
1900    14 16 15
2000    0.0000000 0.0000000
2100    0.3504054 0.0000000
2200    0.3504054 1.2566371
2300    0.7567433 0.0000000
2400    0.6523581 0.6283185
2500    0.7567433 1.2566371
2600    1.1071487 0.0000000
2700    1.0298844 0.3907125
2800    1.0298844 0.8659245
2900    1.1071487 1.2566371
3000    1.3983029 0.2062732
3100    1.3820858 0.6283185
3200    1.3983029 1.0503638
3300    1.7432897 0.4220453
3400    1.7432897 0.8345917
3500    2.0344439 0.6283185
```

```
21600     C ***************************************************************
21700     C *                                                             *
21800     C *       BMF                                                   *
21900     C *                                                             *
22000     C *       SUBROUTINE ASSEMB ( CALLED FROM MAIN PROGRAM )        *
22100     C *                                                             *
22200     C *       THIS SUBROUTINE  ASSEMBLES THE INTEGRATION MATRICES AND *
22300     C *       HENCE FORMS THE MATRIX [ ZM ]. VALUES ARE ASSIGNED TO THE *
22400     C *       NEUMANN BOUNDARY CONDITION, ZQ. IN ORDER TO FORMULATE THE *
22500     C *       ENTRIES OF THE INTEG. MATRICES THE INTEG SUBROUTINE IS *
22600     C *       CALLED.                                               *
22700     C *                                                             *
22800     C ***************************************************************
22900     C *                                                             *
23000     C *       ARRAYS:                                               *
23100     C *          XI, ETA    - CO-ORDS. OF OFF-DIAGONAL INTEGRATION PTS. *
23200     C *          W1         - WEIGHTS OF OFF-DIAGONAL INTEGRATION    *
23300     C *          GAM, DEL   - CO-ORDS. OF DIAGONAL INTEGRATION PTS.  *
23400     C *          W2         - WEIGHTS OF DIAGONAL INTEGRATION        *
23500     C *       ZMXS, ZMYS    - DIAGONAL MATRICES , SEE EQ. ( 4.4.10 ) *
23600     C *       ZMAS, ZMBS, ZMCS, ZMDS - INTEGRATION MATRICES FOR BMF METHOD *
23700     C *          ZM         - FINAL MATRIX                           *
23800     C *                                                             *
23900     C *       VARIABLES:                                            *
24000     C *          N1     - NO. OF PTS IN OFF-DIAGONAL INTEGRATION    *
24100     C *          ID1    - DEGREE OF OFF-DIAGONAL INTEG. SCHEME      *
24200     C *          N2     - NO. OF PTS. IN DIAGONAL INTEGRATION       *
24300     C *          ID2    - DEGREE OF DIAGONAL INTEG. SCHEME          *
24400     C *          ZK     - ( ik )                                    *
24500     C *          IE     - REFERS TO THE ELEMENT BEING INTEGRATED    *
24600     C *        CTH, STH - COSINE AND SINE OF THETA FOR EACH NODAL PT. *
24700     C *                                                             *
24800     C ***************************************************************
24900     C
25000     C
25100     C
25200           SUBROUTINE ASSEMB(SS, TH, PH, IR, IS, IT, ZMAS, ZMBS, ZMCS, ZMDS, ZM
25300          1, ZQ, SFAREA, MODE)
25400     C
25500           IMPLICIT COMPLEX(Z)
25600           DIMENSION SS(3, 1), TH(1), PH(1), IR(1), IS(1), IT(1)
25700          1, ZMAS(1), ZMBS(1), ZMCS(1), ZMDS(1), ZM(1)
25800          1, ZAS(180), ZBS(180), XI(16), ETA(16), GAM(16), DEL(16), W1(16)
25900          1, W2(16), XS(16), YS(16), WS(16), ZCS(180), ZDS(180), ZQ(1)
26000          1, ZMXS(32400), ZMYS(32400)
26100           COMMON NF, XK, XM, N1, ID1, N2, ID2, NV
26200     C
26300           L(I, J)=(J-1)*NF+I
26400           NT=NF/10
26500           XPI=3.1415926
26600           ZALPHA=CMPLX(0.0, 1.0/XK)
26700     C
26800     C  DEFINE THE INTEGRATION PTS. FOR BOTH DIAGONAL AND OFF-DIAGONAL
26900     C  INTEGRATIONS
27000     C
27100           CALL SIMPLX(XI, ETA, W1, N1, ID1)
27200           CALL SIMPLX(GAM, DEL, W2, N2, ID2)
27300     C
27400     C INTEGRATE ELEMENT BY ELEMENT
27500     C
27600           DO 1 IND=1, 2
27700           DO 2 M=1, 5
27800           DO 3 I=1, NV
27900     C
28000           A=TH(I)+(IND-1)*(XPI-2.0*TH(I))
28100           B=PH(I)+(2*M+IND-3)*XPI/5.0
28200           XS(I)=SIN(A)*COS(B)
28300           YS(I)=SIN(A)*SIN(B)
28400           WS(I)=COS(A)
28500         3 CONTINUE
28600     C
28700           DO 4 K=1, NT
28800           IA=IR(K)
28900           IB=IS(K)
29000           IC=IT(K)
29100           IE=NT*(M-1)+K+(IND-1)*NT*5
29200           CALL INTEG(IE, SS, XS, YS, WS, IA, IB, IC, XI, ETA, GAM, DEL
29300          1, ZAS, ZBS, ZCS, ZDS, W1, W2, TH, PH, IR, IS, IT, SFAREA)
29400     C
29500           DO 5 I=1, NF
29600           LIJ=L(I, IE)
29700           ZMAS(LIJ)=ZAS(I)
29800           ZMBS(LIJ)=ZBS(I)
29900           ZMCS(LIJ)=ZCS(I)
30000           ZMDS(LIJ)=ZDS(I)
30100         5 CONTINUE
30200     C
30300         4 CONTINUE
30400         2 CONTINUE
30500         1 CONTINUE
```

```
30600     C
30700     C  FORM TWO DIAGONAL MATRICES ( SEE EQ.  ( 4.4.10 ) )
30800     C
30900           DO 6 I=1,NF
31000           DO 7 J=1,NF
31100           LIJ=L(I,J)
31200           ZMXS(LIJ)=CMPLX(0.0,0.0)
31300           ZMYS(LIJ)=CMPLX(0.0,0.0)
31400         7 CONTINUE
31500         6 CONTINUE
31600           DO 8 I=1,NF
31700           DO 9 J=1,NF
31800           LII=L(I,I)
31900           LIJ=L(I,J)
32000           ZMXS(LII)=ZMXS(LII)+ZMBS(LIJ)
32100           ZMYS(LII)=ZMYS(LII)+ZMCS(LIJ)
32200         9 CONTINUE
32300         8 CONTINUE
32400     C
32500     C  ASSIGN VALUES TO ZQ  ( THE NEUMANN BOUNDARY CONDITION ).
32600     C  ADJUST MATRICES FOR SINGULARITY PTS.  ON THE SURFACE AND
32700     C  FORM THE MATRIX [ ZM ].
32800     C
32900           DO 10 I=1,NF
33000           R=SS(1,I)
33100           S=SS(2,I)
33200           T=SS(3,I)
33300           RC=SQRT(R**2.0+S**2.0+T**2.0)
33400           RS=SQRT(S**2.0+T**2.0)
33500           CTH=R/RC
33600           STH=RS/RC
33700           ZK=CMPLX(0.0,XK)
33800           ZFAC=CEXP(1.5*ZK*XM*CTH*RC)
33900           IF (MODE.EQ.1) GO TO 17
34000           ZQ(I)=(ZK*RC+3.0*XM*CTH)*ZFAC
34100           GO TO 18
34200        17 ZQ(I)=(ZK*RC*CTH+3.0*XM*CTH*CTH-1.5*XM*STH*STH)*ZFAC
34300        18 LII=L(I,I)
34400     C
34500           ZMDS(LII)=ZMDS(LII)+0.5*ZALPHA
34600           ZMAS(LII)=ZMAS(LII)-0.5
34700     C
34800           DO 11 J=1,NF
34900           LIJ=L(I,J)
35000           ZM(LIJ)=ZMAS(LIJ)+ZMCS(LIJ)+ZMXS(LIJ)-ZMYS(LIJ)
35100        11 CONTINUE
35200     C
35300        10 CONTINUE
35400           RETURN
35500           END
```

```
35600     C ***************************************************************************
35700     C *                                                                         *
35800     C *         SUBROUTINE INTEG ( CALLED FROM SUBROUTINE ASSEMB )              *
35900     C *                                                                         *
36000     C *         THIS SUBROUTINE INTEGRATES OVER A SINGLE BOUNDARY               *
36100     C *         ELEMENT FOR THE BURTON AND MILLER FORMULATION.                  *
36200     C *         FOR THE DIAGONAL INTEGRATIONS THE BASE TRIANGLE IS              *
36300     C *         SUBDIVIDED INTO SMALLER TRIANGLES SO THAT A HIGHER              *
36400     C *         ORDER INTEGRATION RESULTS, SEE FIGURE   9   .                   *
36500     C *         THIS SUBROUTINE CALLS THE GFCALC SUBROUTINE.                    *
36600     C *                                                                         *
36700     C ***************************************************************************
36800     C *                                                                         *
36900     C *         VARIABLES:                                                      *
37000     C *             ND    - NUMBER OF SUBDIVISIONS OF THE BASE TRIANGLE       *
37100     C *         ( E0, E0 ) - ORIGIN OF THE BASE TRIANGLE                        *
37200     C *         ( E1, E2 ) - NEW ORIGIN OF A SMALLER TRIANGLE                   *
37300     C *             N3    - NUMBER OF INTEGRATION PTS.  IN REFINED DIAGONAL   *
37400     C *                     INTEGRATION.                                        *
37500     C *         ( XQ, YQ, WQ ) - CO-ORDS. OF THE INTEGRATION PTS.               *
37600     C *                                                                         *
37700     C ***************************************************************************
37800     C
37900     C
38000           SUBROUTINE INTEG(IE, SS, XS, YS, WS, IA, IB, IC, XI, ETA, GAM, DEL
38100          1, ZAS, ZBS, ZCS, ZDS, W1, W2, TH, PH, IR, IS, IT, SFAREA)
38200     C
38300           IMPLICIT COMPLEX(Z)
38400           DIMENSION SS(3, 1), XS(1), YS(1), WS(1), XI(1), ETA(1), RP(3)
38500          1, GAM(1), DEL(1), W1(1), W2(1), ZAS(1), ZBS(1), ZCS(1), ZDS(1), RN(3)
38600          1, TH(1), PH(1), IR(1), IS(1), IT(1), XT(16), YT(16), WT(16)
38700          1, C(400), D(400), WF(400)
38800           COMMON NF, XK, XM, N1, ID1, N2, ID2, NV
38900           NT=NF/10
39000           XPI=3.1415926
39100     C
39200     C ZERO ELEMENT VECTORS
39300     C
39400           DO 1 I=1, NF
39500           ZAS(I)=CMPLX(0.0, 0.0)
39600           ZBS(I)=CMPLX(0.0, 0.0)
39700           ZCS(I)=CMPLX(0.0, 0.0)
39800           ZDS(I)=CMPLX(0.0, 0.0)
39900         1 CONTINUE
40000     C
40100     C  INTEGRATION PTS.  ORIENTATED EQUALLY WITHIN EACH TRIANGLE
40200     C  OF THE SAME SHAPE
40300     C
40400           X1=XS(IB)
40500           Y1=YS(IB)
40600           U1=WS(IB)
40700           X2=XS(IA)
40800           Y2=YS(IA)
40900           U2=WS(IA)
41000           X3=XS(IC)
41100           Y3=YS(IC)
41200           U3=WS(IC)
41300     C
41400     C  CALCULATION OF THE TOTAL SURFACE AREA OF THE DISCRETIZED MODEL
41500     C
41600           RN(1)=(Y1-Y2)*(U1-U3)-(U1-U2)*(Y1-Y3)
41700           RN(2)=(U1-U2)*(X1-X3)-(X1-X2)*(U1-U3)
41800           RN(3)=(X1-X2)*(Y1-Y3)-(Y1-Y2)*(X1-X3)
41900           XLEN=SQRT(RN(1)**2.0+RN(2)**2.0+RN(3)**2.0)
42000           AREA=0.5*XLEN
42100           SFAREA=SFAREA+AREA
42200     C
42300     C  SELECT INTEGRATION PT.  ( 'OFF-DIAGONAL' INTEGRATION )
42400     C
42500           DO 2 K=1, N1
42600           XQ=(X2-X1)*XI(K)+(X3-X1)*ETA(K)+X1
42700           YQ=(Y2-Y1)*XI(K)+(Y3-Y1)*ETA(K)+Y1
42800           WQ=(U2-U1)*XI(K)+(U3-U1)*ETA(K)+U1
42900           W=W1(K)*AREA
43000     C
```

```
C SELECT SINGULARITY PTS.
C (SING. PTS. NOT IN SAME ELEMENT AS INTEG.PT. )
C
      DO 3 IND=1,2
      DO 4 M=1,5
      DO 5 I=1,NV
      A=TH(I)+(IND-1)*(XPI-2.0*TH(I))
      B=PH(I)+(2*M+IND-3)*XPI/5.0
      XT(I)=SIN(A)*COS(B)
      YT(I)=SIN(A)*SIN(B)
      WT(I)=COS(A)
    5 CONTINUE
      DO 6 J=1,NT
      IA=IR(J)
      IB=IS(J)
      IC=IT(J)
      IP=NT*(M-1)+J+(IND-1)*NT*5
      XP1=SS(1,IP)
      YP1=SS(2,IP)
      WP1=SS(3,IP)
      X11=XT(IB)
      Y11=YT(IB)
      U11=WT(IB)
      X22=XT(IA)
      Y22=YT(IA)
      U22=WT(IA)
      X33=XT(IC)
      Y33=YT(IC)
      U33=WT(IC)
C
C  CALCULATION OF A NORMAL VECTOR AT THE SINGULARITY PT. P
C
      RP(1)=(Y11-Y22)*(U11-U33)-(U11-U22)*(Y11-Y33)
      RP(2)=(U11-U22)*(X11-X33)-(X11-X22)*(U11-U33)
      RP(3)=(X11-X22)*(Y11-Y33)-(Y11-Y22)*(X11-X33)
C
C  AVOID THE SINGULARITY PT. OF THE ELEMENT BEING INTEGRATED
C
      IF (IE.EQ.IP) GO TO 6
C
      CALL GFCALC(XP1,YP1,WP1,XQ,YQ,WQ,ZA,ZB,ZC,ZD,RN,RP,IP,IE)
C
      ZAS(IP)=ZAS(IP)+W*ZA
      ZBS(IP)=ZBS(IP)+W*ZB
      ZCS(IP)=ZCS(IP)+W*ZC
      ZDS(IP)=ZDS(IP)+W*ZD
    6 CONTINUE
    4 CONTINUE
    3 CONTINUE
    2 CONTINUE
C
C  CASE FOR SING.PT. & INTEG.PT. IN SAME ELEMENT
C  ( 'DIAGONAL' INTEGRATION )
C
C
C  REFINEMENT OF THE BASE TRIANGLE (SEE FIGURE   9 )
C
      IK=0
      ND=10
      E0=0.0
C
C  THE ORIGIN OF EACH SMALLER TRIANGLE BECOMES ( E1,E2 )
C
      DO 10 I=1,ND
      XD1=(-1.0)**(I+1)/2.0**I
      E1=E0
      E2=E0
      DO 11 M=1,3
      IF (M.NE.2) GO TO 12
      E1=E0
      E2=E0+XD1
   12 CONTINUE
```

```
50300     C
50400     C  POSITIONING OF INTEGRATION PTS.  WITHIN EACH SMALLER TRIANGLE
50500     C
50600           DO 13 J=1,N2
50700              IK=IK+1
50800              C(IK)=XD1*GAM(J)+E1
50900              D(IK)=XD1*DEL(J)+E2
51000              WF(IK)=XD1**2.0*W2(J)
51100          13 CONTINUE
51200              SWAP=E1
51300              E1=E2
51400              E2=SWAP
51500          11 CONTINUE
51600              E0=E0+XD1
51700          10 CONTINUE
51800     C
51900     C  POSITIONING OF INTEGRATION PTS.  WITHIN THE INNER TRIANGLE
52000     C
52100           DO 14 J=1,N2
52200              IK=IK+1
52300              C(IK)=E0-XD1*GAM(J)
52400              D(IK)=E0-XD1*DEL(J)
52500              WF(IK)=XD1**2.0*W2(J)
52600          14 CONTINUE
52700              N3=ND*N2*3+N2
52800     C
52900     C
53000     C  SELECTION OF INTEGRATION PTS.  FOR 'DIAGONAL' INTEGRATION
53100     C
53200           DO 15 J=1,N3
53300           XQ=(X2-X1)*C(J)+(X3-X1)*D(J)+X1
53400           YQ=(Y2-Y1)*C(J)+(Y3-Y1)*D(J)+Y1
53500           WQ=(U2-U1)*C(J)+(U3-U1)*D(J)+U1
53600           W=WF(J)*AREA
53700     C
53800           XP1=SS(1,IE)
53900           YP1=SS(2,IE)
54000           WP1=SS(3,IE)
54100           CALL GFCALC(XP1,YP1,WP1,XQ,YQ,WQ,ZA,ZB,ZC,ZD,RN,RN,IE,IE)
54200     C
54300           ZAS(IE)=ZAS(IE)
54400           ZBS(IE)=ZBS(IE)+W*ZB
54500           ZCS(IE)=ZCS(IE)
54600           ZDS(IE)=ZDS(IE)+W*ZD
54700          15 CONTINUE
54800              RETURN
54900              END
```

```
55000     C ***************************************************************
55100     C *                                                             *
55200     C *        SUBROUTINE GFCALC  ( CALLED FROM SUBROUTINE INTEG )  *
55300     C *                                                             *
55400     C *        THIS SUBROUTINE CALCULATES THE GREENS FN. G(P,Q) ,   *
55500     C *        AND ITS NORMAL DERIVATIVES RELEVANT TO THE BURTON    *
55600     C *        AND MILLER FORMULATION , SEE EQ. ( 5.6.4 ) .         *
55700     C *                                                             *
55800     C ***************************************************************
55900     C *                                                             *
56000     C *        ARRAYS:                                              *
56100     C *           RPQ - VECTOR JOINING POINTS P AND Q               *
56200     C *           RNQ - OUTWARD UNIT NORMAL VECTOR AT Q             *
56300     C *           RNP - OUTWARD UNIT NORMAL VECTOR AT P             *
56400     C *                                                             *
56500     C *        VARIABLES:                                           *
56600     C *           (XQ,YQ,WQ) - CO-ORDINATES OF INTEG. POINT Q       *
56700     C *           (XP,YP,WP) - CO-ORDINATES OF SING. POINT P        *
56800     C *            R1        - MAGNITUDE OF RPQ                     *
56900     C *            PLEN      - MAGNITUDE OF A NORMAL AT P           *
57000     C *            QLEN      - MAGNITUDE OF A NORMAL AT Q           *
57100     C *            PANG      - DOT PRODUCT BETWEEN A NORMAL AT P AND*
57200     C *                        THE POSITION VECTOR OF P             *
57300     C *            QANG      - DOT PRODUCT BETWEEN A NORMAL AT Q AND*
57400     C *                        THE POSITION VECTOR OF Q             *
57500     C *            PDOT      - DOT PRODUCT BETWEEN RPQ AND RNP      *
57600     C *            QDOT      - DOT PRODUCT BETWEEN RPQ AND RNQ      *
57700     C *            XNDOT     - DOT PRODUCT BETWEEN RNQ AND RNP      *
57800     C *            ZALPHA    - COMPLEX COUPLING CONSTANT            *
57900     C *            IE        - ELEMENT THAT IS BEING INTEGRATED     *
58000     C *            IP        - THE SINGULARITY POINT                *
58100     C *            ZGPQ      - THE FREE-SPACE GREENS FN.            *
58200     C *                                                             *
58300     C ***************************************************************
58400     C
58500     C
58600           SUBROUTINE GFCALC(XP,YP,WP,XQ,YQ,WQ,ZA,ZB,ZC,ZD,RN,RP
58700          1,IP,IE)
58800     C
58900     C
59000           IMPLICIT COMPLEX(Z)
59100           DIMENSION RPQ(3),RNQ(3),RN(1),RP(1),RNP(3)
59200           COMMON NF,XK,XM,N1,ID1,N2,ID2,NV
59300     C
59400     C
59500           RPQ(1)=XQ-XP
59600           RPQ(2)=YQ-YP
59700           RPQ(3)=WQ-WP
59800           R1=SQRT(RPQ(1)**2.0+RPQ(2)**2.0+RPQ(3)**2.0)
59900           R11=1.0/R1
60000     C
60100     C  THE UNIT NORMALS RNQ AT Q AND RNP AT P ARE REQUIRED TO BE
60200     C  OUTWARD POINTING.
60300     C
60400           PLEN=SQRT(RP(1)**2.0+RP(2)**2.0+RP(3)**2.0)
60500           QLEN=SQRT(RN(1)**2.0+RN(2)**2.0+RN(3)**2.0)
60600           QANG=RN(1)*XQ+RN(2)*YQ+RN(3)*WQ
60700           PANG=RP(1)*XP+RP(2)*YP+RP(3)*WP
60800           IF (QANG.GE.0.0) GO TO 3
60900           QLEN=-QLEN
61000         3 RNQ(1)=RN(1)/QLEN
61100           RNQ(2)=RN(2)/QLEN
61200           RNQ(3)=RN(3)/QLEN
61300           IF ( PANG.GE.0.0) GO TO 4
61400           PLEN=-PLEN
61500         4 RNP(1)=RP(1)/PLEN
61600           RNP(2)=RP(2)/PLEN
61700           RNP(3)=RP(3)/PLEN
61800           PDOT=RNP(1)*RPQ(1)+RNP(2)*RPQ(2)+RNP(3)*RPQ(3)
61900           XNDOT=RNQ(1)*RNP(1)+RNQ(2)*RNP(2)+RNQ(3)*RNP(3)
62000           QDOT=RNQ(1)*RPQ(1)+RNQ(2)*RPQ(2)+RNQ(3)*RPQ(3)
62100     C
62200     C  SIMPLIFICATION OF DOT PRODUCTS  WHEN INTEG. PT. AND SING. PT.
62300     C  ARE WITHIN THE SAME ELEMENT
62400     C
62500           IF (IE.NE.IP) GO TO 2
62600           PDOT=0.0
62700           XNDOT=1.0
62800           QDOT=0.0
62900         2 CONTINUE
```

```
63000     C
63100     C  CALCULATION OF INTEGRANDS FOR EQUATION ( 5.6.4 )
63200     C
63300           ZALPHA=CMPLX(0.0,1.0/XK)
63400           ZK=CMPLX(0.0,XK)
63500     C
63600           ZGPQ=0.0795775*CEXP(-ZK*R1)*R11
63700           ZA=-ZGPQ*(ZK+R11)*QDOT*R11
63800           ZB=ZALPHA*ZGPQ*XK**2.0*XNDOT
63900           ZC1=-(3.0*R11**2.0+3.0*ZK*R11+ZK**2.0)*QDOT*PDOT*R11**2.0
64000           ZC=(ZC1+R11*(ZK+R11)*XNDOT)*ZALPHA*ZGPQ
64100           ZD=ZGPQ*(1.0+ZALPHA*(ZK+R11)*PDOT*R11)
64200     C
64300           RETURN
64400           END
```

```
64500     C ***********************************************************************
64600     C *                                                                     *
64700     C *       SUBROUTINE SIMPLEX                                            *
64800     C *                                                                     *
64900     C *       THIS SUBROUTINE LISTS THE INTEGRATION POINTS AND              *
65000     C *       WEIGHTS FOR NUMERICAL INTEGRATION OVER THE BASE               *
65100     C *       TRIANGLE.                                                     *
65200     C *       THE FIRST 4 QUADRATURE RULES BELOW ARE SYMMETRIC              *
65300     C *       RULES WHICH HAVE BEEN LISTED BY COWPER [57], THE              *
65400     C *       FINAL RULE REPRESENTS A 16 PT. NON-SYMMETRIC RULE,            *
65500     C *       AS GIVEN IN REFERENCE [55].                                   *
65600     C *                                                                     *
65700     C *       THE VARIABLE ID CORRESPONDS TO THE DEGREE OF THE              *
65800     C *       QUADRATURE RULE .                                             *
65900     C *                                                                     *
66000     C ***********************************************************************
66100     C
66200     C
66300           SUBROUTINE SIMPLX(A,B,W,N,ID)
66400     C
66500           IMPLICIT COMPLEX(Z)
66600           DIMENSION A(1),B(1),W(1),S(4),R(4),U(4),V(4)
66700     C
66800     C
66900     C DEGREE-2: 3 PTS
67000           IF (ID.NE.2) GO TO 1
67100           A(1)=0.1666667
67200           A(3)=0.6666667
67300           A(2)=0.1666667
67400           B(1)=0.1666667
67500           B(3)=0.1666667
67600           B(2)=0.6666667
67700           W(1)=0.3333333
67800           W(2)=0.3333333
67900           W(3)=0.3333333
68000         1 CONTINUE
68100     C
68200     C DEGREE-3: 6 PTS
68300           IF (ID.NE.3) GO TO 2
68400           A(1)=0.816848
68500           A(2)=0.091576
68600           A(3)=0.091576
68700           A(4)=0.108103
68800           A(5)=0.445948
68900           A(6)=0.445948
69000           B(1)=0.091576
69100           B(2)=0.816848
69200           B(3)=0.091576
69300           B(4)=0.445948
69400           B(5)=0.108103
69500           B(6)=0.445948
69600           W(1)=0.109952
69700           W(2)=0.109952
69800           W(3)=0.109952
69900           W(4)=0.223381
70000           W(5)=0.223381
70100           W(6)=0.223381
70200         2 CONTINUE
70300     C
70400     C DEGREE-5: 7 PTS
70500           IF (ID.NE.5) GO TO 3
70600           A(1)=0.3333333
70700           A(2)=0.1012865
70800           A(3)=0.1012865
70900           A(4)=0.7974270
71000           A(5)=0.4701421
71100           A(6)=0.4701421
71200           A(7)=0.0597159
71300           B(1)=0.3333333
71400           B(2)=0.1012865
71500           B(3)=0.7974270
71600           B(4)=0.1012865
71700           B(5)=0.4701421
71800           B(6)=0.0597159
71900           B(7)=0.4701421
72000           W(1)=0.225
72100           W(2)=0.1259392
72200           W(3)=0.1259392
72300           W(4)=0.1259392
72400           W(5)=0.1323941
72500           W(6)=0.1323941
72600           W(7)=0.1323941
72700         3 CONTINUE
```

```
72800     C
72900     C DEGREE-6:  12 PTS
73000           IF (ID.NE.6) GO TO 4
73100           A(1)=0.8738220
73200           A(2)=0.0630890
73300           A(3)=0.0630890
73400           A(4)=0.5014265
73500           A(5)=0.2492867
73600           A(6)=0.2492867
73700           A(7)=0.6365025
73800           A(8)=0.6365025
73900           A(9)=0.3103524
74000           A(10)=0.3103524
74100           A(11)=0.0531450
74200           A(12)=0.0531450
74300           B(1)=0.0630890
74400           B(2)=0.8738220
74500           B(3)=0.0630890
74600           B(4)=0.2492867
74700           B(5)=0.5014265
74800           B(6)=0.2492867
74900           B(7)=0.3103524
75000           B(8)=0.0531450
75100           B(9)=0.6365025
75200           B(10)=0.0531450
75300           B(11)=0.6365025
75400           B(12)=0.3103524
75500           W(1)=0.0508449
75600           W(2)=0.0508449
75700           W(3)=0.0508449
75800           W(4)=0.1167863
75900           W(5)=0.1167863
76000           W(6)=0.1167863
76100           W(7)=0.0828511
76200           W(8)=0.0828511
76300           W(9)=0.0828511
76400           W(10)=0.0828511
76500           W(11)=0.0828511
76600           W(12)=0.0828511
76700         4 CONTINUE
76800     C
76900     C DEGREE-7:  16 PTS
77000           IF (ID.NE.7) GO TO 5
77100           R(1)=0.0694318
77200           R(2)=0.3300095
77300           R(3)=0.6699905
77400           R(4)=0.9305681
77500           S(1)=0.0571042
77600           S(2)=0.2768430
77700           S(3)=0.5835904
77800           S(4)=0.8602401
77900           U(1)=0.1739274
78000           U(2)=0.3260726
78100           U(3)=0.3260726
78200           U(4)=0.1739274
78300           V(1)=0.1355069
78400           V(2)=0.2034646
78500           V(3)=0.1298475
78600           V(4)=0.0311810
78700           K=0
78800           DO 6 I=1,4
78900           DO 7 J=1,4
79000           K=K+1
79100           A(K)=S(J)
79200           B(K)=R(I)*(1.0-S(J))
79300           W(K)=U(I)*V(J)*2.0
79400         7 CONTINUE
79500         6 CONTINUE
79600         5 CONTINUE
79700     C
79800           RETURN
79900           END
```

```
C ***************************************************************
C *                                                             *
C *       SUBROUTINE SOLVE  ( CALLED FROM MAIN PROGRAM )        *
C *                                                             *
C *       THIS SUBROUTINE FORMULATES THE FORCE VECTOR ZF  THEN  *
C *       CALLS THE SOLVER SUBROUTINE IN ORDER TO SOLVE THE     *
C *       MATRIX EQUATION, [ZM][ZPHI]=[ZF], FOR [ZPHI].         *
C *       THE SOLUTION ZPHI IS TRANSFORMED BACK TO THE MEAN     *
C *       FLOW PROBLEM AND IS OUTPUT ALONGSIDE AN ADJUSTED      *
C *       ANALYTIC SOLUTION. THE AVERAGE PERCENTAGE ERROR       *
C *       BETWEEN THE ANALYTIC AND COMPUTED SOLUTIONS IS OUTPUT.*
C *       THE LAST PART OF THIS SUBROUTINE CALLS TWO PLOTTING   *
C *       ROUTINES, PLOTG AND PLOTM. PLOTG GRAPHS THE SURFACE   *
C *       POTENTIAL ( ABSOLUTE VALUE, REAL PART AND IMAGINARY   *
C *       PART ) AGAINST THETA . PLOTM PLOTS CONTOURS OF THE     *
C *       ABSOLUTE POTENTIAL OVER THE SURFACE OF THE DISCRETIZED*
C *       MODEL.                                                *
C *                                                             *
C ***************************************************************
C *                                                             *
C *       ARRAYS:                                               *
C *          THET   - VALUES OF THETA FOR EACH NODE             *
C *          ZF     - THE FORCE VECTOR ( FORMED BELOW )         *
C *          Z      - SURFACE POTENTIAL IN A MEAN FLOW          *
C *          ZEX    - 'EXACT' ANALYTIC SOLUTION                 *
C *       VARIABLES:                                            *
C *          RAD    - NODAL RADIUS                              *
C *          ARAD   - AVERAGE NODAL RADIUS                      *
C *          AVPE   - AVERAGE PERCENTAGE ERROR                  *
C *          ZKN    - (-ik)                                     *
C *          SFAREA- SURFACE AREA OF DISCRETIZED MODEL          *
C *          RC     - DISTANCE TO ELEMENT CENTROID(NODE)        *
C *                                                             *
C ***************************************************************
C
C
      SUBROUTINE SOLVE(ZM, ZQ, TH, PH, IR, IS, IT, SS, ZPHI, ZMDS, SFAREA, MODE)
C
C
      IMPLICIT COMPLEX(Z)
C
      DIMENSION ZQ(1), ZMDS(1), TH(1), PH(1), IR(1), IS(1), IT(1)
     1, SS(3, 1), ZM(1), ZPHI(1), THET(180), ZF(180), Z(180), ZEX(180)
C
      COMMON NF, XK, XM, N1, ID1, N2, ID2, NV
C
      L(I, J)=(J-1)*NF+I
C
      DO 1 I=1, NF
      ZF(I)=CMPLX(0.0, 0.0)
      DO 2 J=1, NF
      LIJ=L(I, J)
      ZF(I)=ZF(I)+ZMDS(LIJ)*ZQ(J)
    2 CONTINUE
    1 CONTINUE
C
      CALL SOLVER(ZM, ZF, ZPHI)
C
C
C  OUTPUT SOLUTION AND CALL PLOT ROUTINES
C
      WRITE(6, 100)
  100 FORMAT(//, 20H SOLUTION AT SURFACE, //,
     16H NODE , 30H X-COORD    Y-COORD  . Z-COORD  , 5X
     1, 21H SOLN (REAL, IMAG, ABS), 20X, 25H EXACT (REAL, IMAG, ABS)   , 13X
     1, 5HTHETA, /)
C
      NT=NF/10
      TOTN=0.0
      TOTD=0.0
      RAD=0.0
      DO 3 J=1, NF
      X=SS(1, J)
      Y=SS(2, J)
      W=SS(3, J)
      RC=SQRT(X*X+Y*Y+W*W)
      RAD=RAD+RC
      CTH=X/RC
      THET(J)=ARCOS(CTH)*18.0/3.1415926
      ZKN=CMPLX(0.0, -XK)
      ZFAC=CEXP(1.5*ZKN*XM*CTH*RC)
      Z(J)=ZPHI(J)*ZFAC
      ZEX(J)=ZEXACT(XM, XK, X, RC, MODE)
      ZEX(J)=ZEX(J)*SFAREA/(4.0*3.14159*RC**2.0)
      WRITE(6, 200)J, SS(1, J), SS(2, J), SS(3, J), Z(J), CABS(Z(J)), ZEX(J)
     1, CABS(ZEX(J)), THET(J)
  200 FORMAT(I4, 3(2X, F8.3), 4X, 2(2(1PE10.3, 2X), 1X, 1PE10.3, 4X), 2X, F9.4)
```

```
88700     C
88800           ERRN=CABS(ZEX(J)-Z(J))
88900           ERRD=CABS(ZEX(J))
89000           TOTN=TOTN+ERRN
89100           TOTD=TOTD+ERRD
89200         3 CONTINUE
89300           AVPE=100.0*TOTN/TOTD
89400           WRITE(6,300)AVPE
89500       300 FORMAT(//,10X,25HAVERAGE PERCENTAGE ERROR=,F10.6)
89600           ARAD=RAD/NF
89700     C
89800     C
89900           CALL PLOTG(Z,THET,NF,XK,XM,ARAD,SFAREA,MODE)
90000           CALL PLOTM(TH,PH,IR,IS,IT,SS,Z)
90100     C
90200           RETURN
90300           END
```

```
90400    C ***************************************************************
90500    C *                                                             *
90600    C *        SUBROUTINE SOLVER ( CALLED FROM SUBROUTINE SOLVE )   *
90700    C *                                                             *
90800    C *        THIS SUBROUTINE SOLVES THE MATRIX EQUATION:          *
90900    C *                                                             *
91000    C *             [ ZM ][ ZPHI ] = [ ZF ]                         *
91100    C *                                                             *
91200    C *        FOR THE VECTOR [ ZPHI ].                             *
91300    C *        THE METHOD OF SOLUTION INVOLVES A STANDARD GAUSS     *
91400    C *        REDUCTION PROCEDURE WITH PARTIAL PIVOTING OF EACH    *
91500    C *        ROW.                                                 *
91600    C *                                                             *
91700    C ***************************************************************
91800    C
91900    C
92000          SUBROUTINE SOLVER(ZM,ZF,ZPHI)
92100    C
92200    C
92300          IMPLICIT COMPLEX(Z)
92400          DIMENSION ZM(1),ZF(1),ZPHI(1)
92500          COMMON NF,XK,XM,N1,ID1,N2,ID2,NV
92600          L(I,J)=(J-1)*NF+I
92700    C
92800          M=NF-1
92900          DO 1 I=1,M
93000    C
93100          MAX=0.0
93200          DO 2 K=I,NF
93300          LKI=L(K,I)
93400          IF (MAX-CABS(ZM(LKI))) 3,3,2
93500        3 IROW=K
93600          MAX=CABS(ZM(LKI))
93700        2 CONTINUE
93800    C
93900          IF (I.EQ.IROW) GO TO 4
94000          ZHANGE=ZF(I)
94100          ZF(I)=ZF(IROW)
94200          ZF(IROW)=ZHANGE
94300          DO 5 J=1,NF
94400          LIJ=L(I,J)
94500          LRJ=L(IROW,J)
94600          ZWAP=ZM(LIJ)
94700          ZM(LIJ)=ZM(LRJ)
94800          ZM(LRJ)=ZWAP
94900        5 CONTINUE
95000        4 IL=I+1
95100          DO 6 J=IL,NF
95200          LII=L(I,I)
95300          LJI=L(J,I)
95400          IF (CABS(ZM(LJI))) 7,6,7
95500        7 DO 8 K=IL,NF
95600          LJK=L(J,K)
95700          LIK=L(I,K)
95800        8 ZM(LJK)=ZM(LJK)-ZM(LIK)*ZM(LJI)/ZM(LII)
95900          ZF(J)=ZF(J)-ZF(I)*ZM(LJI)/ZM(LII)
96000        6 CONTINUE
96100        1 CONTINUE
96200    C
96300    C  BACK SUBSTITUTION
96400    C
96500          LNN=L(NF,NF)
96600          ZPHI(NF)=ZF(NF)/ZM(LNN)
96700          DO  9 I=1,M
96800          K=NF-I
96900          IL=K+1
97000          LKK=L(K,K)
97100          DO 10 J=IL,NF
97200          LKJ=L(K,J)
97300       10 ZF(K)=ZF(K)-ZPHI(J)*ZM(LKJ)
97400          ZPHI(K)=ZF(K)/ZM(LKK)
97500        9 CONTINUE
97600          RETURN
97700          END
```

```
97800     C
97900     C ***************************************************************
98000     C *                                                             *
98100     C *        THE COMPLEX FUNCTION ZEXACT COMPUTES THE 'EXACT'     *
98200     C *        ANALYTIC SOLUTION FOR THE PULSATING AND JUDDERING    *
98300     C *        SPHERE TEST CASES.                                   *
98400     C *                                                             *
98500     C *        THE FOLLOWING ANALYTIC EQUATIONS ARE THE SAME AS     *
98600     C *        EQUATIONS ( 5.2.11 ) AND ( 5.2.12);SEE ALSO          *
98700     C *        REFERENCE [7].                                       *
98800     C *                                                             *
98900     C ***************************************************************
99000     C *                                                             *
99100     C *        VARIABLES:                                           *
99200     C *                  XM - FAR FIELD MACH NO.                    *
99300     C *                  XK - WAVENUMBER                            *
99400     C *                  C  - X CO-ORDINATE OF NODAL POINT          *
99500     C *                  A  - NODAL RADIUS                          *
99600     C *                  MODE - MODE OF VIBRATION                   *
99700     C *                                                             *
99800     C *        FUNCTIONS:                                           *
99900     C *          ZHO  - SPHERICAL HANKEL FN.,2ND KIND,0   ORDER     *
100000    C *          ZHOX - DERIVATIVE OF ZHO                           *
100100    C *          ZH1  - SPHERICAL HANKEL FN.,2ND KIND,1ST ORDER     *
100200    C *          ZH1X - DERIVATIVE OF ZH1                           *
100300    C *          ZH2  - SPHERICAL HANKEL FN.,2ND KIND,2ND ORDER     *
100400    C *          ZH2X - DERIVATIVE OF ZH2                           *
100500    C *                                                             *
100600    C ***************************************************************
100700    C
100800    C
100900          COMPLEX FUNCTION ZEXACT(XM,XK,C,A,MODE)
101000    C
101100    C
101200    C EXACT SOLN FOR PULSATING OR JUDDERING SPHERE
101300    C
101400          IMPLICIT COMPLEX(Z)
101500          R=A
101600          CTH=C/A
101700          XKA=XK*A
101800          XKR=XK*R
101900          A3=A**3.0
102000          ZI=CMPLX(0.0,1.0)
102100          ZEXACT=-ZI*XK*XM*(R+A3*0.5/(R*R))*CTH
102200          IF (MODE.EQ.1) GO TO 1
102300          ZEXACT=CDEXP(ZEXACT)*(ZI*XKA*ZHO(XKR)/ZHOX(XKA)+
102400         11.5*(2.0-XKA*XKA)*XM*CTH*ZH1(XKR)/ZH1X(XKA))/XK
102500          GO TO 2
102600        1 ZEXACT=CDEXP(ZEXACT)*(-XM*XKA*XKA*0.5*ZHO(XKR)/ZHOX(XKA)
102700         1+ZI*XKA*CTH*ZH1(XKR)/ZH1X(XKA)
102800         1+XM*0.5*(3.0-XKA*XKA)*ZH2(XKR)*(3.0*CTH*CTH-1)/ZH2X(XKA))/XK
102900        2 CONTINUE
103000          RETURN
103100          END
103200    C
103300    C
103400    C  SPHERICAL HANKEL FN.,2ND KIND, 0  ORDER
103500    C
103600          COMPLEX FUNCTION ZHO(X)
103700          IMPLICIT COMPLEX(Z)
103800          ZI=CMPLX(0.0,1.0)
103900          ZIX=-ZI*X
104000          ZHO=ZI*CDEXP(ZIX)/X
104100          RETURN
104200          END
104300    C
104400    C
104500    C  DERIVATIVE OF ZHO
104600    C
104700          COMPLEX FUNCTION ZHOX(X)
104800          IMPLICIT COMPLEX(Z)
104900          ZI=CMPLX(0.0,1.0)
105000          ZIX=-ZI*X
105100          ZHOX=-CDEXP(ZIX)*(ZI/(X*X)-1.0/X)
105200          RETURN
105300          END
105400    C
```

```
105500      C
105600      C  SPHERICAL HANKEL FN., 2ND KIND, 1ST ORDER
105700      C
105800            COMPLEX FUNCTION ZH1(X)
105900            IMPLICIT COMPLEX(Z)
106000            ZI=CMPLX(0.0,1.0)
106100            ZIX=-ZI*X
106200            ZH1=CDEXP(ZIX)*(ZI/(X*X)-1.0/X)
106300            RETURN
106400            END
106500      C
106600      C
106700      C  DERIVATIVE OF ZH1
106800      C
106900            COMPLEX FUNCTION ZH1X(X)
107000            IMPLICIT COMPLEX(Z)
107100            ZI=CMPLX(0.0,1.0)
107200            ZIX=-ZI*X
107300            ZH1X=CDEXP(ZIX)*(ZI/X-2.0*ZI/(X**3.0)+2.0/(X*X))
107400            RETURN
107500            END
107600      C
107700      C
107800      C  SPHERICAL HANKEL FN., 2ND KIND, 2ND ORDER
107900      C
108000            COMPLEX FUNCTION ZH2(X)
108100            IMPLICIT COMPLEX(Z)
108200            ZI=CMPLX(0.0,1.0)
108300            ZIX=-ZI*X
108400            ZH2=CDEXP(ZIX)*(ZI*3.0/(X**3.0)-ZI/X-3.0/(X*X))
108500            RETURN
108600            END
108700      C
108800      C
108900      C  DERIVATIVE OF ZH2
109000      C
109100            COMPLEX FUNCTION ZH2X(X)
109200            IMPLICIT COMPLEX(Z)
109300            ZI=CMPLX(0.0,1.0)
109400            ZIX=-ZI*X
109500            ZH2X=CDEXP(ZIX)*(-9.0*ZI/(X**4.0)+4.0*ZI/(X*X)+9.0/(X**3.0)-1.0/X)
109600            RETURN
109700            END
```

```
109800     C ***************************************************************
109900     C *                                                             *
110000     C *       SUBROUTINE PLOTG ( CALLED FROM SUBROUTINE SOLVE )     *
110100     C *                                                             *
110200     C *       THIS SUBROUTINE PLOTS THE ANALYTIC SOLUTION AND THE   *
110300     C *       COMPUTED POTENTIAL FN. AT THE SURFACE AGAINST THETA.  *
110400     C *                                                             *
110500     C ***************************************************************
110600     C *                                                             *
110700     C *       ARRAYS:                                               *
110800     C *          EX  - ABSOLUTE VALUE OF 'EXACT' SOLN.              *
110900     C *          REX - REAL PART      OF 'EXACT' SOLN.              *
111000     C *          AIX - IMAGINARY PART OF 'EXACT' SOLN.              *
111100     C *          COMP- ABSOLUTE VALUE OF COMPUTED SOLN.             *
111200     C *          RC  - REAL PART      OF COMPUTED SOLN.             *
111300     C *          AIC - IMAGINARY PART OF COMPUTED SOLN.             *
111400     C *                                                             *
111500     C ***************************************************************
111600     C
111700     C
111800           SUBROUTINE PLOTG(Z,THET,NF,XK,XM,R,SFAREA,MODE)
111900     C
112000           IMPLICIT COMPLEX(Z)
112100           DIMENSION Z(1),ZX(50),THET(1),RADN(50),COMP(180),EX(50),RC(180)
112200          1,REX(50),FMT(2),AIC(180),AIX(50)
112300     C
112400           DATA FMT/'(F8.3)'/
112500           DATA CHAR1/'0'/
112600           DATA CHAR2/'+'/
112700           DATA CHAR3/'*'/
112800     C
112900     C  CALCULATION OF THE ANALYTIC SOLUTION ( ABSOLUTE VALUE,REAL PART,
113000     C  AND IMAGINARY PART ) IN THE RANGE 0 TO 180 DEGREES.
113100     C
113200           DO 1 I=1,41
113300           W=(1.0-(I-1)/20.0)*R
113400           ZX(I)=ZEXACT(XM,XK,W,R,MODE)
113500           ZX(I)=ZX(I)*SFAREA/(4.0*3.14159*R**2.0)
113600           CTH=W/R
113700           RADN(I)=ARCOS(CTH)
113800           EX(I)=CABS(ZX(I))
113900           REX(I)=REAL(ZX(I))
114000           AIX(I)=AIMAG(ZX(I))
114100         1 CONTINUE
114200     C
114300           DO 2 I=1,NF
114400           COMP(I)=CABS(Z(I))
114500           RC(I)=REAL(Z(I))
114600           AIC(I)=AIMAG(Z(I))
114700           THET(I)=THET(I)*3.1415926/18.0
114800         2 CONTINUE
114900           XMAX=1.60
115000           IF (MODE.EQ.1) XMAX=2.00
115100     C
115200           CALL AINIT(1200)
115300           CALL ASPEED(8)
115400     C
115500     C  SHIFT ORIGIN TO A POSITION 2.5 INS ALONG THE PAPER AND 6 INS UP
115600     C
115700           CALL AORIG(250,500)
115800     C
115900     C  DRAW A BOX 9 IN BY 8 IN
116000     C
116100           CALL ABOX(0,-400,9,8,100,100,3)
116200     C
116300     C  SET UP VERTICAL SCALE
116400     C
116500           XO=-XMAX
116600           XINC=XMAX/4.0
116700           N=9
116800           ISIZE=2
116900           IDIREC=2
117000           CALL ASCALE(-200,-410,0,100,XO,XINC,N,ISIZE,IDIREC,FMT,8)
117100     C
117200     C  SET UP HORIZONTAL SCALE
117300     C
117400           XINC=20.0
117500           N=10
117600           XO=0.0
117700           CALL ASCA(-80,-430,100,0,0,20,N,ISIZE,IDIREC)
117800     C
```

```
117900     C  SET UP X AND Y SCALE FACTORS
118000     C
118100     C  GRAPH THE ANALYTIC SOLN. (ABS,RE,IM) AND THE COMPUTED SURFACE
118200     C  POTENTIAL (ABS,RE,IM).
118300     C
118400           YSCALE=XMAX/4.0
118500           XSCALE=0.3490
118600           CALL ALINED(RADN,EX,41,0.0,0.0,XSCALE,YSCALE,5,5)
118700           CALL ALINEC(THET,COMP,NF,0.0,0.0,XSCALE,YSCALE,CHAR1,-4,-5,1,2)
118800           CALL ALINED(RADN,REX,41,0.0,0.0,XSCALE,YSCALE,5,5)
118900           CALL ALINEC(THET,RC,NF,0.0,0.0,XSCALE,YSCALE,CHAR2,-8,-10,2,2)
119000           CALL ALINED(RADN,AIX,41,0.0,0.0,XSCALE,YSCALE,5,5)
119100           CALL ALINEC(THET,AIC,NF,0.0,0.0,XSCALE,YSCALE,CHAR3,-8,-10,2,2)
119200           CALL AEND
119300           RETURN
119400           END
```

```
C ***********************************************************************
C *                                                                     *
C *       SUBROUTINE PLOTM ( CALLED FROM SUBROUTINE SOLVE )             *
C *                                                                     *
C *       THIS SUBROUTINE PLOTS ,EQUAL INCREMENT, CONTOURS OF THE       *
C *       ABSOLUTE SURFACE POTENTIAL OVER THE SURFACE OF THE            *
C *       DISCRETIZED MODEL.                                            *
C *                                                                     *
C ***********************************************************************
C *                                                                     *
C *       ARRAYS                                                        *
C *          ZVX  - AVERAGE VALUE OF POTENTIAL ASSIGNED TO EACH         *
C *                 VERTEX.                                             *
C *          PHI  - ABSOLUTE VALUE OF ZVX                               *
C *                                                                     *
C *       VARIABLES                                                     *
C *          TE   - TRIANGLE EDGE LENGTH                                *
C *          PINC - INCREMENT IN PHI FOR CONTOURS                       *
C *          KNT  - NO. OF ELEMENTS SURROUNDING EACH VERTEX             *
C *          XL   - DISTANCE BETWEEN I-TH VERTEX AND EACH SING. PT.     *
C *                                                                     *
C ***********************************************************************
C
C
      SUBROUTINE PLOTM(TH,PH,IR,IS,IT,SS,Z)
C
      IMPLICIT COMPLEX(Z)
C
      DIMENSION TH(1),PH(1),IR(1),IS(1),IT(1)
     1,P1(4),P2(4),RN(3),XS(16),YS(16),WS(16),SS(3,1)
     1,ZVX(18),Z(1),PHI(3),IP(3),CTR1(2),CTR2(2)
C
      COMMON NF,XK,XM,N1,ID1,N2,ID2,NV
C
      NT=NF/10
      XPI=3.1415926
      TAU=(SQRT(5.0)+1.0)/2.0
      TE=2.0/(SQRT(TAU+2.0))*0.5198
C
      CALL AINIT(1200)
      CALL ASPEED(8)
      CALL AORIG(500,500)
C
C  LOOP FOR EACH INCREMENT OF PHI
C
      DO 99 PINC=0.0,1.6,0.10
C
C  GENERATE MODEL VERTICES
C
      DO 10 IND=1,2
      DO 11 M=1,5
      DO 12 I=1,NV
      A=TH(I)+(IND-1)*(XPI-2.0*TH(I))
      B=PH(I)+(2*M+IND-3)*XPI/5.0
      XS(I)=SIN(A)*COS(B)
      YS(I)=SIN(A)*SIN(B)
      WS(I)=COS(A)
C
C  DECIDE WHICH ELEMENTS SURROUND THE I-TH VERTEX,THAT IS -
C  DECIDE WHICH SINGULARITY POINTS ARE WITHIN THE RADIAL DISTANCE
C  'TE' FROM THE I-TH VERTEX ( XS(I),YS(I),WS(I) ).
C
C  ASSIGN THE AVERAGE VALUE OF PHI ( FROM THE SURROUNDING ELEMENTS )
C  TO THE COMMON VERTEX.
C
      ZVX(I)=CMPLX(0.0,0.0)
      KNT=0
      DO 4 ICEN=1,NF
      XL1=SS(1,ICEN)-XS(I)
      XL2=SS(2,ICEN)-YS(I)
      XL3=SS(3,ICEN)-WS(I)
      XL=SQRT(XL1**2.0+XL2**2.0+XL3**2.0)
      IF (XL.GT.TE) GO TO 4
      KNT=KNT+1
      ZVX(I)=ZVX(I)+Z(ICEN)
    4 CONTINUE
      ZVX(I)=ZVX(I)/KNT
   12 CONTINUE
```

```
C
C  TAKE THE ABSOLUTE VALUE OF EACH OF THE THREE AVERAGE PHI VALUES
C  REPRESENTED AT THE THREE VERTICES OF EACH TRIANGULAR ELEMENT.
C
C  RANK THESE 3 ABSOLUTE VALUES INTO THE SMALLEST(PS), THE MIDDLE(PM)
C  AND THE BIGGEST(PB) VALUES.
C
      DO 13 K=1,NT
      IA=IR(K)
      IB=IS(K)
      IC=IT(K)
C
      PHI(1)=CABS(ZVX(IA))
      PHI(2)=CABS(ZVX(IB))
      PHI(3)=CABS(ZVX(IC))
      IP(1)=IA
      IP(2)=IB
      IP(3)=IC
C
      DO 6 NN=1,2
      DO 7 N=1,2
      IF (PHI(N+1).GT.PHI(N)) GO TO 7
      SWAP=PHI(N+1)
      PHI(N+1)=PHI(N)
      PHI(N)=SWAP
      CHANGE=IP(N+1)
      IP(N+1)=IP(N)
      IP(N)=CHANGE
    7 CONTINUE
    6 CONTINUE
C
      PS=PHI(1)
      PM=PHI(2)
      PB=PHI(3)
C
      I1=IP(1)
      I2=IP(2)
      I3=IP(3)
C
C  DECIDE WHICH POSITION TO VIEW THE MODEL FROM,  THAT IS -
C  WHICH ELEMENTS ARE TO BE DRAWN.
C
      X1=XS(IA)
      Y1=YS(IA)
      U1=WS(IA)
      X2=XS(IB)
      Y2=YS(IB)
      U2=WS(IB)
      X3=XS(IC)
      Y3=YS(IC)
      U3=WS(IC)
      IE=NT*(M-1)+K+(IND-1)*NT*5
      RN(1)=(Y2-Y1)*(U3-U1)-(U2-U1)*(Y3-Y1)
      RN(2)=(U2-U1)*(X3-X1)-(X2-X1)*(U3-U1)
      RN(3)=(X2-X1)*(Y3-Y1)-(Y2-Y1)*(X3-X1)
      ANG=RN(1)*SS(1,IE)+RN(2)*SS(2,IE)+RN(3)*SS(3,IE)
      IF (ANG.GE.0.0) GO TO 14
      RN(1)=-RN(1)
      RN(2)=-RN(2)
      RN(3)=-RN(3)
   14 IF (RN(2).LE.0.0) GO TO 13
C
C  DECIDE WHETHER THE CONTOUR WILL INTERSECT THE TRIANGULAR
C  ELEMENT UNDER CONSIDERATION.
C
C  IF A CONTOUR CUTS THROUGH AN ELEMENT ,CALCULATE THE POSITION
C  OF EDGE INTERSECTION BY LINEARLY INTERPOLATING ALONG THE EDGE,
C  HENCE CALL SUBROUTINE INTERP.
C
      IF (PINC.GT.PB .OR.  PINC.LT.PS) GO TO 41
      IF (PINC.GT.PS .AND.  PINC.LT.PM) GO TO 8
      CALL INTERP(I2,I3,PM,PB,PINC,CX,CY,CZ,XS,YS,WS)
      CTR1(1)=CX
      CTR2(1)=CZ
      GO TO 9
    8 CALL INTERP(I1,I2,PS,PM,PINC,CX,CY,CZ,XS,YS,WS)
      CTR1(1)=CX
      CTR2(1)=CZ
    9 CALL INTERP(I1,I3,PS,PB,PINC,CX,CY,CZ,XS,YS,WS)
      CTR1(2)=CX
      CTR2(2)=CZ
```

```
135400     C
135500     C  DRAW THE CONTOUR LINE
135600     C
135700           CALL ALINE(CTR1,CTR2,2,0.0,0.0,0.3333,0.3333)
135800     C
135900        41 P1(1)=XS(IA)
136000           P2(1)=WS(IA)
136100           P1(2)=XS(IB)
136200           P2(2)=WS(IB)
136300           P1(3)=XS(IC)
136400           P2(3)=WS(IC)
136500           P1(4)=P1(1)
136600           P2(4)=P2(1)
136700     C
136800     C  DRAW A (DASHED) LINE REPRESENTATION OF THE DISCRETIZED MODEL
136900     C
137000           CALL ALINED(P1,P2,4,0.0,0.0,0.3333,0.3333,10,10)
137100     C
137200        13 CONTINUE
137300        11 CONTINUE
137400        10 CONTINUE
137500        99 CONTINUE
137600           CALL AEND
137700           RETURN
137800           END
137900     C
138000     C
138100           SUBROUTINE INTERP(J,K,PHI1,PHI2,PINC,X1,X2,X3,XS,YS,WS)
138200           DIMENSION XS(1),YS(1),WS(1)
138300     C
138400           Q1=XS(K)-XS(J)
138500           Q2=YS(K)-YS(J)
138600           Q3=WS(K)-WS(J)
138700           XLI=(PINC-PHI1)/(PHI2-PHI1)
138800     C
138900           X1=XS(J)+XLI*Q1
139000           X2=YS(J)+XLI*Q2
139100           X3=WS(J)+XLI*Q3
139200           RETURN
139300           END
139400     C
```

```
1200    C ***************************************************************
1300    C *                                                             *
1400    C *       CHIEF    MAIN PROGRAM.                                *
1500    C *                                                             *
1600    C *       THIS REPRESENTS THE MAIN PROGRAM FOR THE CHIEF METHOD  *
1700    C *       IT IS VERY SIMILAR TO THE BMF MAIN PROGRAM , THE MAIN  *
1800    C *       DIFFERENCE BEING IN THE APPLICATION OF THE RESIDUAL    *
1900    C *       LEAST-SQUARES PROCEDURE . FOR THIS PROCEDURE THE SOLVE *
2000    C *       SUBROUTINE IS CALLED 3 TIMES CORRESPONDING TO THE 3    *
2100    C *       WEIGHTING FACTORS : FS=0.0, 0.5 AND 1.0 .              *
2200    C *                                                             *
2300    C ***************************************************************
2400    C
2500    C                  MAIN PROGRAM.
2600    C
2700          IMPLICIT COMPLEX(Z)
2800          DIMENSION SS(550),SI(550),TH(16),PH(16),IR(18),IS(18),IT(18)
2900         1,ZMGS(32400),ZMHS(32400),ZMGI(32400),ZMHI(32400),ZQ(180),ZPHI(180)
3000          COMMON NF,XK,XM,N1,ID1,N2,ID2,NV
3100          SFAREA=0.0
3200    C
3300          CALL SURFAC(SS,SI,TH,PH,IR,IS,IT,MODE)
3400    C
3500          CALL ASSEMB(SS,SI,TH,PH,IR,IS,IT,ZMHS,ZMHI,ZMGS,ZMGI,ZQ,SFAREA
3600         1,MODE)
3700    C
3800          DO 2 I=1,3
3900          FS=(I-1)*0.5
4000          WRITE(6,3)FS
4100        3 FORMAT(//,31H SOLUTION:  WEIGHT FACTOR ALPHA=,F5.2,/)
4200        2 CALL SOLVE(ZMGS,ZMGI,ZMHS,ZMHI,ZQ,SS,FS,ZPHI,SFAREA,MODE)
4300          RETURN
4400          END
```

```
21600     C ***************************************************************
21700     C *                                                             *
21800     C *       CHIEF                                                 *
21900     C *                                                             *
22000     C *       SUBROUTINE ASSEMB ( CALLED FROM MAIN PROGRAM )        *
22100     C *                                                             *
22200     C *       THIS SUBROUTINE IS SIMILAR TO THE SAME SUBROUTINE OF THE *
22300     C *       BMF METHOD , ALTHOUGH THE FORMULATION OF THE FINAL MATRIX *
22400     C *       [ ZM ] IS DELAYED TILL LATER.                         *
22500     C *                                                             *
22600     C ***************************************************************
22700     C *                                                             *
22800     C *       ARRAYS:                                               *
22900     C *            ZMGS, ZMHS - SURFACE INTEGRATION MATRICES FOR CHIEF *
23000     C *            ZMGI, ZMHI - INTERIOR INTEGRATION MATRICES FOR CHIEF *
23100     C *                                                             *
23200     C *                                                             *
23300     C ***************************************************************
23400     C
23500     C
23600     C
23700           SUBROUTINE ASSEMB(SS, SI, TH, PH, IR, IS, IT
23800          1, ZMHS, ZMHI, ZMGS, ZMGI, ZQ, SFAREA, MODE)
23900     C
24000           IMPLICIT COMPLEX(Z)
24100           DIMENSION SS(3, 1), SI(3, 1), TH(1), PH(1), IR(1), IS(1), IT(1)
24200          1, ZMHS(1), ZMHI(1), ZMGS(1), ZMGI(1), ZQ(1), ZGI(180), ZGS(180)
24300          1, ZHI(180), ZHS(180), XI(16), ETA(16), GAM(16), DEL(16), W1(16)
24400          1, W2(16), XS(16), YS(16), WS(16)
24500           COMMON NF, XK, XM, N1, ID1, N2, ID2, NV
24600     C
24700           L(I, J)=(J-1)*NF+I
24800           NT=NF/10
24900           XPI=3.1415926
25000     C
25100     C SET UP INTEGRATION PTS. ON STANDARD TRIANGLE
25200     C
25300           CALL SIMPLX(XI, ETA, W1, N1, ID1)
25400           CALL SIMPLX(GAM, DEL, W2, N2, ID2)
25500     C
25600     C INTEGRATE ELEMENT BY ELEMENT
25700     C
25800           DO 1 IND=1, 2
25900           DO 2 M=1, 5
26000           DO 3 I=1, NV
26100     C
26200           A=TH(I)+(IND-1)*(XPI-2.0*TH(I))
26300           B=PH(I)+(2*M+IND-3)*XPI/5.0
26400           XS(I)=SIN(A)*COS(B)
26500           YS(I)=SIN(A)*SIN(B)
26600           WS(I)=COS(A)
26700         3 CONTINUE
26800     C
26900           DO 4 K=1, NT
27000           IA=IR(K)
27100           IB=IS(K)
27200           IC=IT(K)
27300           IE=NT*(M-1)+K+(IND-1)*NT*5
27400           CALL INTEG(IE, SS, SI, XS, YS, WS, IA, IB, IC, XI, ETA, GAM, DEL
27500          1, ZGS, ZGI, ZHS, ZHI, W1, W2, SFAREA)
27600     C
27700           DO 5 I=1, NF
27800           LIJ=L(I, IE)
27900           ZMGI(LIJ)=ZGI(I)
28000           ZMGS(LIJ)=ZGS(I)
28100           ZMHI(LIJ)=ZHI(I)
28200           ZMHS(LIJ)=ZHS(I)
28300         5 CONTINUE
28400     C
28500         4 CONTINUE
28600         2 CONTINUE
28700         1 CONTINUE
```

```
C
C ASSIGN VALUES TO ZQ AND ADJUST FOR SING. PTS. ON SURFACE
C
      DO 6 I=1,NF
      R=SS(1,I)
      S=SS(2,I)
      T=SS(3,I)
      RC=SQRT(R**2.0+S**2.0+T**2.0)
      CTH=R/RC
      RSIN=SQRT(S**2.0+T**2.0)
      STH=RSIN/RC
      ZK=CMPLX(0.0,XK)
      ZFAC=CEXP(1.5*ZK*XM*CTH*RC)
      IF (MODE.EQ.1) GO TO 17
      ZQ(I)=(ZK*RC+3.0*XM*CTH)*ZFAC
      GO TO 18
   17 ZQ(I)=(ZK*RC*CTH+3.0*XM*CTH*CTH-1.5*XM*STH*STH)*ZFAC
   18 LII=L(I,I)
    6 ZMGS(LII)=ZMGS(LII)-0.5
      RETURN
      END
```

```
30900    C ***************************************************************************
31000    C *                                                                         *
31100    C *        CHIEF                                                            *
31200    C *                                                                         *
31300    C *        SUBROUTINE INTEG ( CALLED FROM SUBROUTINE ASSEMB )               *
31400    C *                                                                         *
31500    C *        THIS SUBROUTINE INTEGRATES OVER A SINGLE BOUNDARY                *
31600    C *        ELEMENT FOR THE CHIEF METHOD. IN THIS CASE THE GFCALC            *
31700    C *        SUBROUTINE IS CALLED TWICE FOR BOTH THE DIAGONAL AND             *
31800    C *        OFF-DIAGONAL INTEGRATIONS CORRESPONDING TO THE INTERIOR          *
31900    C *        AND SURFACE FORMULATIONS. IN THIS SUBROUTINE  THE                *
32000    C *        DIAGONAL INTEGRATIONS HAVE BEEN PERFORMED USING THE              *
32100    C *        ORIGINAL BASE TRIANGLE.                                          *
32200    C *                                                                         *
32300    C ***************************************************************************
32400    C *                                                                         *
32500    C *        VARIABLES:                                                       *
32600    C *         ( XP1,YP1,WP1) - CO-ORDS. OF SURFACE SINGULARITY PT.            *
32700    C *         ( XP2,YP2,WP2) - CO-ORDS. OF INTERIOR POINT.                    *
32800    C *           ZGPQ1        - GREENS FN. FOR SURFACE SINGULARITY            *
32900    C *           ZGPQ2        - GREENS FN. FOR INTERIOR POINT                 *
33000    C *           ZDGPQ1       - NORMAL DERIVATIVE OF ZGPQ1                    *
33100    C *           ZDGPQ2       - NORMAL DERIVATIVE OF ZGPQ2                    *
33200    C *                                                                         *
33300    C ***************************************************************************
33400    C
33500    C
33600          SUBROUTINE INTEG(IE,SS,SI,XS,YS,WS,IA,IB,IC
33700         1,XI,ETA,GAM,DEL,ZGS,ZGI,ZHS,ZHI,W1,W2,SFAREA)
33800    C
33900          IMPLICIT COMPLEX(Z)
34000          DIMENSION SS(3,1),SI(3,1),XS(1),YS(1),WS(1),XI(1),ETA(1)
34100         1,GAM(1),DEL(1),W1(1),W2(1),ZGS(1),ZGI(1),ZHS(1),ZHI(1),RN(3)
34200          COMMON NF,XK,XM,N1,ID1,N2,ID2,NV
34300          NT=NF/10
34400    C
34500    C ZERO ELEMENT VECTORS
34600    C
34700          DO 1 I=1,NF
34800          ZGS(I)=CMPLX(0.0,0.0)
34900          ZGI(I)=CMPLX(0.0,0.0)
35000          ZHI(I)=CMPLX(0.0,0.0)
35100          ZHS(I)=CMPLX(0.0,0.0)
35200        1 CONTINUE
35300    C
35400    C INTEGRATION PTS. ORIENTATED EQUALLY WITHIN EACH TRIANGLE
35500    C
35600          X1=XS(IB)
35700          Y1=YS(IB)
35800          U1=WS(IB)
35900          X2=XS(IA)
36000          Y2=YS(IA)
36100          U2=WS(IA)
36200          X3=XS(IC)
36300          Y3=YS(IC)
36400          U3=WS(IC)
36500          RN(1)=(Y1-Y2)*(U1-U3)-(U1-U2)*(Y1-Y3)
36600          RN(2)=(U1-U2)*(X1-X3)-(X1-X2)*(U1-U3)
36700          RN(3)=(X1-X2)*(Y1-Y3)-(Y1-Y2)*(X1-X3)
36800          XLEN=SQRT(RN(1)**2.0+RN(2)**2.0+RN(3)**2.0)
36900          AREA=0.5*XLEN
37000          SFAREA=SFAREA+AREA
37100    C
37200    C SELECT INTEGRATION PT.
37300    C
37400          DO 3 J=1,N1
37500          XQ=(X2-X1)*XI(J)+(X3-X1)*ETA(J)+X1
37600          YQ=(Y2-Y1)*XI(J)+(Y3-Y1)*ETA(J)+Y1
37700          WQ=(U2-U1)*XI(J)+(U3-U1)*ETA(J)+U1
37800          W=W1(J)*AREA
```

```
37900     C
38000     C SELECT SINGULARITY PTS.
38100     C (SING.  PTS.  NOT IN SAME ELEMENT AS INTEG. PT. )
38200     C
38300           DO 6 IS=1,NF
38400           XP1=SS(1,IS)
38500           YP1=SS(2,IS)
38600           WP1=SS(3,IS)
38700           XP2=SI(1,IS)
38800           YP2=SI(2,IS)
38900           WP2=SI(3,IS)
39000           IF (IE.EQ.IS) GO TO 6
39100           CALL GFCALC(XP1,YP1,WP1,XQ,YQ,WQ,ZGPQ1,ZDGPQ1,RN,IS,IE,1)
39200           CALL GFCALC(XP2,YP2,WP2,XQ,YQ,WQ,ZGPQ2,ZDGPQ2,RN,IS,IE,2)
39300           ZGS(IS)=ZGS(IS)+W*ZDGPQ1
39400           ZGI(IS)=ZGI(IS)+W*ZDGPQ2
39500           ZHS(IS)=ZHS(IS)+W*ZGPQ1
39600           ZHI(IS)=ZHI(IS)+W*ZGPQ2
39700         6 CONTINUE
39800         3 CONTINUE
39900     C
40000     C CASE FOR SING.PT.  &  INTEG.PT.  IN SAME ELEMENT
40100     C
40200           DO 7 J=1,N2
40300           XQ=(X2-X1)*GAM(J)+(X3-X1)*DEL(J)+X1
40400           YQ=(Y2-Y1)*GAM(J)+(Y3-Y1)*DEL(J)+Y1
40500           WQ=(U2-U1)*GAM(J)+(U3-U1)*DEL(J)+U1
40600           W=W2(J)*AREA
40700           XP1=SS(1,IE)
40800           YP1=SS(2,IE)
40900           WP1=SS(3,IE)
41000           XP2=SI(1,IE)
41100           YP2=SI(2,IE)
41200           WP2=SI(3,IE)
41300           CALL GFCALC(XP1,YP1,WP1,XQ,YQ,WQ,ZGPQ1,ZDGPQ1,RN,IE,IE,1)
41400           CALL GFCALC(XP2,YP2,WP2,XQ,YQ,WQ,ZGPQ2,ZDGPQ2,RN,IE,IE,2)
41500           ZGS(IE)=ZGS(IE)
41600           ZGI(IE)=ZGI(IE)+W*ZDGPQ2
41700           ZHS(IE)=ZHS(IE)+W*ZGPQ1
41800           ZHI(IE)=ZHI(IE)+W*ZGPQ2
41900         7 CONTINUE
42000           RETURN
42100           END
```

```
C ***************************************************************************
C *                                                                         *
C *       SUBROUTINE GFCALC  ( CALLED FROM SUBROUTINE INTEG )               *
C *                                                                         *
C *       THIS SUBROUTINE CALCULATES THE GREENS FN. AND ITS NORMAL          *
C *       DERIVATIVE FOR THE CHIEF METHOD                                   *
C *                                                                         *
C ***************************************************************************
C *                                                                         *
C *       ARRAYS:                                                           *
C *          RPQ - VECTOR JOINING POINTS P AND Q                            *
C *          RNQ - OUTWARD UNIT NORMAL VECTOR AT Q                          *
C *                                                                         *
C *       VARIABLES:                                                        *
C *          XLEN   - MAGNITUDE OF A NORMAL AT Q                            *
C *          ANG    - DOT PRODUCT BETWEEN A NORMAL AT Q AND THE             *
C *                   POSITION VECTOR OF Q                                  *
C *          DOT    - DOT PRODUCT BETWEEN RNQ AND RPQ                       *
C *          ISDUM  - DUMMY VARIABLE FOR INTERIOR OR SURFACE POINTS         *
C *          ZGPQ   - FREE-SPACE GREENS FN.                                 *
C *          ZDGPQ  - NORMAL DERIVATIVE OF ZGPQ                             *
C *                                                                         *
C ***************************************************************************
C
C
      SUBROUTINE GFCALC(XP,YP,WP,XQ,YQ,WQ,ZGPQ,ZDGPQ,RN,IS,IE,ISDUM)
C
C
      IMPLICIT COMPLEX(Z)
      DIMENSION RPQ(3),RNQ(3),RN(1)
      COMMON NF,XK,XM,N1,ID1,N2,ID2,NV
C
C CALCULATE COMPTS. OF VECTOR RPQ( JOINING P & Q)
C AND RNQ (UNIT NORMAL AT Q)
C
      RPQ(1)=XQ-XP
      RPQ(2)=YQ-YP
      RPQ(3)=WQ-WP
      R1=SQRT(RPQ(1)**2.0+RPQ(2)**2.0+RPQ(3)**2.0)
      R11=1.0/R1
      XLEN=SQRT(RN(1)**2.0+RN(2)**2.0+RN(3)**2.0)
      ANG=RN(1)*XQ+RN(2)*YQ+RN(3)*WQ
      IF (ANG.GE.0.0) GO TO 3
      XLEN=-XLEN
    3 RNQ(1)=RN(1)/XLEN
      RNQ(2)=RN(2)/XLEN
      RNQ(3)=RN(3)/XLEN
      DOT=RNQ(1)*RPQ(1)+RNQ(2)*RPQ(2)+RNQ(3)*RPQ(3)
      ZKN=CMPLX(0.0,-XK)
C
C  CALCULATE GREENS FN.  AND ITS NORMAL DERIVATIVE
C
      ZGPQ=0.0795775*CEXP(ZKN*R1)*R11
      IF (IE.NE.IS) GO TO 2
      IF (ISDUM.EQ.2) GO TO 2
      DOT=0.0
    2 ZDGPQ=-ZGPQ*(R11-ZKN)*DOT*R11
C
      RETURN
      END
```

```
80000     C ***************************************************************
80100     C *                                                             *
80200     C *         CHIEF                                               *
80300     C *                                                             *
80400     C *         SUBROUTINE SOLVE ( CALLED FROM MAIN PROGRAM )       *
80500     C *                                                             *
80600     C *         THIS SUBROUTINE IS SIMILAR TO THE SOLVE SUBROUTINE OF *
80700     C *         THE BMF METHOD. THIS ROUTINE ,HOWEVER, FORMALATES TWO *
80800     C *         FORCE VECTORS (ZFS,ZFI) FOR THE SURFACE AND INTERIOR  *
80900     C *         PROBLEMS. THE RESULTING MATRIX EQUATION IS DERIVED    *
81000     C *         USING A RESIDUAL LEAST-SQUARES PROCEDURE. THE REMAINING *
81100     C *         PART OF THE SUBROUTINE IS THE SAME AS FOR THE BMF METHOD.*
81200     C *                                                             *
81300     C ***************************************************************
81400     C
81500     C
81600           SUBROUTINE SOLVE(ZMGS,ZMGI,ZMHS,ZMHI,ZQ,SS,FS,ZPHI,SFAREA,MODE)
81700     C
81800     C
81900           IMPLICIT COMPLEX(Z)
82000     C
82100           DIMENSION ZMGS(1),ZMGI(1),ZMHS(1),ZMHI(1),ZQ(1),ZFS(180)
82200          1,ZFI(180),SS(3,1),ZM(32400),ZPHI(1),THET(180),ZF(180),Z(180)
82300          1,ZEX(180)
82400     C
82500           COMMON NF,XK,XM,N1,ID1,N2,ID2
82600     C
82700           L(I,J)=(J-1)*NF+I
82800     C
82900     C SET UP WEIGHT RATIO FOR SURFACE AND INTERIOR RESIDUALS
83000     C
83100           FI=1.0-FS
83200     C
83300     C SET UP FORCE VECTORS
83400     C
83500           DO 1 I=1,NF
83600           ZFS(I)=CMPLX(0.0,0.0)
83700           ZFI(I)=CMPLX(0.0,0.0)
83800           DO 2 J=1,NF
83900           LIJ=L(I,J)
84000           ZFS(I)=ZFS(I)+ZMHS(LIJ)*ZQ(J)
84100         2 ZFI(I)=ZFI(I)+ZMHI(LIJ)*ZQ(J)
84200         1 CONTINUE
84300     C
84400     C SET MATRIX SYSTEM  [ZM][ZPHI]=[ZF]
84500     C USING LEAST SQUARES TO MINIMISE RESIDUALS
84600     C
84700           DO 3 I=1,NF
84800           ZF(I)=CMPLX(0.0,0.0)
84900           DO 4 J=1,NF
85000           LIJ=L(I,J)
85100           ZM(LIJ)=CMPLX(0.0,0.0)
85200           DO 5 K=1,NF
85300           LKJ=L(K,J)
85400           LKI=L(K,I)
85500         5 ZM(LIJ)=ZM(LIJ)+FS*CONJG(ZMGS(LKI))*ZMGS(LKJ)+
85600          1FI*CONJG(ZMGI(LKI))*ZMGI(LKJ)
85700         4 CONTINUE
85800           DO 6 K=1,NF
85900           LKI=L(K,I)
86000           ZF(I)=ZF(I)+FS*ZMGS(LKI)*CONJG(ZFS(K))+FI*ZMGI(LKI)*CONJG(ZFI(K))
86100         6 CONTINUE
86200           ZF(I)=CONJG(ZF(I))
86300         3 CONTINUE
86400     C
86500     C
86600           CALL SOLVER(ZM,ZF,ZPHI)
86700     C
```

```
      C
      C  OUTPUT SOLUTION AND CALL PLOT ROUTINES
      C
            WRITE(6,100)
        100 FORMAT(//,20H SOLUTION AT SURFACE,//,
           16H NODE ,30H X-COORD    Y-COORD    Z-COORD  ,5X
           1,21H SOLN (REAL,IMAG,ABS),20X,25H EXACT (REAL,IMAG,ABS)    ,13X
           1,5HTHETA,/)
      C
            NT=NF/10
            TOTN=0.0
            TOTD=0.0
            RAD=0.0
            DO 7 J=1,NF
            X=SS(1,J)
            Y=SS(2,J)
            W=SS(3,J)
            RC=SQRT(X*X+Y*Y+W*W)
            RAD=RAD+RC
            CTH=X/RC
            THET(J)=ARCOS(CTH)*18.0/3.1415926
            ZKN=CMPLX(0.0,-XK)
            ZFAC=CEXP(1.5*ZKN*XM*CTH*RC)
            Z(J)=ZPHI(J)*ZFAC
            ZEX(J)=ZEXACT(XM,XK,X,RC,MODE)
            ZEX(J)=ZEX(J)*SFAREA/(4.0*3.14159*RC**2.0)
            WRITE(6,200)J,SS(1,J),SS(2,J),SS(3,J),Z(J),CABS(Z(J)),ZEX(J)
           1,CABS(ZEX(J)),THET(J)
        200 FORMAT(I4,3(2X,F8.3),4X,2(2(1PE10.3,2X),1X,1PE10.3,4X),2X,F9.4)
      C
            ERRN=CABS(ZEX(J)-Z(J))
            ERRD=CABS(ZEX(J))
            TOTN=TOTN+ERRN
            TOTD=TOTD+ERRD
          7 CONTINUE
            AVPE=100.0*TOTN/TOTD
            WRITE(6,300)AVPE
        300 FORMAT(//,10X,25HAVERAGE PERCENTAGE ERROR=,F10.6)
            ARAD=RAD/NF
      C
      C
            CALL PLOTG(Z,THET,NF,XK,XM,ARAD,SFAREA,MODE)
            CALL PLOTM(TH,PH,IR,IS,IT,SS,Z)
      C
            RETURN
            END
```